QUALITY ASSURANCE OF BRIDGE DECK CONCRETE OVERLAYS USING SURFACE RESISTIVITY TESTING

by

David Alex Dillworth

A thesis submitted to the faculty of
The University of North Carolina at Charlotte
in partial fulfillment of the requirements
for the degree of Master of Science in
Construction and Facilities Engineering

Charlotte

2020

Approved by:

____
Dr. Tara Cavalline

____
Dr. Brett Tempest

____
Dr. Alison Sears

ABSTRACT

DAVID ALEX DILLWORTH. Quality Assurance of Bridge Deck Concrete Overlays using Surface Resistivity Testing. (Under the direction of DR. TARA L. CAVALLINE)

Through years of heavy usage, critical transportation components such as bridge decks are repeatedly subjected to stresses from freeze-thaw cycles, chemical attack and the physical loads. These continual stresses and deterioration mechanisms acting on bridge decks contribute to the fact that 11.1% of NCDOT bridges are currently considered structurally deficient (NCDOT 2019). Once a bridge deck becomes moderately to severely deteriorated, an overlay rehabilitation is often employed. Since traffic closures must be minimized, it is essential that the rehabilitation efforts be completed rapidly, potentially resulting in errors. Issues could occur despite quality control (QC) efforts on the part of the contractor, and acceptance inspection and testing on the part of the agency. Errors made in the placement of concrete overlays are often hidden under the finished surface, only later to appear after wear, scaling, and/or loss of cover. It is a challenge to determine the overlay's quality once it is placed and Quality Assurance (QA) inspection and testing measures must be used when evidence of a defective installation is present or is suspected to be present.

In this study, surface resistivity (SR) testing is studied for its viability as an inspection approach for determining the quality of concrete overlays. Bridge deck mockups were developed with regard to potential influencing variables and tested in a methodical sequence. Each mockup is composed of a base concrete, which acts as the existing deck after overlay preparation, the top reinforcing steel mat (epoxy-coated and non-coated),

placed defects, and a different overlay mixture with varying thickness assigned to each mockup. It was expected, through observation of trends evident in heatmaps created from the data, that characteristics of the mockups such as placed voids, overlay thickness variation, details of edge effects, and determine the influence of steel reinforcement could be identified by changes in SR.

Through preliminary testing of cylinders, it was found that although SR readings are affected by non-coated steel reinforcement, SR readings were not significantly affected by epoxy-coated steel reinforcement likely due to an insulating effect of the epoxy coating. The preliminary specimens were also used to quantify the influence of concrete cover and provide cover distance correction factors. Although specific to the particular mixtures used in this study, a similar approach could be used with other mixtures.

The SR meter was effective in determining overlay thickness in the bridge deck mockups and adjustment factors were developed for each overlay. Additionally, it was found that edge effects have more influence on SR than those that have been previously published in the literature, and the meter's orientation with respect to the edge is also a factor influencing the readings. Voids and reinforcement were also detectable through SR readings, although not as readily as expected. Statistical techniques using an array of measurements may be necessary to link SR readings to the presence of voids and reinforcing bars.

As a result of this research, a procedure was developed to be used for field use, borrowing from the SR Testing of Bridge Deck Mockup section within this thesis. Potential modifications and recommendations are offered for adapting this procedure to other potential situations. The procedure developed could potentially be utilized to enhance common concrete overlay testing and inspection protocols, as well as serve as a forensic check on the quality of overlay construction.

ACKNOWLEDGEMENTS

I would like to recognize the individuals and organizations for their contributions to this research work. I have tremendous gratitude for my advisor, Tara Cavalline, Ph.D., P.E., for providing me with the opportunity to research under her guidance. Her expertise and continual encouragement were instrumental in developing this research. I would like to thank Brett Tempest, Ph.D., P.E. for his insightful feedback and for serving on my committee. I would also like to thank Alison Sears, Ph.D. for serving on my committee.

Many thanks to the concrete laboratory team, Ross Newsome, Allison Summers, Joe O'Campo, Wes Maxwell, and several others for their labor and skills needed for batching, mixing, as well as other laboratory operations. Without funding from the NCDOT, their steering committee, and donations from several organizations, this research project would not have been possible.

Above all I would like to thank my wife Lauren for always supporting me in life and throughout my academic journey. Lastly, I want to thank Mom, Dad, my sisters Sara and Leah, my brother Brad, and countless others.

TABLE OF CONTENTS

LIST OF TABLES

LIST OF FIGURES

LIST OF ABBREVIATIONS

AASHTO	American Association of State Highway and Transportation Officials
ACI	American Concrete Institute
ACPA	American Concrete Pavement Association
AEA	Air-Entraining Admixture
ASCE	American Society of Civil Engineers
ASR	Alkali-Silica Reaction
ASTM	American Society for Testing and Materials
BASF	Badische Anilin- und Soda Fabrik
CP	concrete pavement
CF	cubic feet
CY	cubic yard
Cwt	hundredweight
DOT	Department of Transportation
FHWA	Federal Highway Administration
FLDOT	Florida Department of Transportation
F/T	freeze-thaw
VHES	Very-high early strength
VHES-LMC	Very-high early strength latex modified concrete
HPC	High-Performance concrete
IDOT	Illinois Department of Transportation
in	inch

IowaDOT	Iowa Department of Transportation
ITZ	interfacial transition zone
kΩ-cm	kilohms per centimeter
LADOTD	Louisiana Department of Transportation and Development
LMC	Latex Modified Concrete
MAP	Moving Advancements into Practice
$\mu\varepsilon$	micro-strain
MOE	Modulus of Elasticity
MOR	Modulus of Rupture
MnDOT	Minnesota Department of Transportation
MRWR	Mid-range water reducing admixture
NCC	National Concrete Consortium
NCDOT	North Carolina Department of Transportation
NHS	National Highway System
NYSDOT	State of New York Department of Transportation
OPC	ordinary portland cement
PVA	polyvinyl acetate
PVDC	polyvinylidene chloride
PEM	Performance Engineered Mixtures
PC	Polymer concrete
PCA	Portland Cement Association
Pcy	pounds per cubic yards
PPCC	polymer portland cement concrete

PRS	performance-related specifications
Psi	pounds per square inch
QA/QC	Quality Assurance/Quality Control
RCPT	Rapid Chloride Permeability Test
ROC	Rate of change
SAM	Super Air Meter
SBR	styrene-butadiene rubber
SCMs	Supplementary Cementitious Materials
SHAs	State Highway Agencies
SR	SR
SSD	saturated surface dry
TRB	Transportation Research Board
VDOT	Virginia Department of Transportation
w/cm	water/cement ratio
WVDOH	West Virginia Division of Highways
WRA	Water-reducing Admixture
ºF	Degrees Fahrenheit

CHAPTER 1: INTRODUCTION

1.1 Background and significance

Critical transportation infrastructure components such as highway pavements and bridges experience harsh environmental and physical attack from freeze-thaw (F/T) cycles, deleterious chemicals, and vehicle traffic. Rather than replacing bridges that exhibit moderate to severe deterioration of the road surface, rehabilitation using concrete overlays is often the most economical approach to extend the useful life of a bridge. Utilizing concrete overlays help to reduce the costs associated with maintenance and repair that state agencies would otherwise have to fund. Some of the rehabilitation objectives are to waterproof the road surface, repair cracks and spalled concrete, structural strengthening, replace visibly deteriorated concrete, and provide protection for corroded reinforcement (Haber et al. 2017). When concrete overlays are designed using an appropriate concrete mixture, installed properly, and proven curing methods are followed, they can extend a bridge's lifetime 30 years or more (Harrington and Fick 2014).

The Federal Highway Administration (FHWA) has estimated the cost of rehabilitating and replacing structurally deficient highway bridges throughout the U.S. to be near $86 billion (FHWA 2019). The estimate includes bridges from the National Highway System (NHS) and non-NHS bridges. Due to the higher level of exposure, 50-85% of all expenditures for highway bridges go towards deck maintenance, repair, and replacement (Gucunski et al. 2010). That being said, the deck is often the first component of the bridge to be compromised. Visual inspection, the chain drag method, and hammer sounding have historically been the most commonly utilized non-destructive evaluation techniques utilized by state DOTs to detect the occurrence of deterioration and defects within the local medium of concrete pavements and bridge decks. Visual inspection and chain dragging are the initial inspection techniques to identify potential defects or delamination. Those areas are marked for further investigation (Gucunski et al. 2011).

NCDOT has completed an average of 25 overlays each year for the last five years using latex-modified concrete (LMC) or very early high strength (VHES) LMC mixtures (NCDOT 2018). Thorough testing of bridge deck concrete overlays must be further developed and employed to ensure that the quality at completion meets or exceeds specifications and guarantee that the overlay will last for the predicted duration.

1.2 Objectives and scope

The goal of this research study is to investigate the potential of SR testing to be used as an effective means for verifying the quality of newly placed bridge deck concrete overlays. The resistivity of concrete is inversely correlated to the degree of chloride ingress, where concrete with higher resistivity indicates a slower rate of chloride penetration (Polder 2001). Gudimettla and Crawford's (2016) field testing found a moderate correlation between RCPT and SR data at 28 and 56 days. Previously, SR testing is most commonly utilized for predicting the permeability of concrete (related to the rate of chloride ingress), but further research is necessary to demonstrate its viability for use in the quality assurance of concrete overlays. A minimal duration of traffic downtime is a notable consideration when selecting a concrete overlay mixture. This consideration often leads to selecting an overlay that will quickly gain strength and durability in order to open travel lanes for traffic. Consequently, very high early strength (VHES) concrete mixtures are often desirable and selected for use in overlay applications.

In this study, several initial experiments utilizing steel embedded in small cast specimens were performed to investigate the influence of reinforcing steel of different types on SR measurements. Subsequently, several laboratory bridge deck mockups were constructed, each composed of a base concrete, which acts as the existing deck after overlay preparation, the top reinforcing steel mat, and a different overlay mixture with varying thickness assigned to each mockup. By design, the overlay section of the mockups contain defects, namely voids, with their location to be investigated during the testing program. The factors described above are proposed to be detected utilizing the SR meter as a means of evaluating the usefulness of this device for quality assurance (QA) and quality control (QC) for overlay construction.

This information should provide insight into the potential utility of the SR meter for QA and QC of concrete overlays and other types of concrete construction. Results of this study will also provide insight into common factors associated with concrete mixture types and construction details that influence SR readings.

CHAPTER 2: LITERATURE REVIEW

2.1 Bridge deck overlays

Overlays can vary in thickness from 2-10 inches, or greater. There are two types of concrete overlays: bonded, which range from 2-4 in. thick, and unbonded, normally ranging from 6-10 in. thick. Bonded concrete overlays attach to the existing pavement or bridge deck and when in service act integrally as one monolithic slab, in the sense that the overlay becomes a part of the section thickness (Harrington and Fick 2014). The existing deck and overlay must behave monolithically in order to achieve the intended structural integrity. This will mitigate cracking due to the effects of loading and not compromise the durability and service-life requirements of the bridge (Lemieux et al. 2005). For a proper bond to be achieved, care must be given to surface preparation. These bonded overlays require that the existing surface be of sound material, either in-situ or after surface preparation. Alternatively, unbonded concrete overlays do not require that the existing pavement be free of deterioration, as the overlay does not rely on the existing material for to achieve the desired performance and structural capacity (Harrington and Fick 2014). For this research, bonded concrete overlays will be investigated as they are more suitable for bridge deck restoration projects.

2.1.1 General overview and design considerations

When a bridge deck experiences excessive wear, corrosion, or deterioration, the application of an overlay is often used as the most cost effective means to extend its useful life. Apart from a full replacement of the bridge deck, the unsound wearing surface can be removed by hydrodemolition, milling, and other techniques that leave the underlying steel reinforcement intact, and an overlay can be placed. These overlays are most commonly made of highly engineered mixtures which contain polymer admixtures to increase durability. For a specific bridge deck restoration need, there are a variety of bridge deck overlay solutions such as Multi-layer Polymer Overlay which restores skid value and seal cracks and Concrete Overlays. Concrete overlays can be used to match new surface profiles, add structural value, and provide chloride/corrosion protection (Beer 2018).

ElBatanouny (2012) explains that determining the optimum time for rehabilitating a bridge with one of these overlay methods will conserve the limited department maintenance resources. Bridge deck sealers are often used 3 to 6 months after construction but before any deicing salts have been applied. These sealers will generally provide an additional 5 years of service to the bridge deck. Polymer overlays are utilized on bridge decks that are in good to moderate condition and at a median age of 20 years. Polymer overlays provide additional cover for reinforcement and can increase the service life of a bridge deck 25 years. Polymer overlays not only increase the service life of the deck but also improve the skid resistance, appearance, and ride quality (ElBatanouny et al. 2017).

2.1.2 Materials

The selection of constituent materials and their proportions with the consideration of prescribed mechanical and durability performance measures is vital for the production of quality concrete structures. Class AA Concrete is commonly specified for the cast-in-place construction of each essential parts of a bridge (deck, beams, pile cap, barrier rails, end posts, etc.).

The requirements for this class of concrete as defined by NCDOT in their Standard Specifications (2018) are as follows:

- Min. 28 day compressive strength: 4,500 psi
- Cement content range: 639-715 pcy
- Max. w/cm: 0.426 (angular aggregate, air-entrained)
- Max. Slump: 3.5 in.

The requirements for LMC mixtures as defined in the specification differ substantially, most notably the age requirement for compressive strength and slump. Those requirements are listed below:

- Min. 7 day compressive strength: 3,000 psi
- Min. cement content: 658 pcy
- Max. w/cm: 0.40
- Max. Slump: 6 in.

The objective of rehabilitating bridges is not only to restore them to their original condition, but often to exceed the standard specification at the time of former construction. The selection of proven concrete constituent materials intended to extend the bridge's useful life must be made with improved long-term durability performance in consideration. In addition to the variety of durability performance parameters, workability, shrinkage resistance, curing characteristics, and strength can be improved with informed material selection. Furthermore, overlay materials must be selected with thermal expansion in consideration. To prevent cracking resulting from expansion and contraction, the concrete mixture of the overlay shall have an equal or lesser coefficient of thermal expansion than the existing concrete material (Harrington and Fick 2014).

2.1.2.1 Latex admixture

Performance concrete mixtures (PCM) containing polymer emulsion, or simply referred to as latex, offer improved durability protection from the infiltration of deleterious materials that may otherwise find its way to corrosion-sensitive reinforcement steel. Doty (2004) describes LMC as being composed of approximately 1 million-trillion tiny hydrophobic polymer beads that attach to all nonaqueous surfaces and infiltrate the existing microstructure of the hydrodemolished bridge deck. This phenomenon creates a waterproof coating once the overlay is fully hydrated. It is supposed that the water-resistant effect is accomplished by the act of the latex film creating a protective barrier to microcracks and the capillary pore structure within the concrete (Doty 2004).

By replacing part of the mixing water within an overlay mixture with a latex admixture, not only is workability greatly improved, but more importantly, durability is achieved by way of a virtually impermeable bridge deck (Mehta and Monteiro 2016). Mehta and Monteiro (2016) state that the LMC's ability to bond to existing concrete as another impressive characteristic which make it the essential admixture for bridge deck overlay rehabilitation projects, especially in corrosive environments. As a durability related measure, NCDOT typically uses latex admixtures in concrete mixtures for bridge deck overlays (NCDOT 2018).

LMC have been commercially available and utilized since the 50s, beginning with polyvinyl acetate (PVA) or polyvinylidene chloride (PVDC). However, those earlier products have widely been discontinued from concrete overlays due to low wet strength with PVA mixtures, and the suspicion of PVDC as being a leading cause of steel reinforcement corrosion (Mehta and Monteiro 2016). Therefore, styrene-butadiene rubber

(SBR) is commonly preferred for LMC overlay materials, suitable for deck rehabilitation and occasionally new deck construction.

Assaad (2018) found that SBR latex admixtures increase the cohesiveness of the mixture which results in a reduction in flow velocity, passing ability, and reduction of bleeding and segregation. The findings determined that the compressive strength was increased due to the improved bond at the reinforcing steel-concrete and mortar-aggregate interfacial transition zone (ITZ). Further, the reduction of voids in the microstructure produced a concrete with a lower porosity than that of concretes without SBR latex admixtures (Assaad and Issa 2018). LMC also has improved ductility, abrasion and impact resistance, shear bond strength, tensile and flexural strength, and excellent freeze-thaw durability. Furthermore, some latexes provide resistance to acids, alkalies and organic solvents (Kosmatka et al. 2003).

As recommended by ACI Committee 584 (1992) and also required by NCDOT (2006), LMC mixtures shall have a minimum latex admixture content of 24.5 gal/cy and a maximum water content of 18.9 gal/cy. Also, it is imperative that latex materials be stored at moderate temperatures between 40-85° F to avoid freezing or excessive heat.

2.1.2.2 Cementitious materials

In many cases, Type I/II portland cement is specified for bridge deck construction. This is a general-purpose hydraulic cement with moderate sulfate resistance due to its chemical composition. The selection of hydraulic cement has a significant influence on concrete properties due to the changes in matter and energy resulting from the chemical reaction that it has with the mixing water during hydration. In addition to cement selection, the proportional content of cement greatly affects the hydration process which affects setting time, durability and strength (Mehta and Monteiro 2014).

Rehabilitation effort of bridges and pavements require early stiffening of the concrete and a faster return to service; therefore, rapid hardening or Type III hydraulic cement is essential to producing VHES concrete which is often utilized for bridge deck concrete overlays.

2.1.2.3 Aggregate

Due to the fact that aggregates occupy the largest amount of space within a volume of concrete, typically between 60-75% by volume (70-85% by mass) and have a substantial impact on concrete's freshly mixed and hardened properties, as well as mixture proportions, the selection of quality fine and coarse aggregates is critical (Kosmatka et al. 2003). And since aggregates are relatively inexpensive, they are utilized as a filler material intended to minimize the volume of cementitious materials, resulting in a more economical concrete with a decreased paste content (Mehta and Monteiro 2014). Along with economy and improved long-term durability associated with a reduced paste content, constructability is also improved by the selection of the right aggregate characteristics which include grading, absorption, and proportions.

No. 67 coarse aggregates (0.75 in. maximum size) have been widely used in conventional concrete for bridge decks. As concrete overlays can be as thin as 1 in., a smaller aggregate, No.78 (0.5" maximum size), is more functional. The aggregate proportions in concrete overlay mixtures differ as well. NCDOT requires that the percent of fine aggregate as a percent of total aggregate by weight between shall be between 50-55, assuming SSD condition (NCDOT 2018).

2.1.3 Construction methods

The construction methods for installing a concrete overlay begins with the removal of unsound concrete, then the surface, including exposed reinforcement must be cleaned and prepared, then the overlay is batched and placed, and finally the overlay is cured. This general summary is detailed in the following sections.

2.1.3.1 Surface demolition and preparation methods

Depending on the extent of deterioration, anticipated added service-life, and budget, there are two degrees of bridge deck surface demolition preparation for overlay installation: 1) with removal of existing concrete cover; or 2) without removal of existing concrete cover. The concrete cover can be completely removed to expose the reinforcement, and in situations where the concrete surrounding the reinforcement is unsound, that concrete shall be undermined to allow the reinforcement to be encased by the overlay concrete. If the reinforcement is found to be severely corroded and unsound, replacement is required. Hydrodemolition is often the primary method for removal of the unsound or deteriorated concrete cover when applying method 1 (Haber 2017). To secure the bond of the concrete overlay to exposed reinforcement, the concrete surrounding the reinforcing steel must be removed to a minimum clearance of ½ inch (TDOT 2014). Method 2 is followed when the removal of cover concrete is unnecessary. When this degree of surface demolition is selected, milling of the existing deck is utilized to provide a rough bondable interface appropriate for the overlay. On a single bridge deck overlay project, both methods can potentially be utilized on a case-by-case basis.

For both cases, hydrodemolition is preferred over milling or jackhammering because it leaves a clean, rough application surface, as well as undamaged and rust-free reinforcement. Another benefit of hydrodemolition is that it does not induce harmful microcracking of the remaining concrete (Lemieux et al. 2005). This demolition technique breaks down the concrete into gravel-sized pieces for removal without damaging the reinforcement. High-pressure hydrodemolition equipment can convey jets of water at 20-40 gal/min and with pressures of 10,000-35,000 psi. The precision of hydrodemolition equipment allows for concrete removal at depths ranging from 1/8 – 3 inches per pass. Demolition trials of sound and unsound concrete should be performed prior to starting the work to determine the necessary speed, pressure, and overlapping passes required to complete the demolition sufficiently. Once those parameters are determined, the equipment is calibrated, and the removal can begin (Bissonnette et al. 2012).

In construction environments where high chloride levels are present, epoxy-coated reinforcing bars will likely be present. If these bars become nicked or damaged, they must be recoated or touched up with an approved epoxy coating (McDonald 2011). Also, the rebar must be properly supported if dislodged.

The deck surface must remain wet with broomed mortar for the overlay placement but have no standing water or puddling. During minor delays, wet burlap can be used to protect the interface from drying, but delays shall not exceed 30 minutes (PennDOT 2019). Sprinkel (2000) explains that in order to achieve the highest possible bond strength and reach the expected useful life of the overlay, more attention should be directed to surface preparation, proficient placement, and sufficient cure time of the overlay.

2.1.3.2 Batching and placement

The use of a mobile volumetric mixer is vital to producing these high-quality mix designs. Volumetric mixers allow for the contractor to mix onsite, directly within reach of the bridge deck. CemenTech (2019) states that volumetric mixers protect the integrity of the mix by reducing the age of the fresh concrete, reducing tempering water, and reducing segregation of the concrete caused by excessive drum revolutions. The minimum thickness of a latex-modified concrete overlay is 1 inch, not including the surface texturing depth. Concrete overlays shall not span across existing deck expansion joints and be sawcut, rather the overlay must have a discrete expansion joint constructed at the existing expansion joint (Beer 2018).

2.1.3.3 Challenges

Bridge decks sealed with epoxy resin or high molecular-weight methacrylate are sometimes overlaid with microsilica-modified, latex-modified, or super-dense plasticized concretes for complete overlay or repair jobs. The sealers are necessary for prevention of further chloride penetration into the deck, but when it is time for an overlay, the sealers should be removed. Gillum (2001) has found that when a sealer is present at the deck-overlay interface, the expected available bond strength is reduced more than 50%. The determination was made by the direct shear test, tension test, SHRP interfacial bond test, and flexural beam test. Gillum says that the bond strength can be secured if proper surface preparation techniques are implemented.

In an investigated on the behavior of reinforced concrete slab-like elements which utilized ultra-high-performance concrete (UHPC) overlays, Iowa State University determined that by increasing the roughness of the application surface, the bond strength at the interface will be increased. It was suggested that the minimum surface roughness be 0.08 in (2mm) in order to achieve this (Aaleti et al. 2013). Additional to the preparation of the overlay application, proper curing techniques must be followed such as the application of curing compounds and the placement of wet burlap and poly sheeting. The overlay surface must not be excessively textured and must have a flat plane transition at deck joints to reduce vehicle impact on those joints. Sufficient road surface drainage slopes should be planned to eliminate standing water and encourage immediate runoff (Carter et al. 2002).

2.1.3.4 Issues

Cracks formed in overlays provide a pathway for deleterious materials to ingress into the matrix and harm the longevity of the pavement. Cracking of overlays is a common problem but can be mitigated with the proper surface preparation and curing practices suggested by the Texas Department of Transportation (TDOT) (Beer 2018). Cracking may be caused by a cumulation of effects. Other cracking issues are due to the overlay thickness. In a study conducted by Michigan State University which utilized a modified ring shrinkage test (AASHTO PP 34-99), it was found that cracking of overlays can be caused by overlay thickness. For example, as the thickness of an overlay increases, interfacial shear stresses increase and debonding tended to occur, while crack producing tension stresses within the overlay decrease. This occurrence is largely due to shifts in the location of the neutral axis and is most prominent on overlays completed on bridge decks greater than 10 in thick (Shann 2012). Shann (2012) recommends that overlays not be applied to bridge decks that have an original thickness greater than 10 inches.

Very high early strength latex-modified concretes (VHES-LMC) are utilized in bridge deck overlays and pavement repairs to improve construction production efficiency and provide a durable and lasting product. VHES-LMC overlays have increased workability and provide early strength suitable to open for traffic after three hours of concrete placement. VHES-LMC typically has little to no bleed water and reduced water-cement ratio, so plastic shrinkage is likely. In a study performed by Yun and Choi (2014) it was determined that air temperature, relative humidity, concrete temperature, wind speed, and evaporation rate all influence the lack of bleed water during cement hydration and results in map cracking. This type of concrete is most commonly at risk of early age thermal cracking such as map cracking and transverse cracking. Map cracking is caused when water evaporates from the surface of freshly placed concrete faster than it can be replaced by bleed water. Other causes of map cracking are alkali-silica reaction (ASR), F/T reaction, and initial plastic shrinking which results from improper curing methods or use of curing compound that was delayed until after skid-resistant surface texturing or tining (Yun and Choi 2014). The curing compound should be applied once between placement and surface texturing and reapply after surface texturing to mitigate the issue. Other crack reducing techniques are decreasing the hydration temperature, minimize cement paste volume, and reducing free shrinkage (Yun and Choi 2014).

Furthermore, low slump concrete mixtures are more likely to crack. The existing bridge deck acts as a confinement for the overlay so when excessive volumetric changes occur in the overlay, cracking occurs. Transverse cracking is caused by the combination of thermal stresses and drying shrinkage (Yun and Choi 2014).

Quality management in the field prevents poor overlay construction. The quality of the overlay placement work by the constructors is directly correlated to the performance and life span of bridge deck overlays. Premature debonding of high-density concrete overlays can be eliminated when proper care is given to the preparation of the existing deck-overlay interface, especially in regard to rotomilling, sandblasting, and the application of debonding agents at the demolition phase of the repair and providing a dry surface for the application. Haber et al. (2017) noted that corrosion of existing steel reinforcement can be the cause of delamination below the overlay but within the existing concrete. Delamination can also occur either within the overlay or at the overlay and substrate concrete interface, yet the former is highly unlikely. This is often due to poor preparation of the substrate concrete or poor consolidation (Haber et al. 2017). Additional to the preparation of the overlay application, proper curing techniques must be followed.

2.1.4 Quality assurance and control methods

When a bridge is identified for repair, appropriate specification provisions should be provided by agencies (or their contracted designers) and followed by contractors to provide the best possible solution. Recipe specifications or prescriptive specifications are established by state agencies to be strictly followed, which prevents the contractor from altering or improving the process. This is disadvantageous because there is no opportunity for innovation in the changing environment that exists on construction sites or variations in the material resource. Many of today's QA specifications are a combination of materials and methods specifications and QA requirements. The prescriptive measures of materials and methods specifications include specifying the procedures to follow and the equipment and materials to use. QA specifies the desired level of quality. Performance-related Specifications (PRS) specify the desired performance or serviceability level of the concrete mixture and final product. With PRS, the desired level of quality, and the long-term performance can be predicted from acceptance tests (Taylor et al. 2013).

Highway agencies have an interest in ensuring that their pavements meet critical mixture performance requirements, and a QA program provides the specifications for constructing highway components with satisfactory service life. The 28-day strength benchmark used in the past is found to no longer determine quality of construction or durability, nor will it predict length of service life (Cackler et al. 2017). It is necessary to implement a quality monitoring testing program that can be performed during production and construction of concrete so that beneficial mix alterations can be made along the way. Cackler (2017) states the 6 Critical Performance Engineering Mixture Properties adopted from AASHTO 84-17 which includes aggregate stability, transport properties, paste durability, shrinkage, strength, and workability. Rather than agencies prescribing specifications such as minimum or maximum cement content, the contractor is given authority to develop the mixture design to meet the performance requirements of the Quality Control (QC) specifications. Cackler (2017) states that since this approach authorizes the contractor to control the process, they are able to innovate and be more effective. One of the tests proposed to be included into the PEM efforts for bridge deck rehabilitation is the SR test (Cackler et al. 2017).

2.2 NDE for construction quality assurance/control

Non-destructive evaluation (NDE) techniques are valuable QA and QC methods for use on structures because they provide information about the quality of concrete components such as strength evolution, deterioration, cracks and other internal defects such as honeycombing without causing significant harm to the strength and durability of the concrete. Furthermore, NDE techniques are effective in assessing the durability of concrete, determining the position of reinforcement steel, determining the uniformity of concrete, and monitoring long-term changes within the medium (Lorenzi et al. 2012). NDE techniques typically also requires less effort than other approaches, which leads to a reduction of resources and expenditures. The drawback to some NDE techniques include the cost of some NDE tools, the rigor of the analysis required to analyze the data for some tools/techniques, and the level of training required of the technician performing the NDE tasks and data analysis. For example, with regard to data analysis, it should not be assumed that NDE test results will consistently correlate with traditional destructive testing techniques such as compressive strength without developing empirical correlation factors (Taylor et al. 2013).

2.2.1 Introduction to NDE and value to construction

Nondestructive evaluation (NDE) of reinforced concrete is complex due to its composite material nature, and a combination of preparation and placement variables such as mixture design, batching, mixing, and non-uniformity of aggregate supplies. (Gucunski et al. 2011)

A number of research studies have been performed over the past several decades to identify and refine the utility of different NDE tools and techniques for use in the field. For example, a research study by Gucunski et al. (2011) involved the use of a variety of NDE methods to determine the condition of a bridge deck. The evaluation program was conducted at a rate of about 2,500-3,000 square feet per workday. The following methods were utilized, listed in the order of their relative speed of data collection: ground penetrating radar, electrical resistivity, half-cell potential, impact echo, and ultrasonic surface waves. The NDE results were validated using drilled cores and by comparing to records from previous overlay projects (Gucunski et al. 2011). Gucunski et al. (2013), concluded in their research that in order to determine all occurrences of deterioration or defects, the use of more than a single NDE technology is required. Of the 10 NDE technologies utilized in their research detecting the health of concrete bridge decks, ultrasonic surface wave testing was the only technology found to provide information on vertical cracks. Surface wave testing was regarded as just a "fair" technology for that purpose, with the authors stating, "ultrasonic surface wave testing was also the only technology validated as having good potential in concrete deterioration detection and characterization". Electrical resistivity was one of the four viable technologies that had a fair-to-good potential for corrosion detection (Gucunski et al. 2013).

2.2.2 SR

Electrical resistivity is the ability for a material to resist the transfer of ions when subjected to an electrical field. It is mainly influenced by the pore size and interconnectivity of the pore structure (Layssi et al. 2015). Electrical resistivity testing is a method used to detect cracks or paths of moisture within a material's microstructure (Growers and Millard 1999). Additionally, electrical resistivity equipment with the potential to estimate the thickness of concrete pavement slabs is being developed (Taylor et al. 2013).

Resistivity of reinforced concrete is directly associated with the likelihood of corrosion in reinforcing steel and corrosion of the concrete due to chloride diffusion (Proceq 2017). Concrete is an ion conductor, meaning that the electrical conduction happens thought the interconnected pore structure. The permeability of the concrete is an indication of its ability to resist chloride ion penetration (AASHTO 2017) and is the most important criteria for determining the long-term durability of concrete (Kevern 2015, Taylor et al. 2013).

A SR meter is a hand-held, non-destructive evaluation testing tool which has the ability to quickly determine the permeability or the connectivity of a concrete's pore structure. For this research study, the 38 mm (1.5") probe spacing Proceq Resipod SR meter will be used to determine the electrical resistivity of concrete (Figure 2.1). The Resipod uses a spring-loaded four pin array and applies an electrical current that is carried by ions in pore liquid from the outer probes, and the potential difference is measured between the inner probes. Figure 2.2 shows a schematic of the SR meter with the probes engaged demonstrating the applied current and measurement of potential difference. The measurement result is displayed in kilohm-centimeters (kΩ-cm) on the device (Proceq 2017).

FIGURE 2.1: Proceq Resipod SR meter (Proceq 2017)

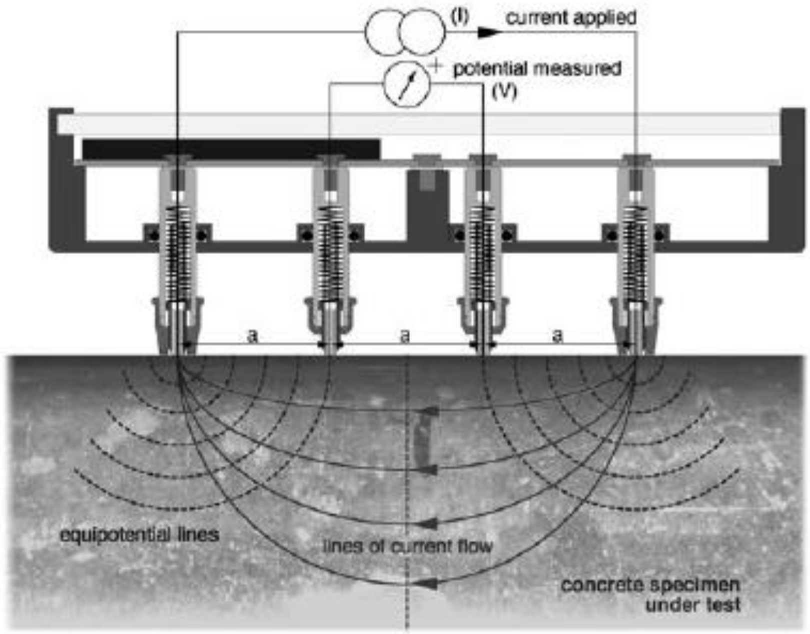

FIGURE 2.2: Proceq Resipod measurement principal (Proceq 2017)

The Resipod has the ability to read the resistivity of a concrete specimen within the range of 1-1000 kΩcm. SR is calculated with the following equation, $\rho = 2\pi aV/I$ [kΩ-cm], where ρ = resistivity [ohm-m], a = electrode separation [m], V = voltage [V], I = current [A]. Proceq, the manufacturer of the Resipod list the following application examples, demonstrating its versatility:

- Estimation of the likelihood of corrosion
- Indication of corrosion rate
- Correlation to chloride permeability
- On site assessment of curing efficiency
- Determination of zonal requirements for cathodic protection systems
- Identification of wet and dry areas in a concrete structure
- Indication of variations in the water/cement ratios within a concrete structure

- Identification of areas within a structure most susceptible to chloride penetration
- Correlation to water permeability of rock

Since SR testing is a relatively simple and straightforward approach compared to many other NDE tools/techniques, it has a fairly small margin of error between users. In a study done by Icenogle and Rupnow (2012), where two tests were conducted by different laboratories on the same material, it was found that the SR readings did not differ by more than 11% (Icenogle and Rupnow 2012).

2.2.2.1 General overview

The approach of SR testing with the Wenner Probe has provided a fairly easy and time efficient method for determining important characteristics about the durability of hardened concrete. Today, the Wenner probe is a well-accepted tool for determining the quality of composition, likelihood of corrosion based on chloride permeability, degree of hydration, and characterization of transport properties as all of the above relate to electrical resistivity of concrete. Compared to previous methods such as rapid chloride permeability test (RCPT) that require intensive specimen preparation and may take days to perform, SR can be measured in minutes, and can be performed in the laboratory or on the jobsite.

The CNS Farnell Concrete Resistivity Meter was one of the early versions of the Wenner probe on the market for testing the electrical resistance of a concrete's pore structure and obtaining understanding of the risk of permeability and corrosion risk of concrete members. The manufacturers state that field use of this device investigates whether or not the embedded steel reinforcement is exhibiting corrosion, the internal structure is compromised, or the rate of chloride penetration resistance of the concrete member is of acceptable levels (CNS Farnell n.d.). Furthermore, electrical resistivity has been used to detect moisture, flaws, and pollution in porous media (Gucunski et al. 2011). Additionally, electrical resistivity was found to detect the presence of cracking during curing and determine the connectivity of the concrete's microstructure (Rajabipour et al. 2004).

Recently, other types of Wenner probe devices have become commercially available for use in measuring SR. One of these devices is the Resipod manufactured by Proceq. As quoted by Proceq (2017), "The Resipod is an evolution of the industry standard CNS Farnell RM MKII resistivity meter, operating on the principle of the Wenner probe.".

2.2.2.2 Use of SR in laboratory setting

Due to the field pattern of the electrical current flow of the Wenner probe, the geometry of the specimen affects the SR measurement, so correction factors were implemented by Florida DOT (2004) to convert readings from a cylindrical specimen to flat surfaces, such as a slab or bridge deck. However, differing values were reported by Kansas Department of Transportation (Jenkins 2015). For example, Jenkins's (2015) findings considered concrete to have a high tendency for chloride penetration to have a SR measurement lower than 7.0 kΩ-cm rather than 12.0 kΩ-cm for a 4 in. x 8 in. cylinder. Table 2.1 shows the correlation of SR of various sample geometries when tested with a Wenner probe with 1.5 in. spacing (Florida DOT 2004).

TABLE 2.1: SR geometry correction factor

	SR (kΩ-cm)		
Chloride Ion Permeability	4 in. x 8 in. Cylinder	6 in. x 12 in. Cylinder	Semi-Infinite Slab (Real)
High	< 12.0	< 9.5	< 6.7
Moderate	12.0 - 21	9.5 - 16.5	6.7 - 11.7
Low	21 - 37	16.5 - 29	11.7 - 20.6
Very Low	37 - 254	29 - 199	20.6 - 141.1
Negligible	> 254	> 199	> 141.1

The geometry correction factor (k) for 4 in. x 8 in. cylinders was established by Spragg et al. (2013) with the utilization of Morris et al.'s (1996) simulations which resulted in the formula below (Equation 2.1). The formula should be used only when the ratio of the diameter to the electrode spacing is less than or equal to 6 or if the ratio of the length to the electrode spacing is less than or equal to 6 ($d/a \leq 6$ or $L/a \leq 6$, where d = diameter, L= length, and a = electrode spacing) (Spragg et al. 2013):

$$k = 1.10 - \frac{0.730}{\frac{d}{a}} + \frac{7.34}{(\frac{d}{a})^2} \quad \text{(Eq. 2.1)}$$

According to Growers and Millard's (1999) experimental findings, to mitigate misleading resistivity measurements, the spacing of the electrode shall be less than 25% of any dimension of the specimen and half the contact area distance from the specimen's edge as there is a restriction of the current flow near the edge. Not following these parameters can result in an overestimation of SR.

2.2.2.3 Use SR in field settings

The primary objective of SR testing is to evaluate the potential of concrete to resist chloride ingress or susceptibility of corrosion to initiate in steel reinforcement. When testing specimens in a laboratory setting or specimens in the field, efforts are made to manipulate both settings to resemble one another in order to produce a one-to-one relationship (Presuel-Moreno et al. 2010). Gucunski et al. (2013) determined that electrical resistivity was not a favorable method for detecting the depth and width of vertical cracks but was somewhat favorable (1 out of 5 rating) for determining characteristics pertaining to delamination of overlays and concrete degradation in bridge decks. In this study, by ranking the overall value of several NDE technologies, it was determined that electrical resistivity was most valuable for evaluating the potential for corrosion in bridge decks.

2.2.2.4 Influences on SR

There are two groups of factors that influence electrical resistivity of concrete, intrinsic factors and factors that affect the resistivity measurement. Intrinsic factors that influence electrical resistivity of concrete include water to cementitious materials ratio (w/cm), characteristics of the pore structure, and aging. Factors that affect the resistivity measurement include moisture content, temperature, specimen geometry, electrode spacing, and the existence of rebar. Larger pores within the concrete and higher temperatures decrease the resistivity reading (Polder 2001).

The permeability of concrete, as well as a number of other properties, can be defined by its w/cm ratio. The higher the w/cm ratio, the more porous the microstructure. This concludes with a lower electrical resistivity of concretes (that do not contain supplementary cementitious materials such as slag) (Rupnow and Icenogle 2012). Chen et al. (2014) reported a 15-20% decrease in electrical resistivity when the w/cm ratio increased from 0.4 to 0.6.

Reinforcement steel embedded within the concrete conducts electrical current more efficiently than the surrounding concrete. Due to that, the current field within reinforced concrete can become distorted, particularly when the cover depth is less than 30 mm (1.18 in) (Proceq 2017). Weydert and Gehlen (1999) determined that when concrete is tested for SR on top and in the parallel orientation of rebar embedded at 10 or 20 mm deep, errors by magnitude of two to six times reduction of the actual resistivity could result. Even when one of the four probes are within 10-20 mm distance of the rebar, the results will contain errors. The error involving rebar will produce resistivity measurements lower than typical or expected. It was also found that the electrical current induced by a Wenner probe can travel through the concrete at a depth approximate to the electrode spacing (Polder 2001).

Sengul and Gjørv (2009) studied the effects of probe spacing on wet-cured slabs with and without steel reinforcement and found minimal differences when measured with varying probe spacings less than 30 mm. However, when electrode spacing increased from 20 mm to 70 mm an approximate resistivity increase of 26% resulted in slabs without embedded reinforcement. When tested on slabs with rebar, a 33% increase was found from testing perpendicular to the rebar and 26% decrease when testing with the meter oriented parallel to the rebar (Sengul and Gjørv 2009).

For reinforcement spacing that is greater than the space between the outer probes (4.5”), the optimum orientation of the meter to the bars is diagonal. When the reinforcement can’t be avoided, it is best to position the meter perpendicular to the bars to minimize its influence. For each location, it is recommended to take 5 readings a few mm apart and then reporting the median of those 5 values (Proceq 2017, Polder 2001). Salehi et al. (2016) performed a study of the effects of different characteristics of concrete specimens containing rebar mesh being tested with the four-point Wenner probe and found that when the densities of the reinforcement mesh increased, the resistivity decreased, and that the effects of rebar diameter are negligible. It was also concluded that when the probe is setup on top of and perpendicular to the bottom rebar and parallel to and between top reinforcement bars, the smallest error would result, as illustrated in Figure 2.2 (Salehi et al. 2016).

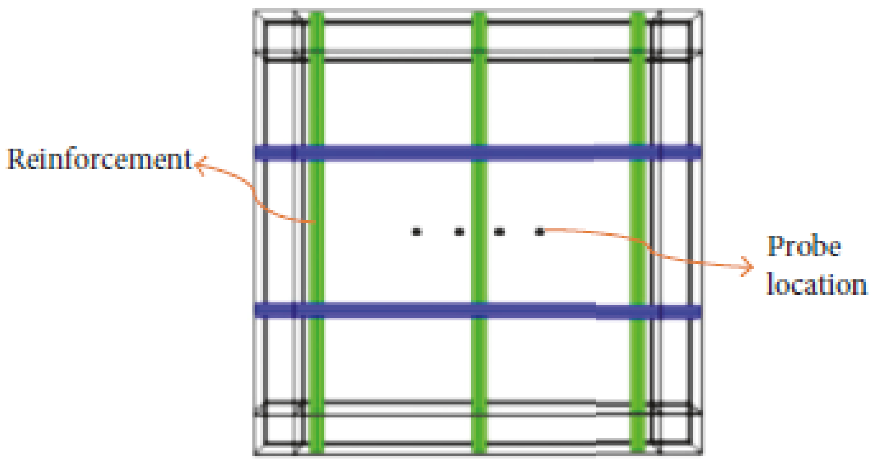

FIGURE 2.3: Probe configuration to reduce SR error

Garzon et al.'s (2014) experimental study of the effects of rebar presence on cylindrical and rectangular prism mortar specimen's electrical resistivity using the four-point Wenner probe confirms those findings. When resistivity measurements are taken directly above the rebar of a double layer mesh, an error will result due to polarization at the concrete and steel interface which acts as a resistance capacitor (Garzon et al. 2014).

The influence that temperature has on the SR of concrete is significant. As the temperature of the concrete increases by one degree, the resistivity measurement can decrease by 3% for saturated concrete and 5% for dry concrete (Proceq 2017), and if the ambient temperature is much higher than the specimen's temperature, the SR will be much lower than expected (Spragg et al. 2013). The effects of temperature on resistivity are due to the fact that electrons move faster at higher temperatures, which causes a higher electrical conductivity, resulting in a decrease in resistivity (Azarsa and Gupta 2017). Another contributing factor of temperature's influence on resistivity is that higher temperatures tend to decrease moisture content which indirectly affects resistivity (Poyet 2009). To help mitigate the influence of temperature, the concrete's temperature and ambient temperature should be monitored and recorded with the resistivity measurements. Reference values of SR are typically quoted for 68°F (Proceq 2017). Millard et al. (1991) and Gowers and Millard (1999) developed a correction factor of 0.33 KΩ-cm/°C to compensate for temperature variation. It is noted, however, that this study only included testing at a limited temperature range.

Due to an increase in ion mobility that is accompanied by increased electrical conductivity, concrete's moisture content has an inverse effect on the SR measurements (Liu and Presuel-Moreno 2014, Larsen et al. 2006). Concrete specimens that were immersed in either water or lime water will likely have a different resistivity than those that were cured in a high humidity setting (Larsen et al. 2006). Larsen et al.'s (2006) research concluded that concrete's resistivity nearly doubled when the degree of saturation decreased from 88% to 77% and the resistivity increased an average of six times when the moisture degree decreased from 88% to 66%. Concrete in an air-dry state will have a higher than expected resistivity reading and sometimes make it impossible to collect the reading (Rupnow and Icenogle 2013). Sengul (2014) found a 50% increase in resistivity of concrete when air-dried versus concrete tested in a saturated condition. Due to less restricted electrical flow of a saturated pore solution, increasing the water content of concrete results in a lower resistivity. For example, fully saturated concrete has a resistivity on the order of 100-1000 ohm-m, while the resistivity of oven-dried concrete can be as high as 10^6 ohm-

m. Care should also be given to surface saturation, as static ponding and the application of pressurized water can lead to inaccurate resistivity measurements of over 30% compared to full laboratory saturation (Marquez 2015).

Gjørv et al. (1977) found that w/cm ratio has an inverse relationship on the electrical resistivity of concrete and later Gucunski et al. (2011) confirmed that finding. This was true of substantially cured concrete and freshly made concrete (Gucunski et al. 2011). In a study performed by Icenogle and Rupnow (2012) where five mixtures at three different w/cm ratios (0.35, 0.50, and 0.65) were tested for SR, it was found that the SR meter (Resipod) successfully identified differences in concrete with different w/cm ratios.

The size of aggregate in the concrete mixture is known to have an impact on SR. Normal weight aggregates will generally be more dense and less porous than the hardened cement paste, thus having a higher resistivity. In a study performed by Sengul (2014) where the effects of two different aggregates sizes were compared, it was found that increasing the aggregate nominal size and content results in a higher resistivity measurement. Morris et al. (1996) reports that concrete with a larger maximum aggregate size will result in a variability of resistivity readings within one specimen. This is likely caused by the size and shape of the interconnected pores, or tortuosity effect, and the amount of interfacial transition zones (ITZ). Aggerates with a higher percentage of smaller particle sizes will develops more ITZ occurrences within the concrete. This is also true of aggregates that have a rough surface texture or irregular particle shape. The ITZ has a greater porosity when compared to the hardened cement paste, which leads to a lower resistivity (Morris et al. 1996). When the nominal aggregate size within the concrete mixture is larger than the resistivity meter's probe spacing, the resistivity reading will likely be impacted (Proceq

2017). In a study performed by Growers and Millard (1999) where specimens of a constant maximum aggregate size were measured for resistivity at changing probe spacings, a 10% increase in the standard deviation was observed as the probe spacing decreased approaching the maximum aggregate size. Figure 2.4 is a graph developed by Growers and Milliard 1999 showing the rate in which the standard deviation percentage increases as the ratio of the contact spacing to maximum aggregate size decreases. To reduce the variance in measurement with the resistivity meter, Growers and Millard (1999) recommends using a device with a probe spacing 1.5 times greater than the maximum nominal aggregate size.

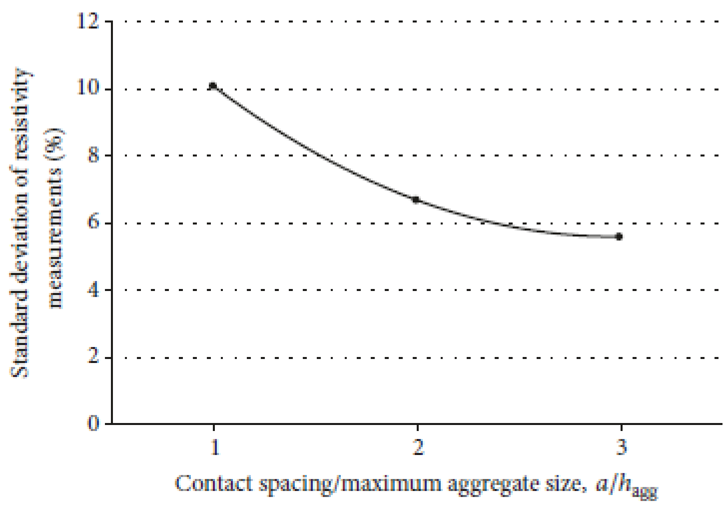

FIGURE 2.4: Effect of contact spacing on resistivity measurement

Resistivity of concrete is also affected by the curing conditions. The curing and/or storage conditions of concrete specimens have a great influence on degree of saturation, degree of hydration, and the pore solution and structure through leaching (Spragg et al. 2013). Weiss et al. (2013) performed a study to determine the curing effects on resistivity. Mortar specimens of the same mixture were subject to three curing conditions: (1) sealed during curing and testing, (2) sealed during curing and saturated during testing, and (3) saturated during curing and testing. Specimens that were sealed both during curing and testing had the highest resistivity. In contrast, specimens that were sealed during curing but saturated during testing had the lowest resistivity. Curing a specimen under water will likely cause a completely different degree of hydration than what would occur in concrete from a field structure (Weiss et al. 2013). Azarsa and Gupta (2017) recommends wetting the specimen prior to performing the resistivity testing.

Resistivity testing is contingent on the initial assumption that concrete is isotropic and homogeneous with semi-finite geometry. When cracks are present within the reach of the imposed current, the electrical resistivity measurement may vary (Azarsa and Gupta 2017). Lataste et al. (2003) performed a study in an effort to locate and identify crack characteristics such as the opening of the crack and bridging degree between the opening and depth of the crack.

The experiment was performed on two reinforced concrete members, a slab in a field setting and beams in a laboratory setting. Rather than a linear electrode orientation of a Wenner probe, an instrument was built where the four electrodes are positioned at the four corners of a square. This instrument is shown in Figure 2.3. The built instrument allows for measuring the resistivity in two orthogonal directions without requiring to rotate the probe ninety degrees between measurements. It was found that when the imposed electrical current was taken orthogonal to the visible water filled cracks, known as conductive cracks, there was no impact on the reading but when tested parallel to the crack a reduction in resistivity was observed. When tested on an insulated crack (air-filled cracks without bridging), an overestimation of resistivity was observed when the imposed current was in the orthogonal orientation, and an underestimation was observed when measured parallel with respect to the crack. In addition, it was also concluded that as the depth of a crack increased, the resistivity measurement also increased.

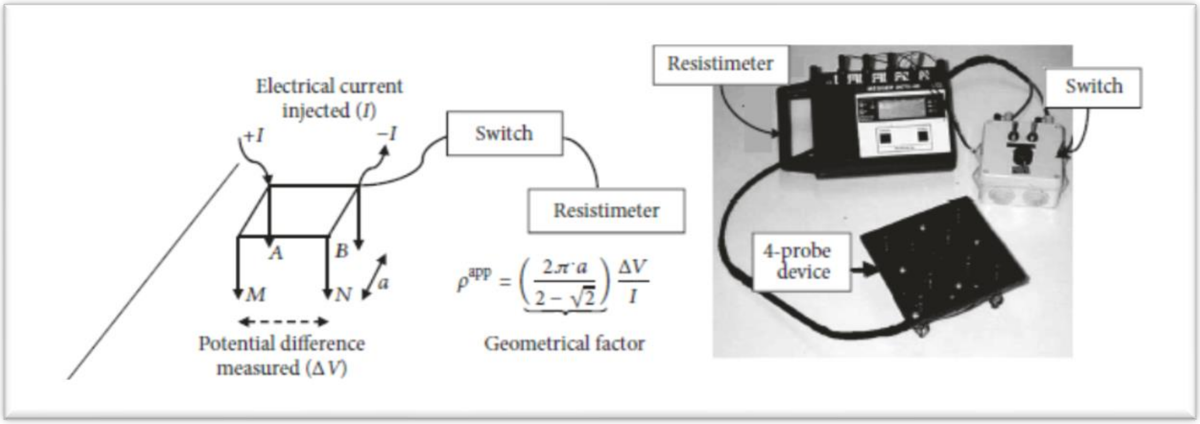

FIGURE 2.5: Four-probe square array principal (Lataste et al. 2003)

Lataste et al.'s (2003) research was based on the assumption that the rebar's influence on the resistivity reading was independent of the presence of cracks. Also, it is possible that the small scale of the concrete specimen could exaggerate the crack's impact on the resistivity reading, and lastly the four corner setup of the probe utilized in the study could possibly produce other measurement errors when compared to the commonly accepted linear Wenner probe configuration (Azarsa and Gupta 2017). Shah and Ribakov's (2008) research on crack assessment and defect detection of concrete structures found that resistivity measurements in the vicinity of insulated cracks produced higher values than that of conductive cracks. Salehi et al. (2015) determined that the depth of cracks did not significantly impact the resistivity measurement on conductive cracks. Furthermore, when the two inner electrodes spanned an insulated crack, the maximum error occurred. The electrical resistivity in this orientation led to about 200% higher results than what was expected of the concrete's resistivity. Microcracking did not significantly affect the resistivity measurement (Morales 2015). Other characteristics that influence the resistivity of concrete are fluid salinity, cement chemistry, admixtures, and defects within the concrete (Gucunski et al. 2011).

2.2.2.5 Use of SR on bridge deck overlays

The Louisiana Department of Transportation has recently accepted SR as a viable quality assurance tool for new and existing concrete and has predicted a savings of over $1.5 million each year by replacing RCPT with SR (Rupnow and Icenogle 2011; Rupnow and Icenogle 2012). Although this seminal study was primarily performed in the laboratory, other studies have focused on use of SR as a field tool, particularly to replace the more intensive and costly RCPT (ASTM 2009). RCPT testing requires that the technicians have significant training and sample preparation is very time consuming (Kevern 2015). Additionally, if evaluating field concrete, cores must be taken, which is a time-consuming, destructive process that can require traffic control, and certainly requires repair of the structure where the cores were removed. SR is showing promise in field applications. For example, Kevern (2016) attempted to utilize the SR meter in field applications and was able to detect the presence of silane and lithium silicate sealers on bridge decks with SR.

2.2.2.5 Limitations of SR testing on bridge decks

Gucunski et al. (2011) explains that manual SR testing along a grid on large-scale surfaces areas such as bridge decks can get tedious and that there are no automated measurement systems on the market at the time of the research to provide a solution. Furthermore, electrodes need galvanic coupling to the surface of the concrete. To provide galvanic coupling, pre-wetting is necessary but over-wetting is a concern. Over-wetting may adversely affect the measurement because the device can possibly be detecting probe-to-probe current flow along the surface of the concrete and not within. To mitigate some of this current leakage from probe to probe, the surface should have a light coating of water and never puddling (Gucunski et al. 2011).

2.3 Research needs

As overlays are often placed quickly with the intention of avoiding traffic delays, and the accompanying fact that overlay concrete mixtures often contain VHES which have a tendency to lose workability and consistency before anticipated, if the overlay gets away from the workers then construction errors are likely to occur. These construction errors can result in unwanted voids or an overlay thickness that does not provide sufficient reinforcement cover. As discussed in previous sections, SR testing of concrete has many benefits including cost, ease of use, and measurements are displayed immediately. Further research is necessary to investigate the potential of SR testing as QA inspection and testing protocol for concrete overlays. SR testing of overlays could possibly be utilized to determine the quality of placement and act as verification or acceptance measure for newly placed bridge deck concrete overlays. Currently, no guidance or standard method exists to support use of the SR meter to evaluate the consistency and integrity of a bridge deck overlay and/or determine its thickness. Additionally, there is only limited information on the effects of different types of reinforcing steel, edges, interfaces between two materials that occur at different depths, and voids on SR readings. Guidance on corrections to SR readings due to these embedded items and voids, as well as edges and discontinuities, would be useful to practitioners hoping to use the SR meter as a QA device for these types of projects.

CHAPTER 3: METHODOLOGY

3.1 Introduction

The primary focus of this research is to investigate the potential usefulness of SR testing as a quality assurance process for determining the condition of recently placed bridge deck concrete overlays. Small-scale specimen and bridge deck mockups were built as the testing specimens. The specimens, particularly the bridge deck mockups, contain common conditions found on typical bridge deck overlay construction projects.

As described in the literature review, one very prominent characteristic of concrete bridge decks that significantly alter SR measurements is embedded steel reinforcement. Bridges that were designed before the introduction of epoxy-coated reinforcement were built using non-coated rebar (black/standard rebar). In an effort to manage variables that can potentially affect the resistivity measurement, a preliminary investigation was carried out on steel reinforced concrete cylinders and miniature slabs to determine whether the SR measurements can differentiate between epoxy-coated and non-coated steel reinforcement. SR tests were performed on the preliminary specimens containing four different concrete mixtures with standard/raw reinforcement and epoxy-coated rebar. The findings of this preliminary investigation were used to determine if epoxy-coated reinforcement steel would be incorporated into the mockups for the second part of this research. This chapter provides an overview of materials, mixture types and proportions, batching of fresh concrete, preparation of preliminary specimens and bridge deck mockups, and the laboratory testing procedures.

3.2 Mixture design

The concrete mixtures prepared for this research study are intended to replicate common mixtures employed by NCDOT for North Carolina bridge deck construction, bridge deck overlays, and bridge deck repair patches. The mixtures were selected from previous research projects implemented by UNC Charlotte under the direction of NCDOT. These mix designs meet Class AA bridge deck specifications which requires a minimum 4,500 psi 28-day compressive strength and a cement content of between 639-715 pounds per cubic yard. The concrete mixtures utilized in this research included:

- A conventional bridge deck mixture (CC)
- A conventional ready-mix bridge deck mixture (CC-RM)
- A latex-modified bridge deck overlay mixture (LMC)
- A very high early strength overlay mixture (VHES)
- A very high early strength latex-modified overlay mixture (VHES-LMC)

The concrete mixtures detailed above are shown below in Table 3.1.

TABLE 3.1: Concrete proportions for bridge deck overlays

Mixture		lb/cy				gal/cy	oz/100# cement	
	w/c	Cement	Water	CA	FA	Latex	MRWR	AEA
CC	0.37	715	265.5	1720	1113	0	7.66	3.65
CC-RM	0.39	572	288.6	1825	1014	-	-	-
LMC	0.39	658	177	1304	1510	17.5	5.55	0
VHES	0.45	658	299	1304	1510	0	15	2.56
VHES-LMC	0.45	658	222	1304	1510	17.5	5.55	0

3.3 Materials description and characterization

The following sections provides information regarding the materials that were utilized for the concrete production as part of the laboratory program of this research. Information such as material manufacturers and suppliers, physical properties, and other characteristics are discussed about the cementitious materials, coarse and fine aggregates, and chemical admixtures.

3.3.1 Cementitious materials

The cementitious materials used for batching the concrete for the laboratory testing program were Ordinary portland cement (OPC) and Very High Early strength cement (VHES). Provided in the following sections are material description, characteristics, and sources for each.

3.3.1.1 Ordinary portland cement

The ordinary portland cement (OPC) utilized for this project is Type I/II cement sourced from Lafarge Holcim in Holly Hill, SC and conforms to ASTM C150, "Standard Specification of Portland Cement" (ASTM 2018). This cement was used in two of the four mixtures produced as part of this research project. The OPC mill report is provided in Appendix A, Figure A.1.

3.3.1.2 Very high early strength cement

Very high early strength concrete is ideal for paving projects that require a fast return to service. The VHES cement utilized in this research study is Rapid Set Cement manufactured by CTS Cement Manufacturing Corporation. The manufacturer requires water curing for a minimum of 1 hour to begin as soon as the moist sheen disappears from the surface. This cement has a specific gravity of 2.97 and is capable of achieving 4,500 psi in 1.5 hours and 8,340 psi at 24 hours. Rapid Set Cement conforms with ASTM C1600, “Standard Specification for Rapid Hardening Hydraulic Cement” (ASTM 2018). The mill report for this cement is provided in Appendix A, Figure A.2.

3.3.2 Coarse aggregate

The coarse aggregate used for the conventional bridge deck concrete mixture for preliminary testing was No. 67 crushed granitic gneiss stone obtained from the Triangle Quarry owned by Wake Stone Corporation in Cary, North Carolina. The No. 67 aggregate has maximum particle size of 1 inch, absorption of 0.04%, and specific gravity of 2.63. Since overlays are regularly thin in section, the three overlay concrete mixtures used No. 78 normal weight aggregates with a maximum particle size of 1/2 inch. The No. 78 aggregate is also a granitic gneiss has an absorption of 0.40% and an apparent specific gravity of 2.663. Both of these aggregates conform to the specifications of ASTM C33, “Standard Specification for Concrete Aggregates.” as well as NCDOT specification 1014-2, “Aggregate for Portland Cement Concrete – Coarse Aggregate” (ASTM 2018, NCDOT 2018) and are typical for North Carolina bridge paving operations. Additional information about the coarse aggregate properties can be found in Appendix A, Figure A.3.

3.3.3 Fine aggregate

The fine aggregate used for all concrete mixtures within this research was silica sand sourced from a natural sand pit in Lemon Springs, North Carolina. This aggregate has an absorption of 0.40%, specific gravity of 2.61, and a fineness modulus of 2.65. Like the coarse aggregate, the fine aggregate also conform to the specifications of ASTM C33, “Standard Specification for Concrete Aggregates”, as well as NCDOT specification 1014-1, “Aggregate for Portland Cement Concrete – Fine Aggregate” (ASTM 2018 and NCDOT

2018). Additional information about the fine aggregate properties is provided in Appendix A, Figure A.4.

3.3.4 Chemical admixtures

The conventional and VHES-non latex concrete mixtures used MasterAir AE200 air entrained admixture (AEA) to assist in achieving the durability-based air content requirements. BASF recommends a dosage rate between 0.125-1.5 fluid ounces per 100 pounds (hundredweight) of cementitious material. To promote workability MasterPolyheed 997 mid-range water reducer was used in each concrete mixture. BASF recommends a dosage rate of 5-13 ounces per hundredweight of cementitious material.

The latex admixture used in two of the three overlay mixtures is Styrofan 1186, which is an aqueous styrene-butadiene polymer type latex manufactured by BASF. Although the manufacturer recommends 24.5 gallons per cubic yard of concrete, the NCDOT approved dosage rate of 17.5 gallons per cubic yard was used. This latex admixture provides a solids content of 48% and mixing water replacement rate of 52%. The Styrofan 1186 has a specific gravity of 2.98 and a unit weight of 8.50 pounds per gallon. For more technical information, the Styrofan 1186 technical data sheet is provided in Appendix A, Figure A.5.

3.4 Batching and mixing procedure

A 6-cubic-foot portable drum mixer (nominal mixing capacity of 3.5 cubic feet) was used to produce the concrete for all preliminary concrete mixtures as well as the mockup overlay concrete and associated cylinders for the secondary research. Due to the large volume demand of the conventional concrete for the base concrete of the mockups, this material was sourced from a local ready mixed concrete supplier.

To help control the moisture content of the aggregate at the time of batching, both coarse and fine aggregates were moved from outside storage hoppers to inside the laboratory at least one week in advance of mixing. This allowed for a stable moisture condition to be achieved, and batch water was modified to account for absorption of the aggregates.

3.4.1 Preliminary tests for influence of reinforcement on SR measurement

The two non-VHES concrete mixtures were proportioned into 2.5 cubic feet batches to fulfil the requirement of 6 – 6 in. x 12 in. cylinders, one slump test (ASTM C143 “Standard Test Method for Slump of Hydraulic-Cement Concrete”), one air test (ASTM “Standard Test Method for Air Content of Freshly Mixed Concrete by the Pressure Method”) and provide additional material for waste. The non-VHES mixtures were batched consecutively on the same day. Similarly, the remaining two VHES mixtures were proportioned into 2.5 cubic feet batches, yet the additional material designated for waste was utilized to produce one miniature slab specimen for each reinforcement condition for each mixture. Figure 3.1 shows three VHES concrete miniature slabs, a miniature slab with epoxy rebar (VES-E), and a miniature slab with standard rebar (VES-S), one without rebar (VES-X). The rebar mat contains four bars which are illustrated by the black lines.

FIGURE 3.1: Miniature slab specimens

Due to the rapid hardening of the Rapid Set cement, one of the VHES concrete mixtures experienced a loss of workability and had to be wasted. Due to that, the VHES concrete mixtures were batched on separate days. The preliminary specimen concrete batching was performed in accordance with ASTM C685, "Standard Specification for Concrete Made by Volumetric Batching and Continuous Mixing" (ASTM 2017).

3.4.2 Bridge deck mockups

The conventional concrete mixture that served as the base concrete for the three overlay mockups, the one control mockup, and associated 4 in. x 8 in. cylinders for the bridge deck mockups were produced with the support of a standard ready mixed concrete truck. The three mockup overlay mixtures were produced and placed at a later date to allow for the base concrete to cure. Similar to the preliminary specimen, the three overlays were batched and mixed with the use of the portable tilting drum mixer in accordance with ASTM C685. "Standard Specification for Concrete Made by Volumetric Batching and Continuous Mixing" (ASTM 2017).

3.5 Fresh concrete test procedures

Described in the following sections are quality control procedures and standards that were utilized to determine characteristics about fresh properties of the concrete. The results of these tests serve to monitor the quality of fresh concrete, to determine that they met target acceptance criteria, and allowed for benchmarking of the data from one mixture to another. Fresh concrete that does not meet these standards within reason shall require remedy efforts, if unsuccessful the mixture would be discarded and reproduced.

3.5.1 Slump

This slump test was performed as a measure of the consistency and flow characteristics of plastic concrete and provides a determination of batch-to-bath uniformity (Mehta and Monteiro 2016). Slump testing was performed following ASTM C143 (ASTM 2015).

3.5.2 Air content

Air content is a durability related acceptance test for concrete that has a potential to be exposed to freezing and thawing environments. The air content of fresh concrete was measured immediately after mixing each bath using the Type B concrete air meter in accordance with ASTM C231(ASTM 2017). Mixtures that met NCDOT air content requirements of 5% ± 1.5% were deemed acceptable (NCDOT 2018).

3.5.3 Unit weight

Fresh unit weight of concrete is another quality control method that suggests whether or not the appropriate material proportions set out by the mixture design were achieved. This determination is most concerned with identifying an excess of the lighter constituent materials such as air and water that are known to diminish durability. The unit weight of fresh concrete was determined by means of the Type B concrete air meter, as it has a known weight and volume. The test was performed according to ASTM C138, “Standard Test Method for Density (Unit Weight), Yield, and Air Content (Gravimetric) of Concrete” (ASTM 2017).

3.5.4 Temperature

The cement hydration process is directly impacted by temperatures that are either too high or too low. Extreme temperature will likely compromise the quality of the concrete in regard to strength and durability. The temperature of fresh concrete was measured within 5 minutes after the mixing process concluded. The test was performed in accordance with AASHTO T309, “Temperature of Freshly Mixed Portland Cement Concrete” (AASHTO 2015).

3.6 Preparation and curing of test specimens

Test specimens were prepared in accordance with ASTM C192, “Standard Practice for Making and Curing Concrete Test Specimens in the Laboratory” (ASTM 2018). Prior to casting, a form release agent was applied to cylindrical specimen casings to facilitate demolding. OPC containing concrete specimens were covered with plastic for 24 hours prior to removing casings. The concrete mixtures that contain VHES cement reach a hardened state much earlier, they were covered with plastic for 1 hour before being demolded. Once specimens were demolded, they were placed in the moist curing room only to be removed during testing. The moist curing room conforms with ASTM C511, “Standard Specification for Mixing Rooms, Moist Cabinets, Moist Rooms, and Water Storage Tanks Used in the Testing of Hydraulic Cements and Concretes” (ASTM 2013)

3.6.1 Preparation and curing of preliminary specimens

As previously mentioned in the introduction, the steel reinforcement variable which effects the SR measurement must be understood and controlled in order to accurately represent the condition of the concrete. In an effort to manage that variable, a preliminary investigation was carried out on concrete cylinders and miniature slabs, both containing reinforcement, to determine whether the SR meter can differentiate between epoxy-coated and non-coated steel reinforcement. The results of this preliminary investigation were intended to be the deciding factor of whether or not to incorporate epoxy-coated reinforcement steel into the mockups for the primary research. The query which initiated this preliminary investigation is: will the thin epoxy coating that encases the steel reinforcement provide sufficient insulation so that the current applied by the SR meter has no contact with the highly conductible steel? The answer to this question was observed in the form of a variation or non-variation in SR magnitude in the direct vicinity of the epoxy-coated reinforcement steel. As concluded by Polder (2002), the most obvious indication of this influence (2-6x reduction in SR) is a substantial decrease in magnitude of SR when the probe is orientated on top of and parallel to the epoxy-coated steel reinforcement.

SR tests were performed on cylinders and miniature slab specimens prepared using four different concrete mixtures, two different rebar types as well as instances of no reinforcement.

3.6.1.1 Preparation and curing of 6 in. x 12 in. cylinders

Each concrete mixture was cast into 6 in. x 12 in. cylinders. A single No. 6 (3/4 in.) rebar was embedded longitudinally into selected cylinders as follows:

(1) with a single standard rebar - two cylinders per mixture,

(2) with a single epoxy-coated rebar - two cylinders per mixture,

(3) no reinforcement - two cylinders per mixture.

Table 3.2 shows the number of cylinders measured for SR for each pairing of concrete and rebar type.

TABLE 3.2: Number of 6 in. x 12 in. cylinders for preliminary testing

Type of reinforcement	Number of Cylinders			
	Conventional Concrete	Latex-modified concrete	VHES concrete	VHES Latex-Modified Concrete
Standard rebar	2	2	2	2
Epoxy coated rebar	2	2	2	2
No rebar	2	2	2	2

In cylinders containing reinforcement, the No. 6 bar was placed off-center longitudinally through the cylinder, providing differing cover dimensions for the SR testing. Rebar was placed approximately 1.5 in. from the outside surface of the cylinders, as shown in Figure 3.2. The intentions of this approach was to provide insight into the influence of rebar depth on the SR measurement, and also mirrors the mockup tests, which will have rebar placed at varying depths of cover.

FIGURE 3.2: Typical 6 in. x 12 in. reinforced cylinder

After the concrete cylinders were cast, they were covered with plastic to promote curing without moisture loss. Cylinders cast from the two conventional (non-VHES) concrete mixtures were allowed to cure for 24 hours in laboratory conditions prior to demolding, then were tested for SR at 1 day (24 hours). After the 1-day tests, cylinders were placed in UNC Charlotte's moist curing room and removed only for the 3, 7, 14, 28, 56, and 90-day SR tests.

Cylinders cast from the two VHES mixtures were also covered with plastic to promote curing without moisture loss. At 1 hour, the cylinders were demolded, and SR tests were performed at 1 hour, 2 hours, and 4 hours. The VHES cylinders were then placed in the moist curing room to follow the same testing schedule utilized for the conventional (non-VHES) concrete test specimens. At 120 days, all cylinders (CC, LMC, VHES-LMC, VHES-non latex) were relocated to an environmental chamber programmed to retain a constant temperature of 73 ± 3°F with a relative humidity of 50 ± 4% to allow them to reach a steady yet unsaturated state, and SR testing resumed.

3.6.1.2 Preparation and curing of miniature slabs

As an intermediary sized testing specimen between the preliminary 6 in. x 12 in. cylinders and the more extensive small-scale slab mockups, miniature slabs were constructed and tested as part of this preliminary work. The miniature slabs served to better understand the influence of reinforcing steel and orientation of test on measured SR, Figure 3.3 shows the containers utilized as concrete forms for the miniature slabs with the 3 rebar conditions – unreinforced (at top), uncoated rebar (middle) and epoxy-coated rebar (bottom). The No. 6 reinforcement was placed 6 in.-on-center to maintain the same spacing as the mockups. The forms at the left of Figure 3.3 were filled with VHES concrete, the forms on the right of Figure 3.3 were filled with VHES-LMC. After being filled with concrete, the boxes were placed on a vibrating table to assist with consolidation of the concrete around the reinforcement. Since these boxes were cast using rapid setting VHES concrete, they were cured and tested following the schedule and procedure previously utilized for the VHES cylinders (1, 2, 4 hours, then 1, 3, 7, 14, 28, 56, and 90 days).

FIGURE 3.3: Miniature slab forms

3.6.2 Preparation and curing of bridge deck mockups

The primary test specimens of this research are the four bridge deck mockups. In order to offer adaptability of laboratory testing protocol to field testing, the bridge deck mockups were developed to resemble a 10-inch-thick section of a typical cast-in-place reinforced concrete bridge deck. In developing the mockups, consideration was given to steel reinforcement diameter and spacing as set forth by typical bridge deck construction practices, except for the inclusion of the top steel reinforcement mat only.

The steel reinforcement that would typically be found in the lower portion of bridge decks was omitted due to the fact that the reach of the SR meter's current field is limited with respect to depth. It is suspected that the lower reinforcement mat would impose no influence on SR. Figure 3.4 shows the plan view schematic of a typical bridge deck mockup form including the top reinforcement mat and the 12-inch clear space for control measurements and does not display the placed void material.

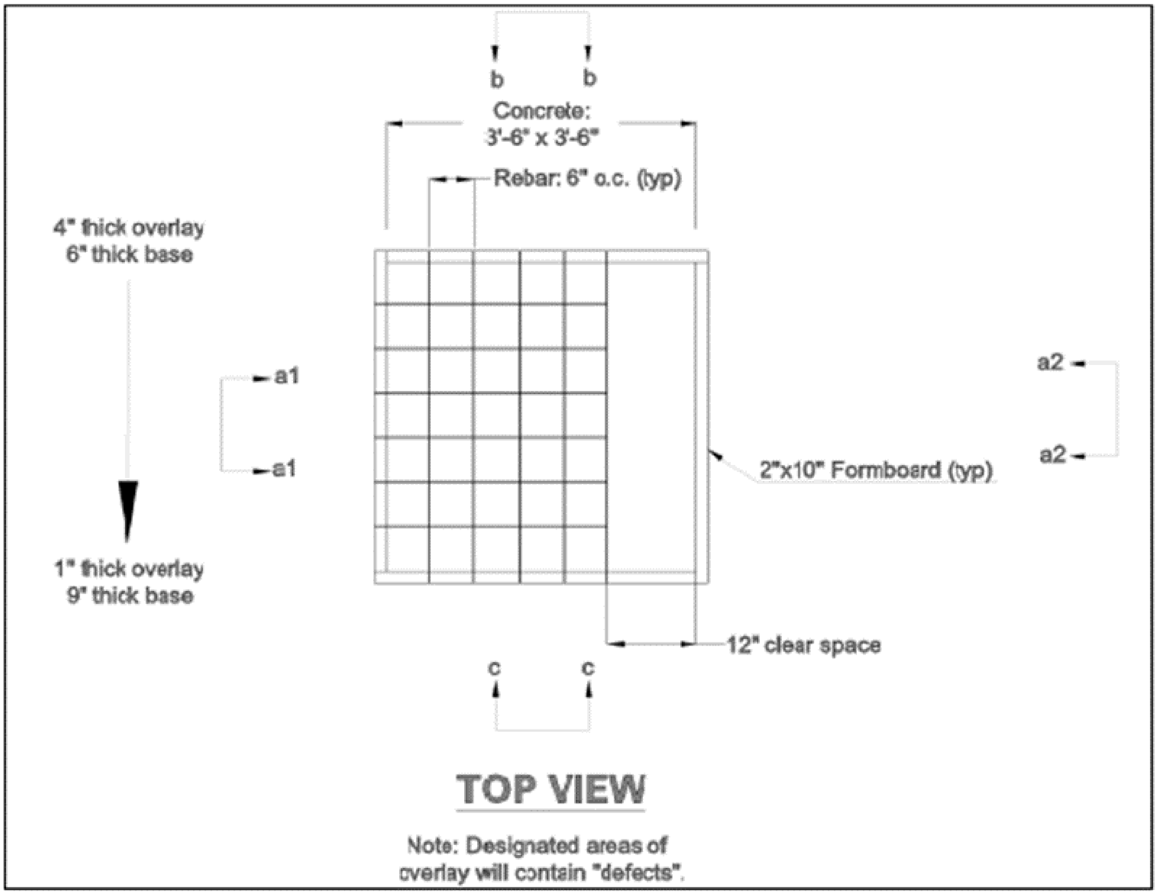

FIGURE 3.4: Plan view of typical bridge deck mockup schematic

Figure 3.5 provided more detail of the steel reinforcement mat showing the division line between the epoxy-coated and non-coated steel reinforcement, as well as dimensioning. At the reinforcement division line, the reinforcement is simply butted end-to-end, without connection. The steel reinforcement mat within each mockup is composed of No. 6 epoxy coated and standard or non-coated transverse and lateral reinforcement strands spaced at 6 inches on center.

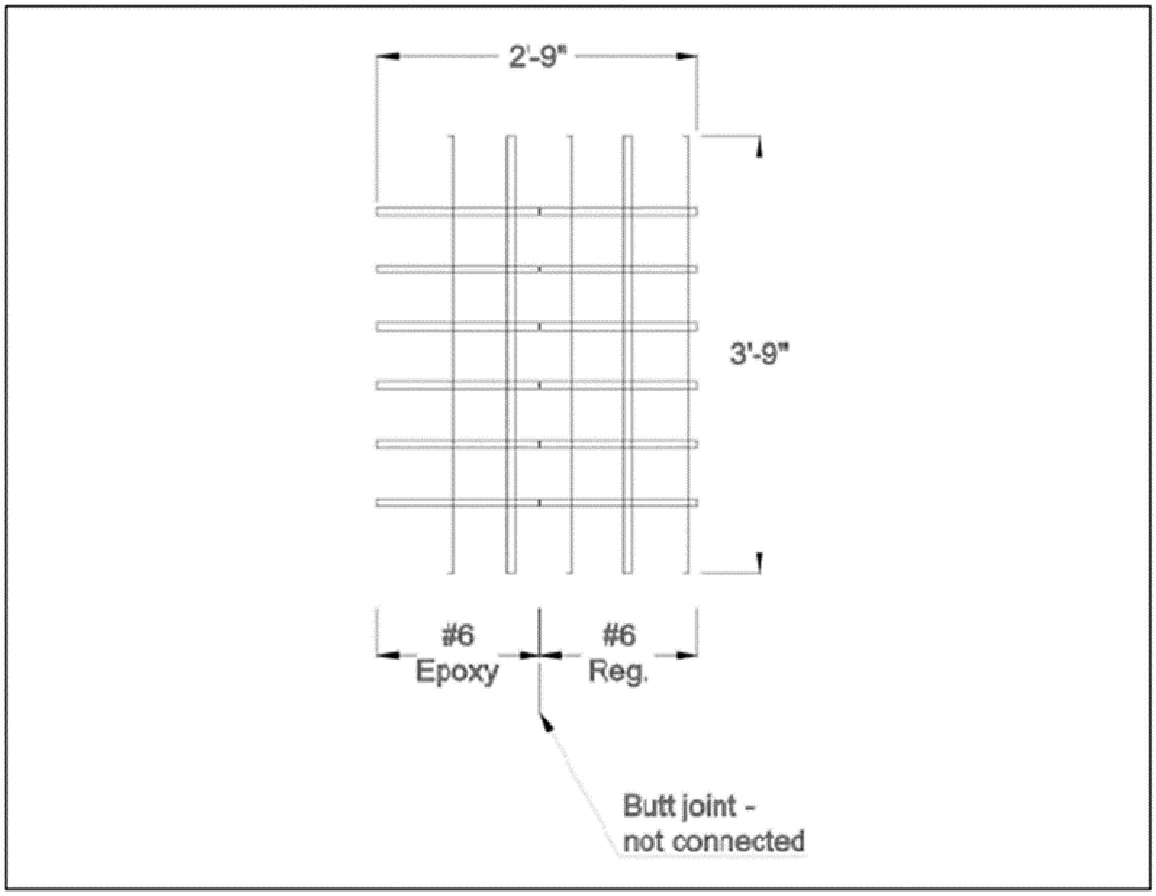

FIGURE 3.5: Typical bridge deck mockup steel reinforcement mat

Each mockup contains a different concrete mixture configuration. The single control mockup was filled entirely with a conventional concrete (CC) bridge deck mixture recommended by NCDOT, and the remaining three mockups contain the CC only as the base layer, then a different overlay concrete mixture was poured on top of each. To create a varying thickness overlay, the base concrete was intentionally poured and finished out of level. Figure 3.6 shows a section view of a typical bridge deck mockup. As depicted in the figure, the base concrete and overlay concrete thickness varies from left-to-right. The full schematics for the bridge deck mockups can be found in Appendix B.

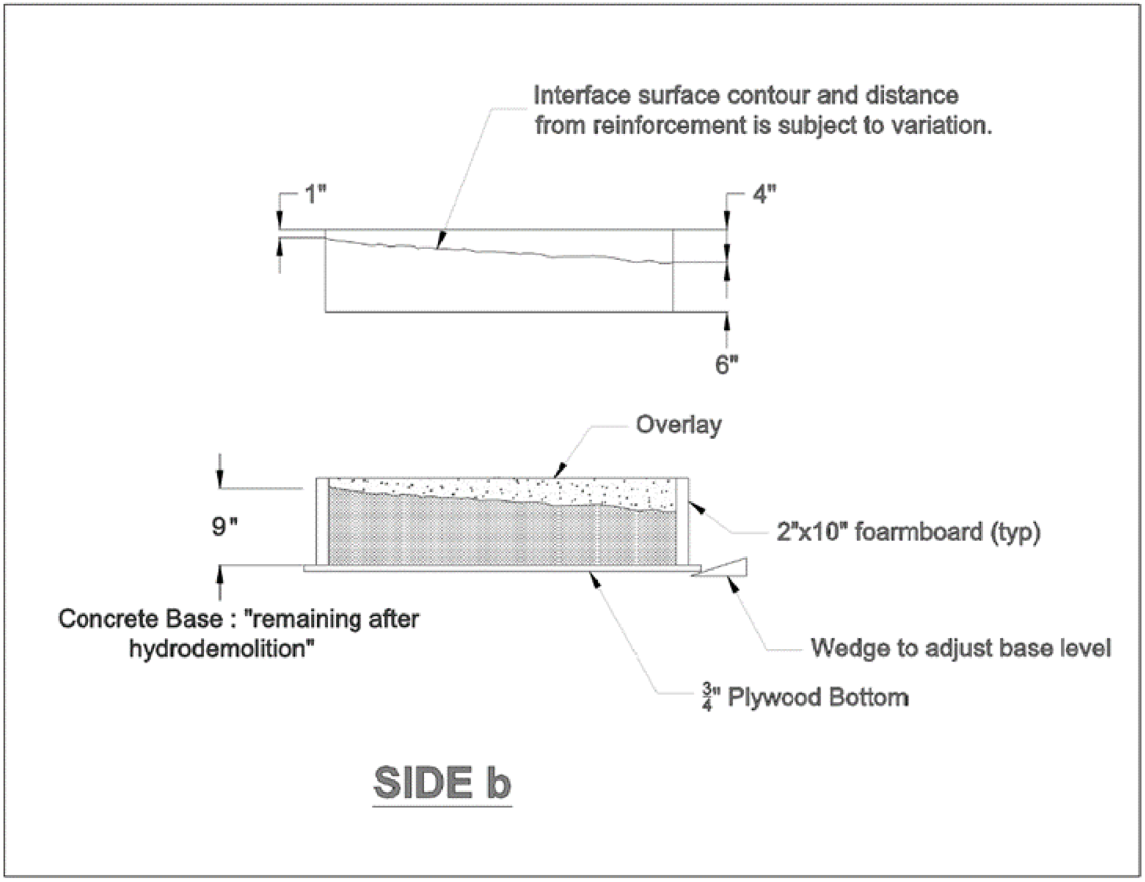

FIGURE 3.6: Typical bridge deck mockup section view

The bridge deck mockup forms were built using 2-inch x 10-inch lumber for the sides and plywood on the bottom. To provide a moisture loss barrier, the mockup forms were lined with 3 mil. polyethylene sheeting. Once the forms were built, the steel reinforcement was placed and supported through predrilled holes on three of the four form walls then tied with standard reinforcement ties. The mockups were built to be carted around the laboratory on a pallet jack. Figure 3.7 shows a typical completed mockup form containing epoxy-coated reinforcement (left), standard reinforcement (middle), and a non-reinforced section (right).

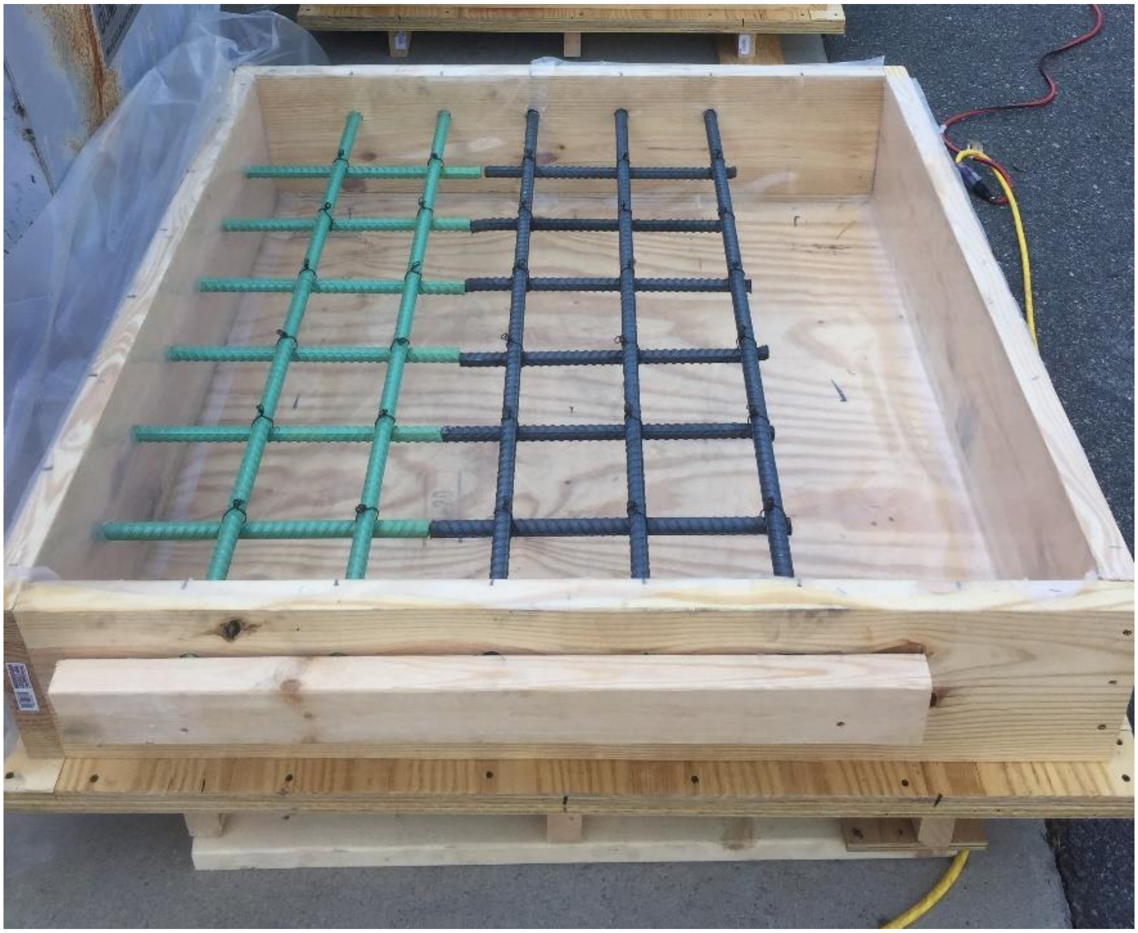

FIGURE 3.7: Typical bridge deck mockup form

The control mockup and overlay bases were all poured together then the overlays were poured on top at a later date, after 7 days of curing of the base concrete. The three overlays mixtures are as follows, Latex-modified concrete (LMC), Very High Early Strength Latex Modified Concrete (VHES-LMC), and Very High Early Strength (VHES) concrete. The conventional concrete was placed by a ready-mixed concrete truck outside of the UNC Charlotte Smith Lab, and the three overlays were batched, mixed, and placed in the laboratory. During placement, an electric handheld concrete vibrator was utilized to assist with consolidation.

After pouring the conventional concrete for the control mockup and the base sections for the three overlay mockups, the mockups were left in place outside and moist cured for 7 days to allow for curing per NCDOT's specifications. Therefore, the 1 day and 3-day SR testing of the control mockup was performed outside of the laboratory. On the 7th day, the moist curing concluded, and the mockups were relocated inside for the duration of the testing program. Figure 3.8 is an image of the control mockup (foreground) and the three overlay mockups after the base concrete has been moist cured for 7 days, and prior to pouring the overlay concrete.

FIGURE 3.8: Control mockup and three overlay mockups pre-overlay

The volume of concrete required to fill each mockup overlay and accompanying 4 in. x 8 in. cylinders for each of the three mixtures (LMC, VHES-LMC, and VHES) exceeded the volume provided by the portable drum mixer. Therefore, each overlay mixture was divided into a pair of equally proportioned mixes, one mixture for the cylinders and one mixture for the overlay. The overlay mixing and placement process extended over three consecutive days. Days one, two, and three of mixing were designated for the LMC, VHES-LMC and VHES concrete mixtures respectively. On each day of overlay placement, the mockup was prepared with glued in place polyether foam material intended to replicate voids that could potentially occur in a full-scale overlay placement. It is expected that this semi-frigid foam will hold its shape, not allowing concrete material, with the exception of water to enter. Throughout the research testing program, it is anticipated that these voids could be detected with the SR meter as revealed by a decrease in magnitude of SR when compared to surrounding, more homogeneous concrete. Figure 3.9 shows an image of the void material used within each mockup overlay.

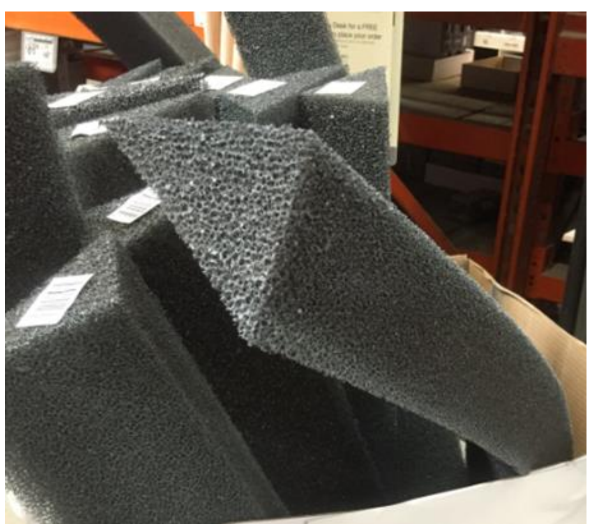

FIGURE 3.9: Polyether foam void material

Figure 3.10 shows the mockups a month after the base concrete has been poured and void material glued in place. Each mockup contains one additional void from the previous. The LMC mockup was prepared with six voids as depicted in Figure 3.10a. An additional void (bottom left-hand corner of Figure 3.10b) was included on the VHES-LMC mockup for a total of seven voids, and the VHES mockup contains two additional voids ([1]bottom left-hand corner and [2] top right-hand corner of Figure 3.10c for a total of eight voids.

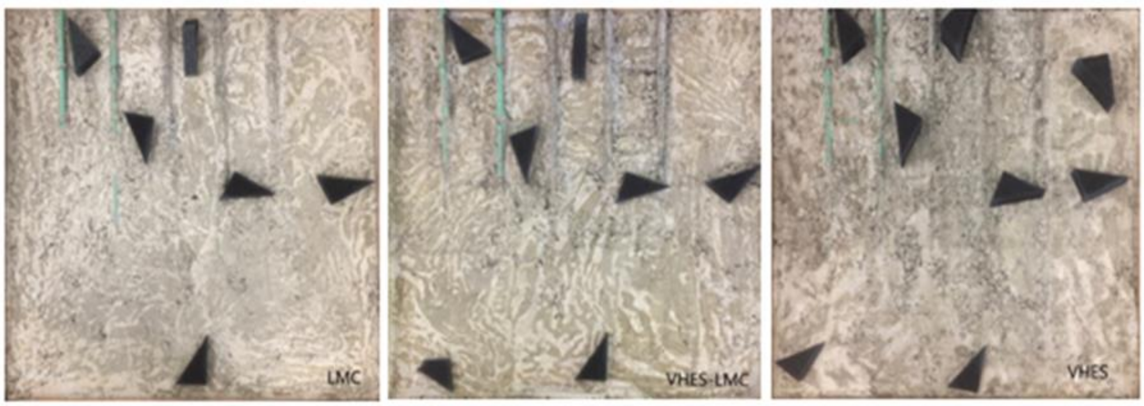

FIGURE 3.10: Mockup void placement - (a) LMC, (b) VHES-LMC, and (c) VHES

The bridge deck mockups containing Type I/II cement (conventional concrete, latex modified concrete) were cured after finishing with wet burlap under polyethylene sheets in an effort to maintain the desired moist conditions for the 7 day curing period (NCDOT 2012). The overlay concrete containing the VHES cement were cured similarly to non-VHES mockups except for the curing duration was reduced from 7 days to a one hour curing period, as recommended by the cement manufacture (CTS).

3.7 Hardened concrete test procedures

This section of the thesis details the tests performed on the hardened concrete specimens. SR of preliminary specimens, mockups and accompanying mockup 4 in. by 8 in. cylinders, compressive strength of 4 in. x 8 in.

3.7.1 SR testing

3.7.1.1 SR testing of 6 in. x 12 in. cylinders

The Resipod SR Meter manufactured by Proceq was used to take SR measurements on the preliminary 6 in. x 12 in. specimens following the AASHTO T 358 Standard Method of Test for SR Indication of Concrete's Ability to Resist Chloride Ion Penetration test method. SR was measured on two replicates of each concrete type and reinforcement configuration at the four circumferential points shown in Figure 3.11. The influences of mixture type, reinforcement type, and depth of cover on SR measurements were evaluated with attention given to the comparison of measurements at quadrant 1 with other quadrants.

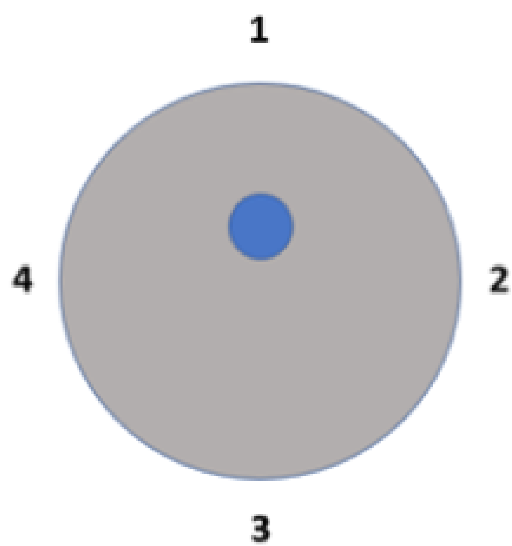

FIGURE 3.11: 6 in. x 12 in. cylinder SR measurement locations

3.7.1.2 SR testing of miniature slabs

At each scheduled testing age, SR measurements were made using the SR meter at 22 locations on the top surface of the miniature slabs. Figure 3.12 shows a typical miniature slab, with the rebar locations shown in black. Testing locations and alignment of the SR meter are highlighted in blue.

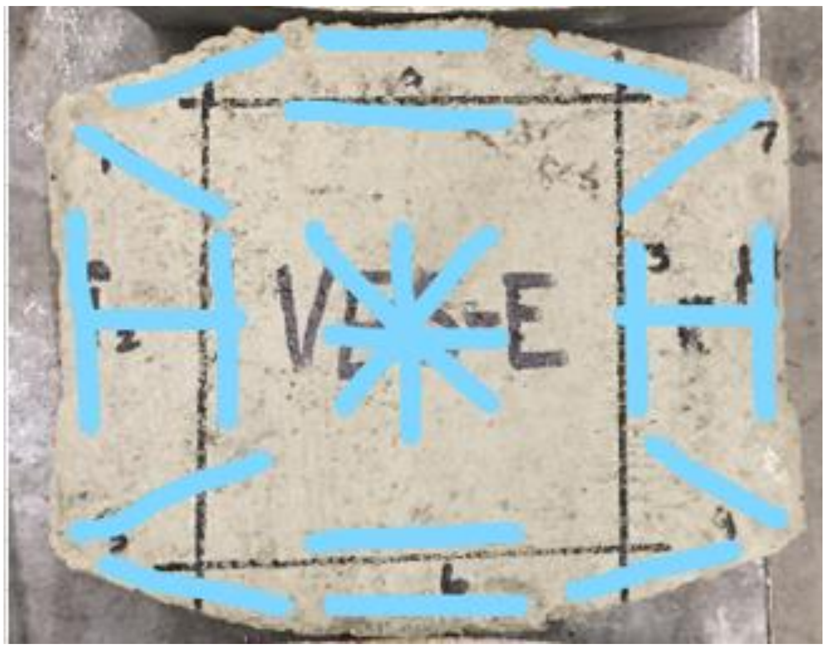

FIGURE 3.12: Typical miniature slab with location and orientation of rebar (shown in black) and test locations (shown in blue)

3.7.1.3 SR testing of bridge deck mockups

The bridge deck mockups were measured for SR at designated points arranged in a 13 x 13 cell grid (169 points) across the top surface. For the SR meter's current to successfully enter and pass through the pore liquid water must be added to the mockups surface. Roughly 1 gallon of water divided into three pours was used to saturate the 3.5 ft. by 3.5 ft. testing area per orientation. The water was poured onto the surface so that it is fully covered without spillover, allowing to absorb and reapplying several times to account for evaporation. The desired saturation is achieved when the SR measurement no longer drifts and subsides at a reasonable magnitude. The points were measured with the SR meter positioned in three different orientations with respect to image of Figure 3.14.

Each point was measured with the particular orientation to fulfill 169 points before beginning the next orientation. The points were measured in a sequence from left-to-right, top-to-bottom starting with the top left point in the following orientations, diagonal, horizontal, then vertical. An extension was temporarily attached to the meter to make the data collection from the standing position easier (Figure 3.13).

FIGURE 3.13: SR meter from standing position

Figure 3.15 shows the testing point grid layout represented by the lines drawn on the mockup where many of the testing points (even cells) are made between the grid sections. The data was collected on an Excel table with color conditioning formatting ranging from green (high) to red (low) to help better visualize areas of different SR magnitudes. The three orientations were averaged at each age per cell and the standard deviation was calculated. The standard deviation aspect of the data analysis was intended to reveal where the different orientations per cell will differentiate between one another.

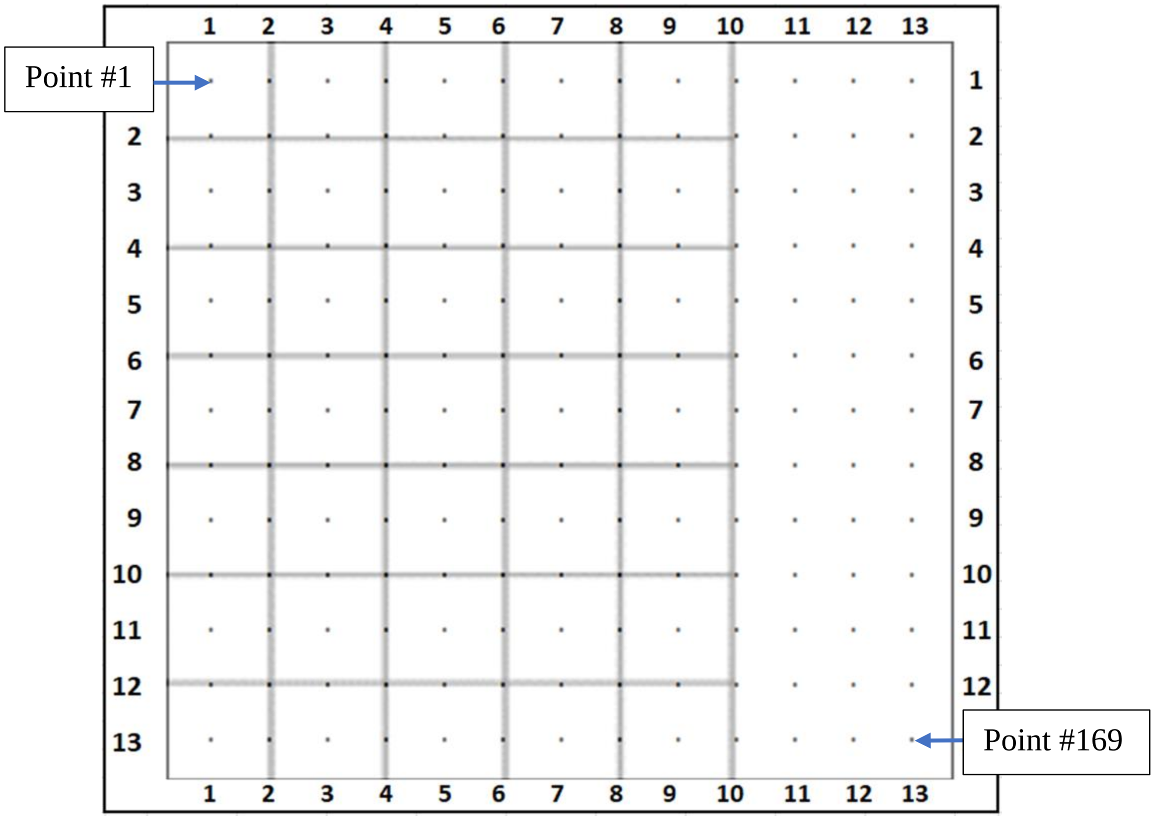

FIGURE 3.14: Testing sequence for SR of mockups

FIGURE 3.15: Mockup showing grid layout marking

3.7.3 Compressive strength test of 4 in. x 8 in. cylinders

The compressive strength tests were performed after the resistivity measurement on the 4 in. x 8 in. cylinders that were cast from the bridge deck mockup concrete. The compressive strength was tested in accordance with ASTM C39, “Standard Test Method for Compressive Strength of Cylindrical Concrete Specimens” (ASTM 2018). Two cylinders of each OPC mixture were tested at the following ages: 1, 7, 28, 56, and 90 days after casting. Two cylinders for each VHES mixture were tested at the following ages: 1, 2, 4 hours and 1, 7, 28, 56, and 90 days.

CHAPTER 4: TEST RESULTS

4.1 SR of 6 in. x 12 in. cylinders

The results of the preliminary investigation of the influence of steel reinforcement on SR measurements is discussed in the following sections.

4.1.1 SR radar analysis of 6 in. x 12 in. cylinders

Figures 4.1a, 4.1b, and 4.1c show the SR measurement at each point (1-4) around the circumference of the cylinders cast from the conventional concrete mixture. As can be observed in Figure 4.1 and at the bottom of Figures 4.1b and 4.1c, the reinforcement is offset towards point 1 on the cylinder. The radar chart represents the end view of the cylinders with the numbers 1-4 correlating the circumferential positions on the diagrams.

If the radar plots in Figure 4.1a, 4.1b, and 4.1c are compared, the influence of the standard rebar on the resistivity measurement can be readily observed, particularly near position 1 (where the reinforcement is closest to the surface). This drop in SR is evident in both the data tables and the radar plots. Readings at position 1 for the conventional rebar (Figure 4.1b) are lower than those at position 1 for the unreinforced cylinder (Figure 4.1a) and for the cylinder with epoxy-coated rebar (Figure 4.1c).

This testing showed that uncoated reinforcement will influence (decrease) SR measurements and that the proximity of the reinforcement to the meter influences the decrease in the resistivity measurement. However, the radar chart showing resistivity tests of the unreinforced cylinders (Figure 4.1a) and of cylinders with epoxy-coated reinforcement (Figure 4.1c) appear to be similar. It therefore appears that the SR measurement is not influenced by the epoxy-coated reinforcement. This is likely due to an insulating effect of the epoxy coating.

Conventional Concrete (NO Latex)																								
	1-CC				2-CC				1-CC-Standard				2-CC-Standard				1-CC-Epoxy				2-CC-Epoxy			
	1	2	3	4	1	2	3	4	1	2	3	4	1	2	3	4	1	2	3	4	1	2	3	4
1d	3.2	3.3	3.2	3.3	3.2	3.3	3.3	3.6	2.5	3.0	2.9	3.2	2.4	3.5	3.0	2.9	3.6	3.7	3.4	3.1	3.5	3.7	3.3	3.7
3d	4.9	5.3	5.5	4.7	5.0	4.5	5.3	5.0	3.6	5.1	5.1	4.5	3.7	4.8	4.3	5.2	4.8	5.3	4.6	4.8	5.2	4.9	4.6	5.6
7d	6.1	6.4	6.6	5.9	6.3	6.0	6.2	6.2	4.4	5.6	5.5	5.6	4.5	5.5	5.3	5.5	6.3	6.3	5.9	5.8	6.4	6.4	6.5	6.2
14d	7.1	7.2	7.6	7.0	7.4	7.0	7.2	7.2	5.2	7.1	6.5	6.6	4.8	6.2	6.2	6.8	7.1	7.3	6.8	6.7	7.5	7.3	7.2	7.4
28d	8.5	8.7	9.1	8.6	9.1	8.5	9.0	8.9	6.2	8.0	8.0	8.1	5.8	7.5	7.8	8.0	8.5	8.5	8.4	8.1	8.9	8.1	8.0	8.6
56d	9.3	9.2	9.7	9.2	9.4	9.1	9.6	9.2	6.6	8.5	8.4	8.6	6.3	8.4	8.3	9.2	9.8	9.2	9.7	9.6	9.6	10.0	9.3	8.9
90d	11.7	11.4	11.8	11.5	11.4	11.3	11.4	11.4	7.9	10.5	10.2	10.6	7.7	9.9	9.9	10.2	11.4	11.9	11.5	10.9	11.6	11.3	11.6	11.4

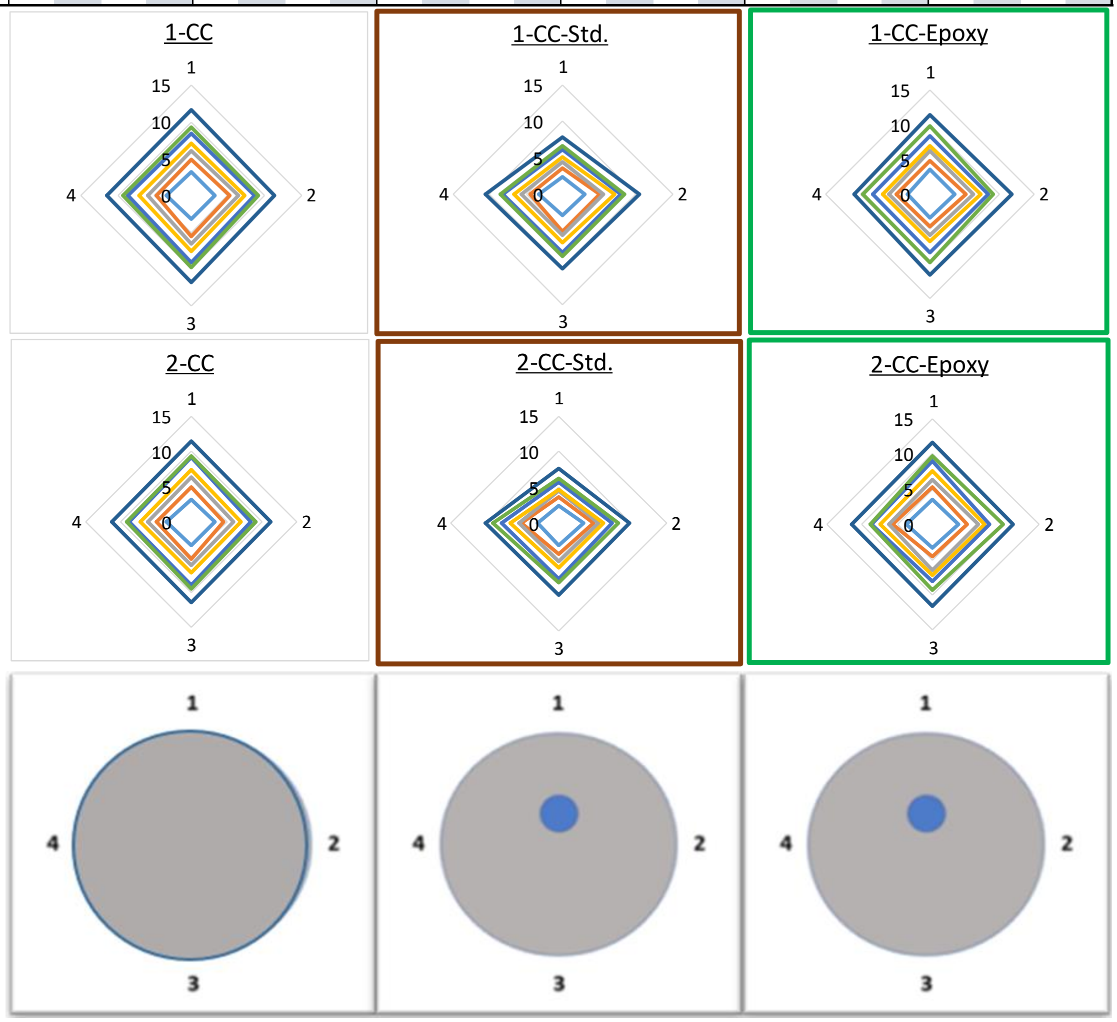

Figure 4.1a: Data, radar plot, and schematic of conventional concrete with no rebar

Figure 4.1b: Data, radar plot, and schematic of conventional concrete with standard rebar

Figure 4.1c: Data, radar plot, and schematic of conventional concrete with epoxy-coated rebar

FIGURE 4.1: SR radar analysis for preliminary CC cylinders

A similar trend can be observed in measurements for the LMC, shown in Figures 4.2a through 4.2c. The influence of the uncoated reinforcement on SR readings is clearly evident in the radar plot for Figure 4.2b, particularly at location 1 where the bar is closest to the surface of the cylinder. The epoxy coated rebar (Figure 4.2c) does not appear to influence the SR readings, which are very similar to those obtained for the unreinforced cylinder (Figure 4.2a). Note the overall increase in SR measurements for all LMC mixtures, which indicates a lower permeability and higher durability performance of this mixture compared to the conventional concrete mixture.

Latex Modified Concrete (LMC)																								
	1-LMC				2-LMC				1-LMC-Standard				2-LMC-Standard				1-LMC-Epoxy				2-LMC-Epoxy			
	1	2	3	4	1	2	3	4	1	2	3	4	1	2	3	4	1	2	3	4	1	2	3	4
1d	3.4	3.6	3.8	3.7	3.5	3.4	3.4	3.6	2.4	3.1	3.0	3.1	2.3	2.9	3.0	3.1	3.7	3.6	3.4	3.5	3.7	3.5	3.5	3.7
3d	7.1	7.2	7.7	7.5	7.6	7.7	7.0	7.1	4.8	6.6	6.3	6.4	5.1	6.5	6.1	6.3	7.9	7.3	7.4	7.3	7.6	7.4	7.2	7.4
7d	9.4	9.9	9.7	9.7	9.6	9.7	9.3	9.5	6.2	8.3	9.1	8.5	6.9	8.3	8.3	8.1	10.0	9.3	9.5	9.3	9.9	9.3	9.3	9.4
14d	11.1	11.2	11.2	11.1	11.3	11.4	10.9	11.1	7.7	9.8	10.1	9.8	8.0	9.9	9.8	9.7	11.5	11.2	11.4	11.0	11.4	11.3	11.0	11.1
28d	13.2	13.5	13.4	13.4	13.8	13.6	13.2	13.5	9.1	11.5	11.7	12.1	9.0	11.5	11.4	11.4	14.1	13.1	13.3	13.1	13.6	13.6	12.7	13.1
56d	14.2	15.0	14.9	14.7	15.1	15.1	13.9	14.3	9.4	12.8	14.1	13.0	9.6	12.7	12.4	12.7	14.9	14.3	14.6	14.5	14.8	14.5	13.8	14.4
90d	17.5	17.7	17.8	17.3	17.5	18.0	17.0	18.0	11.5	15.6	15.9	15.3	12.2	15.5	15.4	15.3	18.5	17.6	17.4	17.2	17.7	17.4	17.2	17.4

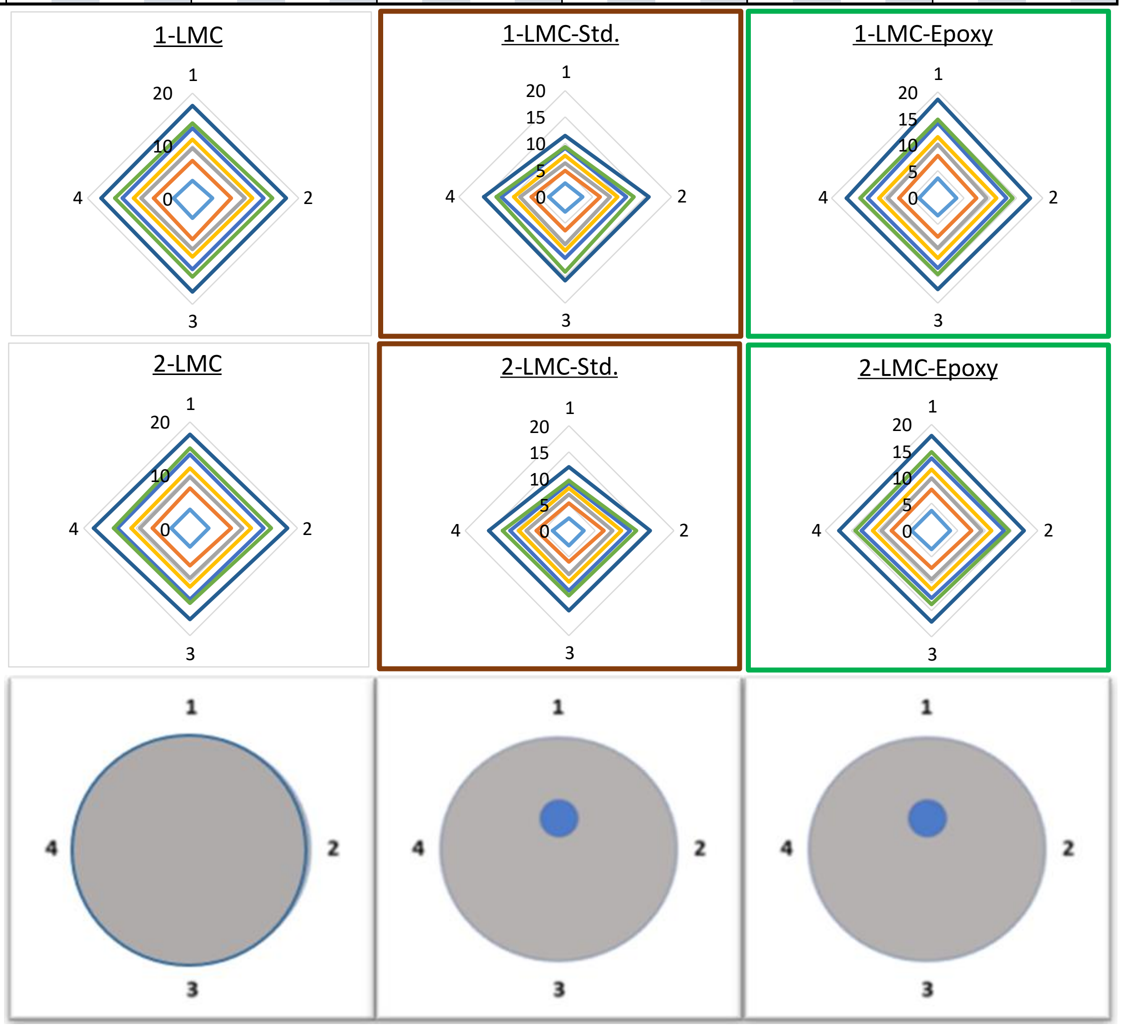

Figure 4.2a: Data, radar plot, and schematic of latex-modified concrete with no rebar

Figure 4.2b: Data, radar plot, and schematic of latex-modified concrete with standard rebar

Figure 4.2c: Data, radar plot, and schematic of latex-modified concrete with epoxy-coated rebar

FIGURE 4.2: SR radar analysis for preliminary LMC cylinders

Test results for cylinders cast with the VHES mixture are shown in Figures 4.3a through 4.3c. The influence of the uncoated reinforcement on the SR of the VHES concrete cylinders (Figure 4.3b) is again evident when compared to the unreinforced cylinder and the cylinder containing the epoxy coated reinforcement (Figure 4.3c). Of note, the SR values of the VHES concrete are much higher than those of the conventional concrete and LMC. The resistivity values at 7 days were lower than the measurements at 3 days. It is suspected that this reduction in resistivity is the result of the VHES cylinders increasing in humidity/moisture content due to being stored in the moist curing room.

Very High Early Strength Concrete (No Latex)																								
	1-VHES				2-VHES				1-VHES-Standard				2-VHES-Standard				1-VHES-Epoxy				2-VHES-Epoxy			
	1	2	3	4	1	2	3	4	1	2	3	4	1	2	3	4	1	2	3	4	1	2	3	4
1h	2.7	3.1	3.1	3.1	3.1	3.5	3.3	3.1	2.4	3.0	3.3	3.1	2.7	3.4	3.3	3.3	3.3	3.5	3.2	3.1	2.9	2.8	3.0	3.2
2h	4.8	5.3	5.4	5.4	5.1	6.0	5.1	5.4	3.5	4.2	4.6	4.2	3.7	4.3	4.7	4.9	5.1	5.6	5.1	5.2	5.0	4.5	4.9	5.0
4h	7.9	9.1	9.1	9.6	9.0	10.9	10.1	8.8	6.0	7.3	7.5	7.0	5.6	7.3	7.6	7.7	9.0	9.1	7.9	8.1	9.0	8.3	7.9	8.8
1d	35.1	41.1	38.2	38.5	37.0	42.1	38.0	36.8	24.2	30.6	31.7	30.1	23.2	29.6	32.9	30.7	39.9	38.6	34.7	36.3	43.7	38.8	36.8	39.1
3d	38.8	41.3	42.1	42.8	43.2	48.4	42.4	41.9	27.4	32.7	33.6	33.6	24.5	31.7	36.5	33.4	46.5	42.0	43.7	44.3	43.6	41.6	38.5	39.5
7d	38.9	40.2	41.1	41.1	41.8	44.9	41.7	43.2	25.9	33.0	32.5	31.9	22.6	31.7	35.9	34.1	40.1	40.6	39.4	38.0	43.1	40.1	37.8	41.5
14d	30.7	32.1	32.1	32.2	31.7	32.9	31.4	33.8	20.4	28.3	29.3	25.1	20.6	26.8	29.0	27.9	31.9	32.6	30.3	30.4	31.4	28.3	29.2	30.9
28d	19.8	21.2	20.4	20.4	19.5	21.3	20.2	21.9	11.4	16.2	17.6	16.3	13.6	16.5	18.2	17.8	19.4	19.7	18.6	19.0	18.8	17.9	18.0	19.0
56d	14.3	15.3	14.7	15.5	14.8	16.0	15.3	14.9	8.7	12.4	13.0	12.5	10.0	12.3	13.2	13.0	15.0	14.9	13.8	15.0	14.8	14.1	14.5	14.8
90d	13.8	15.2	14.8	15.5	15.0	16.5	15.8	14.9	8.6	12.3	13.0	12.1	9.7	12.0	13.3	13.1	14.9	14.4	13.9	14.4	14.6	14.1	14.2	14.5

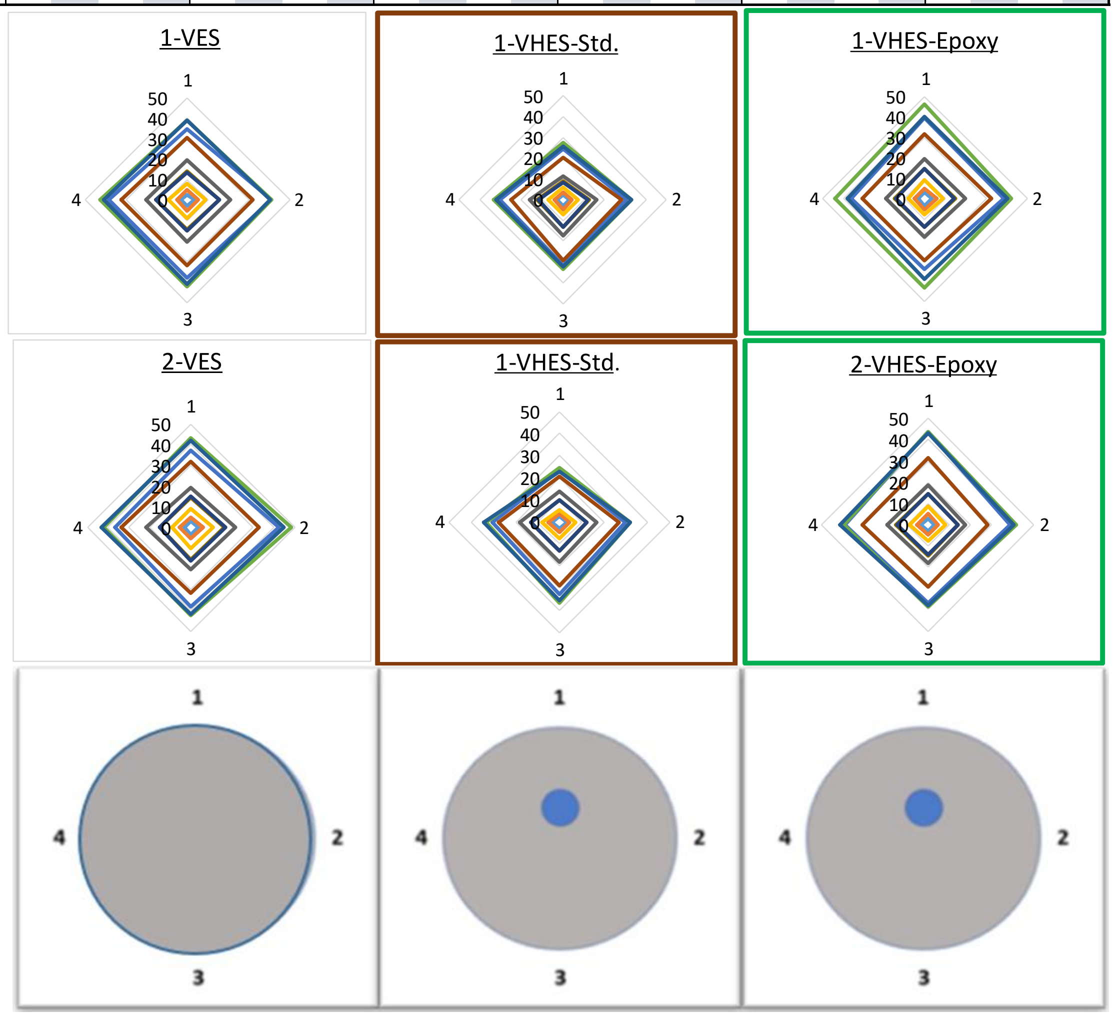

Figure 4.3a: Data, radar plot, and schematic of VHES concrete with no rebar

Figure 4.3b: Data, radar plot, and schematic of VHES concrete with standard rebar

Figure 4.3c: Data, radar plot, and schematic of VHES concrete with epoxy-coated rebar

FIGURE 4.3: SR radar analysis for preliminary VHES cylinders

Test results for cylinders cast with the VHES-LMC are shown in Figures 4.4a through 4.4c. The influence of the uncoated reinforcement on the SR of the VHES LMC cylinders (Figure 4.4b) is again evident when compared to the unreinforced cylinder and the cylinder containing the epoxy coated reinforcement (Figure 4.4c). Of note, the SR values of the VHES-LMC concrete are substantially higher than those of the conventional concrete, the LMC, and the VHES concrete. Similar to the trends observed in the VHES mixture, the resistivity values appeared to peak at 3 days, and then lower readings were measured at 7 days and 14 days.

Very High Early Strength Latex Modified Concrete																								
	1-VHES-LMC				2-VHES-LMC				1-VHES-LMC-Std.				2-VHES-LMC-Std.				1-VHES-LMC-Epoxy				2-VHES-LMC-Epoxy			
	1	2	3	4	1	2	3	4	1	2	3	4	1	2	3	4	1	2	3	4	1	2	3	4
1h	3.9	3.9	3.7	4.0	4.1	4.1	4.2	4.3	3.6	3.9	4.3	4.1	3.5	4.1	4.5	4.5	4.4	4.0	4.5	4.5	4.2	4.2	4.3	4.4
2h	9.8	9.8	9.7	9.7	10.6	10.1	9.8	9.9	7.5	9.2	9.5	9.4	7.7	9.1	9.8	9.6	11.2	10.7	11.2	11.3	10.5	10.7	10.2	11.4
4h	26.2	26.0	25.9	25.1	26.2	26.4	26.2	26.9	21.5	24.5	25.9	24.7	20.5	25.8	24.8	26.2	31.8	26.2	28.4	28.2	29.5	28.8	28.9	28.9
1d	65.5	69.3	67.9	69.1	69.1	67.9	64.2	67.2	54.5	61.6	68.3	63.4	51.9	60.6	65.7	60.3	71.9	69.1	71.5	71.0	79.7	68.1	68.1	68.1
3d	86.6	84.1	87.5	88.5	86.0	87.6	83.7	88.3	72.2	77.9	87.6	73.9	65.5	74.6	87.0	74.3	108	87.3	91.3	86.4	94.6	92.9	85.7	85.2
7d	88.9	85.4	84.0	85.2	84.3	85.5	81.5	84.7	72.3	78.6	82.4	73.6	63.1	75.1	81.8	70.2	102	88.8	89.1	85.5	89.9	93.1	84.0	81.6
14d	76.7	72.6	71.7	71.8	72.2	74.3	68.9	72.9	56.3	60.2	70.7	62.2	52.1	58.8	70.8	57.4	84.6	70.6	74.3	70.9	72.5	75.8	71.2	74.1
28d	49.8	47.7	46.3	47.8	49.2	48.7	46.7	49.2	33.1	36.1	43.5	36.2	30.2	39.2	43.9	37.0	49.1	46.7	46.2	46.0	46.4	47.8	42.8	45.2
56d	33.8	33.0	32.0	32.1	33.2	33.3	33.3	34.1	22.4	28.5	30.1	26.2	21.3	27.5	30.1	26.9	35.5	32.4	34.5	32.5	32.7	31.7	31.9	32.7
90d	33.3	33.6	32.4	33.4	33.2	32.5	33.4	33.6	23.9	27.9	30.8	28.6	21.8	27.9	30.7	27.6	36.5	32.8	34.4	33.0	34.3	34.2	31.8	33.7

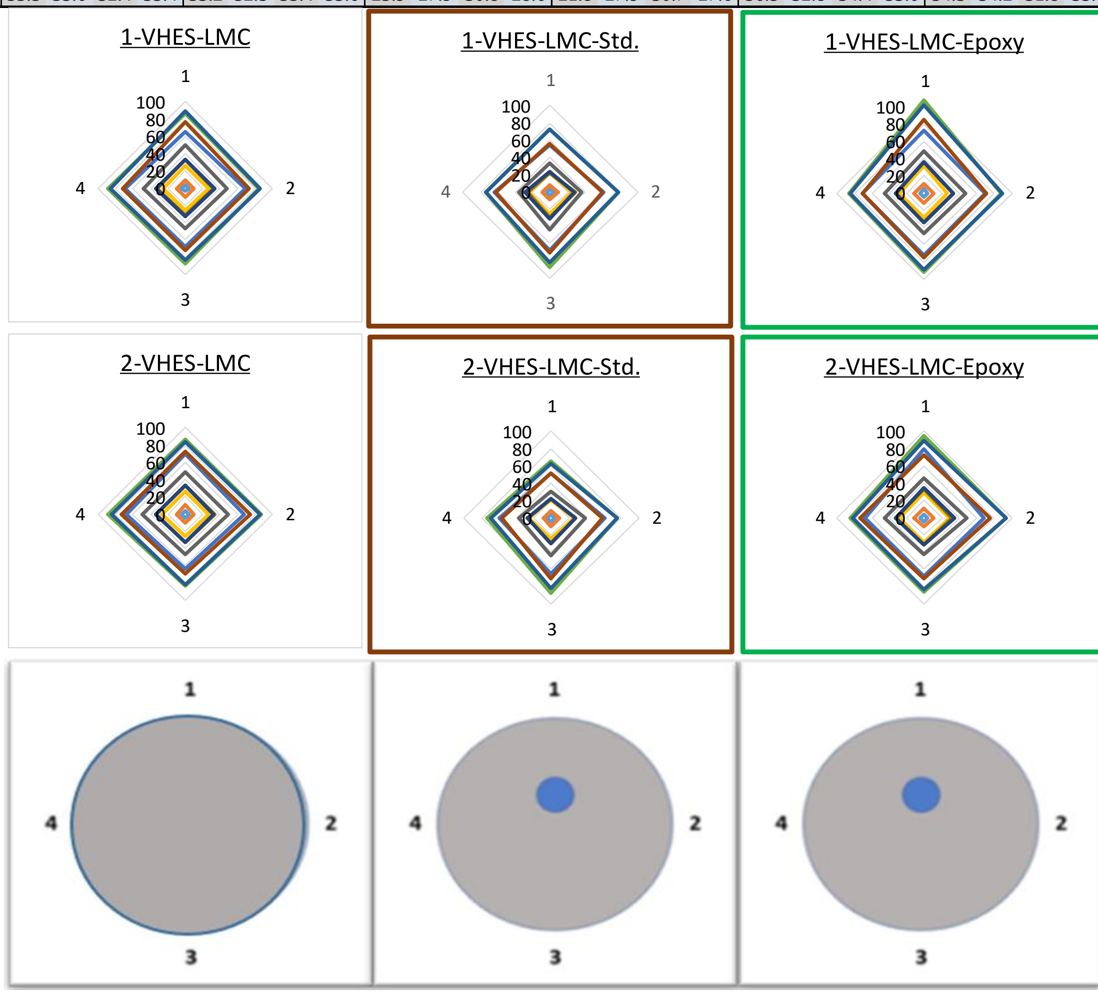

Figure 4.4a: Data, radar plot, and schematic of VHES latex-modified concrete with no rebar

Figure 4.4b: Data, radar plot, and schematic of VHES latex-modified concrete with standard rebar

Figure 4.4c: Data, radar plot, and schematic of VHES latex-modified concrete with epoxy-coated rebar

FIGURE 4.4: SR radar analysis for preliminary VHES-LMC cylinders

4.1.2 SR versus cover analysis of 6 in. x 12 in. cylinders

From the previous analysis, it was found that the uncoated steel reinforcement greatly influences SR. Further analysis was conducted to better understand to what degree the concrete cover changed the SR when measured on top of and parallel to the bar. To facilitate this, the SR measurements from quadrant 1 were compared to those taken from quadrant 3 on each of the preliminary cylinders reinforced with uncoated steel reinforcement. The cover depth for these cylinders averaged 1.5 in. at quadrant 1, 3.75 in. at quadrant 3, and roughly 2.9 in. at quadrants 2 and 4 as depicted in Figure 4.5.

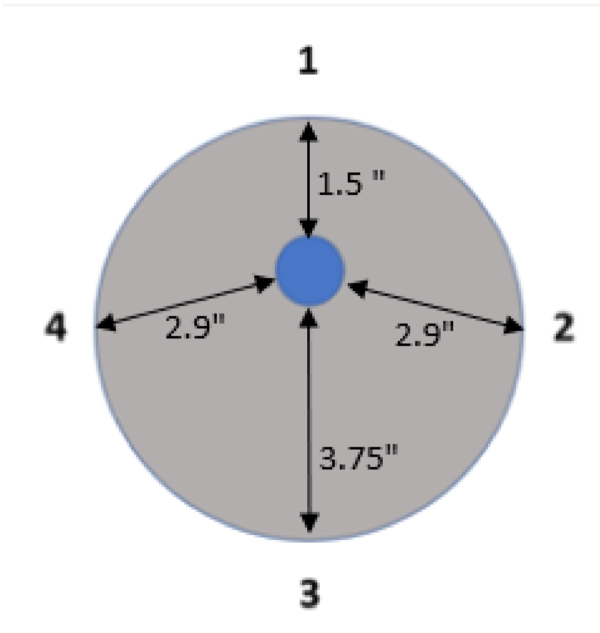

FIGURE 4.5: Cover depth of preliminary cylinders

In Figures 4.6 – 4.9, the SR measurements are plotted for 1.5 in. (quadrant 1) and 3.75 in. (quadrant 3) of cover at each age, and a trendline connects the pair of measurements. Each figure named above is of one concrete mixture and the bold black trendline with arrow endpoints as well as the equation of the line shows the average of those trendlines. These trendlines are expected to demonstrate how the SR reading is influenced by variable of cover depth on uncoated reinforcing steel. Of note, the dotted lines in Figures 4.6 – 4.9 are of the later ages (14 days and older) and the solid lines are of early ages (7 days and earlier). The magnitude of SR in the CC and LMC mixtures (Figure 4.6 and 4.7) increases with age, while the VHES and VHES-LMC mixtures (Figures 4.8 and 4.9) are more variable and skip around. Additionally, the 56 and 90 day trendlines are virtually identical in the VHES and VHES-LMC mixtures.

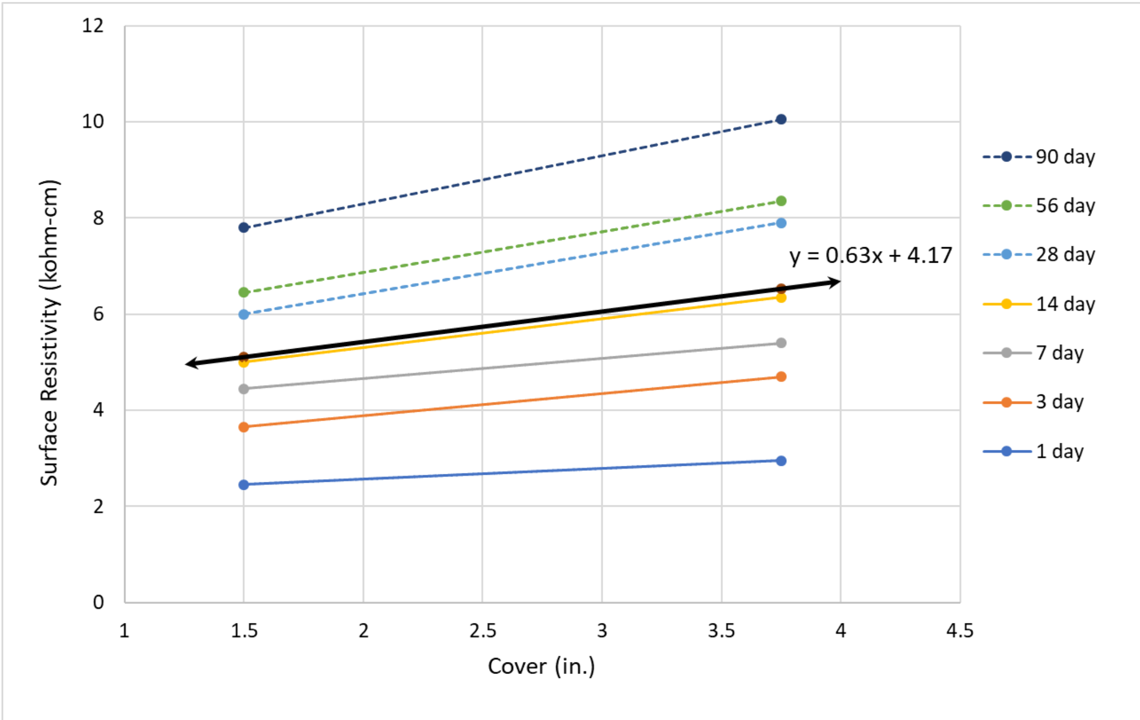

FIGURE 4.6: SR versus concrete cover at selected concrete ages – CC mixture

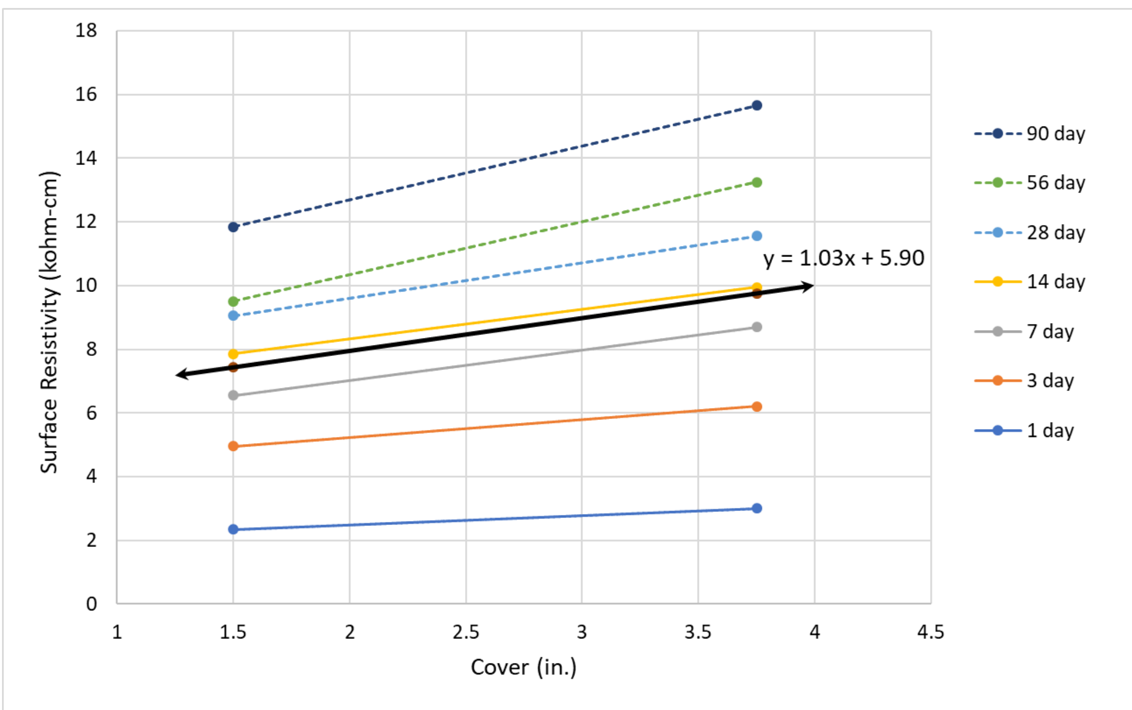

FIGURE 4.7: SR versus concrete cover at selected concrete ages – LMC mixture

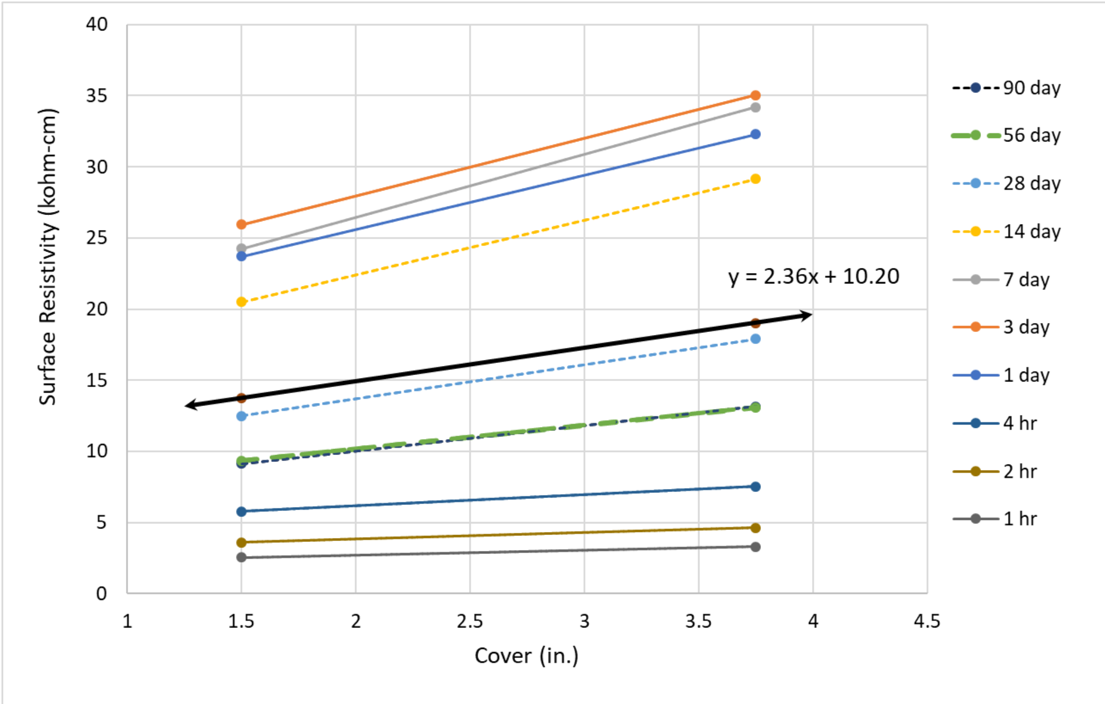

FIGURE 4.8: SR versus concrete cover at selected concrete ages – VHES Mixture

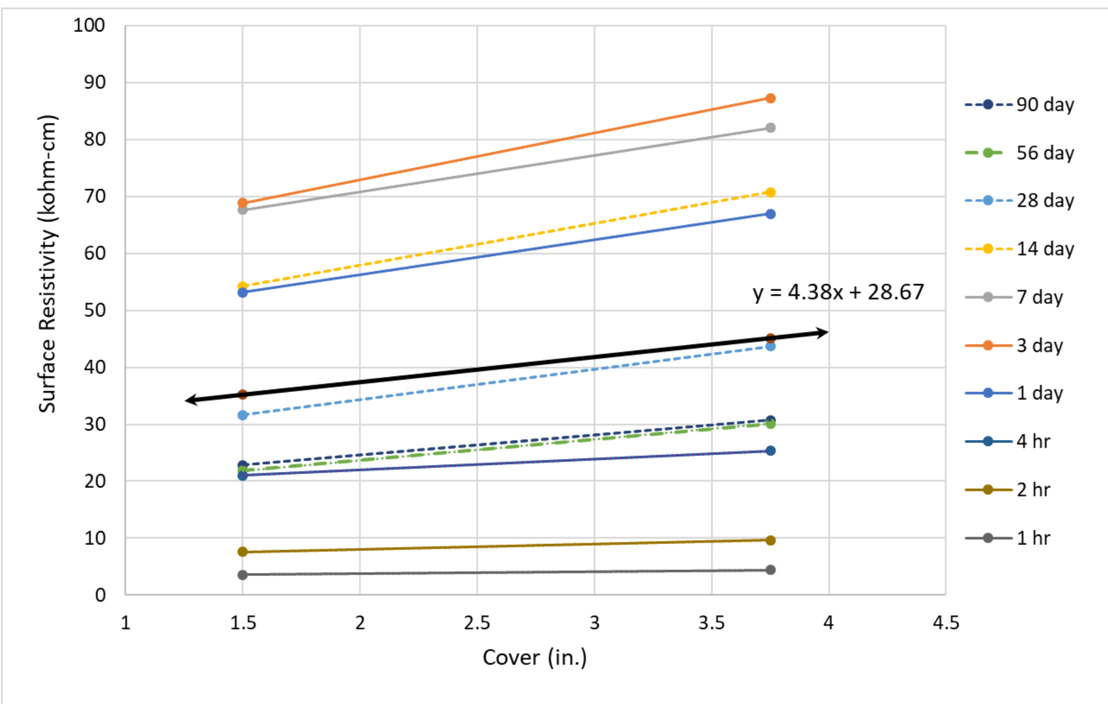

FIGURE 4.9: SR versus concrete cover pre age – VHES-LMC mixture

Table 4.1 provides all of the trendline equations for Figures 4.6 – 4.9, where the x-variable represents the concrete cover distance (in.) and the y variable represents SR (kohm-cm). These trendline equations can be used to estimate the degree of influence of cover on SR measurements. For example, in regard to the CC mixture at 1 day ($y = 0.22x + 2.1$), the cover depth (x variable) can be estimated by entering the measured SR value (measured on top of and parallel) into the y variable of the equation. So, if SR is measured to be 2.5 kohm-cm at 1 day, the cover depth may be near 1.8 in., or if the SR was measured to be 2.8 kohm-cm, the cover depth may be near 3.2 in. Or in regard to the VHES-LMC mixture at 56 day ($y = 3.7x + 16$), if the SR is measured to be 21 and 24 kohm-cm, the cover depths can be estimated to be 1.4 and 2.2 in. respectively. As the SR value increases when compared to another measurement when measured directly on top of and parallel to the same steel reinforcement bar of the same condition, it is hypothesized that the cover depth is increasing at the rate provided in Table 4.1. The estimated change in SR per each 0.5 in. increment of cover depth is arranged by mixture and age in Table 4.2.

These findings are specific to the concrete mixtures (materials and proportions) used for this study. However, a similar simple set of experiments could be performed with other materials and mixture proportions to identify trendlines and changes in SR for different cover depths. Similar to other resistivity tests, this approach assumes the concrete is homogeneous with regard to material, moisture, and temperature. Also, it is helpful to knowing the average SR of an unreinforced cylinder of the concrete being evaluated (per the standard AASHTO T358 test protocol) to indicate that the measured SR is within reason, and not an outlier. Furthermore, this research was conducted on cover depths between 1.5 in. and 3.75 in., so cover depths beyond this range may not be supported by this work.

TABLE 4.1: Equation of the line for each age and mixture (X = cover, Y =SR)

age	CC Figure 4.6	LMC Figure 4.7	VHES Figure 4.8	VHES-LMC Figure 4.9
1 hour			y = 0.33x + 2.1	y= 0.33x + 3.0
2 hour			y = 0.46x + 2.9	y = 0.91x + 6.2
4 hour			y = 0.78x + 4.6	y = 1.9x + 18
1 day	y = 0.22x + 2.1	y = 0.29x + 1.9	y = 3.8x + 18	y = 6.1x + 44
3 day	y = 0.47x + 3.0	y = 0.56x + 4.1	y = 4.01x + 20	y = 8.2x + 56
7 day	y = 0.42x + 3.8	y = 0.96x + 5.1	y =4.4x + 18	y = 6.4x + 58
14 day	y = 0.60x + 4.1	y = 0.93x + 6.5	y = 3.8x + 15	y = 7.4x + 43
28 day	y = 0.84x + 4.7	y = 1.1x + 7.4	y = 2.4x + 8.9	y = 5.4x + 24
56 day	y = 0.84x + 5.2	y = 1.7x + 7.0	y = 1.67x + 6.9	y = 3.7x + 16
90 day	y = 1.0x + 6.3	y = 1.7x + 9.3	y = 1.8x + 6.5	y = 3.5x + 18

TABLE 4.2: Change in SR (kohm-cm) per change in cover depth (increments of 0.5 in.)

age	CC	LMC	VHES	VHES-LMC
1 hour			0.2	0.2
2 hour			0.2	0.5
4 hour			0.4	1.0
1 day	0.1	0.1	0.2	3.1
3 day	0.2	0.3	2.0	4.1
7 day	0.2	0.5	2.2	3.2
14 day	0.3	0.5	1.9	3.7
28 day	0.4	0.6	1.2	2.7
56 day	0.4	0.9	0.8	1.9
90 day	0.5	0.9	0.9	1.8

Figure 4.10 compares the bold black lines from the above figures (CC, LMC, VHES, and VHES-LMC) and similar to Figures 4.6 – 4.9 , the bold black trendline with arrow endpoints and equation of the line is the average of each mixture. As a confirmation of the accuracy of the trendlines, the 2.9 in. cover depth (Figure 4.5) was introduced by

averaging the SR measurements of all ages of quadrant 2 and 4. The average SR measurement of the 2.9 in. (quadrant 2 and 4) cover is plotted on Figure 4.10 for each concrete mixture. Of note, the 2.9 in. cover plots very closely to each respective trendline, with the closest one being the average (bold black trendline). This infers that due to the circular distribution of the SR meter's field (Figure 2.2) objects are detectable to the same degree whether they are centrically or eccentrically located below the measuring point.

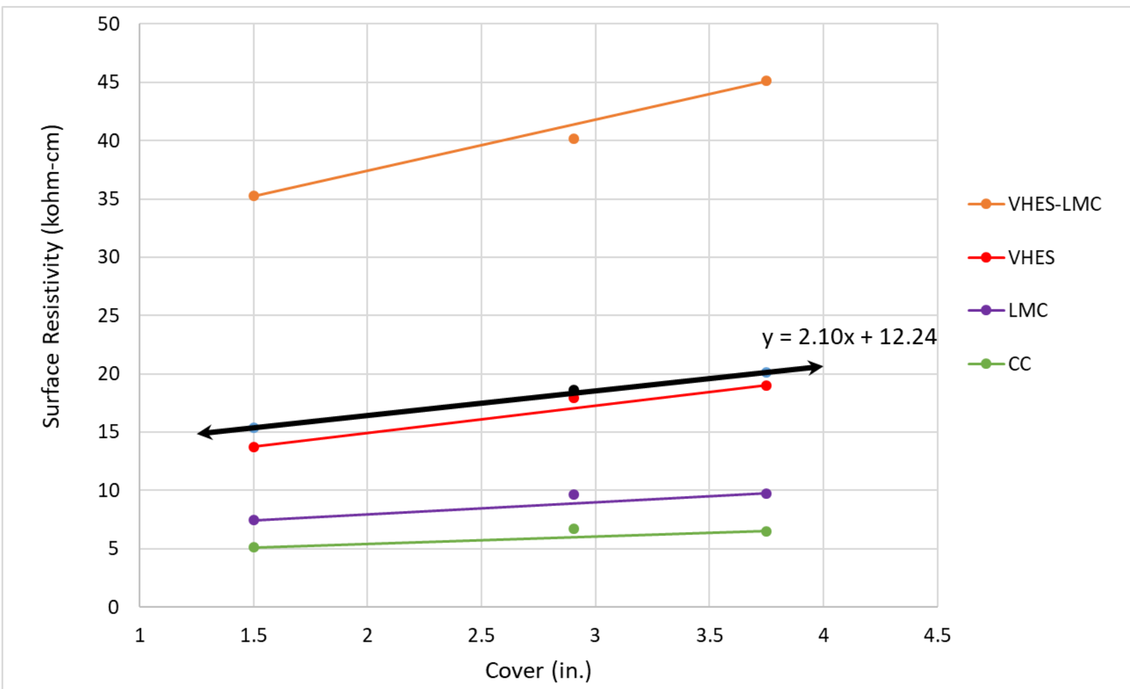

FIGURE 4.10: SR versus concrete cover for each mixture age average

In Figures 4.6, the slopes tend to increase gradually by age with an even transition. The trendline slopes in Figure 4.7 also gradually increases yet there is a slight drop in SR at the 1.5 in. cover measurement between 28 and 56 days. The trendlines of the VHES-LMC and VHES mixtures (Figure 4.8 and 4.9) as well as their evolution over time do not have the same predictable increase. For example, at the early ages (1-4 hour) the slopes are similar, then towards the middle ages (1-28 days) the slopes are slightly increasing and translated in the positive y-direction, then at the later ages (56 and 90 day), the trendlines are more similar to the earlier ages (1-4 hour). Also, in Figure 4.10, the gradual increase in slope of trendline exists between the different concrete mixtures, exactly corelating to the SR of the concretes. For example, the VHES-LMC concrete has an overall higher than LMC. The y-intercept value in each trendline equation is somewhat proportional the relative SR magnitude per mixture. The average trendline slope of each mixture increases in the following order (Figure 4.10):

1. CC: y = 0.63x + 4.17
2. LMC: y = 1.03x + 5.90
3. VHES: y = 2.36x + 10.20
4. VHES-LMC: y = 4.38x + 28.56

Figure 4.11 is a SR versus time graph for the 6” x 12” preliminary cylinders (dashed lines) that illustrates the peak in SR of the VHES-LMC and VHES concrete mixtures. The two solid trendlines in Figure 4.11 are the average of similar mixtures (CC averaged with LMC and VHES averaged with VHES-LMC). It is suspected that this peak in SR at 3 day is the result of the rapid hydration taking place within the VHES and VHES-LMC cylinders which increases the water requirements during early curing, resulting in a dehydrated medium when compared to non-VHES concrete mixtures. As discussed in the literature, heat and low moisture content both inversely corelated to SR. In a sense, the VHES containing concretes may be in a state of low moisture content (dehydrated) during this time, and due to being stored in the moist curing room, over time the moisture content stabilizes, resulting in the leveling off of SR.

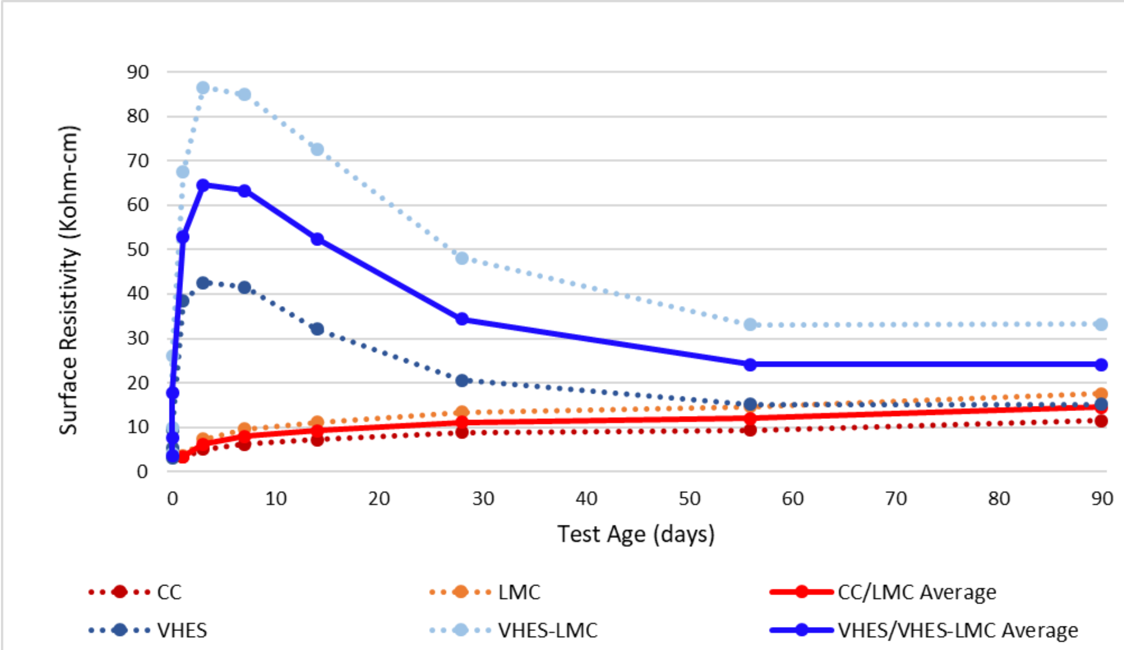

FIGURE 4.11: SR of preliminary 6 in. x 12 in. cylinders

4.2 SR results for miniature slabs

In Figures 4.12 – 4.14, the results of the SR testing of the VHES miniature slab at 7 days are shown in the following reinforcement conditions, without reinforcement (Figure 4.12), with uncoated steel reinforcement (Figure 4.13), and with epoxy-coated reinforcement (Figure 4.14). It was found that the SR readings of the remaining ages of the VHES miniature slabs as well as all of the ages of the VHES-LMC miniature slabs have a similar distribution in the change in SR. The complete dataset of the miniature slab measurement results are provided in Appendix C. The groups of cells where each number is repeated 4-5 times represents one SR measurement along that group of cells. The blue highlight in Figures 4.12 – 4.14 represents the rebar location.

SR measurements made around the perimeter of each box were found to have the highest magnitude. Areas near the center of the box and on top of the rebar positioned in the y-axis direction tended to have the lowest SR measurements. The rebars in the y-axis direction are closer to the testing surface than the rebars in the x-axis direction, which may explain some of the changes in magnitude in the readings in perpendicular directions. The lower resistivity observed when measurements were made on top of the rebar closer to the surface (in the y-axis direction) correlates to the findings from the preliminary reinforced concrete cylinder tests. These miniature slabs clearly indicated the potential for edge effects to notably increase SR measurements. Also, they provided an early indication of the influence of the reinforcement mat, identified by a decrease in SR.

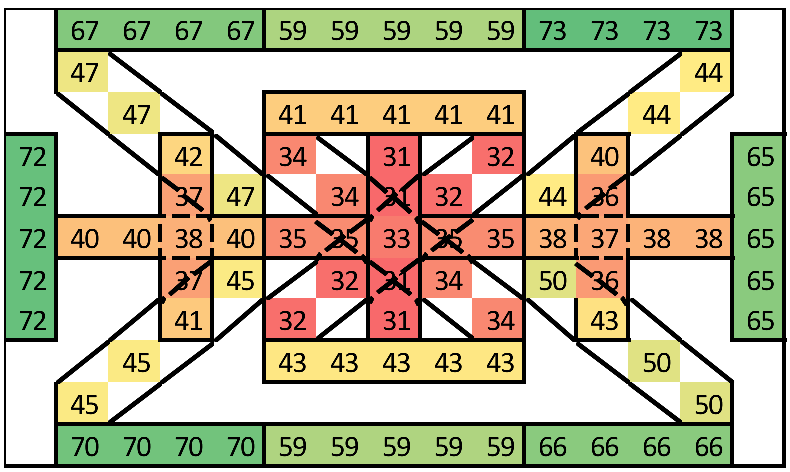

FIGURE 4.12: VHES miniature slab 7-day SR - no reinforcement

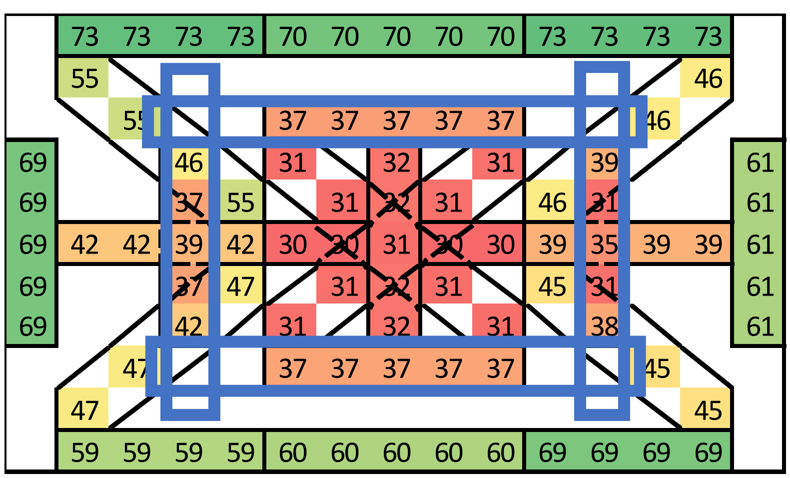

FIGURE 4.13: VHES miniature slab 7-day SR - standard reinforcement

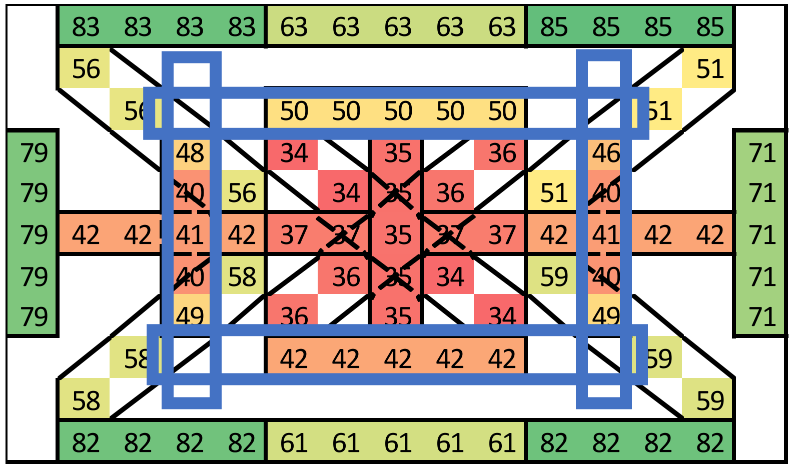

FIGURE 4.14: VHES miniature slab 7-day SR - epoxy reinforcement

4.3 SR results of mockups

The results of the mockup analysis including edge effects and the primary analysis is discussed in the following sections.

4.3.1 Edge effects analyzed on control mockup

Due to the 3-dimensional nature of the current field induced by the SR meter during measurement, consideration should be given to the fact that influences will exist when that current field is restricted by the edge of a homogeneous material such as concrete. When SR is measured in the close proximity of the edge of a concrete member, the reading will be influenced by what is often referred to as edge effect. The literature mentions this occurrence and general reasoning, yet it has not been found to be quantified with respect to the orientation of the meter with respect to the edge in question. In Growers and Milliard (1999), it is stated that the user shall keep a distance of at least twice the probe spacing from the specimen's edge to eliminate what is known as edge effects. For example, the Resipod has a probe spacing of 1.5 in. which requires a 3 in. setback form the edge.

Due to the lack of explanation of edge effects, an experiment to quantify this influence was performed on the control mockup at 90 days within the zone of the mockup not containing reinforcing steel (shown in Figure 4.15, with the gray rectangle indicating the position of the first reinforcing bar). A grid system was marked out on the mockup consisting of 9 columns and 10 rows, shown in black. Due to the slight content variation of concrete's natural makeup and consequently the effect it has on SR, 9 columns were chosen with the intention to recognize outlier measurements and provide ample data to be averaged resulting in a more robust analysis. The distance in inches from the edge is represented by the rows starting from the bottom of the figure, where row 1 represents 1 in. from the edge, row 2 represents 2 in. from the edge, etc. At each column-row intersection the mockup was measured for SR in the three orientations with respect to the specimen's edge (diagonal, parallel "horizontal", and perpendicular "vertical"). When measuring in the diagonal and vertical orientation, the meter was positioned so that the probe closest to the edge may lie directly over the "distance of interest," not the measurement point, which would be the center of the probe span. In contrast, when measuring in the horizontal orientation, the meter was positioned so that the center of the probe span (center of four probes) lie directly over the "distance of interest". Figure 4.15 shows the SR meter positioned in each orientation, where the vertical orientation (a.) distance of interest is 2 in. set back at column 3, the horizontal (b.) distance of interest is 1 in. set back at column 6, and the diagonal (c.) distance of interest is 2 in. set back at column 8. Although the measurement is technically taken at the center of the four probes, the setback distance is the distance between concrete's edge and the center of the probe closest to the edge.

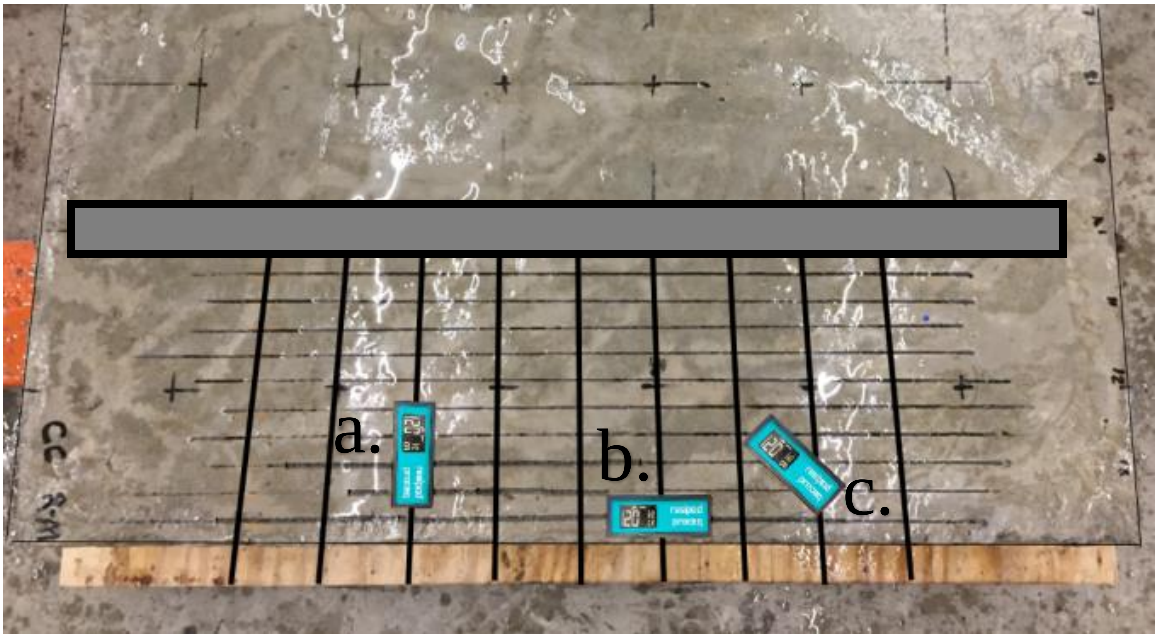

FIGURE 4.15: Edge effect specimen

The measurements were recorded on an Excel sheet with color conditional formatting and arranged by orientation. Figure 4.16 shows the collected data in each orientation with row averages. The measurements at the top of each orientation's figure, row 10 to approximately row 5, are expected to be influenced by the non-coated steel reinforcement shown with the gray rectangular box in Figure 4.15 due to the close proximity of the SR meter. This was expected to be most noticeable in the diagonal and vertical orientation, as those orientation result in the meter being positioned on top of and closest to the non-coated steel reinforcement.

Edge distance (in.)	Horizontal Orientation										Average
	1	2	3	4	5	6	7	8	9		
10	15	16	17	18	17	15	18	20	18		17.1
9	16	17	18	17	15	16	16	18	17		16.5
8	16	17	18	18	18	16	15	16	19		17.0
7	17	18	18	18	18	19	21	17	20		18.2
6	18	19	17	18	19	19	18	21	21		18.8
5	19	18	19	17	17	18	19	18	18		18.1
4	20	21	18	19	21	17	18	19	24		19.6
3	19	21	19	20	19	23	20	21	23		20.6
2	21	21	22	24	23	22	24	24	25		22.8
1	24	26	23	26	28	30	31	30	30		27.6

Edge distance (in.)	Diagonal Orientation										Average
	1	2	3	4	5	6	7	8	9		
10	18	18	19	18	18	16	17	18	19		17.9
9	17	19	17	18	16	16	16	18	17		17.0
8	18	18	16	18	18	16	19	17	20		17.8
7	18	18	17	19	16	19	16	18	18		17.6
6	18	18	18	19	17	19	18	18	14		17.8
5	19	17	19	17	16	16	17	17	15		17.0
4	18	19	19	19	18	17	20	16	19		18.2
3	18	18	18	18	19	20	18	17	20		18.4
2	20	21	22	18	19	21	21	20	22		20.4
1	20	21	21	21	21	24	23	23	25		22.2

Edge distance (in.)	Vertical Orientation										Average
	1	2	3	4	5	6	7	8	9		
10	17	18	17	18	17	17	19	19	19		17.8
9	18	18	17	17	19	17	15	19	18		17.6
8	17	18	16	17	17	16	20	17	16		17.0
7	17	18	16	17	16	16	18	18	16		16.8
6	17	19	18	18	19	16	16	18	17		17.4
5	18	18	17	15	18	17	20	16	17		17.3
4	18	19	16	17	16	17	17	18	18		17.2
3	19	20	17	19	21	17	18	20	18		18.6
2	19	19	19	16	21	17	21	19	17		18.6
1	19	22	21	20	18	20	23	21	22		20.5

FIGURE 4.16: SR edge effects of each orientation

When analyzing the data in Figure 4.16, greater consideration was given to the averages, rather than the dataset in each column, as the averages summarize those data points. As described above, the vertical and diagonal orientations are expected to be most influenced by the steel reinforcement in rows 10-5, as recognized by a decrease in magnitude. As far as the edge effect, rows 4-1 were observed. Each orientation in Figure 4.16 show slightly different trends as the meter approaches the edge, yet they are all in agreement that the measurement is highest at the edge, then the measurements continue to decrease as they are taken further away from the edge. Figure 4.17 is a sample of the mockup data clearly showing the edge effects as illustrated by the relatively higher SR value (greener in color) of the perimeter cells (rows and columns 1 and 13).

	Rebar										No Rebar		
	1	**2**	**3**	**4**	**5**	**6**	**7**	**8**	**9**	**10**	**11**	**12**	**13**
1	4.8	4.6	4.8	4.7	4.4	3.8	4.4	4.2	4.2	4	4.1	4.3	4.8
2	4.8	4.5	4.4	4.2	4.3	4.1	4	4	4.1	4.2	4.1	4.4	4.7
3	4.8	4.4	4.3	4.2	4.1	4	4.1	4	4.1	4.1	4.1	4.3	4.9
4	4.8	4.5	4.2	4.2	4.2	4.1	4.1	4	4	4.2	4.2	4.4	4.6
5	4.6	4.3	4.2	4.3	4	4	4.1	4.1	3.9	3.9	4	4.3	4.9
6	4.8	4.4	4.3	4.1	4.1	4	4	4	3.8	3.8	4	4.2	5
7	4.6	4.3	4.2	4	4.1	4	4	4	3.9	3.9	4	4.2	5.3
8	4.7	4.4	4.2	4.2	4.2	3.8	4.2	3.9	3.9	3.8	3.8	3.9	4.6
9	5.1	4.4	4.2	4.1	4.1	4	3.8	4	3.7	3.9	3.9	4.1	4.3
10	5.1	4.2	4.1	3.9	3.8	4	4.1	3.8	3.7	3.9	4.1	4.1	4.3
11	5.1	4.4	4.1	4	3.8	3.9	4	3.9	3.8	4	4.2	4.5	4.6
12	5	4.5	4.3	4.2	4.2	4.2	4.7	4.4	4.1	4.3	4.4	4.5	5
13	5.5	4.9	4.7	4.6	4.4	4.4	4.9	4.4	4.4	4.5	4.6	4.9	5.4

FIGURE 4.17: Edge effects shown on the 3 day LMC mockup – average orientation

In Figure 4.18, the average SR per row is graphed for each orientation. The horizontal orientation in Figure 4.18 displays the most obvious influence of edge effects. It is hypothesized that since the meter is positioned parallel to the edge (horizontal orientation), that more of the current field comes into contact with the edge, resulting in an increase in SR. In the diagonal orientation, less of the current field contacts the edge, resulting in less of a prominent influence. Lastly, the vertical orientation, where the current field is perpendicular to the edge, even less of an influence is observed. The current field for each orientation is illustrated in Figure 4.19 with the four linear dots representing the electrodes and the ovals representing the lines of current flow. Refer back to Chapter 2, Figure 2.2 Proceq Resipod measurement principal for an illustration of the current flow lines from the profile perspective. In conclusion, as a general rule of thumb to avoid these effects in the field, it is recommended to stay at least 5 in. away from the edge when the parallel or diagonal orientation is used and at least 4 in. away when the perpendicular orientation is being used to avoid edge effects.

Distance from Edge (in.)	SR Average
10	17.1
9	16.5
8	17.0
7	18.2
6	18.8
5	18.1
4	19.6
3	20.6
2	22.8
1	27.6

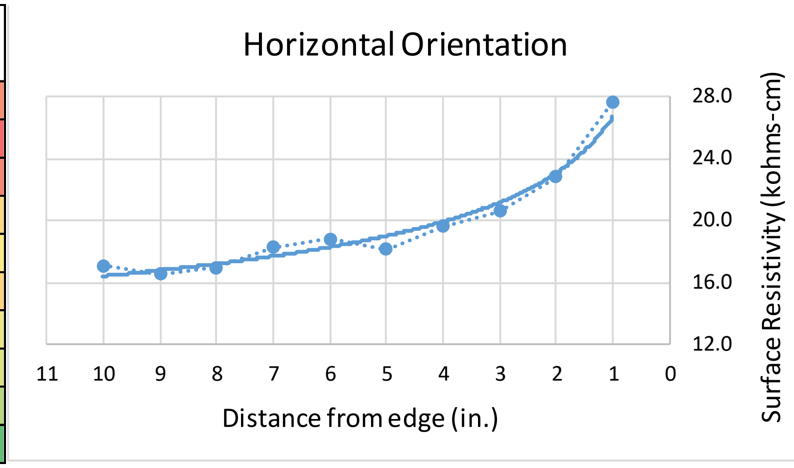

Distance from Edge (in.)	SR Average
10	17.9
9	17.0
8	17.8
7	17.6
6	17.8
5	17.0
4	18.2
3	18.4
2	20.4
1	22.2

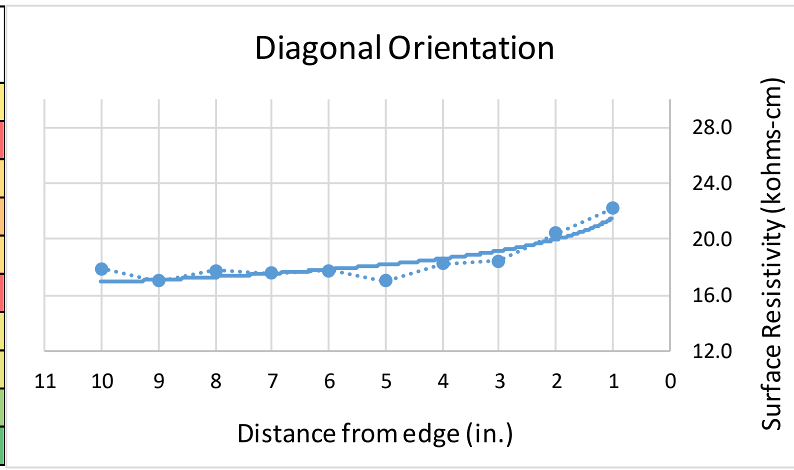

Distance from Edge (in.)	SR Average
10	17.8
9	17.6
8	17.0
7	16.8
6	17.4
5	17.3
4	17.2
3	18.6
2	18.6
1	20.5

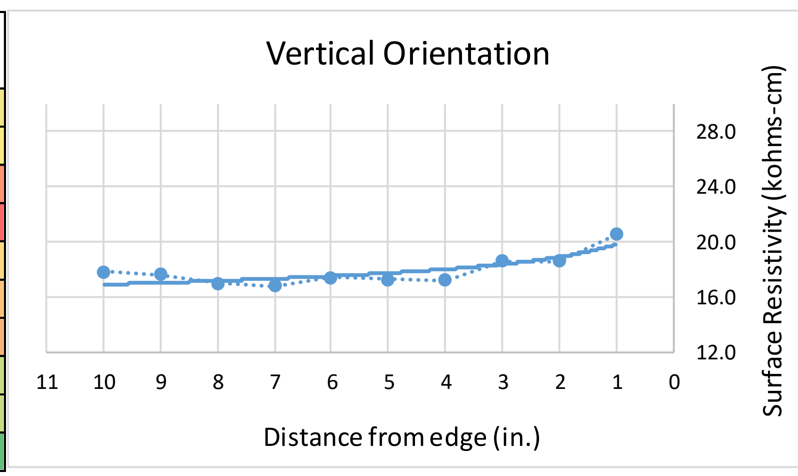

FIGURE 4.18: Graphical representation of SR edge effects

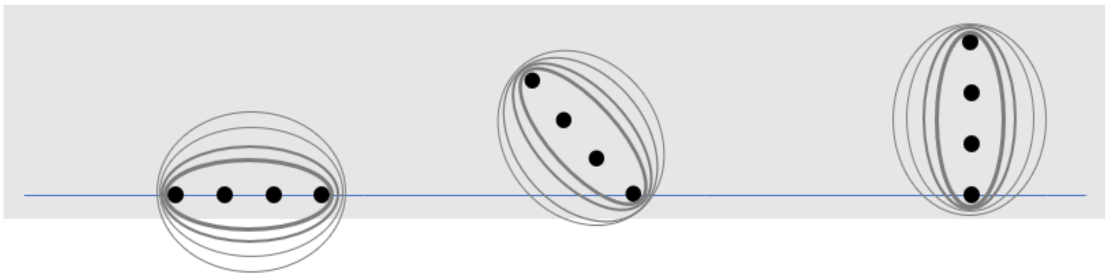

FIGURE 4.19: Edge effects theory - SR current field

4.3.2 Primary analysis of mockups

The objective of the primary analysis of the mockups is to investigate the potential of SR testing as a QA measure to locate defects such as voids within concrete overlays to identify changes in overlay thickness. The recognition of changes in overlay thickness is anticipated to be characterized as continual or gradual, spanning over an area larger than that of the SR meter’s electrical current field. It is hypothesized that small areas of overlay depth changes could potentially be misleading and appear as a void or other defect, rather than overlay thickness variation. Moreover, the detection of steel reinforcement was observed, although other more specialized and effective reinforcement locating methods are widely utilized in industry.

As explained in previous sections, the three overlay mockups were equipped with low-density foam material to simulate voids (Figure 4.19), and the overlays were placed with a gradual increase in thickness from roughly 1 in. on one side of the mockup (row 13) to roughly 4 in. on the opposite side (row 1). The control mockup only contains the steel reinforcement mat (epoxy-coated and non-coated) which is identical to the three overlay mockups and there are no deliberately placed voids or variation in thickness. The purpose of the control mockup is to act as a typical bridge deck to be compare to the other three mockups which are each based on a different overlay.

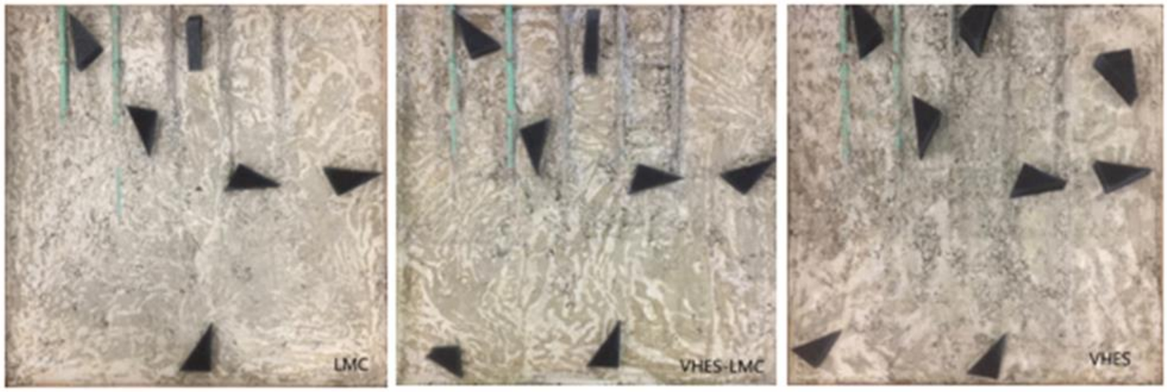

FIGURE 4.20: Mockup void locations - (a) LMC, (b) VHES-LMC, and (c) VHES

While pouring the base concrete for the mockups, the goal was to create an out-of-level flat plane (from 1 in. to 4 in.) to facilitate the overlay thickness variation. Due to the physical restrictions of the reinforcement mat and the roughened texture of the base slab required to achieve a bond with the topping slab, a perfectly flat surface was not used. Figures D.8, D.16, and D.26 in Appendix D are the heat maps generated by a 3D laser scanner where a point cloud surface scan was created. The simplified overlay thicknesses measurement for each can be found in the following overlay mockup sub-sections (Figures 4.25, 4.37, and 4.49). The purpose of this surface analysis was to identify the discrepancies in elevation between the intended plane and what was produced.

The 7-day age measurements were selected for analysis for each mockup because they appear to reveal the most obvious trends of overlay thickness. Those will be presented in the following sections for each, and the entire mockup data collection arranged by overlay type in order of increasing age can be found in Appendix D.

4.3.2.1 Control mockup

The control mockup data in this section (Figure 4.20 – 4.24) includes diagonal, horizontal, and vertical orientations, the average and standard deviation per cell of those orientations, and two row analyses datasets acquired at age 7 days. The analysis titled "Row Average - All Points" consists of the average all 13 points per row and analysis titled "Row Average – No Vertical Rebar" consists of measurements at all non-vertical reinforcement points. The points measured for the ladder analysis of the control mockup are columns 1, 3, 5, 7, 9, 11, 12, and 13. Both of the Row Average analyses are averaged in the white cell at the bottom of each figure. The final averages (white cells) are to be compared with the intention of identifying the influence of reinforcement. The complete SR data/heatmaps of other ages (1, 3, 14, 28, 56, and 90 day) of the control mockup can be found in Appendix D.

	Diagonal													Row Average	
	Rebar										No Rebar			All points	No vert. rebar
Reading #	1	2	3	4	5	6	7	8	9	10	11	12	13		
1	3.6	3	3	3.6	3.5	3.5	3.7	3.6	3.6	3.6	3.6	3.2	3.7	3.48	3.49
2	3.1	3.1	3.6	3	3.1	3.3	3.5	3.7	4.1	3.2	3.2	3.3	3.7	3.38	3.45
3	3.1	3.1	3.5	3.1	2.9	3.1	2.8	3.3	3.6	3.2	3.2	3.3	4	3.25	3.30
4	3.4	3.3	3.4	3.2	3	3.1	3.3	3.4	3.5	3.6	3.3	3.1	3.3	3.30	3.29
5	3.4	3.2	3.6	3.8	2.9	3.1	3.3	3.3	3.4	3.8	3	3.1	3.4	3.33	3.26
6	3	3.2	3.4	3.3	3.6	3.5	3.4	2.9	3.4	2.9	3.2	3.3	3.7	3.29	3.38
7	3.3	3.4	3.1	3.6	3.3	3.3	3.1	2.7	3.3	3	3	3.2	3.9	3.25	3.28
8	3.4	3.1	3.4	3.6	3.3	3.4	3.1	3.3	3.6	3.3	3.1	3	3.6	3.33	3.31
9	3.3	3.1	3.2	2.9	3.4	3.7	3.7	3.9	3.1	3.4	3.2	2.9	3.7	3.35	3.31
10	3.1	3.1	3.2	2.9	3.4	2.9	3.6	3.4	3.3	3.4	3	3.3	3.4	3.23	3.29
11	3.2	3.4	3.4	2.7	3.1	3.1	3.3	3.7	3	3.5	3.2	3.3	3.3	3.25	3.23
12	3.3	3.6	3.2	3.2	3.3	3	3.7	3.7	3.1	3.2	3.5	3.1	3.4	3.33	3.33
13	3.6	3.7	3.6	3.2	3.5	3.4	3.7	3.9	3.4	3.5	3.1	3.3	3.6	3.50	3.48
														3.327	3.337

FIGURE 4.21: Control mockup – diagonal orientation 7 day SR reading

	Horizontal													Row Average	
	Rebar										No Rebar			All points	No vert. rebar
Reading #	1	2	3	4	5	6	7	8	9	10	11	12	13		
1	3.3	3.3	3.5	3.7	3.3	3.3	2.9	3.1	3.5	3.6	3.4	3.2	3.7	3.37	3.35
2	3.2	3.3	3.3	3.5	3.1	3.2	3.3	3	3.5	3.3	3.5	3	3.7	3.30	3.33
3	3.4	3.1	3.4	3.6	3.1	2.9	3.4	3.6	3.4	3.3	3.3	2.9	3.7	3.32	3.33
4	3.6	3.2	3	3.2	3	3.2	3.3	3.6	3.3	3.3	3.3	3.6	3.6	3.32	3.34
5	4	3.5	3.8	3.7	3.2	3.3	3.4	3.6	3.3	3.3	3	3.1	3.7	3.45	3.44
6	3.7	3.6	3.3	3.2	2.8	3	3.4	2.8	3.3	3.1	3	2.9	3.6	3.21	3.25
7	3.3	3.1	3.4	3.1	3.3	3.6	3	3.1	3.2	3.1	2.9	3.3	3.7	3.24	3.26
8	3.4	3.3	3.3	3.7	3.1	3.1	3.4	3.9	3.7	3.6	3.3	3.5	3.7	3.46	3.43
9	3.7	3.2	2.9	3.2	3	3.3	3.5	3.6	3.4	3.3	2.9	2.9	4	3.30	3.29
10	3.5	3.3	3.3	2.9	3.3	3.3	3.1	3.6	3.8	3.3	3.5	3.6	4.2	3.44	3.54
11	3.5	3.4	3.4	3.6	3.4	3.5	3.1	3.3	3.7	3.4	3.1	3.4	3.6	3.42	3.40
12	3.4	3.6	3.1	2.9	3.4	3.5	3.4	3.3	3	3.3	3.4	3.2	3.6	3.32	3.31
13	4	3.4	3.6	3.4	3.3	3.4	3	3.7	3.5	3.3	3.1	2.9	3.3	3.38	3.34
														3.347	3.353

FIGURE 4.22: Control mockup – horizontal orientation 7 day SR reading

Vertical														Row Average	
	Rebar										No Rebar			All points	No vert. rebar
Reading #	1	2	3	4	5	6	7	8	9	10	11	12	13		
1	3.6	3.5	3.4	3.7	3.6	4	3.6	3.3	4	3.6	3.5	3.2	4.1	3.62	3.63
2	3.5	3.5	3.5	3.2	3	3.4	3.8	3.5	3.6	3.6	3.2	3.1	3.8	3.44	3.44
3	3.4	3.3	2.8	3.1	3.5	3	3.7	3.5	3.7	3.4	3.2	3.2	3.8	3.35	3.41
4	3.1	3.5	3.5	3.4	2.9	3	3.7	3.4	3.2	3.9	3.3	3.4	3.6	3.38	3.34
5	3.4	3.6	3.7	3.9	2.9	3.5	2.9	3.4	3.1	3.3	3.3	3.3	3.3	3.35	3.24
6	3.6	3.3	3.3	3.6	3.1	3.6	3.1	3.4	3.4	2.9	2.8	3.3	3.8	3.32	3.30
7	3.3	3.5	3.3	3.7	3.3	3.3	3.9	3.3	3.4	3.7	3.2	3.6	4	3.50	3.50
8	3.3	3.1	3.2	3.3	3.3	3.2	3.4	3.3	3.3	3.6	3.1	3.3	3.5	3.30	3.30
9	3.3	3.1	3.1	3	3.3	3.2	3.3	3.7	3.5	3.5	3.2	3.1	3.7	3.31	3.31
10	3.1	3.2	3.1	3.2	3.1	3.4	3.4	3.3	3.5	3	3.1	3.3	3.8	3.27	3.30
11	3.3	2.9	3.2	2.9	3.1	3.6	3.6	3.1	3.6	2.9	3.1	3.3	3.8	3.26	3.38
12	3.4	3.5	3.5	3.2	3.2	3.5	3.1	3.1	3.2	3.4	3.5	3.3	3.4	3.33	3.33
13	4.1	4.1	3.5	4.1	3.1	3.4	3.7	3.8	3.7	3.7	3.6	3.7	3.4	3.68	3.60
														3.394	3.389

FIGURE 4.23: Control mockup – vertical orientation 7 day SR reading

Average														Row Average	
	Rebar										No Rebar			All points	No vert. rebar
Reading #	1	2	3	4	5	6	7	8	9	10	11	12	13		
1	3.5	3.3	3.3	3.7	3.5	3.6	3.4	3.3	3.7	3.6	3.5	3.2	3.8	3.49	3.49
2	3.3	3.3	3.5	3.2	3.1	3.3	3.5	3.4	3.7	3.4	3.3	3.1	3.7	3.37	3.40
3	3.3	3.2	3.2	3.3	3.2	3	3.3	3.5	3.6	3.3	3.2	3.1	3.8	3.31	3.35
4	3.4	3.3	3.3	3.3	3	3.1	3.4	3.5	3.3	3.6	3.3	3.4	3.5	3.33	3.32
5	3.6	3.4	3.7	3.8	3	3.3	3.2	3.4	3.3	3.5	3.1	3.2	3.5	3.38	3.31
6	3.4	3.4	3.3	3.4	3.2	3.4	3.3	3	3.4	3	3	3.2	3.7	3.27	3.31
7	3.3	3.3	3.3	3.5	3.3	3.4	3.3	3	3.3	3.3	3	3.4	3.9	3.33	3.35
8	3.4	3.2	3.3	3.5	3.2	3.2	3.3	3.5	3.5	3.5	3.2	3.3	3.6	3.36	3.35
9	3.4	3.1	3.1	3	3.2	3.4	3.5	3.7	3.3	3.4	3.1	3	3.8	3.32	3.30
10	3.2	3.2	3.2	3	3.3	3.2	3.4	3.4	3.5	3.2	3.2	3.4	3.8	3.31	3.38
11	3.3	3.2	3.3	3.1	3.2	3.4	3.3	3.4	3.4	3.3	3.1	3.3	3.6	3.31	3.33
12	3.4	3.6	3.3	3.1	3.3	3.3	3.4	3.4	3.1	3.3	3.5	3.2	3.5	3.33	3.32
13	3.9	3.7	3.6	3.6	3.3	3.4	3.5	3.8	3.5	3.5	3.3	3.3	3.4	3.52	3.47
														3.356	3.360

FIGURE 4.24: Control mockup –average of orientations 7 day SR reading

Standard Deviation													
	Rebar										No Rebar		
Reading #	**1**	**2**	**3**	**4**	**5**	**6**	**7**	**8**	**9**	**10**	**11**	**12**	**13**
1	0.2	0.3	0.3	0.1	0.2	0.4	0.4	0.3	0.3	0	0.1	0	0.2
2	0.2	0.2	0.2	0.3	0.1	0.1	0.3	0.4	0.3	0.2	0.2	0.2	0.1
3	0.2	0.1	0.4	0.3	0.3	0.1	0.5	0.2	0.2	0.1	0.1	0.2	0.2
4	0.3	0.2	0.3	0.1	0.1	0.1	0.2	0.1	0.2	0.3	0	0.3	0.2
5	0.3	0.2	0.1	0.1	0.2	0.2	0.3	0.2	0.2	0.3	0.2	0.1	0.2
6	0.4	0.2	0.1	0.2	0.4	0.3	0.2	0.3	0.1	0.1	0.2	0.2	0.1
7	0	0.2	0.2	0.3	0	0.2	0.5	0.3	0.1	0.4	0.2	0.2	0.2
8	0.1	0.1	0.1	0.2	0.1	0.2	0.2	0.3	0.2	0.2	0.1	0.3	0.1
9	0.2	0.1	0.2	0.2	0.2	0.3	0.2	0.2	0.2	0.1	0.2	0.1	0.2
10	0.2	0.1	0.1	0.2	0.2	0.3	0.3	0.2	0.3	0.2	0.3	0.2	0.4
11	0.2	0.3	0.1	0.5	0.2	0.3	0.3	0.3	0.4	0.3	0.1	0.1	0.3
12	0.1	0.1	0.2	0.2	0.1	0.3	0.3	0.3	0.1	0.1	0.1	0.1	0.1
13	0.3	0.4	0.1	0.5	0.2	0	0.4	0.1	0.2	0.2	0.3	0.4	0.2

FIGURE 4.25: Control mockup – standard deviation of 7 day SR readings

The heatmaps (Figures 4.20 – 4.24) do not show a distinct pattern to facilitate the detection of steel reinforcement. It is expected that the mockup would have the lowest SR reading when the SR meter is parallel and on top of the non-coated steel reinforcement. This would be found in Figure 4.20 – 4.23 in columns 5, 7, and 9. Furthermore, when observing Figure 4.22 (vertical orientation) "Row Average" analysis and comparing "all points" to that of "no vertical rebar", an expected differentiation could not be made. To the contrary, the "all points" average, which includes reinforcement was higher than the "no vertical rebar" average.

4.3.2.2 LMC overlay mockup

As stated in previous sections, the overlay thickness changes from one side of the mockup to the other (row 1 to row 13). Figure 4.26 shows the thickness measurements which were extracted from the 3D surface scan. The thickness measurements were taken at points between the reinforcement bars (bold lines) and are presented in color conditional formatting where the darker green represents greater thicknesses, as illustrated in the figure. The other variable introduced into the mockups are voids. Figure 4.27 represents the general areas where the voids were places with reference to row and column designation as labeled around the figure.

The LMC overlay mockup analysis includes the same orientation analysis (diagonal, horizontal, vertical, average and standard deviation per cell), as well as the two row averages identical to the control mockup but due to the addition of void material, an additional set of row averages was included. This dataset was also acquired at the 7 day age. The analysis titled “Row average - No vertical rebar/No voids” are a collection of measurements excluding those instances and are averaged with the intention of identify the influence of voids and steel reinforcement on SR. Those measurements are found on the right side column of the Figures 4.28 – 4.31. The “Row average - No vertical rebar/No voids” measurement points include no more than the non-vertical rebar columns 1, 3, 5, 7, 9, 11, 12, and 13, and selected cells are excluded per row where void material was placed. The complete SR data/heatmaps of other ages (1, 3, 14, 28, 56, and 90 day) of the LMC mockup can be found in Appendix D.

2.9	3.0	3.3	3.3	3.5	4.0	3.5
2.8	3.0	2.9	3.1	3.0	3.3	3.4
2.0	2.6	2.6	2.8	2.9	3.1	3.2
1.6	2.3	2.6	2.6	2.7	2.7	2.5
1.6	2.1	2.3	2.3	2.3	2.1	2.2
1.5	1.7	1.9	2.0	1.8	1.5	1.8
1.2	1.0	1.2	1.3	1.4	1.2	1.3

FIGURE 4.26: LMC mockup overlay thickness measurements

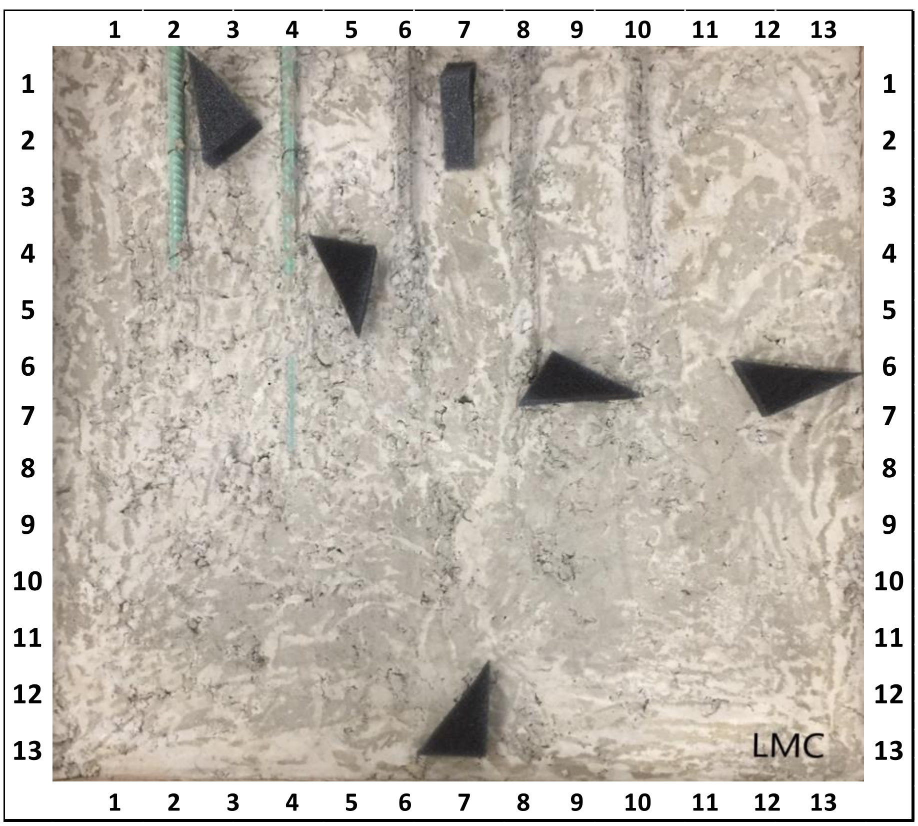

FIGURE 4.27: LMC mockup void locations

	Diagonal													Row Average		
	Rebar										No Rebar			All	No vert	No vert
	1	2	3	4	5	6	7	8	9	10	11	12	13	Points	bar	bar/void
1	6.5	6.6	6.7	6.6	6.3	6.1	6.4	5.7	6.2	5.6	5.8	6.2	6.3	6.231	6.300	6.286
2	6.7	5.9	5.9	5.8	5.8	5.4	5.7	6.6	5.6	5.8	5.6	5.7	5.3	5.831	5.788	5.788
3	6.6	6.5	5.6	5.9	5.6	5.5	5.3	5	5.8	5.7	5.8	5.6	6.4	5.792	5.838	5.838
4	5.6	5.4	5.5	5.7	6.3	5.7	5.7	5.7	5.3	5.9	5.7	5.9	6	5.723	5.750	5.750
5	6.2	6.1	5.9	5.7	5.5	5.9	5.7	5.4	5.2	5.3	5.7	5.7	6	5.715	5.738	5.771
6	6.3	5.7	5.6	5.3	4.8	5.8	5.5	5.5	5.4	5.3	5.1	6.1	6.6	5.615	5.675	5.614
7	6.4	5.7	6	5.1	5.2	5.3	5.3	5.5	5.2	5.4	5.5	5.8	6.5	5.608	5.738	5.817
8	6.7	6	5.9	5.4	5.3	5.2	5.5	5.3	5	5.3	5	5.5	5.9	5.538	5.600	5.600
9	6.8	5.9	5.7	5.4	5.2	5.2	5.3	5.3	5.1	5.3	5.3	5.7	5.9	5.548	5.625	5.625
10	6.9	5.9	5.5	5.3	5.2	5.7	5.6	5.1	4.8	5	5.3	5.5	5.6	5.492	5.550	5.550
11	6.7	6.1	5.3	5.4	5	5.2	5.3	4.9	5.2	5.3	5.7	5.9	6.1	5.548	5.650	5.650
12	6.7	5.9	5.7	5.7	5.7	5.7	6	5.4	5.3	5.7	5.7	5.7	6.6	5.831	5.925	5.925
13	7.1	6.4	6	6.5	5.9	5.8	6.5	5.5	5.9	5.9	6	6.7	7.4	6.277	6.438	6.429
														5.750	5.816	5.819

FIGURE 4.28: LMC overlay mockup – SR diagonal orientation at 7 days

	Horizontal													Row Average		
	Rebar										No Rebar			All	No vert	No vert
	1	2	3	4	5	6	7	8	9	10	11	12	13	Points	bar	bar/void
1	6.5	6	6.5	6.1	5.7	4.9	5.8	5.9	5.8	5.6	5.3	6	6.1	5.862	5.963	5.986
2	7.3	6.6	6	6.2	6.1	5.6	5.7	5.5	5.4	5.8	5.8	5.9	6.5	6.031	6.088	6.088
3	7	6.4	6.2	5.9	5.7	5.6	6	5	5.3	5.9	5.7	6.1	6.7	5.962	6.088	6.088
4	5.9	6.3	5.9	5.4	5.5	5.8	5.5	5.6	5.5	5.9	5.8	6.1	6.6	5.831	5.850	5.850
5	6.4	6.1	6.1	5.8	5.3	5.9	5.9	6	5.6	5.6	5.8	6	6.5	5.923	5.950	6.043
6	6.3	5.8	5.9	5.5	5.8	5.6	5.7	5.8	5.5	5.6	5.5	6	7.6	5.892	6.038	6.043
7	6.5	6	5.8	5.5	5.3	5.4	5.4	5.5	5.3	5.4	5.8	5.7	6.3	5.685	5.763	5.850
8	6.3	5.8	5.9	5.5	5.4	5.3	5.4	5.4	4.9	5.3	5.3	5.5	6.2	5.554	5.613	5.613
9	7.2	6.1	5.5	5.6	5.6	5.7	5.3	5.4	5	5.3	5.4	5.5	6.3	5.685	5.725	5.725
10	6.9	6	5.7	5.6	5	5.4	5.7	5.4	4.8	5.2	5.5	5.7	5.3	5.554	5.575	5.575
11	7	6	5.6	5.3	5.5	5.4	5.3	5	5.1	5.6	6.1	5.9	6.1	5.685	5.825	5.825
12	7.2	6	5.6	5.8	5.7	5.7	5.9	6.1	5.3	5.5	5.9	6	6.4	5.931	6.000	6.000
13	7.1	6.2	6.5	6.1	5.8	5.7	6.3	5.9	5.4	5.7	5.2	6.2	7.3	6.108	6.225	6.214
														5.823	5.900	5.915

FIGURE 4.29: LMC overlay mockup – SR horizontal orientation at 7 days

	Vertical													Row Average		
	Rebar										No Rebar			All	No vert	No vert
	1	2	3	4	5	6	7	8	9	10	11	12	13	Points	bar	bar/void
1	7	6.5	6.8	6.5	6.4	5.1	5.3	6	5.9	5.8	5.4	6	6.4	6.087	6.154	6.271
2	6.6	6.3	6.1	6.1	5.9	5.5	5.7	5.4	5.7	5.5	5.7	6	6.5	5.923	6.025	6.025
3	6.2	6.3	5.9	5.6	5.5	5.3	5.2	5.4	5.7	5.6	6	5.8	6.9	5.800	5.900	5.900
4	6.6	6.6	5.8	5.7	6	5.4	5.6	5.8	5.7	5.8	6.3	5.8	6.4	5.962	6.025	6.025
5	6.9	6	5.9	5.7	5.9	5.7	5.6	5.6	5.6	5.6	6	6.3	6.5	5.946	6.088	6.114
6	5.4	5.7	6	5.9	5.8	5.7	5.5	5.6	5.2	5.3	5.5	6.1	6.6	5.715	5.763	5.714
7	5.5	6.1	5.9	6.2	5.7	5.6	5.5	5.4	5.4	5.5	5.4	5.7	6.3	5.708	5.675	5.717
8	6.8	5.9	5.9	5.8	5.5	5.3	5.3	5.4	5.3	5.3	5.4	5.7	5.8	5.646	5.713	5.713
9	6.5	6	5.7	5.4	5.3	5.2	5.3	5.4	5.4	5.4	5.6	5.8	5.9	5.608	5.688	5.688
10	6.6	6	5.6	5.4	5	5.3	5.6	5.1	5.2	5.2	5.5	5.8	5.7	5.541	5.625	5.625
11	6.7	6.1	5.5	5.3	5	5.3	5.5	5.2	5.2	5.3	5.6	5.1	5.8	5.508	5.550	5.550
12	6.5	6	5.9	5.6	5.3	5.6	6.2	5.5	5.3	5.8	6	5.6	6.4	5.823	5.900	5.900
13	7.4	6.4	6.5	6.1	6.2	6.3	6.8	6.2	6.4	6.6	6.6	6.6	7.5	6.585	6.750	6.743
														5.835	5.912	5.922

FIGURE 4.30: LMC overlay mockup – SR vertical orientation at 7 days

	Average													Row Average		
	Rebar										No Rebar			All	No vert	No vert
	1	2	3	4	5	6	7	8	9	10	11	12	13	Points	bar	bar/void
1	6.7	6.4	6.7	6.4	6.1	5.4	5.8	5.9	6	5.7	5.5	6.1	6.3	6.060	6.139	6.181
2	6.9	6.3	6	6	5.9	5.5	5.7	5.8	5.6	5.7	5.7	5.9	6.1	5.928	5.967	5.967
3	6.6	6.4	5.9	5.8	5.6	5.5	5.5	5.1	5.6	5.7	5.8	5.8	6.7	5.851	5.942	5.942
4	6	6.1	5.7	5.6	5.9	5.6	5.6	5.7	5.5	5.9	5.9	5.9	6.3	5.838	5.875	5.875
5	6.5	6.1	6	5.7	5.6	5.8	5.7	5.7	5.5	5.5	5.8	6	6.3	5.862	5.925	5.976
6	6	5.7	5.8	5.6	5.5	5.7	5.6	5.6	5.4	5.4	5.4	6.1	6.9	5.741	5.825	5.790
7	6.1	5.9	5.9	5.6	5.4	5.4	5.4	5.5	5.3	5.4	5.6	5.7	6.4	5.667	5.725	5.794
8	6.6	5.9	5.9	5.6	5.4	5.3	5.4	5.4	5.1	5.3	5.2	5.6	6	5.579	5.642	5.642
9	6.8	6	5.6	5.5	5.4	5.4	5.3	5.4	5.2	5.3	5.4	5.7	6	5.614	5.679	5.679
10	6.8	6	5.6	5.4	5.1	5.5	5.6	5.2	4.9	5.1	5.4	5.7	5.5	5.529	5.583	5.583
11	6.8	6.1	5.5	5.3	5.2	5.3	5.4	5	5.2	5.4	5.8	5.6	6	5.580	5.675	5.675
12	6.8	6	5.7	5.7	5.6	5.7	6	5.7	5.3	5.7	5.9	5.8	6.5	5.862	5.942	5.942
13	7.2	6.3	6.3	6.2	6	5.9	6.5	5.9	5.9	6.1	5.9	6.5	7.4	6.323	6.471	6.462
														5.803	5.876	5.885

FIGURE 4.31: LMC overlay mockup – SR average of orientations at 7 days

Standard Deviation													
	Rebar										No Rebar		
	1	**2**	**3**	**4**	**5**	**6**	**7**	**8**	**9**	**10**	**11**	**12**	**13**
1	0.3	0.3	0.2	0.3	0.4	0.6	0.5	0.2	0.2	0.1	0.3	0.1	0.2
2	0.4	0.4	0.1	0.2	0.2	0.1	0	0.7	0.2	0.2	0.1	0.2	0.7
3	0.4	0.1	0.3	0.2	0.1	0.2	0.4	0.2	0.3	0.2	0.2	0.3	0.3
4	0.5	0.6	0.2	0.2	0.4	0.2	0.1	0.1	0.2	0.1	0.3	0.2	0.3
5	0.4	0.1	0.1	0.1	0.3	0.1	0.2	0.3	0.2	0.2	0.2	0.3	0.3
6	0.5	0.1	0.2	0.3	0.6	0.1	0.1	0.2	0.2	0.2	0.2	0.1	0.6
7	0.6	0.2	0.1	0.6	0.3	0.2	0.1	0.1	0.1	0.1	0.2	0.1	0.1
8	0.3	0.1	0	0.2	0.1	0.1	0.1	0.1	0.2	0	0.2	0.1	0.2
9	0.4	0.1	0.1	0.1	0.2	0.3	0	0	0.2	0.1	0.2	0.2	0.2
10	0.2	0.1	0.1	0.2	0.1	0.2	0.1	0.2	0.2	0.1	0.1	0.2	0.2
11	0.2	0.1	0.2	0.1	0.3	0.1	0.1	0.2	0.1	0.2	0.3	0.5	0.2
12	0.4	0.1	0.2	0.1	0.2	0.1	0.2	0.4	0	0.2	0.2	0.2	0.1
13	0.2	0.1	0.3	0.2	0.2	0.3	0.3	0.4	0.5	0.5	0.7	0.3	0.1

FIGURE 4.32: LMC mockup – SR standard deviation at 7 days

Due to edge effects that were discussed in previous sections, it was noticed that the SR around the perimeter of the mockups (rows 1 and 13 and columns 1 and 13) was generally higher than that of the areas within the perimeter. By disregarding those cells for a moment and using the "Row Average" analysis (the three columns right side of Figure 4.28 – 4.31), a trend can be observed where an increase in SR occurs as the overlay thickness increases. Note that the overlay is at its thickest at row 1 (appx 3.75 in.) and at its thinnest at row 13 (1.25 in.). Figure 4.33 shows how the overlay thickness influences SR at each age. The data used was from the average of orientation measurements row analysis from the LMC mockups at each age (Appendix D – LMC: 1, 3, 7, 14, 28, 56, and 90 day), and rows 1 and 13 were left out due to edge effects. As a general rule of thumb, it is recommended to stay at least 5 in. away from the edge when the parallel or diagonal orientation is used and at least 4 in. away when the perpendicular orientation is being used to avoid edge effects. The measurements taken on top of the reinforcement were also left out, leaving 5 rows. A linear trend occurs at early ages but by day 28, the trend becomes less linear with a dip near 2.1 in. The black trendline is average of all ages of the LMC overlay. The equation of the line shows a positive correlation between SR and overlay thickness. It is hypothesized that the slope of the average trendline validates that the LMC overlay and conventional concrete base have similar SR.

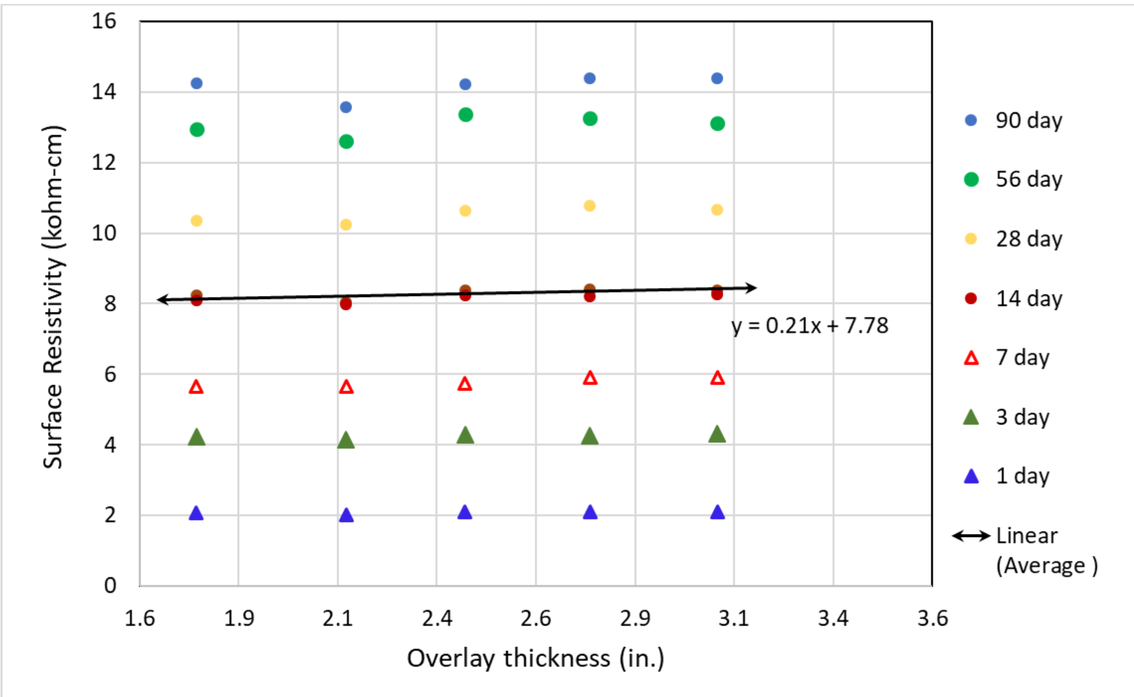

FIGURE 4.33: SR versus LMC overlay thickness

Based on Figure 4.33, Table 4.3 shows the line slope equations taken from each age and the calculated rate of change (ROC) correction factor that can be used to estimate SR as the overlay thickness changes in 1 in. increments. For example, at 7 days and 28 days, as the LMC overlay thickness increased by 1 in., the SR can be expected to increase by 0.2 and 0.4 kohm-cm respectively. It is noted that this is a fairly small change.

TABLE 4.3: LMC line slope equation and ROC (overlay thickness vs. SR)

Age	Line slope equation	Rate of change
1 day	y = 0.03x + 2.00	0.0
3 day	y = 0.09x + 4.02	0.1
7 day	y = 0.24x + 5.18	0.2
14 day	y = 0.16x + 7.78	0.2
28 day	y = 0.35x + 9.69	0.4
56 day	y = 0.29x + 12.36	0.3
90 day	y = 0.31x + 13.41	0.3

In Figure 4.34, the rate of change of SR per change in overlay thickness by 1 in. increments is graphed. Similar to Figure 4.33, the ROC starts out linear (predictable) and towards 14 and 28 days this rate becomes more unstable then evens out between 56 and 90 days. Overall, the graph shows a positive trend where the LMC overlay thickness influence of SR specific to this research can be estimated using the rate of change correction factors in Table 4.3.

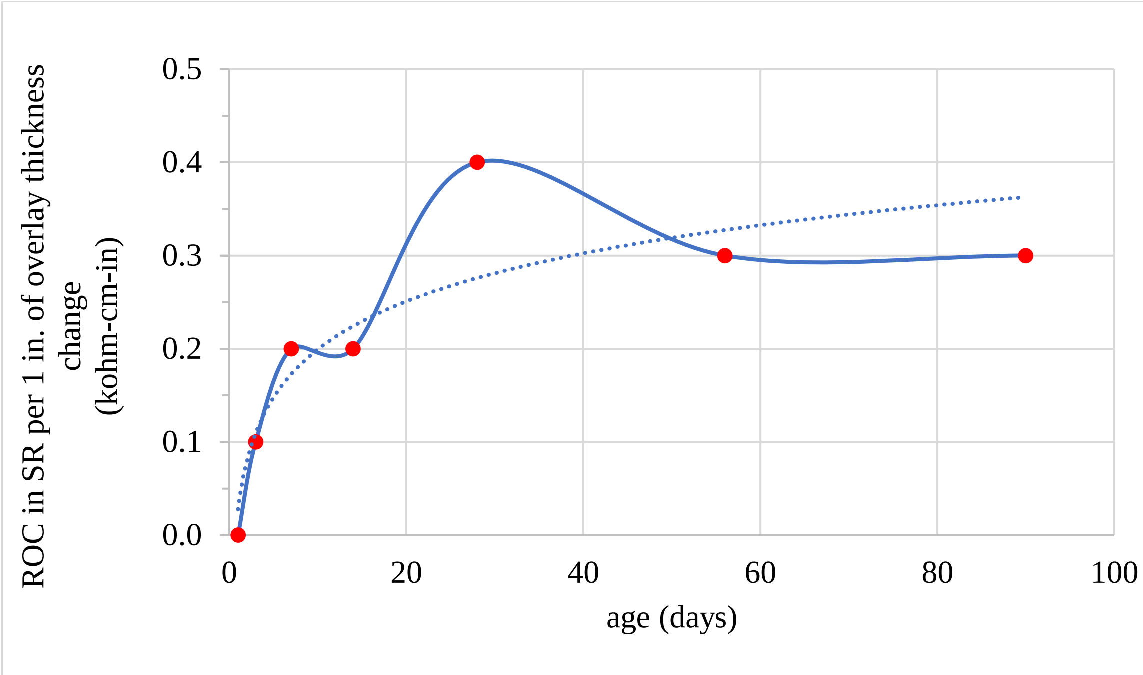

FIGURE 4.34: LMC rate of change per age (overlay thickness vs. SR)

With regard to void detection, by observation of the various orientations in the heatmaps alone (Figures 4.28 – 4.31), the voids were not explicitly identified by the expected orange or red cell appearance correlating with a decrease in SR magnitude. For visual reference, Figure 4.35, the 7 day horizontal SR data with the voids superimposed on top (black shapes) is provided. The average orientation was selected, yet no clear detection was made so further analysis was conducted and is discussed in later sections.

Average													
	Rebar										No Rebar		
	1	**2**	**3**	**4**	**5**	**6**	**7**	**8**	**9**	**10**	**11**	**12**	**13**
1	6.7	6.4	6.7	6.4	6.1	5.4	5.8	5.9	6	5.7	5.5	6.1	6.3
2	6.9	6.3	6	6	5.9	5.5	5.7	5.8	5.6	5.7	5.7	5.9	6.1
3	6.6	6.4	5.9	5.8	5.6	5.5	5.5	5.1	5.6	5.7	5.8	5.8	6.7
4	6	6.1	5.7	5.6	5.9	5.6	5.6	5.7	5.5	5.9	5.9	5.9	6.3
5	6.5	6.1	6	5.7	[illegible]	5.8	5.7	5.7	5.5	5.5	5.8	6	6.3
6	6	5.7	5.8	5.6	5.5	5.7	5.6	5.6	5.4	5.4	5.4	6.1	6.9
7	6.1	5.9	5.9	5.6	5.4	5.4	5.4	5.5	5.3	5.4	5.6	5.7	6.4
8	6.6	5.9	5.9	5.6	5.4	5.3	5.4	5.4	5.1	5.3	5.2	5.6	6
9	6.8	6	5.6	5.5	5.4	5.4	5.3	5.4	5.2	5.3	5.4	5.7	6
10	6.8	6	5.6	5.4	5.1	5.5	5.6	5.2	4.9	5.1	5.4	5.7	5.5
11	6.8	6.1	5.5	5.3	5.2	5.3	5.4	5	5.2	5.4	5.8	5.6	6
12	6.8	6	5.7	5.7	5.6	5.7	6	5.7	5.3	5.7	5.9	5.8	6.5
13	7.2	6.3	6.3	6.2	6	5.9	6.5	5.9	5.9	6.1	5.9	6.5	7.4

FIGURE 4.35: Voids superimposed on LMC mockup - 7 day average SR data

Figures 4.36 – 4.39 shows the degree of influence that the voids and reinforcement have on the SR measurement. This was accomplished by taking the average of all cells at each age with the following list of exclusions/inclusions, “No exclusions”, “No vertical reinforcement”, “No reinforcement”, “No reinforcement or voids”, “Vertical reinforcement only”, and “Vertical standard rebar only”.

The exclusions /inclusions are defined as follows:

- No exclusions - average of all (169) measurements
- No vertical rebar - average of 169 points excluding vertical rebar
- No rebar - average of 169 points excluding all rebar
- No rebar or voids - average of 169 points excluding all rebar and voids
- Vertical rebar only - including only measurements at vertical rebar
- Vertical standard rebar only - including only measurements at vertical standard rebar (non-coated)

Each exclusion/inclusion designation is separated into its own line which is graphed in Figures 4.36 – 4.39. The four figures are the diagonal (Figure 4.36), horizontal (Figure 4.37), vertical orientation (Figure 4.38), and average of orientations (Figure 4.39).

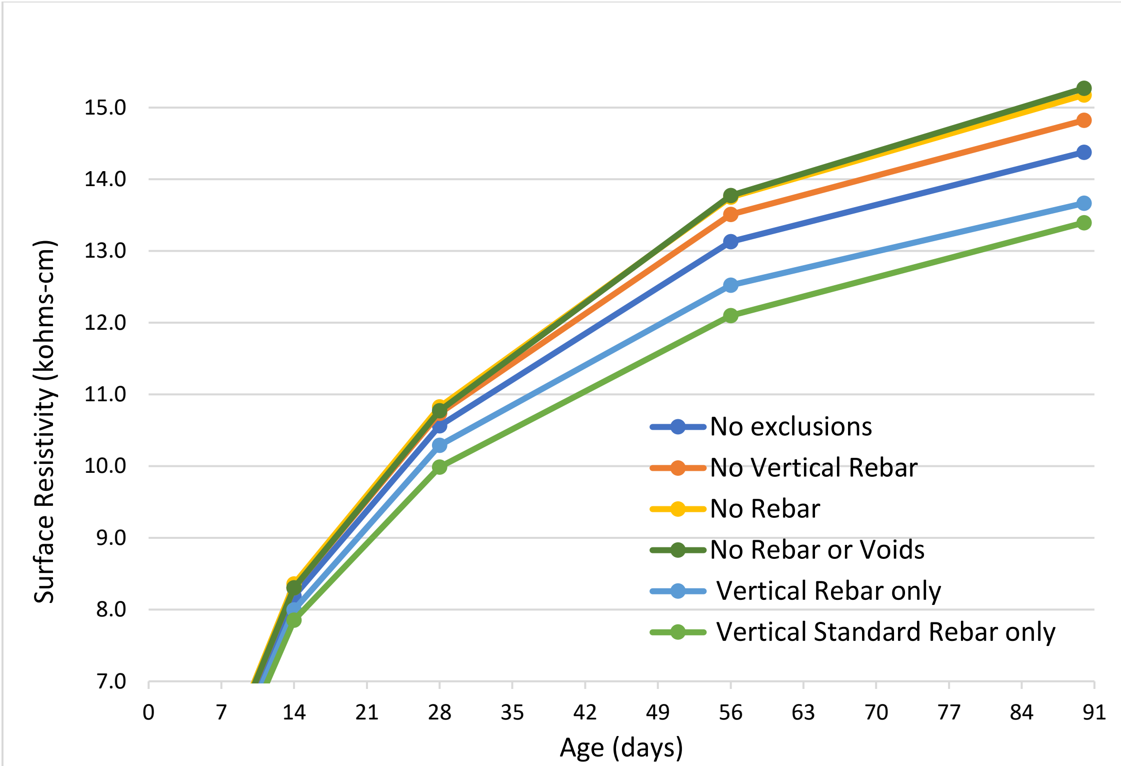

FIGURE 4.36: LMC mockup - SR diagonal orientation with different exclusions

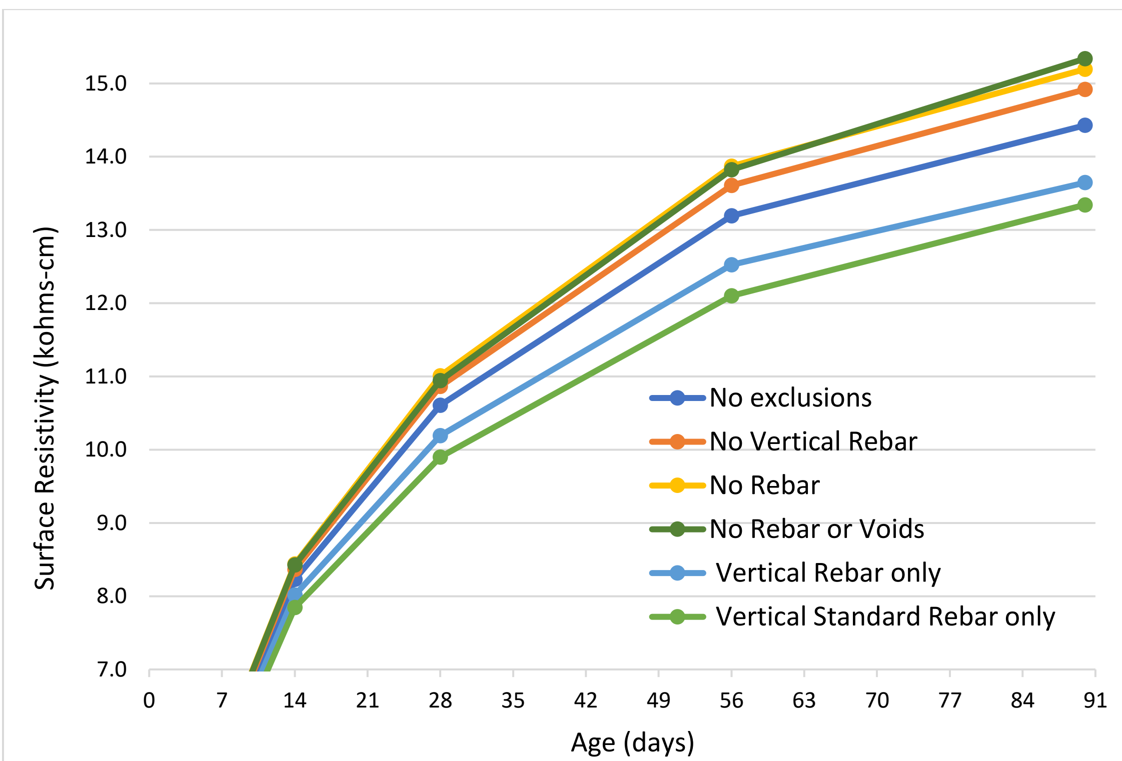

FIGURE 4.37: LMC mockup - SR horizontal orientation with different exclusions

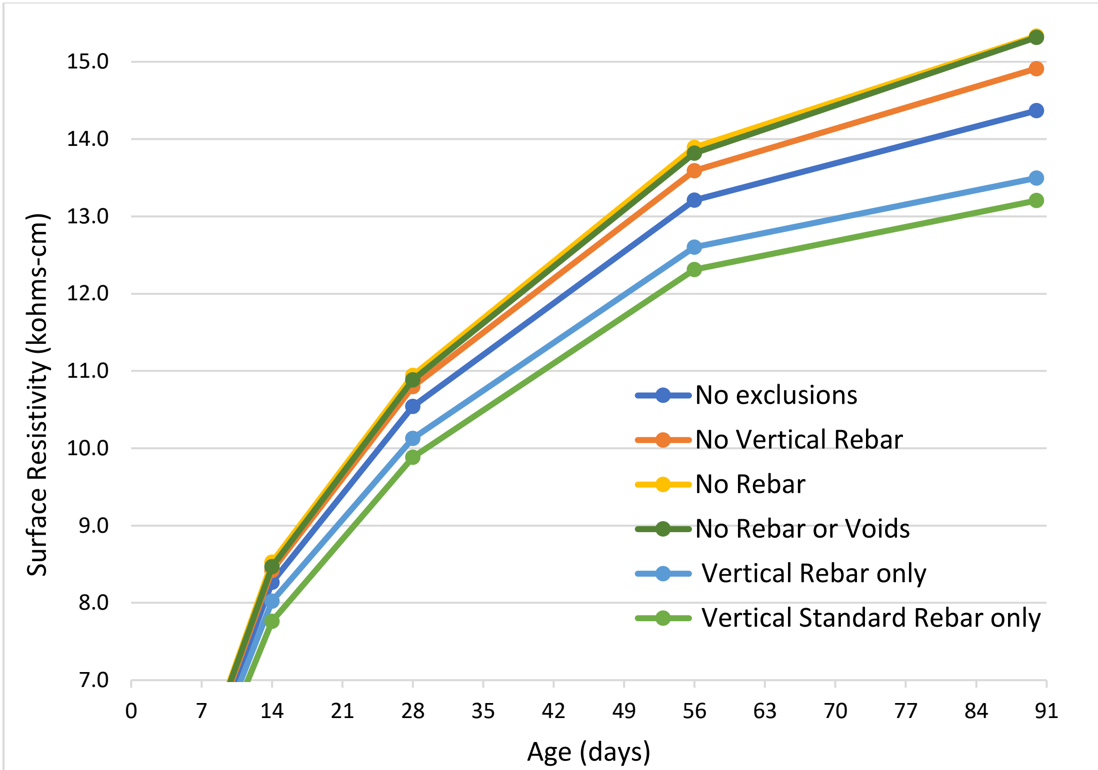

FIGURE 4.38: LMC mockup - SR vertical orientation with different exclusions

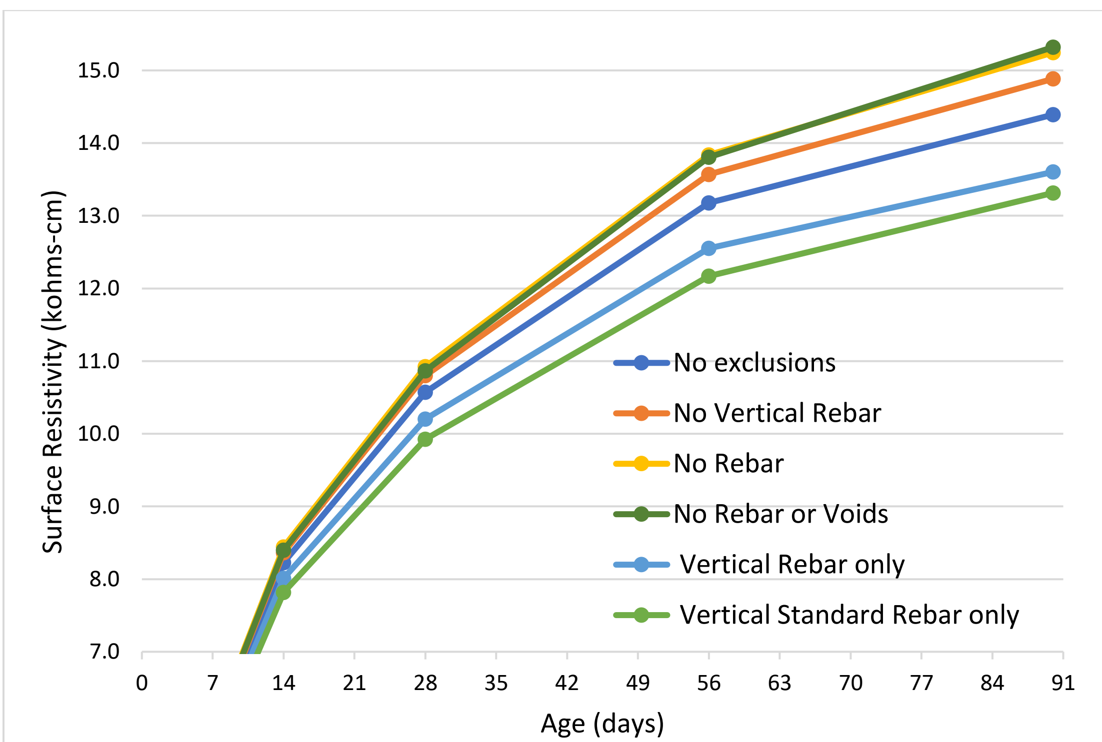

FIGURE 4.39: LMC mockup - SR average of orientations with different exclusions

By observing Figure 4.37, the average measurements of “Vertical standard reinforcement only” are of the lowest magnitude, and the average measurements of “No reinforcement” and “No reinforcement or voids” were of the highest SR, as expected due to the fact that steel reinforcement and voids will produce SR results lower than expected. Another observation made is the 90 day data point of the “No exclusion” designation resides lower than when reinforcement and voids were excluded and higher than when reinforcement was the only inclusion. Each of the observations discussed above show a similar trend across each SR meter orientation.

4.3.2.3 VHES overlay mockup

The identical method of overlay thickness variation performed for the LMC and VHES-LMC mockups was employed for the VHES. Correspondingly, Figure 4.40 shows the thickness measurement extracted from the 3D surface scan which were taken at points between the reinforcement strands (bold lines) and are presented in color conditional formatting where the darker green represents greater thicknesses, as illustrated in the figure. The voids introduced into the mockups are displayed in Figure 4.41. Note the row and column labeling around the figure.

The VHES overlay mockup analysis includes the same perspectives as the LMC mockup with the addition of two void (Figure 4.41). This dataset was also acquired at the 7 day age. Again, the row average analyses are intended to identify the influence of voids and steel reinforcement on SR. Those measurements are found on the right three columns of Figures 4.42 – 4.45. The “Row average – All points” measurements include every measurement point (13 points). The analysis titled “Row average – No vertical rebar” contain measurements at columns 1, 3, 5, 7, 9, 11, 12, and 13. The “Row average - No vertical rebar/No voids" measurement points begin with the same non-vertical rebar location framework (columns 1, 3, 5, 7, 9, 11, 12, and 13) and selected cells are excluded per row where void material was placed (Figure 4.41). The complete SR data/heatmaps of other ages (1, 4 hr., 1, 3, 14, 28, 56, and 90 day) of the VHES mockup can be found in Appendix D.

3.5	3.3	3.5	3.8	3.8	3.9	4.0
3.2	2.9	3.0	3.0	3.1	3.3	3.7
3.3	2.8	2.9	3.1	2.8	2.9	3.3
3.0	2.6	2.8	2.7	2.6	2.7	3.0
2.5	2.2	2.4	2.3	2.3	2.3	2.5
2.0	1.7	1.8	1.8	1.9	1.7	2.0
1.7	1.5	1.5	1.4	1.3	1.4	1.4

FIGURE 4.40: VHES mockup overlay thickness measurements

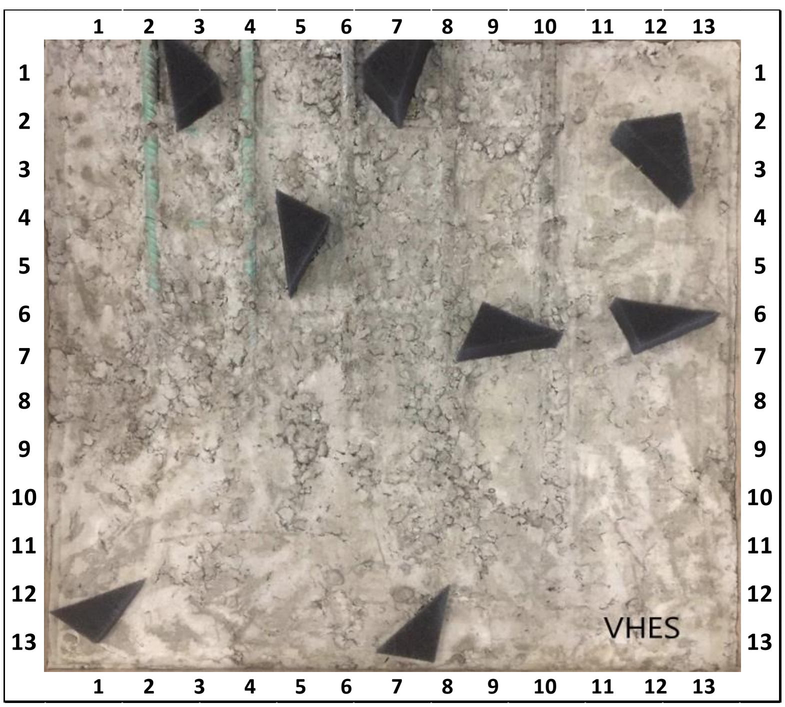

FIGURE 4.41: VHES mockup void locations

	Diagonal													Row Average		
	Rebar										No Rebar			All	No vert	No vert
	1	2	3	4	5	6	7	8	9	10	11	12	13	Points	bar	bar/void
1	11	8.8	9	7.9	8.3	7.9	8.7	7.8	7.5	8	7.9	7.8	8	8.34	8.50	8.50
2	9	8.7	8.1	7.8	9.1	7.9	7.1	7.2	6.9	7.7	7.7	7.6	8.6	7.95	8.01	8.01
3	8.4	8.1	7.5	7.8	7.6	7.6	7.8	7.4	7.7	7.2	8.2	7.6	9.8	7.90	8.08	8.14
4	8.5	8.5	8.3	8.2	7.6	6.6	7.5	7.9	7.9	7.6	8.2	8.2	8.7	7.98	8.11	8.11
5	8.5	8.7	7.6	8.4	8.5	6.5	7.7	8.2	7.9	8.9	8.5	9	9.4	8.29	8.39	8.37
6	9.2	8.3	8.6	8.2	8.2	8.7	8.3	8	7.5	8	9	9.3	9.5	8.52	8.70	8.61
7	9.7	9.6	9.1	8	8.5	8.3	8.6	9.6	9	8.9	8.6	9.1	10	9.03	9.13	8.90
8	8.9	9	8.8	8.8	8.5	8.8	8.8	8.5	9.5	8.7	9	10	10	9.05	9.23	9.23
9	9.3	9.2	8.7	9.3	9.2	9.2	8.8	8.7	8.7	9	10	10	11	9.37	9.55	9.55
10	9.8	9.9	9.3	9.9	9.7	9.2	9.8	9.7	9.4	9.4	11	11	12	9.95	10.15	10.15
11	11	10	9.7	10	10	9.7	10	10	9.1	9.9	11	11	12	10.18	10.33	10.33
12	12	10	9.5	9.8	11	10	9.3	10	9.5	10	11	11	12	10.37	10.54	10.54
13	13	11	11	11	10	9.5	12	11	10	11	11	11	12	10.96	11.27	10.94
														9.068	9.228	9.183

FIGURE 4.42: VHES overlay mockup – SR diagonal orientation at 7 days

	Horizontal													Row Average		
	Rebar										No Rebar			All	No vert	No vert
	1	2	3	4	5	6	7	8	9	10	11	12	13	Points	bar	bar/void
1	9	8.3	8	7.1	7.3	7.6	7.7	7.8	6.8	6.9	6.3	6.6	9.2	7.58	7.61	7.72
2	8.5	7.4	7	6.5	7.3	7.2	7	6.9	7	7.2	7	7.5	8.9	7.34	7.53	7.53
3	8.7	7.2	7	6.6	7.1	7	7.1	7	6.8	7.5	7.4	7.6	9.2	7.40	7.61	7.61
4	8.6	7.7	7.5	7	7	6.7	7	7.3	7.4	7.6	7.7	7.9	9.6	7.62	7.84	7.84
5	8.2	7.9	6.9	8.1	8.1	7.3	7.3	7.5	7.3	7.8	8.2	8.9	10	7.97	8.13	8.13
6	8.6	7.6	7.3	7	7.1	8.1	7.6	7.3	7.2	7.7	8.4	8.7	9.8	7.88	8.09	8.00
7	9.4	8.2	7.4	6.5	7	8.2	7	8.2	8	7.3	8	8.8	9.6	7.97	8.15	7.76
8	9	7.8	8.3	8.4	7.9	8	8.2	8.9	7.9	8.3	8.4	9.2	10	8.49	8.62	8.62
9	9	8.6	8.2	8.5	8.5	9	8.8	8.8	8.4	9.1	8.9	9.4	10	8.88	8.93	8.93
10	10	9	8.9	8.8	8.8	8.9	8.6	9.2	9.3	9.3	9.8	11	11	9.41	9.64	9.64
11	11	9.4	9	8.9	9.4	9.2	9	9.1	9.2	9.7	10	10	11	9.58	9.78	9.78
12	11	9.5	9.1	9.3	9.7	9.5	9.2	9.5	9.1	9.4	9.5	10	11	9.68	9.84	9.84
13	12	9.7	9.5	9.5	9.1	8.9	9.3	9.4	8.7	9.9	10	10	11	9.82	10.03	9.78
														8.431	8.597	8.551

FIGURE 4.43: VHES overlay mockup – SR horizontal orientation at 7 days

	Vertical													Row Average		
	Rebar										No Rebar			All Points	No vert bar	No vert bar/void
	1	2	3	4	5	6	7	8	9	10	11	12	13			
1	9.1	8.3	8	7.3	7.8	7.5	8.9	7.3	7.4	8	7.4	7.7	8.2	7.92	8.06	7.98
2	7.5	7.7	7.4	6.5	6.8	6.7	6.8	6.6	6.4	6.5	6.7	6.7	7.9	6.94	7.03	7.03
3	7.6	7.6	6.4	6.5	6.7	6.7	6.8	7	6.8	7	7	7.4	8.4	7.07	7.14	7.10
4	7.2	7.6	7.2	7.3	7.3	5.8	7.1	7.1	7	6.9	7	7.9	8.3	7.21	7.38	7.38
5	7.6	8.1	6.9	7.7	7.8	5.6	7.1	7	6.9	6.7	7.7	8.4	8.7	7.40	7.64	7.61
6	8.4	8.1	7.7	7.8	7.8	7.4	6.4	7.7	6.9	8.1	7.8	9	9.1	7.86	7.89	7.73
7	7.9	7.8	8.1	7.1	7.6	7.6	7.5	7.2	7	6	8.2	9.3	9.4	7.75	8.13	7.86
8	8.2	8	7.9	8.2	8.2	8	8	7.8	7.9	8.6	8.4	8.7	9.2	8.24	8.31	8.31
9	8.5	8.6	8.4	8.5	8.8	8.3	8	7.7	8	7.8	9.1	9.7	9.4	8.53	8.74	8.74
10	9.4	8.7	8.1	8.3	8.7	8.5	8.6	8.5	8.1	8.9	9.4	9.8	10	8.85	9.03	9.03
11	9	9.4	8.9	8.7	9.3	8.4	9.1	8.7	8.2	9.5	9.9	9.8	11	9.22	9.39	9.39
12	9.7	9.3	8.4	8.7	9.2	8.5	9.1	9.2	9.1	9.5	9.8	11	11	9.44	9.69	9.69
13	11	10	9.3	9.5	9.5	9.5	10	9.4	8.9	10	11	11	12	10.06	10.26	10.08
														8.191	8.360	8.302

FIGURE 4.44: VHES overlay mockup – SR vertical orientation at 7 days

	Average													Row Average		
	Rebar										No Rebar			All Points	No vert bar	No vert bar/void
	1	2	3	4	5	6	7	8	9	10	11	12	13			
1	9.6	8.5	8.3	7.4	7.8	7.7	8.4	7.6	7.2	7.6	7.2	7.4	8.5	7.95	8.06	8.07
2	8.3	7.9	7.5	6.9	7.7	7.3	7	6.9	6.8	7.1	7.1	7.3	8.5	7.41	7.52	7.52
3	8.2	7.6	7	7	7.1	7.1	7.2	7.1	7.1	7.2	7.5	7.5	9.1	7.46	7.61	7.62
4	8.1	7.9	7.7	7.5	7.3	6.4	7.2	7.4	7.4	7.4	7.6	8	8.9	7.60	7.78	7.78
5	8.1	8.2	7.1	8.1	8.1	6.5	7.4	7.6	7.4	7.8	8.1	8.8	9.4	7.89	8.05	8.04
6	8.7	8	7.9	7.7	7.7	8.1	7.4	7.7	7.2	7.9	8.4	9	9.5	8.09	8.23	8.11
7	9	8.5	8.2	7.2	7.7	8	7.7	8.3	8	7.4	8.3	9.1	9.8	8.25	8.47	8.17
8	8.7	8.3	8.3	8.5	8.2	8.3	8.3	8.4	8.4	8.5	8.6	9.3	9.8	8.59	8.72	8.72
9	8.9	8.8	8.4	8.8	8.8	8.8	8.5	8.4	8.4	8.6	9.5	9.7	10	8.92	9.07	9.07
10	9.8	9.2	8.8	9	9.1	8.9	9	9.1	8.9	9.2	9.9	10	11	9.40	9.60	9.60
11	10	9.6	9.2	9.2	9.6	9.1	9.4	9.3	8.8	9.7	10	10	11	9.66	9.83	9.83
12	11	9.7	9	9.3	9.8	9.4	9.2	9.6	9.2	9.7	10	11	11	9.83	10.02	10.02
13	12	10	9.8	9.9	9.6	9.3	10	9.9	9.3	10	11	11	12	10.28	10.52	10.27
														8.564	8.728	8.679

FIGURE 4.45: VHES overlay mockup – SR average of orientations at 7 days

Standard Deviation													
	Rebar										No Rebar		
	1	**2**	**3**	**4**	**5**	**6**	**7**	**8**	**9**	**10**	**11**	**12**	**13**
1	1	0.3	0.6	0.4	0.5	0.2	0.6	0.3	0.4	0.6	0.8	0.7	0.6
2	0.8	0.7	0.6	0.8	1.2	0.6	0.2	0.3	0.3	0.6	0.5	0.5	0.5
3	0.6	0.5	0.6	0.7	0.5	0.5	0.5	0.2	0.5	0.3	0.6	0.1	0.7
4	0.8	0.5	0.6	0.6	0.3	0.5	0.3	0.4	0.5	0.4	0.6	0.2	0.7
5	0.5	0.4	0.4	0.4	0.4	0.9	0.3	0.6	0.5	1.1	0.4	0.3	0.7
6	0.4	0.4	0.7	0.6	0.6	0.7	1	0.4	0.3	0.2	0.6	0.3	0.4
7	1	0.9	0.9	0.8	0.8	0.4	0.8	1.2	1	1.5	0.3	0.3	0.5
8	0.4	0.6	0.5	0.3	0.3	0.5	0.4	0.6	0.9	0.2	0.3	0.7	0.6
9	0.4	0.3	0.3	0.5	0.4	0.5	0.5	0.6	0.4	0.7	0.8	0.3	1
10	0.4	0.6	0.6	0.8	0.6	0.4	0.7	0.6	0.7	0.3	0.6	0.5	1
11	0.9	0.3	0.4	0.7	0.4	0.7	0.6	0.7	0.6	0.2	0.3	0.4	0.7
12	1.1	0.5	0.6	0.6	0.7	0.8	0.1	0.5	0.2	0.4	0.7	0.4	0.2
13	0.7	0.5	0.6	0.6	0.6	0.3	1.3	0.9	0.9	0.4	0.5	0.6	0.5

FIGURE 4.46: VHES mockup – SR standard deviation at 7 days

Similar to the LMC analysis of overlay thickness influence on SR, Figure 4.47 is provided for the VHES overlay. The data used was from the average of orientation measurements row analysis from the VHES mockups at each age (Appendix D – VHES: 1 hour, 4 hour, 1, 3, 7, 14, 28, 56, and 90 day), and rows 1 and 13 were omitted due to edge effects. The measurements taken on top of the reinforcement were also omitted , leaving 5 rows. Similar to the VHES-LMC analysis, a low pitch linear trend occurs at the very early ages (1-4 hour) depicting a similar SR between base concrete and overlay concrete, but by day 1, the trend becomes less linear and more negative with a notable change in slope between 2.6 and 2.9 in. Differing from the VHES-LMC overlay thickness analysis, the trendlines at day 1 and beyond are of higher SR than the earlier ages. This indicates that for the VHES and VHES-LMC mockup, the overlay thickness has a greater influence on SR when the overlay is at least 1 day old.

The black trendline is average of all ages of the VHES overlay. The equation of the line shows a negative correlation between SR and overlay thickness, although at day 1 and 4 the correlation is almost one-to-one (low slope). It is hypothesized that the slope of the average trendline validates that the VHES overlay and conventional concrete base have dissimilar SR magnitude and the instability of the trendlines at later ages resembles the theory discussed about the SR evolution of VHES cements in the preliminary cylinder analysis in previous sections (Figure 4.11)

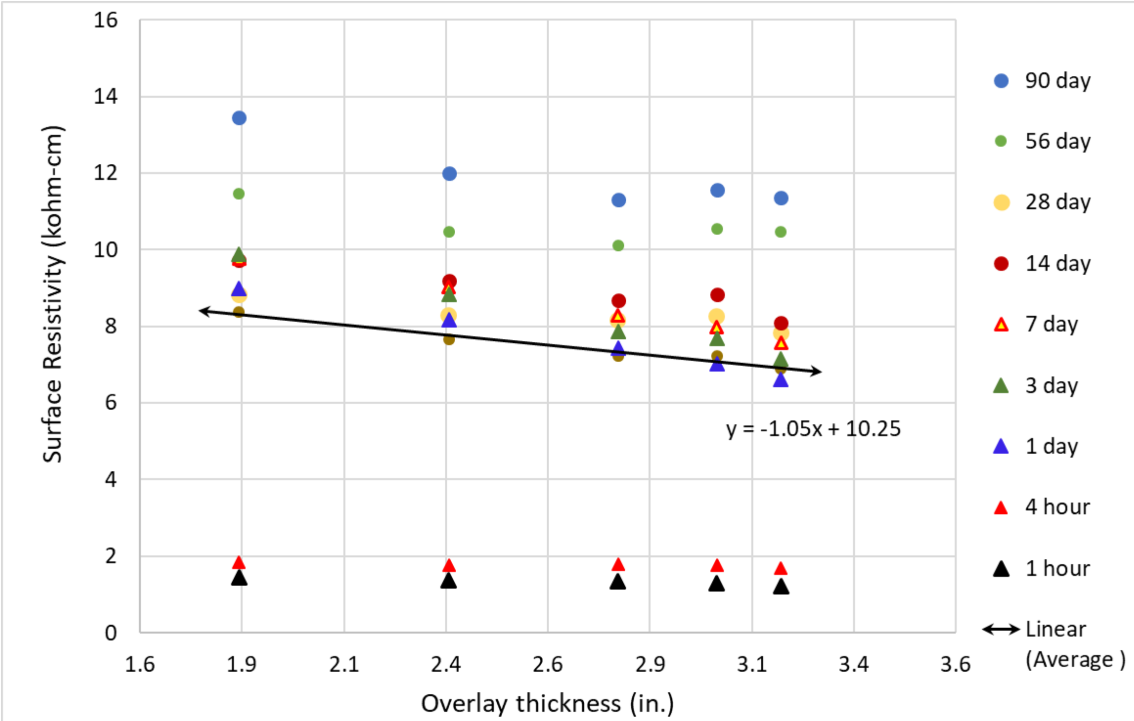

FIGURE 4.47: SR versus VHES overlay thickness

Based on Figure 4.47, Table 4.4 shows the trendline equation slope taken from each age and the calculated rate of change factor that can be used to estimate SR as the overlay thickness changes in 1 in. increments. For example, at 7 days and 28 days, as the VHES-LMC overlay thickness increased by 1 in., the SR decrease by 1.6 and 0.6 kohm-cm respectively.

TABLE 4.4: VHES line slope equation and ROC (overlay thickness vs. SR)

Age	Line slope equation	Rate of change
1 hour	y = -0.15x + 1.74	-0.2
4 hour	y = -0.1x + 2.0	-0.1
1 day	y = -1.75x + 12.25	-1.8
3 day	y = -1.99x + 13.53	-2.0
7 day	y = -1.62x + 12.80	-1.6
14 day	y = -1.06x + 11.70	-1.1
28 day	y = -0.60x + 9.86	-0.6
56 day	y = -0.70x + 12.44	-0.7
90 day	y = -1.51x + 15.92	-1.5

In Figure 4.48, the rate of change of SR per change in overlay thickness by 1 in. increments is graphed. The rate of change in SR decreases substantially having a negative correlation with overlay thickness where it reaches a turning point in the positive direction, yet the rate of change between SR and overlay thickness does not have a positive correlation. Overall, the graph shows a negative trend where the VHES overlay thickness influence on SR specific to this research can be estimated using Table 4.4.

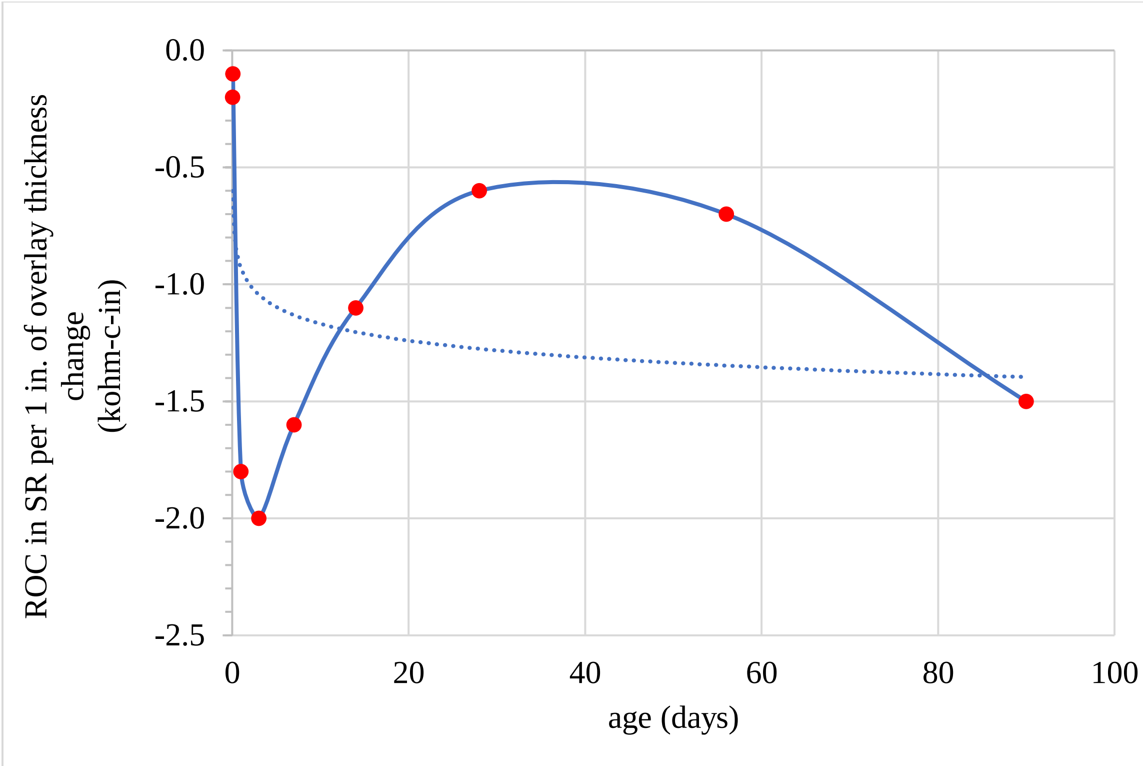

FIGURE 4.48: ROC of VHES

Similar to the previous mockups (LMC and VHES-LMC), edge effects were identified (recognized by higher SR values around perimeter cells) also voids were not explicitly identified by the expected orange or red cell appearance correlating with a decrease in SR magnitude. Figure 4.492, the 7 day average SR data with the voids superimposed on top (black shapes) is provided. Again, the average of all orientation was selected for analysis, and no clear detection of those voids was made so further analysis was conducted.

Average													
	Rebar										No Rebar		
	1	2	3	4	5	6	7	8	9	10	11	12	13
1	9.6	8.5	8.3	7.4	7.8	7.7	8.4	7.6	7.2	7.6	7.2	7.4	8.5
2	8.3	7.9	7.5	6.9	7.7	7.3	7	6.9	6.8	7.1	7.1	7.3	8.5
3	8.2	7.6	7	7	7.1	7.1	7.2	7.1	7.1	7.2	7.5	7.5	9.1
4	8.1	7.9	7.7	7.5	7.3	6.4	7.2	7.4	7.4	7.4	7.6	8	8.9
5	8.1	8.2	7.1	8.1	8.1	6.5	7.4	7.6	7.4	7.8	8.1	8.8	9.4
6	8.7	8	7.9	7.7	7.7	8.1	7.4	7.7	7.2	7.9	8.4	9	9.5
7	9	8.5	8.2	7.2	7.7	8	7.7	8.3	8	7.4	8.3	9.1	9.8
8	8.7	8.3	8.3	8.5	8.2	8.3	8.3	8.4	8.4	8.5	8.6	9.3	9.8
9	8.9	8.8	8.4	8.8	8.8	8.8	8.5	8.4	8.4	8.6	9.5	9.7	10
10	9.8	9.2	8.8	9	9.1	8.9	9	9.1	8.9	9.2	9.9	10	11
11	10	9.6	9.2	9.2	9.6	9.1	9.4	9.3	8.8	9.7	10	10	11
12	11	9.7	9	9.3	9.8	9.4	9.2	9.6	9.2	9.7	10	11	11
13	12	10	9.8	9.9	9.6	9.3	10	9.9	9.3	10	11	11	12

FIGURE 4.49: Voids superimposed on VHES mockup - 7 day average SR data

Figures 4.50 – 4.53 shows the degree of influence that the voids and reinforcement have on the SR measurement. Like the previous mockup analyses, this was accomplished by taking the average of all of the cells at each age with the following list of exclusions/inclusions, “No exclusions”, “No vertical reinforcement”, “No reinforcement”, “No reinforcement or voids”, “Vertical reinforcement only”, and “Vertical standard rebar only”. Each exclusion/inclusion designation is separated into its own line which is graphed in the following figures. The four figures are the diagonal (Figure 4.50), horizontal (Figure 4.51), vertical orientation (Figure 4.52), and average of orientations (Figure 4.53).

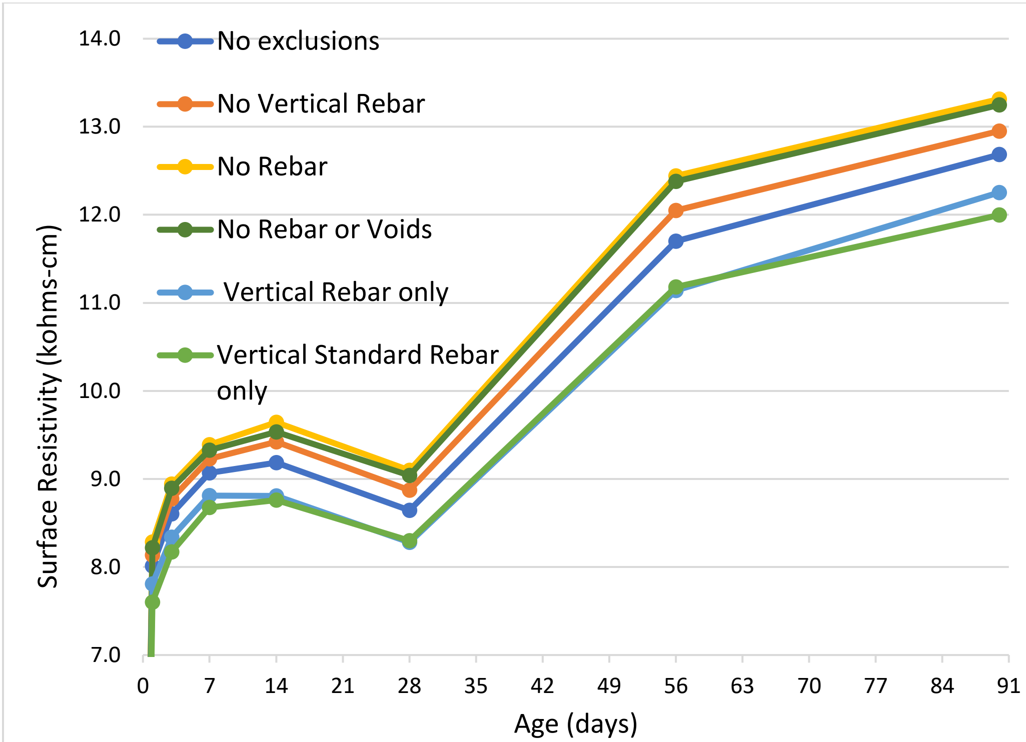

FIGURE 4.50: VHES mockup diagonal orientation with different exclusions

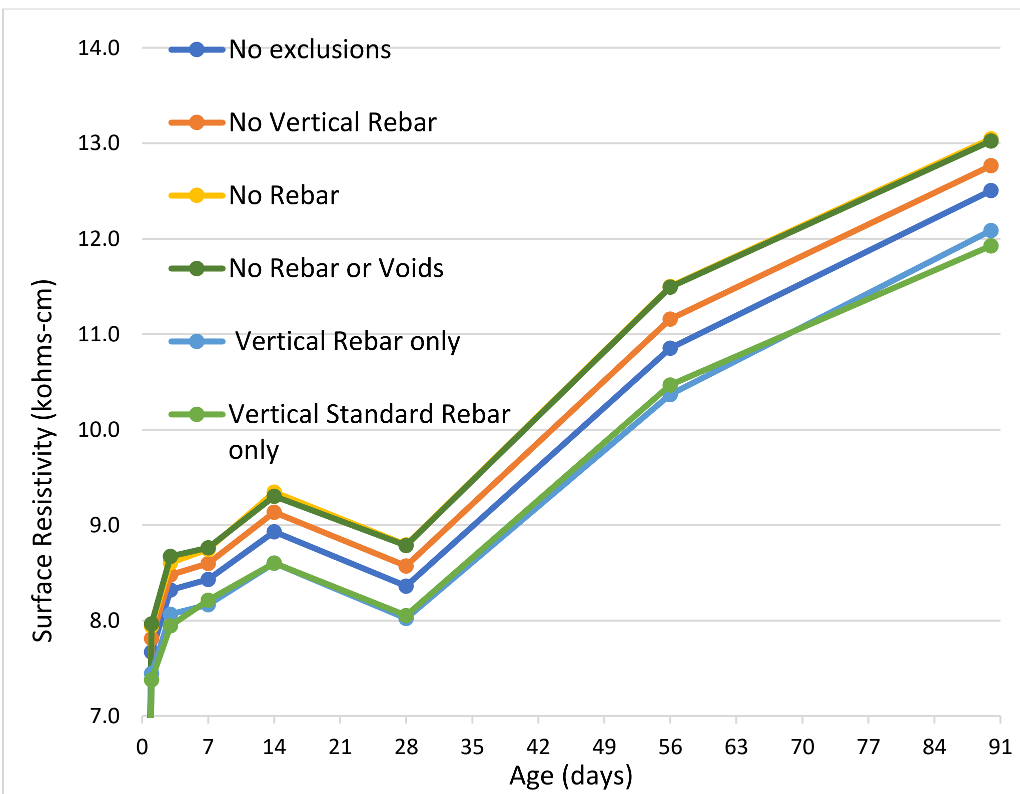

FIGURE 4.51: VHES mockup horizontal orientation with different exclusions

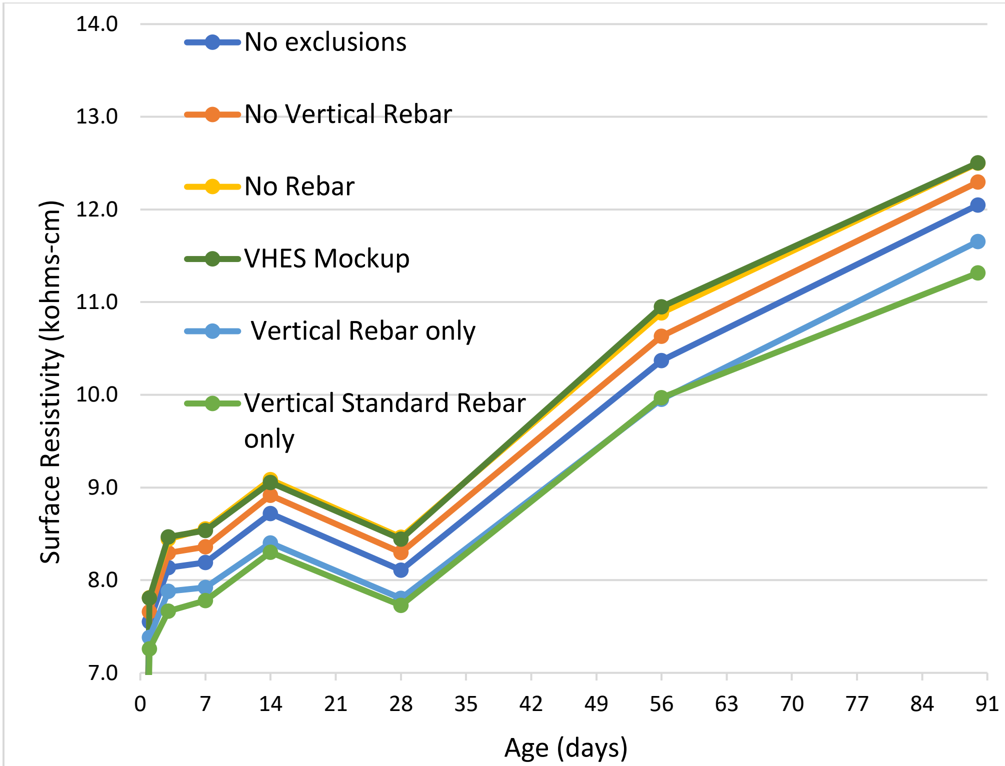

FIGURE 4.52: VHES mockup vertical orientation with different exclusions

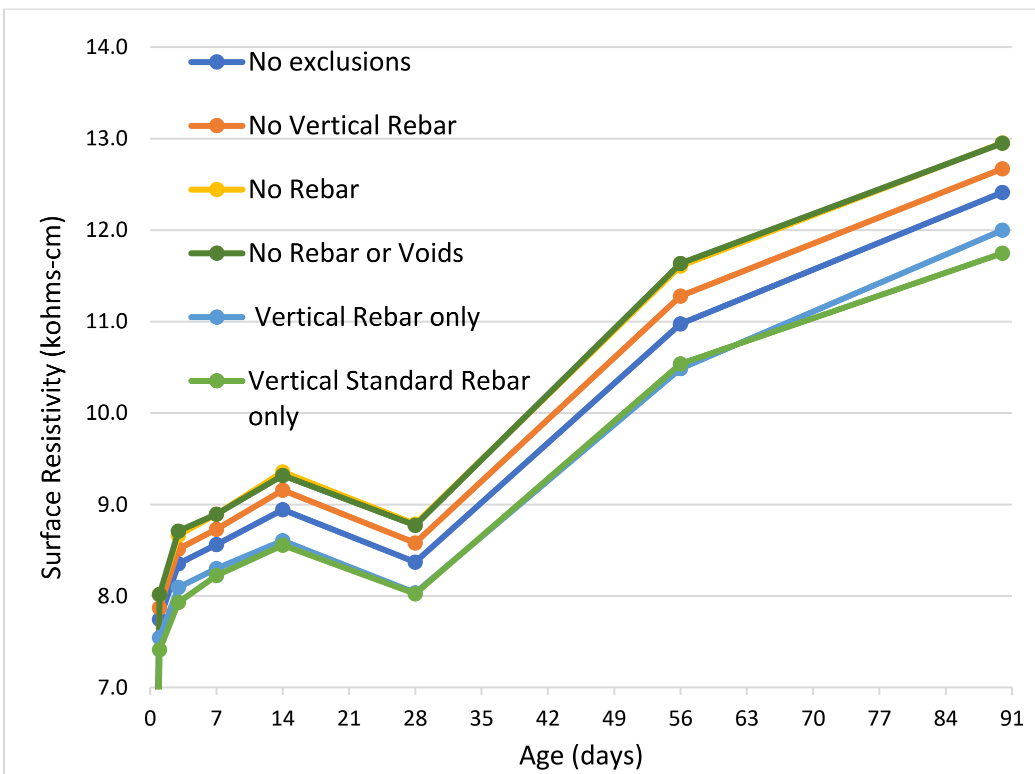

FIGURE 4.53: VHES mockup average of orientations with different exclusions

Each orientation and designation (Figures 4.50- 4.53) shows a similar dip at the 28 day SR testing. The basis for this occurrence may be related to 1) the water availability in the VHES mockup at this age, due to the rapid hydration) and 2) the ability of water applied prior to testing to penetrate the mockup. Overall, the vertical orientation datapoints are slightly lower than that of the diagonal and horizontal orientation. This may be the result of meter being positioned parallel to the steel reinforcement at each testing location, regardless of whether or not the meter is precisely on top of the steel.

Similar to the LMC and VHES-LMC mockups, the “No exclusions” designation (plotted line) resides in the middle of other inclusion/exclusion designations. The “No rebar” and “no rebar/voids” designations (plotted lines) track very similarly throughout the testing duration in all orientations and are the highest designations. Throughout the testing duration, the “Vertical rebar only” and “Vertical standard rebar only” designations show a similar magnitude and trend in all orientations, with the “vertical standard rebar only” designation tracking slightly lower on average, as expected. By the 90 day testing age, the “Vertical standard rebar only” designation falls relatively significantly, possibly confirming the greater influence of non-coated steel reinforcement on SR.

4.3.2.4 VHES-LMC overlay mockup

The identical method of overlay thickness variation was employed for the VHES-LMC mockup, yet the measurements vary from mockup to mockup for reasons explained in previous sections. Similarly, Figure 4.54 shows the thickness measurement extracted from the 3D surface scan which were taken at points between the reinforcement bars (bold lines) and are presented in color conditional formatting where the darker green represents greater thicknesses, as illustrated in the figure. The voids introduced into the mockups are displayed in Figure 4.55. Note the row and column labeling around the figure which are similar to the other mockups.

The VHES-LMC overlay mockup analysis includes the same perspectives as the LMC and VHES mockup with the addition of another void (Figure 4.55). This dataset was also acquired at the 7 day age. Again, the analysis titled “Row average - No vertical rebar/No voids” are a collection of measurements excluding those instances and are averaged with the intention of identify the influence of voids and steel reinforcement on SR. Those measurements are found on the right side of the Figures 4.56 – 4.59. The “Row average – All points” measurements include every measurement point (13 points). The analysis titled “Row average – No vertical rebar” contain measurements at columns 1, 3, 5, 7, 9, 11, 12, and 13. The “Row average - No vertical rebar/No voids” measurement points begin with the same non-vertical rebar location framework (columns 1, 3, 5, 7, 9, 11, 12, and 13) and selected cells are excluded per row where void material was placed (Figure 4.40). The complete SR data/heatmaps of other ages (1, 4 hr., 1, 3, 14, 28, 56, and 90 day) of the VHES-LMC mockup can be found in Appendix D.

3.4	3.6	4.0	3.6	4.0	4.2	3.8
3.3	3.1	3.2	3.2	3.1	3.3	3.8
2.8	2.8	2.9	2.9	2.9	2.8	3.3
2.4	2.4	2.6	2.7	2.6	2.7	2.5
2.3	2.4	2.4	2.5	2.4	2.5	2.3
1.8	1.9	2.0	2.0	2.0	1.9	1.8
1.4	1.5	1.8	1.4	1.3	1.4	1.4

FIGURE 4.54: VHES-LMC mockup overlay thickness measurements

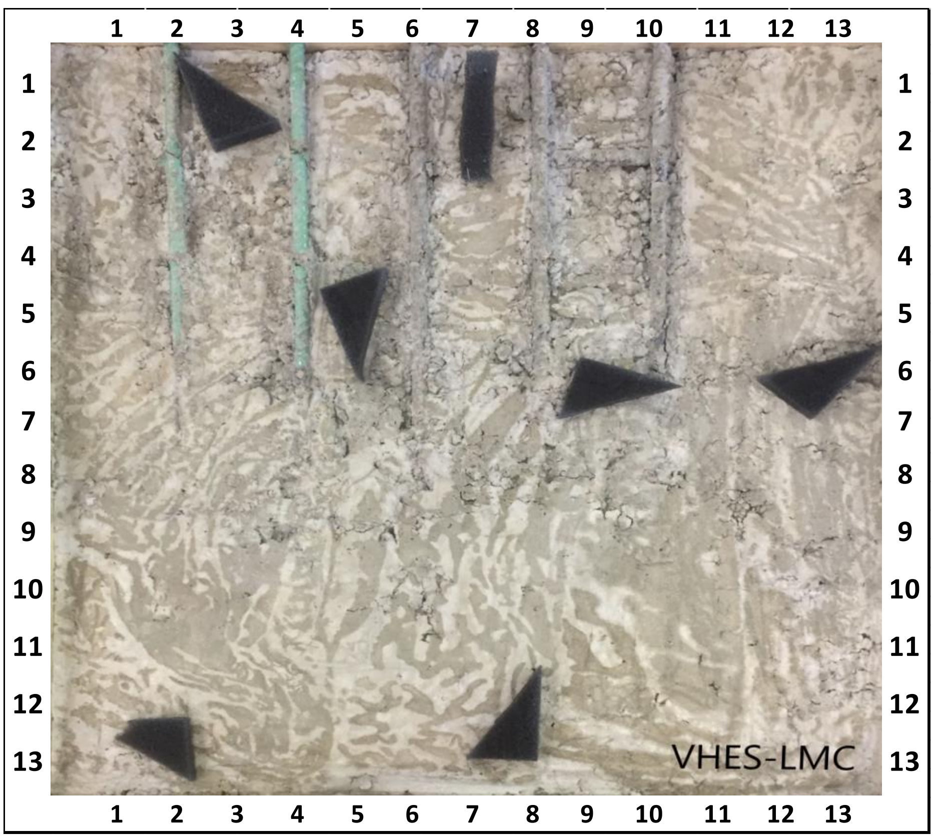

FIGURE 4.55: VHES-LMC mockup void locations

Diagonal														Row Average		
	Rebar										No Rebar			All Points	No vert bar	No vert bar/void
	1	2	3	4	5	6	7	8	9	10	11	12	13			
1	16	12	12	13	11	12	12	9.6	11	12	11	11	12	11.877	11.963	11.950
2	13	11	12	10	9.4	10	9.3	9.6	9.8	11	11	11	12	10.762	10.988	10.988
3	13	12	9.6	11	12	12	11	10	10	11	11	11	13	11.223	11.213	11.100
4	13	13	13	12	11	11	11	9.4	11	10	11	12	12	11.469	11.688	11.688
5	13	14	13	12	11	11	11	12	11	11	12	11	13	11.933	11.925	11.920
6	13	14	13	13	12	12	13	12	12	12	12	12	11	12.446	12.363	12.533
7	13	13	14	12	12	12	12	13	13	13	13	13	13	12.823	12.800	12.829
8	15	13	14	13	12	14	13	14	14	14	13	14	14	13.731	13.800	13.800
9	16	14	14	14	14	14	13	14	15	14	14	16	16	14.300	14.575	14.575
10	17	15	15	13	14	13	13	15	15	16	15	15	18	14.885	15.125	15.125
11	16	15	16	16	15	15	14	15	15	16	16	17	19	15.823	16.163	16.163
12	16	17	16	18	17	17	18	17	16	17	17	18	20	17.231	17.250	17.250
13	18	17	16	18	17	17	19	19	18	18	18	18	17	17.708	17.650	17.300
														13.555	13.654	13.632

FIGURE 4.56: VHES-LMC overlay mockup – SR diagonal orientation at 7 days

Horizontal														Row Average		
											No Rebar			All Points	No vert bar	No vert bar/void
	1	2	3	4	5	6	7	8	9	10	11	12	13			
1	13	13	12	11	11	9.6	10	9.6	10	10	9.6	10	12	10.838	11.013	11.050
2	12	11	11	9.2	9	9.4	8.9	8.7	9.8	9.7	9.5	10	13	10.115	10.413	10.413
3	13	12	10	9.8	10	11	9.1	8.6	9	9.7	10	11	12	10.269	10.413	10.471
4	14	13	12	12	10	9.1	8.9	9.5	10	10	11	11	13	10.933	11.125	11.125
5	12	13	13	12	11	11	11	11	11	12	11	10	13	11.631	11.588	11.660
6	14	14	12	12	12	11	11	12	11	12	12	11	12	11.962	11.925	12.050
7	13	13	13	12	13	12	12	13	12	14	12	12	13	12.477	12.400	12.443
8	15	14	13	13	12	13	12	13	13	14	13	13	14	13.169	13.163	13.163
9	15	15	14	12	13	13	11	14	14	14	13	14	15	13.700	13.700	13.700
10	16	15	14	14	13	13	13	15	14	15	14	15	17	14.469	14.550	14.550
11	17	16	15	15	15	15	14	15	15	16	15	18	20	15.738	16.000	16.000
12	18	16	16	16	17	17	17	16	16	16	15	17	18	16.377	16.688	16.688
13	19	18	16	16	16	16	18	20	17	16	16	18	17	17.200	17.113	16.733
														12.991	13.084	13.080

FIGURE 4.57: VHES-LMC overlay mockup – SR horizontal orientation at 7 days

	Vertical													Row Average		
											No Rebar			All Points	No vert bar	No vert bar/void
	1	2	3	4	5	6	7	8	9	10	11	12	13			
1	13	12	11	11	11	11	11	9.5	11	10	11	11	12	11.069	11.388	11.500
2	13	10	11	9.3	9.4	9.7	9.7	9.8	9.4	9	11	10	11	10.162	10.513	10.513
3	13	11	9.8	9.3	9.8	9.8	9.6	11	9	9.6	10	9.5	11	10.133	10.229	10.290
4	13	12	11	11	9.5	10	9.8	9.8	11	10	10	10	12	10.685	10.700	10.700
5	12	13	12	12	11	12	11	11	11	11	10	11	12	11.277	11.088	11.080
6	13	13	13	12	12	12	11	12	12	11	11	11	10	11.738	11.650	11.950
7	13	13	12	13	11	12	12	12	11	13	12	11	12	12.192	11.838	11.914
8	14	12	13	13	12	13	12	13	13	14	13	13	14	12.846	12.763	12.763
9	15	13	13	12	13	13	12	15	13	13	13	13	14	13.123	13.138	13.138
10	16	15	14	13	13	13	13	15	14	15	14	15	16	14.269	14.338	14.338
11	16	15	15	15	14	14	15	14	15	15	15	16	18	15.138	15.400	15.400
12	16	16	16	17	16	16	15	17	16	15	16	18	19	16.323	16.400	16.400
13	16	17	16	17	16	16	16	18	16	17	17	17	17	16.800	16.563	16.650
														12.750	12.770	12.818

FIGURE 4.58: VHES-LMC overlay mockup – SR vertical orientation at 7 days

	Average													Row Average		
	Rebar										No Rebar			All Points	No vert bar	No vert bar/void
	1	2	3	4	5	6	7	8	9	10	11	12	13			
1	14	12	12	12	11	11	11	9.6	11	11	10	11	12	11.262	11.454	11.500
2	13	11	11	9.6	9.3	9.8	9.3	9.4	9.7	9.8	11	10	12	10.346	10.638	10.638
3	13	12	9.8	9.9	11	11	9.8	9.7	9.3	10	10	11	12	10.542	10.618	10.620
4	13	12	12	12	10	10	10	9.6	11	10	11	11	12	11.029	11.171	11.171
5	12	13	12	12	11	11	11	11	11	11	11	11	13	11.614	11.533	11.553
6	14	13	13	12	12	12	12	12	12	12	11	12	11	12.049	11.979	12.178
7	13	13	13	12	12	12	12	13	12	13	12	12	13	12.497	12.346	12.395
8	15	13	13	13	12	13	12	13	13	14	13	13	14	13.249	13.242	13.242
9	15	14	14	13	13	13	12	14	14	14	13	14	15	13.708	13.804	13.804
10	16	15	14	14	13	13	13	15	14	15	14	15	17	14.541	14.671	14.671
11	16	15	15	15	15	15	14	15	15	15	15	17	19	15.567	15.854	15.854
12	17	16	16	17	17	17	17	16	16	16	16	17	19	16.644	16.779	16.779
13	18	18	16	17	16	17	18	19	17	17	17	18	17	17.236	17.108	16.894
														13.099	13.169	13.177

FIGURE 4.59: VHES-LMC overlay mockup – SR average of orientations at 7 days

Standard Deviation													
	Rebar										No Rebar		
	1	**2**	**3**	**4**	**5**	**6**	**7**	**8**	**9**	**10**	**11**	**12**	**13**
1	1.3	0.5	0.2	1.4	0.2	1.2	1.1	0.1	0.6	0.9	0.6	0.6	0.2
2	0.5	0.6	0.4	0.6	0.2	0.4	0.4	0.6	0.2	0.8	1	0.5	0.9
3	0.2	0.9	0.3	0.7	1.2	1.2	0.8	1	0.6	0.7	0.3	1	0.7
4	0.4	0.8	0.8	0.1	0.7	1	1.2	0.2	0.4	0.1	0.6	0.8	0.6
5	0.3	0.4	0.6	0.3	0.4	0.3	0.4	0.6	0.3	0.3	0.7	0.6	0.9
6	0.4	0.7	0.5	0.6	0.2	0.6	1.1	0.4	0.6	0.2	0.8	0.6	0.8
7	0.3	0.2	0.8	0.8	0.8	0.3	0.1	0.2	0.7	0.1	0.7	0.6	0.8
8	0.9	0.7	0.9	0.1	0.3	0.6	0.7	0.4	1	0.3	0.1	0.9	0.2
9	0.3	1.1	1	0.8	0.6	0.3	1.2	0.2	1.1	0.7	0.6	1.4	0.7
10	0.8	0.3	0.4	0.6	0.3	0.2	0.2	0.5	0.4	0.8	0.5	0.2	1
11	0.6	0.8	0.9	0.2	0.5	0.5	0.5	0.5	0.2	0.3	0.6	1	0.7
12	0.8	0.8	0.1	0.9	0.8	0.5	1.3	0.6	0.1	1.3	0.8	0.9	1.1
13	1.2	0.8	0.1	0.8	0.5	0.6	1.4	0.7	0.8	0.9	0.7	0.3	0.5

FIGURE 4.60: VHES-LMC mockup – SR standard deviation at 7 days

Similar to the LMC and VHES analysis of overlay thickness influence on SR, Figure 4.61 is provided for the VHES-LMC overlay. The data used was from the average of orientation measurements row analysis from the VHES-LMC mockups at each age (Appendix D – VHES-LMC: 1 hour, 4 hour, 1, 3, 7, 14, 28, 56, and 90 day), and rows 1 and 13 were left out due to edge effects. The measurements taken on top of the reinforcement were also omitted, leaving 5 rows. Similar to the LMC analysis, a low slope linear trend occurs at early ages (1-4 hour) depicting a similar SR, but by day 1, the trend becomes less linear and more negative with a dip between 2.4 and 2.9 in. The bold black trendline is average of all ages of the VHES-LMC overlay. The equation of the line shows a negative correlation between SR and overlay thickness. It is hypothesized that the slope of the average trendline validates that the VHES-LMC overlay and conventional concrete base have dissimilar SR magnitude and the instability of the trendlines at later ages resembles the theory discussed about the SR evolution of VHES cements in the preliminary cylinder analysis in previous sections (Figure 4.11)

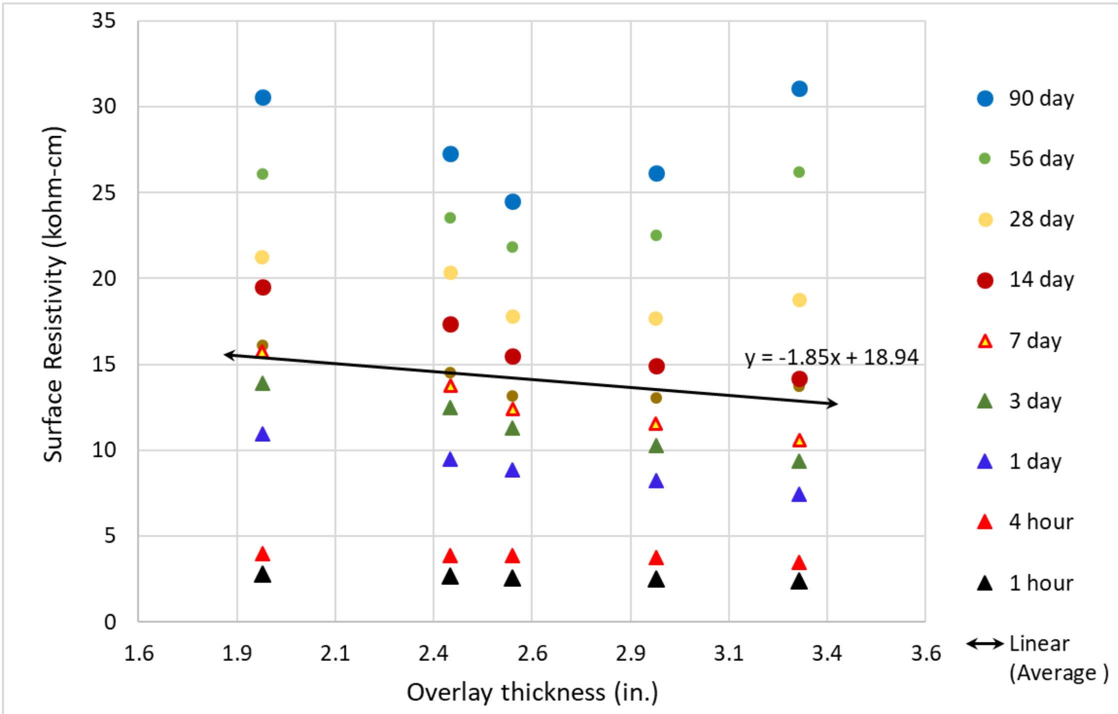

FIGURE 4.61: SR versus VHES-LMC overlay thickness

Based on Figure 4.61, Table 4.5 shows the line slope equation taken from each age and the calculated rate of change factor that can be used to estimate SR as the overlay thickness changes in 1 in. increments. For example, at 7 days and 28 days, as the VHES-LMC overlay thickness increased by 1 in., the SR decrease by 3.8 and 2.2 kohm-cm respectively.

TABLE 4.5: VHES-LMC line slope equation and ROC (overlay thickness vs. SR)

Age	Line slope equation	Rate of change
1 hour	y = -0.28x + 3.31	-0.3
4 hour	y = -0.37x + 4.75	-0.4
1 day	y = -2.54x + 15.61	-2.5
3 day	y = -3.41x + 20.36	-3.4
7 day	y = -3.81x + 22.77	-3.8
14 day	y = -3.97x + 26.64	-4.0
28 day	y = -2.17x + 24.84	-2.2
56 day	y = -0.16x + 24.44	-0.2
90 day	y = 0.07x + 27.74	-0.1

In Figure 4.62, the rate of change of SR per change in overlay thickness by 1 in. increments is graphed. Similar to Figure 4.61, the rate of change starts out linear (predictable) by day 28 the trend becomes less linear. In Figure 4.46 the rate of change in SR decreases substantially having a negative correlation with overlay thickness where it reaches a turning point in the positive direction, yet the rate of change between SR and overlay thickness does not have a positive correlation. Overall, the graph shows a negative trend where the VHES-LMC overlay thickness influence on SR specific to this research can be estimated using Table 4.5.

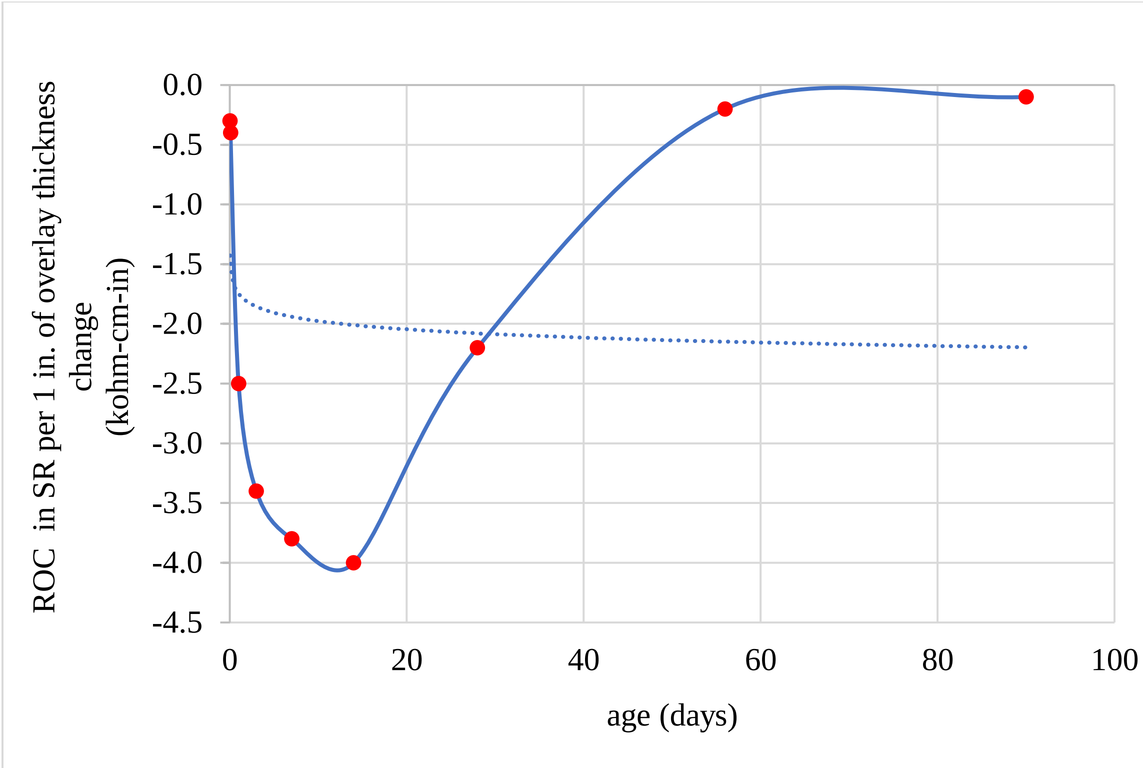

FIGURE 4.62: ROC of VHES-LMC

Similar to the previous mockup (LMC), voids were not explicitly identified in the VHES-LMC mockup by the expected orange or red cell appearance correlating with a decrease in SR magnitude. Also, edge effects were identified in the VHES-LMC mockups but not to the extent as in the LMC mockup. Figure 4.63, the 7 day average SR data with the voids superimposed on top (black shapes) is provided. The average of all orientation was selected, and again no clear detection was made so further analysis was conducted.

Average													
	Rebar										No Rebar		
Reading #	1	2	3	4	5	6	7	8	9	10	11	12	13
1	3.5	3.3	3.3	3.7	3.5	3.6	3.4	3.3	3.7	3.6	3.5	3.2	3.8
2	3.3	3.3	3.5	3.2	3.1	3.3	3.5	3.4	3.7	3.4	3.3	3.1	3.7
3	3.3	3.2	3.2	3.3	3.2	3	3.3	3.5	3.6	3.3	3.2	3.1	3.8
4	3.4	3.3	3.3	3.3	3	3.1	3.4	3.5	3.3	3.6	3.3	3.4	3.5
5	3.6	3.4	3.7	3.8	3	3.3	3.2	3.4	3.3	3.5	3.1	3.2	3.5
6	3.4	3.4	3.3	3.4	3.2	3.4	3.3	3	3.4	3	3	3.2	3.7
7	3.3	3.3	3.3	3.5	3.3	3.4	3.3	3	3.3	3.3	3	3.4	3.9
8	3.4	3.2	3.3	3.5	3.2	3.2	3.3	3.5	3.5	3.5	3.2	3.3	3.6
9	3.4	3.1	3.1	3	3.2	3.4	3.5	3.7	3.3	3.4	3.1	3	3.8
10	3.2	3.2	3.2	3	3.3	3.2	3.4	3.4	3.5	3.2	3.2	3.4	3.8
11	3.3	3.2	3.3	3.1	3.2	3.4	3.3	3.4	3.4	3.3	3.1	3.3	3.6
12	3.4	3.6	3.3	3.1	3.3	3.3	3.4	3.4	3.1	3.3	3.5	3.2	3.5
13	3.9	3.7	3.6	3.6	3.3	3.4	3.5	3.8	3.5	3.5	3.3	3.3	3.4

FIGURE 4.63: Voids superimposed on VHES-LMC mockup - 7 day average SR data

Figures 4.64 – 4.67 shows the degree of influence that the voids and reinforcement have on the SR measurement. This was accomplished by taking the average of all of the cells at each age with the following list of exclusions/inclusions, “No exclusions”, “No vertical reinforcement”, “No reinforcement”, “No reinforcement or voids”, “Vertical reinforcement only”, and “Vertical standard rebar only”. Each exclusion/inclusion designation is separated into its own line which is graphed in the following figures. The four figures are the diagonal (Figure 4.64), horizontal (Figure 4.65), vertical orientation (Figure 4.66), and average of orientations (Figure 4.67).

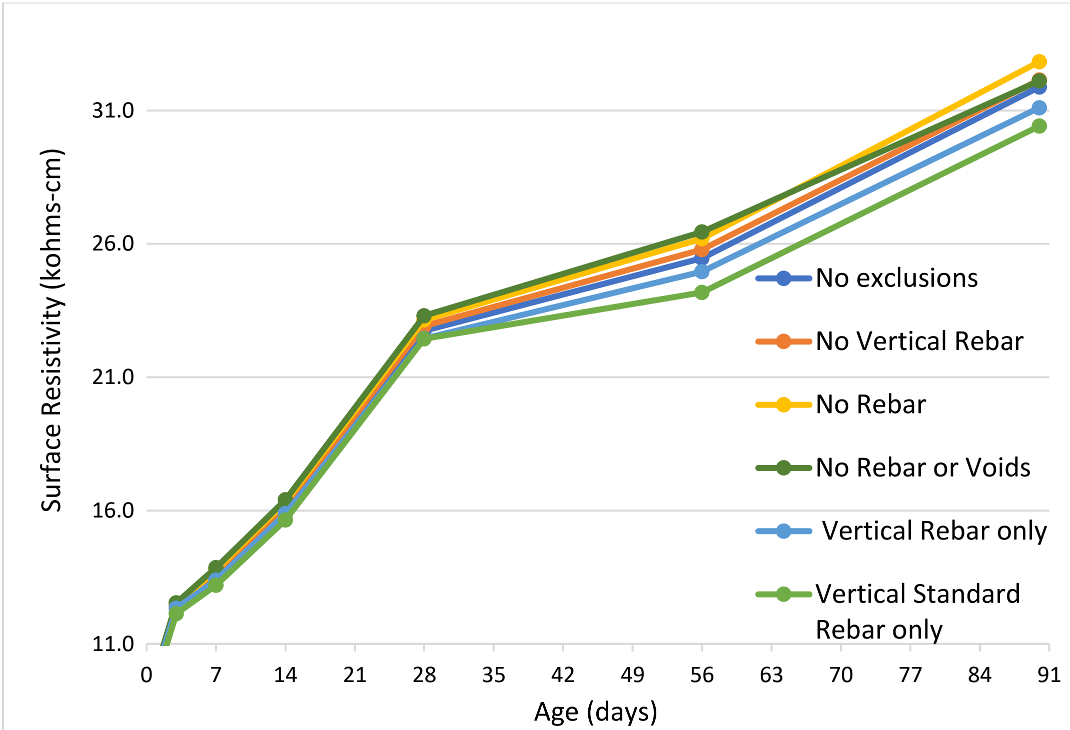

FIGURE 4.64: VHES-LMC mockup diagonal orientation with different exclusions

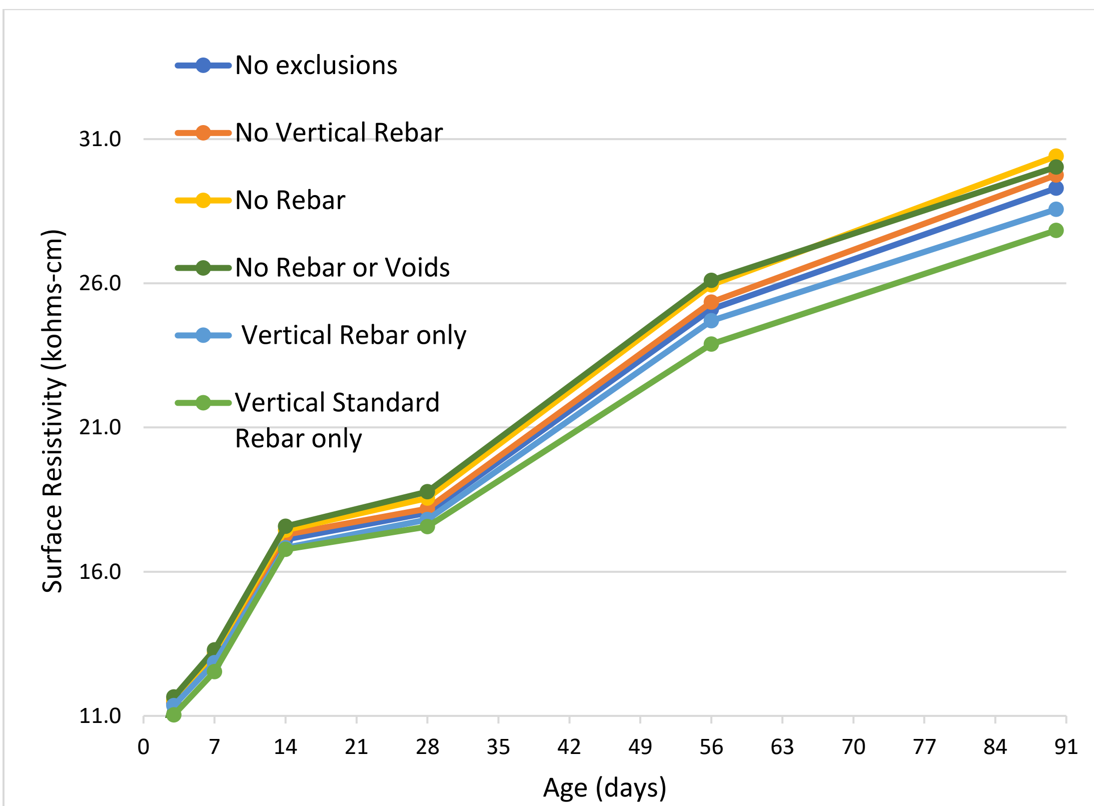

FIGURE 4.65: VHES-LMC mockup horizontal orientation with different exclusions

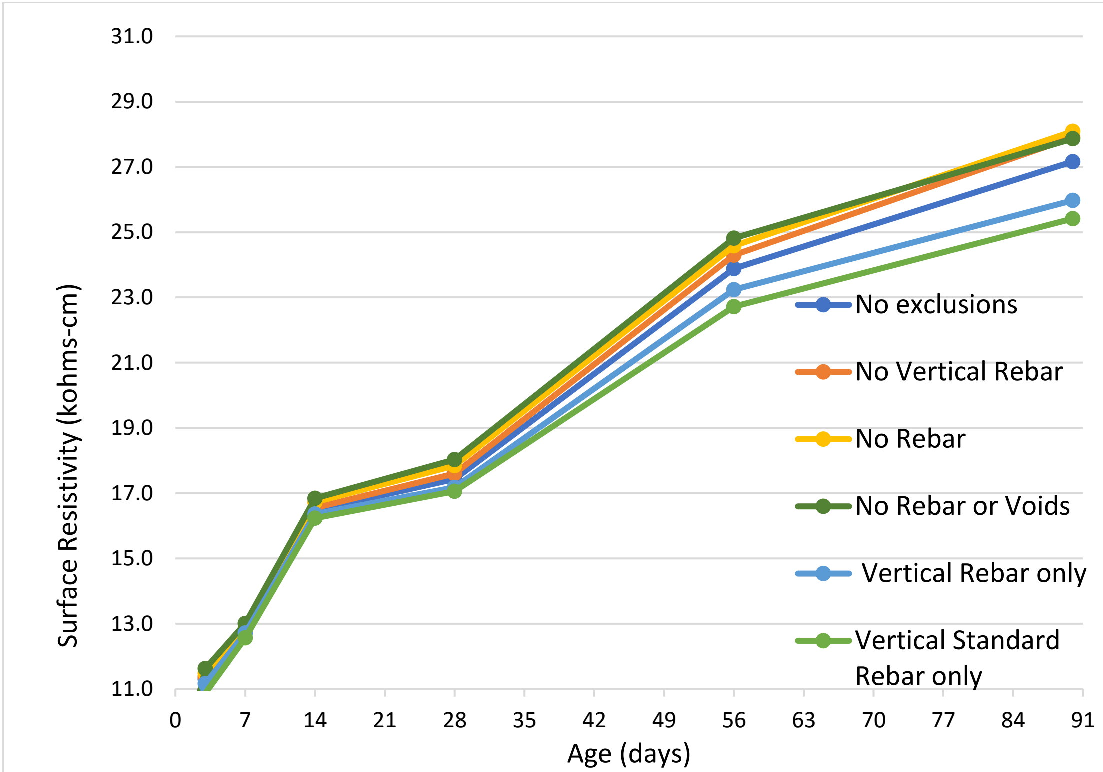

FIGURE 4.66: VHES-LMC mockup vertical orientation with different orientations

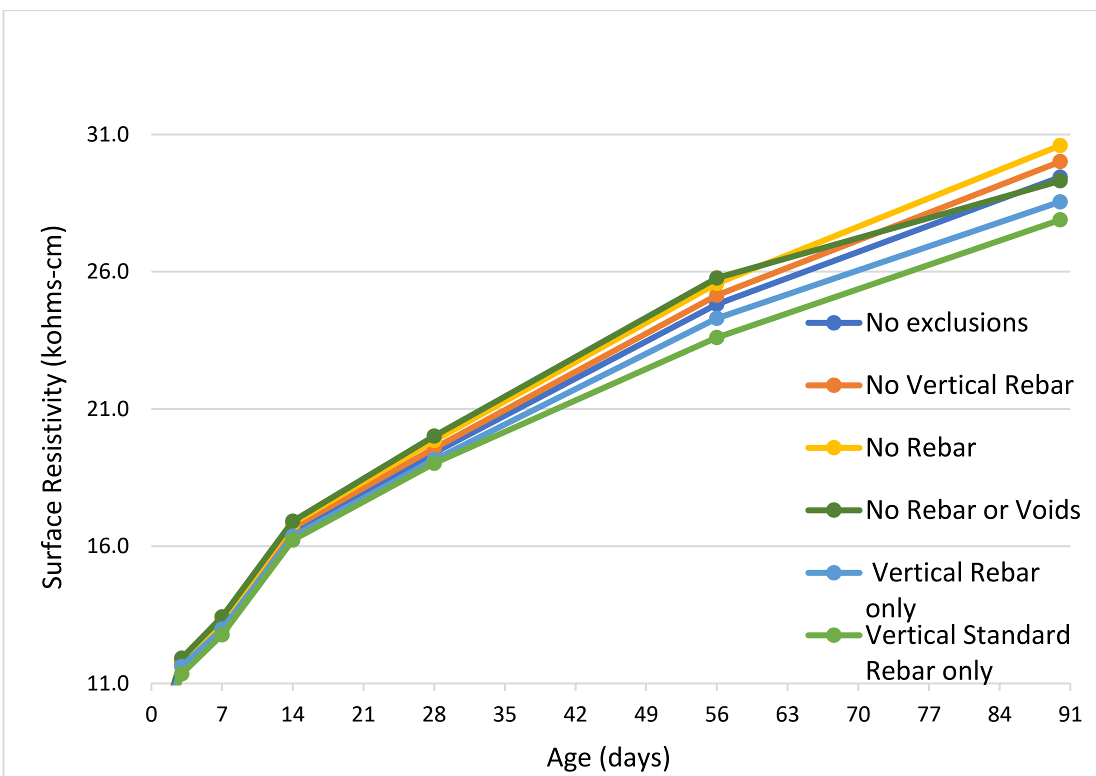

FIGURE 4.67: VHES-LMC mockup average of orientations with different exclusions

For an overall perspective, the average magnitude of SR decreases by orientation to the reinforcing bars in the following order, diagonal, horizontal, then vertical. This incidence was not found in the LMC mockup (Figures 4.36 – 4.39). This is because when the meter is in the vertical orientation, the current field parallel to the reinforcement, resulting in more influence on the resistivity, correlating to a lower SR. It should also be understood that the mockups were tested in that same order by orientation (diagonal, horizontal, then vertical), while applying water each round of testing, resulting in a higher saturation of water, if the material can absorb it. As discussed in the literature, an increase in water content has a negative influence on SR magnitude. Unlike the LMC mockup discussed in previous sections, there is a noticeable dip in the trendlines in the horizontal and vertical orientations, but not in the diagonal orientation. The reason for this occurrence is not understood at this time.

Similar to the previous mockup, by observing Figures 4.64 – 4.67, it is concluded that the average measurements of "Vertical standard reinforcement only" are of the lowest magnitude, and the average measurements of "No reinforcement" were of the highest SR, as expected and show a similar trend across the orientations and average of orientations. But the designation "No reinforcement or voids" did not fall into the similar rank as in the LMC mockup analysis in Figure 4.67, the LMC average inclusion/exclusion figure. Most notably, the 90 day "No reinforcement or voids" data point within the average of orientation graph (Figure 4.67) did not increase as much in SR, following the other designations. Rather the designation with the greatest SR at 90 days was the "No reinforcement", or reinforcement exclusion perspective, as could be expected. Similar to the LMC mockup analysis, the "No exclusions" designation often fell between SR-increasing exclusions and above designations that are expected to decrease SR. This aligns with a hypothesis that the "No exclusions" is somewhat of an average or benchmark when analyzing inclusions and exclusions.

4.5 SR and compressive strength test results of 4 in. x 8 in. cylinders

In addition to the SR analysis of the mockups, as introduced in previous sections, 4 in. by 8 in. concrete cylinders were cast from each concrete mixture to accompany each mockup. These cylinders were tested for SR and then the same cylinders were reused to be tested for compressive strength at each age. Table 4.6 shows SR results and Figure 4.68 is the graph illustrating the evolution of SR (dashed trendlines). The two solid trendlines in Figure 4.68 are the average of similar mixtures (CC averaged with LMC and VHES averaged with VHES-LMC). The compressive strength results can be found in Table 4.7 and the compressive strength evolution is graphed in Figure 4.69.

TABLE 4.6: SR (kohm-cm) results of CC ready-mix, LMC, VHES, and VHES-LMC 4 in. x 8 in. cylinders

	CC Ready-mix				LMC				VHES				VHES-LMC			
	specimens 1-3				specimens 1-3				specimens 1-3				specimens 1-3			
	1	2	3	avg.	1	2	3	avg.	1	2	3	avg.	1	2	3	avg.
Q 1									2.4	2.4	2.4		5.3	6.0	5.9	
Q 2									2.4	2.2	2.5		5.7	6.0	5.7	
Q 3									2.6	2.3	2.2		5.5	6.2	5.7	
Q 4									2.3	2.1	2.2		5.5	6.5	5.9	
1 hr. avg.									2.4	2.3	2.3	2.3	5.5	6.2	5.8	5.8
Q 1									3.1	2.8	3.0		6.5	6.6	6.9	
Q 2									2.9	2.7	2.9		6.3	6.7	6.7	
Q 3									2.9	2.7	3.0		6.1	6.6	7.0	
Q 4									3.0	2.9	3.1		6.0	6.5	7.0	
2 hr. avg.									3.0	2.8	3.0	2.9	6.2	6.6	6.9	6.6
Q 1									3.3	3.6	3.7		9.7	10.7	10.2	
Q 2									2.9	3.4	3.6		9.1	10.8	10.3	
Q 3									2.8	3.7	3.9		9.2	10.7	11.2	
Q 4									3.2	3.4	3.3		9.8	10.1	10.3	
4 hr. avg.									3.1	3.5	3.6	3.4	9.5	10.6	10.5	10.2
Q 1	2.4	2.2	2.1		4.7	4.4	4.6		5.0	8.0	8.1		10.2	9.9	10.9	
Q 2	2.3	2.3	2.0		4.4	4.3	4.4		4.5	7.3	7.8		10.3	10.5	11.0	
Q 3	2.1	2.3	2.1		4.5	4.2	4.5		5.3	8.8	8.0		10.0	10.9	10.2	
Q 4	2.2	2.2	2.9		4.6	4.3	4.5		5.7	8.4	8.2		9.9	10.1	10.0	
1 day avg.	2.3	2.3	2.3	2.3	4.6	4.3	4.5	4.4	5.1	8.1	8.0	7.1	10.1	10.4	10.5	10.3
Q 1	2.5	2.6	2.7		8.0	7.8	8.0		7.8	7.1	8.9		11.4	10.7	9.8	
Q 2	2.8	2.6	2.3		7.8	8.1	7.9		7.6	6.9	9.5		11.9	10.0	9.4	
Q 3	2.9	2.8	2.7		8.3	8.4	8.0		6.9	6.9	8.9		11.0	10.0	8.9	
Q 4	2.5	2.8	2.7		7.6	7.8	8.0		6.7	7.2	9.2		11.5	10.4	9.8	
3 day avg.	2.7	2.7	2.6	2.7	7.9	8.0	8.0	8.0	7.3	7.0	9.1	7.8	11.5	10.3	9.5	10.4
Q 1	3.5	3.5	3.5		9.6	9.8	9.7		7.1	6.7	10.1		11.9	10.3	10.1	
Q 2	3.3	3.7	3.5		9.6	9.4	9.5		7.0	6.7	10.3		11.3	12.2	10.6	
Q 3	3.4	3.3	3.8		9.6	9.8	9.8		7.5	6.4	10.2		12.1	11.7	9.6	
Q 4	3.5	3.4	3.6		9.4	10.1	10.1		6.8	6.5	9.9		11.3	11.0	10.1	
7 day avg.	3.4	3.5	3.6	3.5	9.6	9.8	9.8	9.7	7.1	6.6	10.1	7.9	11.7	11.3	10.1	11.0
Q 1	4.7	4.9	4.8		11.7	11.5	11.7		10.2	9.8	10.5		11.3	9.9	10.7	
Q 2	4.7	4.4	4.8		10.5	11.8	11.0		10.3	10.9	10.6		11.1	10.0	10.9	
Q 3	4.6	4.4	4.2		11.3	11.6	11.7		10.0	10.4	10.8		11.0	9.6	10.8	
Q 4	4.3	4.1	4.6		10.8	11.7	11.8		10.6	10.7	10.5		11.2	9.9	10.9	
14 day avg.	4.6	4.5	4.6	4.5	11.1	11.7	11.6	11.4	10.3	10.5	10.6	10.4	11.2	9.9	10.8	10.6
Q 1	6.1	5.8	6.1		13.7	14.4	14.0		10.6	11.9	11.5		13.4	12.9	13.0	
Q 2	6.0	6.4	6.3		14.3	14.3	14.6		11.8	11.8	11.0		13.2	14.1	13.7	
Q 3	5.6	6.6	6.2		13.8	14.1	14.2		11.5	11.4	11.8		13.6	13.6	12.2	
Q 4	5.8	6.2	5.8		14.1	14.4	14.0		10.7	10.9	11.2		15.0	13.1	13.5	
28 day avg.	5.9	6.3	6.1	6.1	14.0	14.3	14.2	14.2	11.2	11.5	11.4	11.3	13.8	13.4	13.1	13.4
Q 1	9.3	10.4	9.8		17.1	17.1	17.2		13.0	12.3	14.1		14.9	19.6	14.1	
Q 2	9.8	10.0	10.0		17.5	17.3	18.4		13.4	11.0	13.4		14.4	17.6	14.5	
Q 3	9.0	10.8	9.4		16.7	16.7	17.6		12.8	12.3	13.9		14.5	19.8	14.7	
Q 4	9.2	10.3	9.2		17.9	17.2	17.8		12.4	12.8	13.4		14.3	18.7	15.1	
56 day avg.	9.3	10.4	9.6	9.8	17.3	17.1	17.8	17.4	12.9	12.1	13.7	12.9	14.5	18.9	14.6	16.0
Q 1	14.3	15.3	14.3		20.4	19.5	19.8		16.0	15.4	14.4		23.3	30.0	20.0	
Q 2	14.8	14.7	14.0		20.1	19.8	19.8		16.2	14.4	11.9		19.2	30.8	20.5	
Q 3	13.9	14.1	13.7		20.1	20.1	21.0		16.4	14.2	12.7		18.8	35.0	19.8	
Q 4	14.0	14.6	14.6		18.7	19.4	20.3		15.7	14.0	13.6		18.1	32.0	19.9	
90 day avg.	14.3	14.7	14.2	14.4	19.8	19.7	20.2	19.9	16.1	14.5	13.2	14.6	19.9	32.0	20.1	24.0

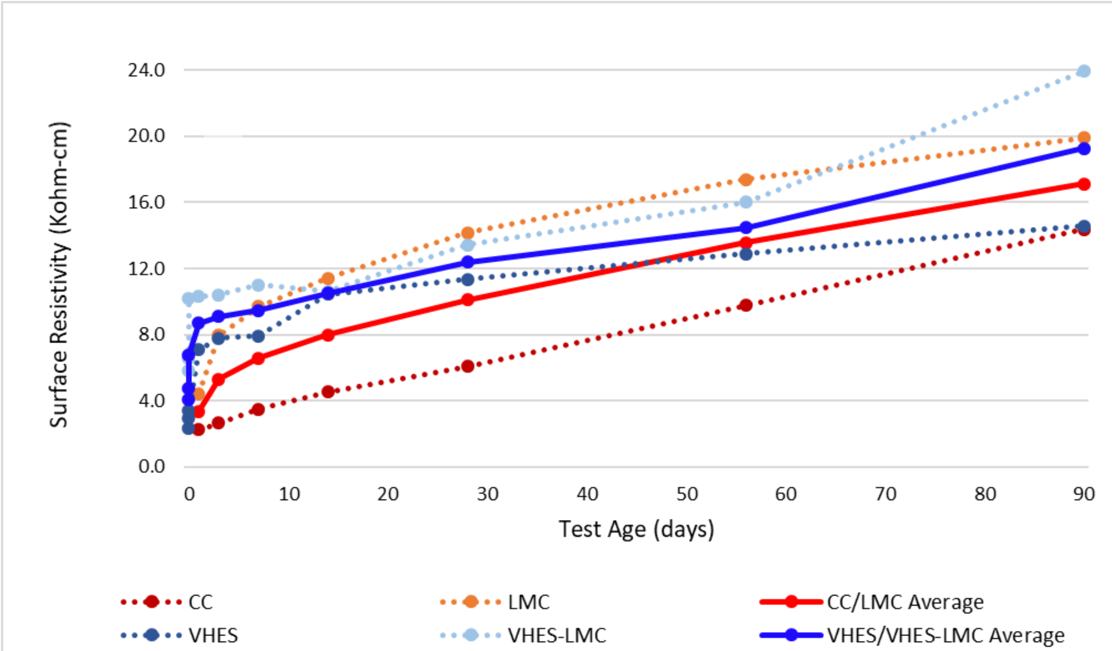

FIGURE 4.68: SR (kohm-cm) graph of CC ready-mix, LMC, VHES, and VHES-LMC 4 in. x 8 in. mockup cylinders

TABLE 4.7: Compressive strength (psi) results of CC ready-mix, LMC, VHES, and VHES-LMC 4 in. x 8 in. mockup cylinder

	CC Ready-mix				LMC				VHES				VHES-LMC			
age	1	2	3	Avg.	1	2	3	Avg.	1	2	3	Avg.	1	2	3	Avg.
1 hr									1,563	1,514	1,682	1,586	2,983	2,964	3,096	3,014
2 hr									2,188	2,015	1,940	2,048	3,393	3,412	3,180	3,328
4 hr									2,719	2,660	2,529	2,636	3,917	3,963	3,824	3,902
1 day	1,817	1,734	1,998	1,850	3,377	3,297	3,447	3,373	3,049	2,816	3,152	3,006	4,296	4,455	4,396	4,382
3 day	3,572	4,375	4,127	4,025	5,339	5,494	5,329	5,387	3,201	3,227	3,264	3,230	4,461	4,904	5,030	4,798
7 day	5,551	5,392	5,611	5,518	6,449	6,495	6,455	6,467	4,061	4,166	3,374	3,867	5,099	5,121	5,108	5,109
14 day	7,336	6,874	6,135	6,782	6,789	6,654	6,919	6,787	5,182	4,138	5,634	4,985	5,744	5,737	5,865	5,782
28 day	7,759	7,543	6,881	7,394	7,237	7,102	7,140	7,160	5,714	5,800	5,612	5,709	6,319	6,074	6,002	6,132
56 day	7,800	8,278	8,320	8,133	8,630	7,912	7,953	8,165	6,014	6,023	6,236	6,091	6,342	6,768	6,501	6,537
90 day	8,973	9,332	9,392	9,233	9,328	8,699	8,858	8,962	6,452	6,541	6,466	6,486	7,219	7,073	7,156	7,149

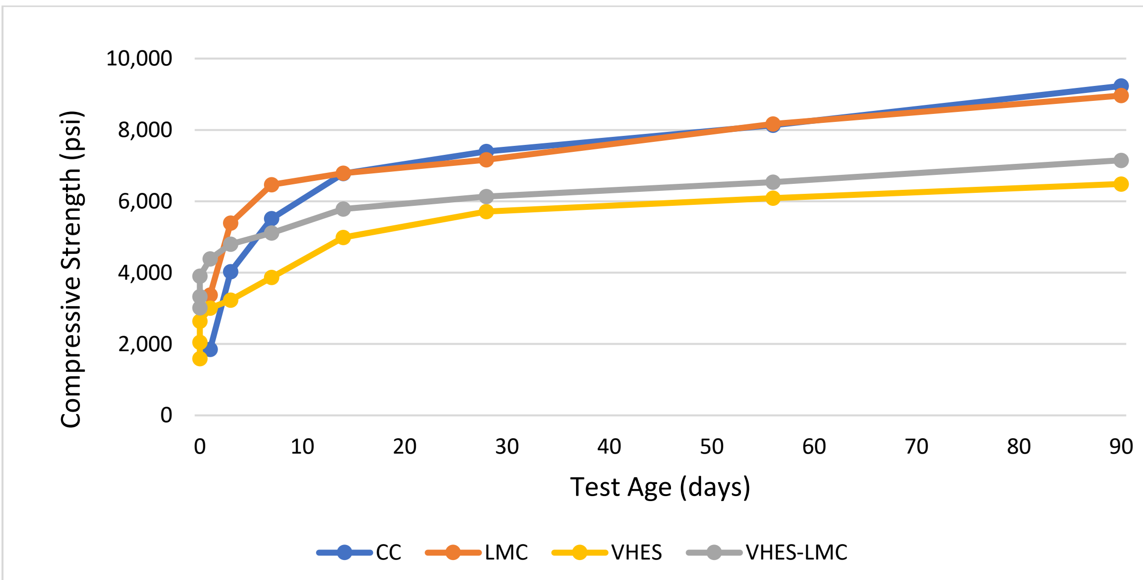

FIGURE 4.69: Compressive strength (psi) graph of CC ready-mix, LMC, VHES, and VHES-LMC 4 in. x 8 in. mockup cylinder

4.6 Summary of findings

4.6.1 Finding from SR on preliminary cylinders

The preliminary cylinders were developed to provide an understanding of how SR is influenced by different concrete mixtures that could potentially be utilized in bridge deck overlays. Also, these cylinders provided information about the influence that epoxy-coated steel reinforcement steel may have on SR versus standard, non-coated steel reinforcement. The following is a summary of those findings:

- Concrete mixtures with latex admixtures tend to produce slightly higher, yet similar SR measurements than that of concrete mixtures without the latex admixture at each of the test ages. For example, the trendline of LMC concrete mixture is translated in the positive y-direction when compared to the CC mixture in Figure 4.11 in previous sections.
- The two concrete mixtures with very high early strength cement, VHES-LMC and VHES, produce very high and rapid SR gain within the first three days, where they reach a peak of approximately 85 kohm-cm and 40 kohm-cm respectively, compared to approximately 10 kohm-cm 3 day measurement for the LMC and CC mixtures. The LMC and CC mixtures do not exhibit this peak at 3 days, rather the expected gradual SR gain. These findings are illustrated in Figure 4.11 in previous sections.
- It is theorized that this peak in SR at 3 day is the result of the rapid hydration taking place within the VHES and VHES-LMC cylinders which increases the water demand during early curing, resulting in a relatively low humidity concrete at this

time, when compared to non-VHES concrete mixtures. As discussed in the literature, temperature and moisture content are both inversely corelated to SR.

- As expected, the non-coated steel reinforcement significantly influences the SR measurement as depicted in the radar graphs of Figures 4.1b, 4.2b, 4.3b, and 4.4b. Table 4.2 from previous sections shows the SR change for each mixture as the cover depth changes in 0.5 in increments. As an example, with regard to the VHES mixture at day 3, it is estimated that SR will be about 2.0 kohm-cm higher when measured over steel reinforcement with 1.5 in. of cover versus 1 in. of cover (0.5 in. difference). It is noted that the anticipated changes in SR for cover depth are specific to these mixtures. However, a similar approach could identify these trends for other mixtures with different materials and proportions. The stark difference between the different types of mixtures, however, illustrates that significantly different behavior can be expected for different cover depths for different mixtures.
- SR was not influenced by the epoxy-coated steel embedded into selected cylinders, as the radar graphs of these cylinders (Figures 4.1a, 4.2a, 4.3a, and 4.4a) closely resemble graphs of cylinders with no steel reinforcement (Figures 4.1c, 4.2c, 4.3c, and 4.4c).

4.6.2 Findings from SR tests on miniature slabs

The miniature slabs were developed during the analysis of the preliminary cylinders as a transitional, or linking specimen to the primary specimen, the bridge deck mockup. They were a fundamental next step intended to better understand the influence of reinforcement mesh on SR before the mockups were built. The following is a summary of those findings:

- SR values were always lower in the center of the miniature slabs (surrounded by the reinforcement mat), compared to the perimeter, for all mixtures at each age of testing. This is likely due to edge effects and the influence of the reinforcement mat density, which was analyzed in previous sections.
- Similar to the preliminary cylinders, the miniature slabs containing very high early strength cement and or latex admixtures were higher than that of the conventional concrete mixture at each of the test ages.

4.6.3 Findings from SR tests on the bridge deck mockups

The bridge deck mockups were the primary specimens utilized in this research. By the thorough analysis of the preliminary mockups and miniature slabs, the characteristics, variables, and geometry of the mockups were refined. The following is a summary of the findings resulting from this research in order of greatest to least significant:

- The overlay thickness change was found to be very detectable in the heatmaps of SR in each orientation. Furthermore, it was apparent in the Row average analysis of many of the mockups and correction factors were developed for each mixture in Table 4.3 (LMC), Table 4.4 (VHES-LMC), and Table 4.5 (VHES). These correction factors are specific to only these mixtures/materials/proportions.

However, additional work could be done to explore the role of materials and proportions for each type of mixture on those correction factors.

- The edge effect analysis demonstrated that SR is influenced by the edge of a concrete member and to a differing degree depending on the orientation of the meter with respect to the edge. The rank of orientation influence of edge effects on SR is horizontal, diagonal, then vertical, with horizontal being the most influential. As a general rule of thumb, it is recommended to stay at least 5 in. away from the edge when the parallel or diagonal orientation is used and at least 4 in. away when the perpendicular orientation is being used to avoid edge effects. The non-coated steel reinforcement influenced SR at depths of 2.5 in. rather than the maximum depth of 1.18 in. as published by (Proceq 2017). Although, this finding was not observed in the heat maps as expected. The graphical trendlines of characteristic inclusion/exclusions was necessary to support this finding.
- A few of the placed voids in some of the mockups were confirmed using SR. Although this finding was not strongly observed in the heat maps, review of the graphical trendlines of void inclusion/exclusions provided the ability to show these voids, supporting this finding.
- Overall, it was hoped that the SR meter could be found useful to identify intentionally placed voids in the slabs. There is a chance that the material utilized to produce the artificial voids was influenced by the mix water, prewetting water, or other moisture, influencing the readings. The 6 inch spacing of the reinforcing grid may have also influenced the SR readings to the extent that voids were not discernable. Future work could attempt to utilize another type of material, or

different sizes/shapes of voids, to further explore the potential of SR to locate the voids.

CHAPTER 5: BRIDGE DECK OVERLAY TESTING PROTOCOL

5.1 Identify area of concern and define perimeter

If the deck overlay area of concern is large, it will need to be analyzed in sections. The section size utilized in this research was a 3.5 ft. by 3.5 ft. area with reinforcement spaced 6 in. on center, although different areas and reinforcement spacings can be investigated. The area to be inspected shall be determined by either by visual inspection, hammer sounding, chain dragging, or as notated during the overlay pour as an area of concern and outline with paint. Hammer sounding and chain dragging should be performed following ASTM D4580 Standard Practice for Measuring Delaminations in Concrete Bridge Decks by Sounding procedure. Clean the testing area, removing debris and any substance that may prohibit the electrical current from making necessary contact with the concrete's pore liquid.

5.2 Locate the reinforcement

Within the testing perimeter, locate the longitudinal and transverse reinforcement with a reinforcement locating device. Since one orientation of bar is embedded below the other, the use of a depth determining device may assist in improving this evaluation. The location of each rebar should be marked and notated as such based on differing depths. Once marked, the reinforcement mat will act as the datapoint grid for the measurement sequence. Figure 5.1 is an example of a bridge deck with 6 in. on-center reinforcement spacing. This spacing allow for measurements to be taken on top of the reinforcement, as well as centered between two bars. Bridge decks with reinforcement at greater spacing (9 in. on-center) may provide one extra testing point equally spaced between bars so expanding or modifying the grid could be necessary.

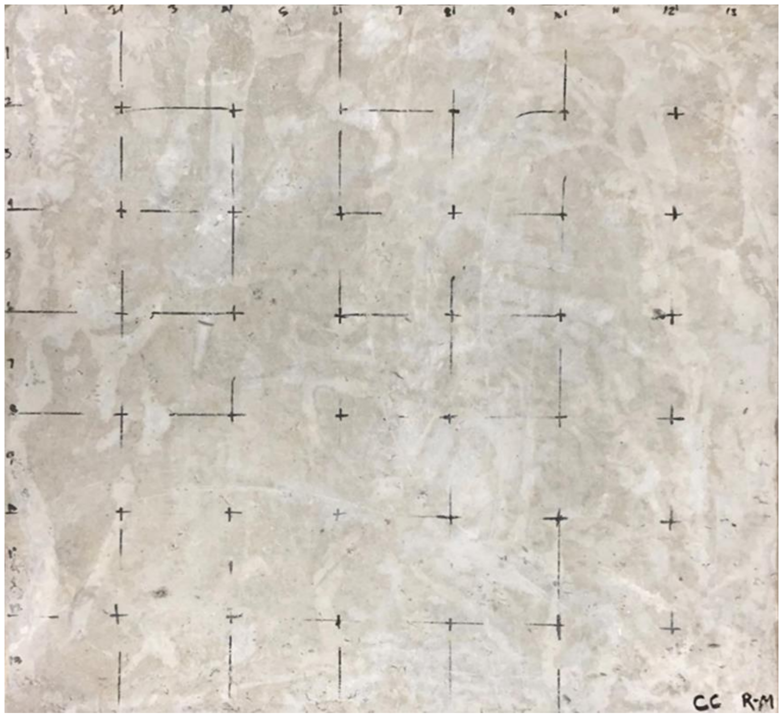

FIGURE 5.1: Bridge deck area to be analyzed

Due to the considerable surface wetting requirements, it is important that the markings be made with a durable colorant such as construction marking spray paint, permanent marker, or waterproof paint pen to avoid unintended removal, yet the markings should not be indefinite.

5.3 Define the desired testing sequence

Utilizing the reinforcement grid that was marked out in the previous section, create a testing sequence or follow the one provided in Figure 5.2, while modifying as appropriate to meet project-specific constraints and the intent of the investigation. Establishing a grid system (rows and columns indicated by numbers) can help with accurate identification of testing locations and recording of the measurements, and the grid system spacing can be tightened or widened to suit the project's specific needs and evaluation objectives. The testing sequence provided in Figure 5.2 consists of 169 points spaced 3 in. apart perpendicularly (reinforcement spaced 6 in. on center) illustrated by the dots on the figure. Testing points will lie between the reinforcement, at reinforcement intersections, and on top of reinforcement mid-spans. It is recommended to analyze one or more test areas of this general size as the data collection, maintenance, and analysis will require less effort. As a general rule of thumb, it is recommended to stay at least 5 in. away from the edge when the parallel or diagonal orientation is used and at least 4 in. away when the perpendicular orientation is being used to avoid edge effects.

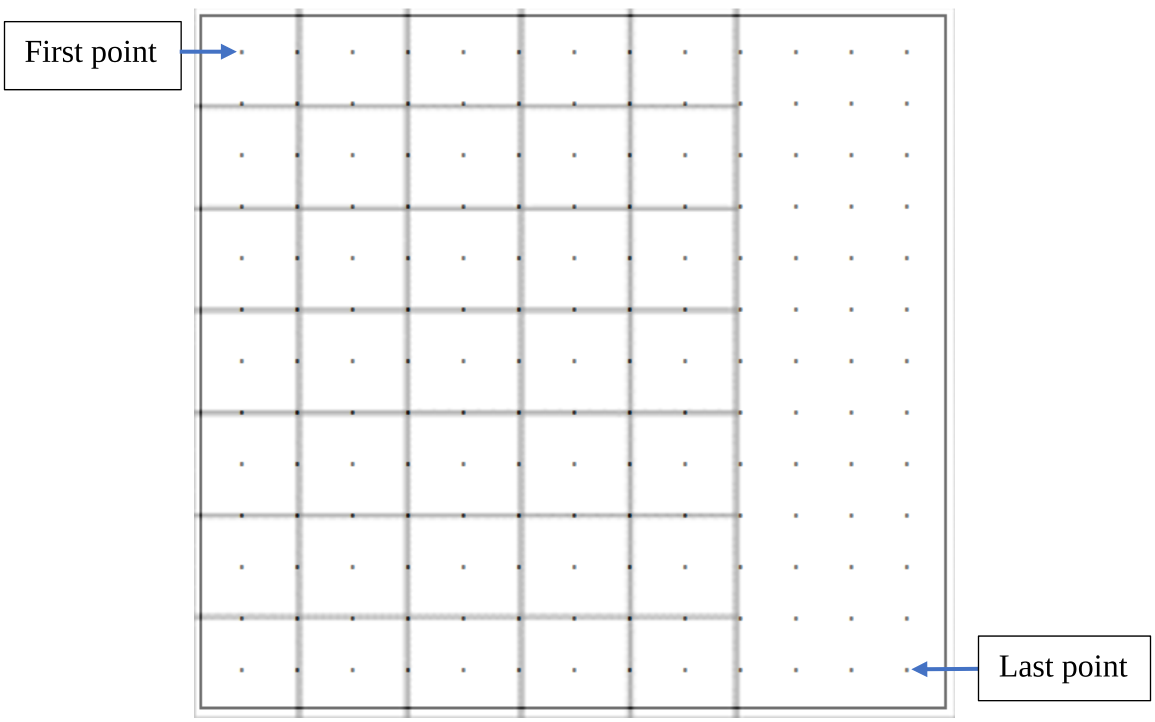

FIGURE 5.2: Proposed testing sequence for SR of mockups

5.4 Wetting testing area

The following wetting protocol is based on an air-conditioned laboratory setting. Depending on environmental conditions such as temperature and humidity, modifications are recommended. The goal of wetting the concrete is to provide ample water so that the current has the ability to be transmitted through the concrete. Excessive ponding must be avoided, since the current can travel across this surface water, affecting the readings. For the testing of slabs performed as part of this study, roughly 1 gallon of water divided into three pours was used to saturate the 3.5 ft. by 3.5 ft. testing area per orientation. Pour enough water onto the surface so that it is fully covered without spillover. Allow to absorb then reapply several times accounting for evaporation. The desired saturation is achieved when the SR measurement no longer drifts and stabilizes at a reasonable magnitude. Once the prewetting procedure has been performed, and the surface appears wet but there is no ponded water, data collection can begin. Note that as the surface dries, the testing area should be continually rewetted by adding water using a sponge or rag, then brushing the surface to remove ponded water.

5.5 SR data collection

Now that each testing point is defined, SR can be measured at each point following the defined testing sequence (Figure 5.2). It is recommended to test each point with the meter orientated diagonally, transverse, and longitudinal with respect to the bridge centerline. To measure the points, center the SR meter's 4 probes over the desired point and engage, waiting for the result be become stable and document the reading. Each point should be measured twice and averaged. If the SR value drifts, revisit section 6.4 Wetting testing area. Test all of the points using one orientation before beginning the following orientation.

In this research, two approaches of data collection were utilized. If two technicians are available, the measurements can be taken my one and called out to the colleague, and he or she will record them into an Excel spreadsheet. If only one technician is available, he or she can call out the measurements to a voice recorder and once all points are measured within an orientation, enter the measurements into the Excel file while listening to the recording. The SR meter is a hand-held device and to reduce the influence of being bent over on measurements and to improve ergonomics, an extended handle (pvc conduit, wood block, duct tape, and bungee cord) was attached to the meter for taking measurements in the standing position.

FIGURE 5.3: Measuring SR in the standing position

5.6 Data analysis

As a visual identifier of voids and overlay thickness variation, it is recommended to collect the data in an Excel type grid arrangement using color conditional formatting per cell to create heat maps. If three testing orientations are used, heatmaps could be created for each orientation as well as one for the average of orientation, and one heatmap of the standard deviation (which shows the magnitude of variation between orientations) for a total of five heatmaps. In this research, the five heatmaps were created for each age. Of these orientations, the diagonal orientation is the most valuable as it is less influenced by reinforcement, yet it still can detect voids or determine overlay thickness tapering. Often times, an overlay is composed of VHES cement so, the area of concern within the bridge deck can be tested and analyzed starting at one hour, repeating the process at the desired interval until satisfied.

The heatmaps of the three orientations can be analyzed by direct comparison. For example, the orientation that results in the meter being on top of and parallel to a top reinforcement strand (least amount of cover) is expected to be of the least magnitude. Also, if testing between bars and one of the orientations is much lower than the other two, as signaled by the standard deviation, it is possible that a somewhat linear void exists below that outlier orientation. This is hypothesized but was not proven with this research. It is assumed that voids closer to the surface would be more obvious of this hypothesis.

Also, the standard deviation can help potentially identify if the measurements were taken without ample moisture of the testing area. Greater discrepancies in orientation results could be interpreted as the reinforcement cover being relatively low, the reinforcement spacing being close to, equal to, or less than that of the SR meter's current field, or that the concrete has not been saturated sufficiently. The most obvious characteristic indicator was overlay thickness change.

In the study used to develop this protocol, the overlay thickness change was observed in several of the heatmaps. Figure 5.4 is an example if the overlay thickness change in the VHES-LMC mockup utilizing the average of orientations. The identification of overlay thickness change is significant and is identified by the SR increasing/decreasing magnitude per row or column as a whole. In Figure 5.4a, the magnitude of SR increases from row 1 where the overlay thickness averages 1.3 in. to row 13 where the overlay thickness averages 3.8 in.

	1	2	3	4	5	6	7	8	9	10	11	12	13
1	13	11	10	9.7	10	9.8	10	10	9.3	9	9.1	9.7	11
2	11	10	9.3	8.5	8.5	8.5	8.6	8.4	8.6	8.6	9.1	9.1	10
3	12	11	8.6	9.3	10	9.5	8.4	8.4	8.4	8.2	8.8	8.9	10
4	12	11	10	10	9.6	9	9	8.8	9.2	9	9.3	9.1	11
5	11	12	11	11	9.7	10	9.9	9.7	10	9.9	9.4	9.5	11
6	12	12	12	11	10	11	11	11	10	10	9.8	10	10
7	12	12	12	11	12	11	10	11	11	12	11	11	12
8	13	11	12	11	11	11	11	11	11	12	11	11	13
9	14	13	12	13	12	12	11	12	12	12	12	13	14
10	15	14	13	12	12	12	12	12	13	14	13	14	16
11	14	14	14	14	13	13	12	13	13	14	14	15	16
12	16	16	15	15	15	15	15	15	14	14	13	15	17
13	17	16	15	15	15	15	16	18	15	16	16	16	16

3.4	3.6	4.0	3.6	4.0	4.2	3.8
3.3	3.1	3.2	3.2	3.1	3.3	3.8
2.8	2.8	2.9	2.9	2.9	2.8	3.3
2.4	2.4	2.6	2.7	2.6	2.7	2.5
2.3	2.4	2.4	2.5	2.4	2.5	2.3
1.8	1.9	2.0	2.0	2.0	1.9	1.8
1.4	1.5	1.8	1.4	1.3	1.4	1.4

FIGURE 5.4: SR (left) versus overlay thickness change in inches (right) (VHES-LMC 14 day average orientation)

SR can be measured in areas of known thickness and then used as a benchmark magnitude to evaluate other unknown overlay thickness. The operator must compile multiple SR measurements at varying (but known) overlay thicknesses in order to determine the ROC in thickness of a particular overlay/base combination. The benchmark values are used to calibrate or determine the range of expected SR values within a specific concrete overlay. This method of thickness detection works when the heatmap plotted measurements resemble distinct lines of varying SR as depicted in Figure 5.4. For greater resolution, more particularly in identifying voids, the data should be plotted graphically to help illustrate trends in resistivity and to note obvious inconsistencies that may indicate changes in thickness, voids, or other discontinuities.

CHAPTER 6: CONCLUSIONS AND RECOMMENDATIONS

The potential utility of SR for evaluation of bridge deck concrete overlays has been studied in this research. This thesis presents laboratory testing of concrete specimens and bridge deck mockups with accompanying cylinders, with the intention of developing an effective field testing protocol for QA of concrete overlay construction. Gaps in the knowledge identified through a literature review, along with an agency's request supported the need for this research. In an effort to provide adaptable research and methods, several common bridge deck and concrete overlay mixtures were evaluated in resembling conditions to those found in the field. Due to the known, but not quantified, influence of a number of construction conditions on SR measurements, the influencing factors were thoroughly investigated in order to understand and quantify their effects on SR measurements. The results were also used to provide insight into the ability of the SR measurement to be used to assess overlay thickness and quality, and to allow the user to understand changes in SR measurements due to construction factors such as edges, reinforcement of different types, and overlay thicknesses.

In this chapter, several research findings from the laboratory testing program are presented. Additionally, a SR evaluation protocol for concrete overlays is provided as well as recommendations for future research.

6.1 Findings and Conclusions

The laboratory testing of preliminary cylinders, preliminary miniatures slabs, and bridge deck mockups with accompanying cylinders each composed of four concrete mixtures provided useful information about the potential of SR testing of bridge deck concrete overlays.

In the following list, the findings are ranked based on significance and strength conformation utilizing SR starting with the strongest finding.

1. SR readings are not significantly affected by epoxy-coated steel reinforcement. SR readings are, however, influenced by steel reinforcement that is not epoxy coated.
2. SR readings can be used to identify changes in overlay thickness. The overlay thickness can be predicted based on benchmark values using SR readings obtained over an area, given that the overlay thickness is known in a portion of the test area.
3. The edge of a concrete material influences SR measurements at a distance of 4-5 in depending on meter orientation. Readings taken in the parallel and diagonal orientation are most affected, while readings taken in the perpendicular orientation are least effected by edge effects.
4. Non-coated steel reinforcement cover can be quantified using SR measurements, provided that the reinforcing mat is not densely placed and does not influence measurements.
5. It is suspected that dense reinforcement mats affect the SR measurements. The location of non-coated steel reinforcement was not readily detectable in the mockups.
6. Voids were not readily detectable in the mockups. It is suspected that the reinforcement mat posed interference or that void material was insubstantial.

These key findings, as well as other developments are further described below:

- From 6 in x 12 in. preliminary cylinder radar plot of the influence of steel reinforcement analysis, it was found that SR readings are not influenced by epoxy-coated steel reinforcement while non-coated steel reinforcement was detectable. This was determined by the similar resemblance between SR readings made on non-reinforced concrete cylinders and cylinders reinforced with epoxy-coated steel reinforcement. This is likely due to an insulating effect of the epoxy coating. This finding was common amongst all concrete mixtures within the research and at each age tested.
- Correction factors for SR measurements taken on top of and parallel to non-coated steel reinforcement were developed utilizing the preliminary 6 in. x 12 in. cylinders. Correlations varied by type of concrete mixture and age. A positive correlation was found between cover depth and SR. As the concrete aged, the slope of trendlines steepened. This finding was common amongst all concrete mixtures. On average, concrete mixtures with the highest overall SR had the steepest trendline slopes for cover (in.) versus SR (kohm-cm) in the following order, CC, LMC, VHES, then VHES-LMC. Correction factors specific to these mixtures are provided in Table 4.2. Similar approaches could be used for concrete mixtures of different materials and proportions.
- It was found that the SR measurements for the VHES and VHES-LMC concrete mixtures increase at early ages, peaking sharply at 3 days then fall significantly to level off substantially at 56 and 90 days. It is suspected that this early age peak is due to the rapid hydration of these VHES cements at early ages to facilitate early

strength gain, which dries the concrete as it densifies the microstructure. During curing at later ages, the concrete begins to replenish its pore liquid in the moist curing room, the SR tends to decrease.

- In the miniature slab analysis, it was found that SR tended to be the highest around the perimeter of the specimen and lower in the center within the reinforcement and at the lowest on top of and parallel with the steel reinforcement with the least concrete cover. These miniature slabs provided and early indication of the potential for edge effects to notably increase SR measurements and the influence of the reinforcement mat, identified by a decrease in SR.
- The edge effect analysis conducted on the control mockup provided insight into the influence of the proximity of meter to the edge, as well as the orientation of the meter with respect to the edge. The greatest magnitude of influence occurred when the meter is oriented parallel to the edge and the least when the meter was oriented perpendicular to the edge. The diagonal orientation degree of influence was between the other orientations, as could be expected. SR measured in the parallel and diagonal orientation began to be influenced by the edge between 4 – 5 in. of distance from the edge, and the perpendicular orientation began to be influenced between 3 - 4 in. of distance from the edge. This finding is slightly greater than what was found in the literature (Growers and Millard 1999) which provided an overall rule of thumb of at least two times the distance of the probe spacing, or 3 in. total, indicating that practitioners in the field or laboratory should be closer to four or five inches of distance from an edge, when the probe spacing is set at 1.5 in. As a general rule of thumb, it is recommended to stay at least 5 in. away from

the edge when the parallel or diagonal orientation is used and at least 4 in. away when the perpendicular orientation is being used to avoid edge effects.

- By observing the heatmaps of the primary mockup analysis, it was found overlay thickness variation is detectable by the SR measurements. The LMC overlay had a positive correlation with overlay thickness and SR amongst virtually all ages. The VHES and VHES-LMC overlays had a negative correlation with overlay thickness and SR amongst all ages. Correction factors specific to these mixtures were developed for each mixture included in this study (varying by age) and can be found in Tables 4.2 (LMC), 4.3 (VHES), and 4.4 (VHES-LMC). Similar approaches could be used for concrete mixtures of different materials and proportions. The trendlines created for the LMC overlay analysis were most uniform, potentially being more predictable. On the contrary, the SR measurements for VHES and VHES-LMC mixtures were less stable, potentially introducing more variability into the measurements and reducing the utility of the models. It is hypothesized that the relatively poorer relationships between the VHES and VHES-LMC mixture overlay thicknesses versus SR are due to the rapid early age hydration and drying that occurs in the VHES cement.
- Estimating overlay thickness can be accomplished by using benchmark SR values from a known overlay of varying thickness and determining a ROC in SR per each thickness increment. The ROC is multiplied by the SR values of the overlay being estimated. The benchmark values will also provide an expected range of SR for the overlay. The overlays being compared must share similar characteristics such as concrete mixture, temperature, and age.

- Intentionally placed voids in the mockups could not be readily detected using the SR measurement heatmaps alone. Additional analysis was necessary to assist in identifying voids, including graphing of measurements and comparing measurements of locations of known voids to measurements of datapoints of no voids. Trendlines were graphed and the influence of the voids on the SR measurements were observed by a decrease in SR in measurements at points where the voids were included.
- Similar to the detection of voids in the mockups, the steel reinforcement was not visually apparent in the SR measurement heatmaps alone, so further analysis was necessary where data points were graphed comparing instances of measurements at points were voids were placed, to instances of measurements at points where no voids existed. Trendlines were graphed and the influence of the voids on SR measurements was evident by a decrease in SR in points where the voids were included.
- Since the influence of steel reinforcement on SR was described in the literature and then confirmed by the preliminary cylinders, it was expected to see similar obvious trend in the mockups. This did not occur without finer graphical analysis, so it is suspected that the congested reinforcement mat as a whole, combined with the change in material and slope of the overlay may have influenced the SR measurements around the reinforcing. For example, measurements taken between steel reinforcement and on top of steel reinforcement were both influenced to a similar degree, and a distinction between those testing points could not be identified by the SR meter.

- An extended handle was temporarily fashioned to the SR meter to allow for taking measurements on deck surfaces in the standing position, rather than kneeling. The digital display is visible from this position and the data can be called out to another technician or recorded with a voice recorder. This approach makes the data collection on a flat surface much easier and could be utilized to support field use of the SR meter.

6.2 Recommendations for future research

1. The non-coated steel reinforcement was easily detected in the preliminary specimens, but the detection was not so obvious in the mockups. Further research is necessary to determine whether interference by the reinforcement mat exists and to what degree. The reinforcement mat in this research was spaced 6 in. on center (typical of many bridge decks), so it is proposed that specimens be developed with a range of reinforcement mat spacings to be measured for SR with the intention of determining at what spacing the SR measurement begins to be influenced by the mat. These specimens should be built without introducing other variables such as overlay thickness variation, placed voids, etc. The proposed specimens should be measured at several positions and meter orientations including but not limited to parallel, perpendicular, and diagonal orientation, on top of reinforcement, centered between reinforcement, etc. The data should be entered into color conditional formatting for analysis using an approach similar to that performed herein.

2. The voids were not obviously identified in the heat maps of the mockups. Further research is necessary to determine the cause of this, such as void material selection, thickness of concrete cover on top of voids, and the interference by the reinforcement mat. Materials used for the voids should be selected to duplicate natural voids or honeycombing

that might occur in actual conditions. These specimens should also be built without introducing other variables such as overlay thickness variation, reinforcement, etc. in an effort to remove potential interference and unwanted influences.

REFERENCES

Aaleti, Sriram, Sritharan, S. and Abu-Hawash, A. (2013) “Innovative UHPC-Normal Concrete Composite Bridge Deck.” RILEM-fib-AFGC International Symposium on Ultra-High Performance Fiber-Reinforced Concrete.

American Association of State Highway and Transportation Officials (AASHTO) (2017) Standard Method of Test for SR Indication of Concrete’s Ability to Resist Chloride Ion Penetration. AASHTO T 358-17 American Association of State Highway and Transportation Officials. Washington, D.C.

American Association of State Highway and Transportation Officials (AASHTO). (2015). “Standard Method of Test for Temperature of Freshly Mixed Portland Cement Concrete.” T 309-15, American Association of State Highway and Transportation Officials, Washington, DC.

American Society for Testing and Materials (ASTM). (2018). ASTM Standard C33/C33M-18 “Standard Specification for Concrete Aggregates.” ASTM International, West Conshohocken, PA. DOI: 10.1520/C0033_C0033M-18. www.astm.org

American Society for Testing and Materials (ASTM). (2018). ASTM Standard C39/C39M-18 “Standard Test Method for Compressive Strength of Cylindrical Concrete Specimens.” ASTM International, West Conshohocken, PA. DOI: 10.1520/C0039_C0039M-18. www.astm.org

American Society for Testing and Materials (ASTM). (2017). ASTM Standard C138/C138M-17a “Standard Test Method for Density (Unit Weight), Yield, and Air Content (Gravimetric) of Concrete.” ASTM International, West Conshohocken, PA. DOI: 10.1520/C0138_C0138M-17A. www.astm.org

American Society for Testing and Materials (ASTM). (2015). ASTM Standard C143/C143M-15a “Standard Test Method for Slump of Hydraulic-Cement Concrete.” ASTM International, West Conshohocken, PA. DOI: 10.1520/C0143_C0143M-15A. www.astm.org

American Society for Testing and Materials (ASTM). (2018). ASTM Standard C150/C150M-18 “Standard Specification for Portland Cement.” ASTM International, West Conshohocken, PA. DOI: 10.1520/C0150_C0150M-18. www.astm.org

American Society for Testing and Materials (ASTM). (2018). ASTM Standard C192/C192M-18 “Standard Practice for Making and Curing Concrete Test Specimens in the Laboratory.” ASTM International, West Conshohocken, PA. DOI: 10.1520/C0192_C0192M-18. www.astm.org

American Society for Testing and Materials (ASTM). (2017). ASTM Standard C231/C231M-17a “Standard Test Method for Air Content of Freshly Mixed Concrete by the Pressure Method.” ASTM International, West Conshohocken, PA. DOI: 10.1520/C0231_C0231M-17A. www.astm.org

American Society for Testing and Materials (ASTM). (2013). ASTM Standard C511-13 “Standard Specification for Mixing Rooms, Moist Cabinets, Moist Rooms, and Water Storage Tanks Used in the Testing of Hydraulic Cements and Concretes.” ASTM International, West Conshohocken, PA. DOI: 10.1520/C0511-13. www.astm.org

American Society for Testing and Materials (ASTM). (2017). ASTM Standard C685/C685M-17 “Standard Specification for Concrete Made by Volumetric Batching and Continuous Mixing.” ASTM International, West Conshohocken, PA. DOI: 10.1520/C0685_C0685M-17. www.astm.org

ACI Committee 228, “Nondestructive test methods for evaluation of concrete in structures,” Tech. Rep. ACI 228.2R-98, American Concrete Institute, Farmington Hills, Michigan, USA, 2004.

ACI Committee 548. (1992) Standard Specification for Latex-Modified Concrete (LMC) Overlays (ACI 548.4) Materials Journal, Volume 89, Issue 5, pg. 521-526

Assaad, J. and Issa, C. (2018) Stability and Bond Properties of Latex-Modified Semi-Lightweight Flowable Concrete. American Concrete Institute (ACI). Materials Journal, Issue 4, Volume 115, pg. 519-530.

Azarsa, P. and Gupta, R. (2017) Electrical Resistivity of Concrete for Durability Evaluation: A Review. Advances in Material Science and Engineering, Volume 2017, Hindawi Publishing Corporation.

Beer, D. (2010) Bridge Deck Concrete Overlays. Challenges and Inspections. Texas Department of Transportation.

Bissonnette, B., Vaysburd, A. and Fay, K. (2012) “Best Practices for preparing Concrete Surfaces Prior to Repairs and Overlays.” Reclamation Managing Water in the West. U.S. Department of the Interior Bureau of Reclamation Technical Service Center. Denver, CO. Report Number: MERL 12-17.

Cackler, T., Harrington, D. and Taylor, P.C. (2017, May) “Performance Engineered Mixtures (PEM) for Concrete Pavements.” CP Road Map Brief, April 2017. National Concrete Pavement Technology Center. Ames, IA.

Cackler, T., Praul, M. and Duval, R. (2017, July) “Developing a Quality Assurance Program for Implementing Performance Engineered Mixtures for Concrete Pavements.” CP Road MAP Brief, July 2017. National Concrete Pavement Technology Center. Ames, IA.

Carter, P., Gurjar, S. and Wong, J. (2002) “Debonding of Highway Bridge Deck Overlays.” Concrete International. Alberta, Canada.

Chen, C.-T., Chang, J.-J. and Yeih, W.-C. (2014) “The effects of specimen parameters on the resistivity of concrete,” Construction and Building Materials, vol. 71, pp. 35–43

Concrete Resistivity Meter. CNS Farnell Limited. Hertfordshire, England. Retrieved from: www.cnsfarnell.com

ElBatanouny, M., Nadelman, E., Kurth, J. and Krauss, P. (2017) “Use of Polymer Overlays or Sealers on New Bridges.” Final Report. WJE Associates Inc. The Iowa Highway Research Board TR-717.

Federal Highway Administration (FHWA) (2019) “Bridge Replacement Unit Cost 2019”, Safety & Management, Bridge Inspection, National Bridge Inventory. Retrieved from: https://www.fhwa.dot.gov/bridge/nbi/sd2019.cfm

Garzon, A. J., Sanchez, J., Andrade, C., Rebolledo, N., Menéndez, E. and Fullea, J. (2014) Modification of four point method to measure the concrete electrical resistivity in presence of reinforcing bars,” Cement and Concrete Composites, vol. 53, pp. 249–257

Gillum, A., Shahrooz, B. and Cole, J. (2011) Bond Strength between Sealed Bridge Deck and Concrete Overlays. American Concrete Institute (ACI). Structural Journal, Vol. 98, Issue 6, pg. 872-879.

Gjørv, O. E., Vennesland, Ø, and El-Busiady, A. H. S. (1977) “Electrical Resistivity of Concrete in the Oceans” 9th Annual Offshore Technology Conference, Houston TX, USA, pp. 581-588.

Gowers, K. R. and Millard, S. G. (1999) Measurement of Concrete Resistivity for Assessment of Corrosion Severity of Steel Using Wenner Technique. ACI Materials Journal, Vol. 96, No. 5, pp. 536–542.

Gucunski, N., Nazarian, S., Wiggenhauser, H., and Kutrubes, D. (2010) “Nondestructive Testing to Identify Concrete Bridge Deck Deterioration”, SHRP 2-FEHRL Workshop R06-A, Brussels, Belgium

Gucunski, N. (2011) Comprehensive Bridge Deck Deterioration Mapping of Nine Bridges by Nondestructive Evaluation Technologies. Report SPR-NDEB(90)-8H-00, FWHA, U.S. Department of Transportation, Washington, D.C.

Gucunski, N. (2013) Nondestructive Testing to Identify Concrete Bridge Deck Deterioration. Repost S2-R06A-RR-1, TRB, U.S. Department of Transportation, Washington, D.C.

Gudimettla, J. and Crawford, G. (2016) “Resistivity tests for concrete—recent field experience,” ACI Materials Journal, vol. 113, no. 4

Haber, Z. B., Munoz, J. F. and Gaybeal, B. A. (2017) Field Testing of an Ultra-High Performance Concrete Overlay. U.S. Department of Transportation Federal Highway Administration, Publication No. FHWA-HRT-17-096. McLean, VA

Harrington, D. and Fick, G. (2014) Guide to Concrete Overlays: Sustainable Solutions for Resurfacing and Rehabilitating Existing Pavements, 3rd Edition. ACPA Publication TB021.03P. National Concrete Pavement Technology Center Institute for Transportation.

Icenogle, P. and Rupnow T. (2012) SR Measurements for Quality Assurance Pave the Way to Savings in Louisiana. Louisiana Transportation Research Center. Baton Rouge, LA

Jenkins, A. (2015) “ SR as an alternative for rapid chloride permeability test of hardened concrete,” Tech. Report FHWA-KS-14-15, Kansas Department of Transportation Bureau of Research, Topeka, KS.

Jones R (1962) Non-destructive testing of concrete. Cambridge University Press, London

Kevern, J., Halmen, C., Hudson, D. and Trautman, B. (2016). “Evaluation of SR for Concrete Quality Assurance in Missouri.” Transportation Research Board.

Kosmatka, S.H., Kerkhoff, B., and Panarese, W.C. (2003). Design and Control of Concrete Mixtures. 14th Edition. Portland Cement Association, Skokie, IL.

Larsen, C. K., Sellevold, E. J., Østvik, J.-M., and Vennesland, Ø. (2006) “Electrical resistivity of concrete—Part II: influence of moisture content and temperature,” in Proceedings of the 2nd International RILEM Symposium on Advances in Concrete through Science and Engineering

Lataste, J. F., Sirieix, C., Breysse, D., and Frappa, M. (2003) “Electrical resistivity measurement applied to cracking assessment on reinforced concrete structures in civil engineering,” NDT & E International, vol. 36, no. 6, pp. 383–394.

Layssi, H., Ghods, P., Alizadeh, A. R. and Salehi, M. (2015) “Electrical resistivity of concrete,” Concrete International, pp. 41–46.

Lee, Y. H. and Oh, T. (2016) “The measurement of P-, S- , and R-wave velocities to evaluate the condition of reinforced and prestressed concrete slabs,” Advances in

Material Science and Engineering, vol. 2016, Article ID 1548215, Hindawi Publishing Corporation.

Lemieux, M., R. Gagné, B. Bissonnette, and M. Lachemi. (2005) Behavior of Overlaid Reinforced Concrete Slab Panels Under Cyclic Loading—Effect of Interface Location and Overlay Thickness. ACI Structural Journal, Vol. 102, No. 3, pp. 454–461.

Liu, Y. and Presuel-Moreno, F. J. (2014) "Normalization of temperature effects on concrete resistivity by method using Arrhenius law," *ACI Materials Journal*, vol. 111, no. 4, pp.433-443.

Lorenzi A., Fonseca Caetano L., Campagnolo J. L. and Silva Filho LCP (2012) Analyzing two different data processing strategies for monitoring concrete structures using ultrasonic pulse velocity. Revista Alconpat Int 2(3):182–194

Marquez, J. M. S. (2015) *Influence of saturation and geometry on surface electrical resistivity measurements [M.S. thesis],*Concordia University, Montreal, Canada

McDonald, D. (2011). "Guidelines for Inspection and Acceptance of Epoxy-Coated Reinforcing Steel at the Jobsite." Epoxy Interest Group. Retrieved from: http://www.epoxyinterestgroup.org/index.cfm/_api/render/file/?method=inline&fileID=9C0262EF-BFDB-0C20-74CCB04EFC53D686

Millard, S. G., Harrison, J. A. and Gowers, K. R. (1991) "Practical measurements of concrete resistivity," *British Journal Non-destructive Testing,* vol. 33, pp. 59-63.

Morales, M. (2015) "Experimental investigation of the effects of embedded rebar, cracks, chloride ingress and corrosion on electrical resistivity measurements of reinforced concrete," Master, Oregon State University

Morris, W., Moreno, E.I. and Sag¨u´es, A.A. (1996) "Practical evaluation of resistivity of concrete in test cylinders using a Wenner array probe," Cement and Concrete Research, vol. 26, no. 12, pp. 1779–1787

North Carolina Department of Transportation (NCDOT). (2018). Standard Specifications for Roads and Structures: Division 10: Materials. Raleigh, North Carolina.

Polder, R. B. (2001) "Test methods for onsite measurement of resistivity of concrete—a RILEM TC-154 technical recommendation," Construction and Building Materials, vol. 15, no. 2-3, pp. 125–131

Poyet, S. (2009) "Experimental investigation of the effects of temperature on the first desorption isotherm of concrete," *Cement and Concrete Research,* vol. 39, no. 11, pp. 1052-1059

Rajabipour, F., Weiss, J., and Abraham, D. M. (2004) “Insitu electrical conductivity measurements to assess moisture and ionic transport in concrete (A discussion of critical features that influence the measurements),” School of Civil Engineering, Purdue University, Indiana

Rupnow, T. and Icenogle, P. (2011) “SR Measurements Evaluated as Alternative to the Rapid Chloride Permeability Test for Quality Assurance and Acceptance.” Final Report, Report No. FHWA/LA.11/479

Rupnow, T. and Icenogle, P. (2012) “Evaluation of SR Measurements as an Alternative to the Rapid Chloride Permeability Test for Quality Assurance and Acceptance.” Transportation Research Record: Journal of the Transportation Research Board, Vol. 2290/2012 Concrete Materials, 8 pgs.

Salehi, M., Ghods, P. and Burkan Isgor, O. (2016) “Numerical investigation of the role of embedded reinforcement mesh on electrical resistivity measurements of concrete using the Wenner probe technique”, Materials and Structures, vol. 49, no. 1-2, pp. 301–316

Salehi, M., Ghods, P. and Isgor, O. B. (2015) “Numerical study on the effect of cracking on SR of plain and reinforced concrete elements,” Journal of Materials in Civil Engineering, vol.27, no. 12, Article ID 04015053

Sansalone, M. J., and Streett, W. B. (1999) “The Impact-Echo Method”, NDTnet, vol.3, no.2. Retrieved from: https://www.ndt.net/article/0298/streett/streett.htm#author

Sengul, O. (2014) “Use of electrical resistivity as an indicator for durability,” Construction and Building Materials, vol. 73, pp. 434–441

Sengul, O. and Gjørv, O. E. (2009) “Effect of embedded steel on electrical resistivity measurements on concrete structures,” *ACI Materials Journal*, vol. 106, no. 1

Shah, A.A., and Ribakov, Y. (2008) “Non-destructive measurements of crack assessment and defect detection in concrete structures,” Materials and Design, vol. 29, no. 1, pp. 61–69

Shann, S. V. 2012. Application of Ultra High Performance Concrete (UHPC) as a Thin-Bonded Overlay for Concrete Bridge Decks. M.S. Thesis, Michigan Technological University

Spragg, R., Bu, Y., Snyder, K., Bentz, D. and Weiss, J. (2013) “Electrical testing of cement-based materials: role of testing techniques, sample conditioning,” Tech. Rep. FHWA/IN/JTRP-2013/28, Purdue University

Spragg, R., Villani, C., Snyder, K., Bentz, D., Bullard, J. and Weiss, J. (2013) “Factors that influence electrical resistivity measurements in cementitious systems,” Journal of the Transportation Research Board, vol. 2342, pp. 90–98

Sprinkel, M. (2000) Evaluation of Latex-Modified and Silica Fume Concrete Overlays Placed on Six Bridges in Virginia. Virginia Transportation Research Council.

Taylor, P., Tennis, P., Obla, K., Ram, P., Van Dam, T. and Dylla, H. (2013). Durability of Concrete. Transportation Research Circular No. E-C171. TRB Committee AFN30. Transportation Research Board, Washington, DC.

Udegbunam, O., Yaman, I. O., Aklan, H. and Hohm, T. (1999) Developing a Rapid Measure of Concrete Permeability for Use in QNQC Specifications, Proceedings of the Transportation Research Board, Paper no. 990565.

Weiss, J., Snyder, K., Bullard, J. and Bentz, D. (2013) "Using a saturation function to interpret the electrical properties of partially saturated concrete," Journal of Materials in Civil Engineering, vol. 25, no. 8, pp. 1097–1106

Weydert, R. and Gehlen, C. (1999) Electrolytic Resistivity of Cover Concrete: Relevance, Measurement and Interpretation. Eighth Int. Conf. on Durability of Materials and Components. Vancouver, Canada.

Yun, K.. Choi, P. (2014). "Cause and controls of cracking at bridge deck overlay switch very-early strength latex-modified concrete." Construction and Building Materials. Science Direct.

Holcim

Material Certification Report

Material: Portland Cement
Type: I-II (MH)

Test Period: 18-Sep-2019 to 19-Sep-2019
Date Issued: 14-Oct-2019

Certification

This cement meets the specifications of ASTM C150 and AASHTO M85 for Type I-II (MH) cement.

General Information

Supplier:	Holcim (US) Inc. d/b/a LafargeHolcim US	Source Location:	Holly Hill Plant Silo: 18
Address:	8700 West Bryn Mawr Ave Chicago, IL 60631		2173 Gardner Blvd Holly Hill, SC 29059
Contact:		Contact:	Scott Poaps / (803) 496-2995

The following is based on average test data during the test period. The data is typical of product shipped from this source; individual shipments may vary.

Test Data on ASTM Standard Requirements

Chemical			Physical		
Item	**Limit [1]**	**Result**	**Item**	**Limit [1]**	**Result**
SiO_2 (%)	-	20.1	Air Content (%)	12 max	7
Al_2O_3 (%)	6.0 max	4.8	Blaine Fineness (m^2/kg)	260-430	404
Fe_2O_3 (%)	6.0 max	3.5			
CaO (%)	-	63.6	Autoclave Expansion (%) (C151)	0.80 max	-0.04
MgO (%)	6.0 max	1.4	Compressive Strength MPa (psi)		
SO_3 (%) [2]	3.0 max	3.2	3 day	10.0 (1450) min	31.0 (4500)
Loss on Ignition (%) [5]	3.5 max	1.9	7 day	17.0 (2470) min	38.4 (5570)
Insoluble Residue (%)	1.50 max	0.35	28 day (previous month's data)	-	46.9 (6800)
CO_2 (%)	-	1.0			
$CaCO_3$ in Limestone (%)	70 min	88	Initial Vicat (minutes)	45-375	125
Potential Phase Compositions [3]:					
C_3S (%)	-	56	Mortar Bar Expansion (%) (C1038)	0.020 max	0.003
C_2S (%)	-	15			
C_3A (%)	8 max	7			
C_4AF (%)	-	11			
$C_3S + 4.75C_3A$ (%)	100 max	88			

Test Data on ASTM Optional Requirements

Chemical			Physical		
Item	**Limit [1]**	**Result**	**Item**	**Limit [1]**	**Result**
Equivalent Alkalies (%)	-	0.48	Heat of Hydration kJ/kg (cal/g) (ASTM C1702) 3 Days [4]	-	267 (64)

Notes (*1-9)

1 - Dashes in the Limit / Result columns mean Not Applicable.
2 - It is permissible to exceed the specification limit provided that ASTM C1038 Mortar Bar Expansion does not exceed 0.020% at 14 days.
3 - Adjusted per Annex A1.6 of ASTM C150 and AASHTO M85.
4 - Test results represent the most recent value and is provided for information only.
5 - Limit = 3.0 when limestone is not an ingredient in the final cement product
9/18/2019
Grind 261

Additional Data

Item	Limestone	Inorganic Processing Addition	Base Cement Phase Composition	Result
Amount (%)	2.6	0.7	C_3S (%)	58
SiO_2 (%)	2.7	30.3	C_2S (%)	15
Al_2O_3 (%)	0.7	11.0	C_3A (%)	7
Fe_2O_3 (%)	0.8	0.7	C_4AF (%)	11
CaO (%)	50.1	41.4		
SO_3 (%)	0.6	2.0		

Printed: 10/14/2019 3:10:27 PM

Version: 180412

Scott Poaps
Scott Poaps,
Quality Manager

FIGURE A.1 Ordinary portland cement mill report

CTS Rapid Set

MILL CERTIFICATE
RAPID SET CEMENT
May 3, 2019

Reported To: CTS Cement Manufacturing Corporation

Project: Bulk Cement Stock

PLANT	Juarez, Plant 1
RAPID SET CEMENT, BULK	9408 tons (8535 mt)
IDENTIFICATION, lot number	J63
SPECIFIC GRAVITY	2.97
TIME OF SETTING, Minutes (ASTM C191 MODIFIED)	
INITIAL	18
FINAL	23
COMPRESSIVE STRENGTH – PSI (MPa)	
3 HOURS	6870 (47.4)
24 HOURS	8340 (57.5)

Tested in accordance with ASTM C109 as modified by CTS 101-17.

This cement was sampled from Juarez Plant 1 and test results shown herein are representative of the Rapid Set® cement identified with the above lot number.

Seller, having no control over the use of Rapid Set® cement, will not guarantee finished work in which it is used.

CTS CEMENT MANUFACTURING COMPANY

Authorized Representative

See California all-purpose acknowledgement certificate Attachment.

Controlled Copy – Do Not Duplicate

CTS 8-032 Rev. NC 09/13/18

CTS CEMENT MANUFACTURING CORP. | AN EMPLOYEE-OWNED COMPANY
12442 KNOTT ST., GARDEN GROVE, CA 92841 | 800.929.3030 | CTSCEMENT.COM

FIGURE A.2: Very high early strength cement mill report

A.S.T.M. C 127 Standard Test Method for Specific Gravity and Absorption of Coarse Aggregate

Date Sampled	Material	Control Number	Bulk - Dry	Bulk - Saturated Surface Dry	Apparent	Absorption	Laboratory	Technician	Comments
		Triangle							
April 4, 2018	# 67	T-1	2.632	2.644	2.663	0.4%	WSC Central	C. Gastiger	Dark Gray Material

FIGURE A.3: # 67 Coarse aggregate specific gravity and absorption report

A.S.T.M. C - 131 Standard Test Method for Resistance to Degradation of Small-Size Coarse Aggregate by Abrasion and Impact in the Los Angeles Machine

Date Sampled	Material	Control Number	Grading	Percent Loss	Laboratory	Technician	Comments
		Triangle					
April 4, 2018	# 67	T-1	B	47	WSC Central	C. Gastiger	Dark Gray Material

FIGURE A.4: #67 Coarse aggregate LA abrasion test report

A.S.T.M. C - 136 Standard Test Method for Sieve Analysis of Fine and Coarse Aggregate

Date Sampled	Material	Control Number	Percent Passing															Soil Mortar				
			2"	1 1/2"	1"	3/4"	1/2"	3/8"	#4	#8	#10	#16	#30	#40	#50	#100	#200	LL	PI	#30	#40	#200
		Triangle																				
April 4, 2018	# 67	T-1			100	98	59	38	5	3												

FIGURE A. 5 # 67 coarse aggregate sieve analysis report

Sample Status: Complete

NORTH CAROLINA DEPARTMENT OF TRANSPORTATION
MATERIALS AND TESTS UNIT
1801 BLUE RIDGE RD. RALEIGH, N.C. 27607
01/31/2018
Fine Aggregate Test Yearly

Hicams No.: 889572
T.I.P. No.:
Work Order No.:
Contract No.:
Field ID: FA122-1
P.O./Other No.:
County: Harnett
Engineer:
Date Sampled: 12/01/2017
Received: 12/13/2017
Reported: 01/29/2018
Sampled By: Christian, Guy C
Test Category: Verification
Sampled From: Stockpile - 1
Contractor:
Represented Qty.: 10000.000 TON
Prod./Suppl.: G.S. Materials
Facility: Hall Pit - Lemon Springs
Material: Yearly Quality Check for Fine Aggregate (Strength, Soundness, etc.)

Test No.: AASHTO T112, T19, T27, T104, T71, T84
QA Indicator: N
Location of Source: Stockpile
Property Owner:

SIEVE ANALYSIS

Sieve Size	Percent Passing
3/8"	100
# 4	100
# 8	98
#16	86
# 30	41
# 40	
# 50	9
# 80	
# 100	2
# 200	1.0
Fineness Modulus	2.65
Deleterious Substance	0.4

STRUCTURAL STRENGTH

Compression Test on 2 inch Cubes

Strength Ratio: 3-Day: 112.7 %
7 Day: 118.7 %

Color: 2
Sp.Grav.: 2.61
Absorp.: 0.40 %
Soundness: 3.1 % Loss

Unit Weight
Solid 163.1 lbs/ft3
Dry & Rodded 101.6 lbs/ft3

Comments:

Chun Kun Su

Chun Kun Su P.E.
GeoMaterials Workgroup Supervisor

cc: G.S. Materials

FIGURE A.6: Fine aggregate report

Client :		**Date :** 06/24/2020	
Project/Contract :			
Placement :			
Usage :			
Mix Design No. : 11AB	**Description :** 4500 NC AAF # 67		

Compressive Strength	11ABCFNPE	**Submittal No.**	
Aggregate Size	#67	**Plant**	Reames Road, Charlotte
Air %	4.5% to 7.5%	**Volume**	27.12 ft³
w/cm Ratio	0.39	**U.W.**	142.8 lb/ft³
Slump	2.00 to 3.00in	**Slump with SuperP**	

Constituents and Suppliers	**Quantity**	**Sp. Gr.**	**Volume**
	(yd³)	**SSD**	
Cement - 101 - CEMENT - Type I/II - Cemex, Knoxville	572 lb	3.150	2.91 ft³
Additive - 108 - FLY ASH - Type F - SEFA, Winyah Station	172 lb	2.300	1.20 ft³
Water - 800 - WATER - - - -	34.6 Gal	1.000	4.63 ft³
Stone - 167 - #67 - Crushed granite - BV Hedrick, Lake Norman	1825 lb	2.770	10.55 ft³
Sand - 301 - SAND - Natural sand - Hanson, Pageland	1014 lb	2.620	6.20 ft³
Admixture - 431 - RETARDER - Daratard 17 - Grace, Cambridge	3.00 oz/cwt	1.000	0.02 ft³ /
Admixture - 441 - AIR - Darex II - Grace, Cambridge	1.00 oz/yd³	1.000	0.00 ft³ /
Admixture - 410 - NORMAL - Zyla 640 - Grace, Cambridge	2.00 oz/cwt	1.000	0.02 ft³ /
Air Volume			1.63 ft³
Total	3872 lb		27.12 ft³
Optional Products :			

Remarks :
MAX WATER 36.6 Gals/cyd
; 1 oz/yard AE is a default value. Batcher must enter sufficent dosage

Prepared by : Patrick Baker, Lab Supervisor	Approved by :
Date : 01/11/2016	Date : / /

FIGURE A.7: Ready-mix conventional AA concrete mix design report

Construction
Technical Data Sheet

BASF
We create chemistry

Styrofan® 1186

Chemical Nature	**Aqueous styrene-butadiene copolymer dispersion for use in concrete modification.**		

Properties

Typical Properties	Solids content	%	ca. 48
	pH		ca. 10
	Viscosity at 23 °C (Brookfield RVT, Spindle #1, at 20 rpm)	mPa s	ca. 38
Other properties of the dispersion	Surface Tension	dynes/cm	ca. 32
	Specific Gravity	lbs/gal	ca. 8.5
		g/cm³	ca. 1.01
	Bound Styrene	%	ca. 66
	Average Particle Size	µm	ca. 0.2
	Dispersion type		anionic
	Coagulum (100 mesh)	Wt. %	< 0.1
	Sensitivity to frost	cycles	ca. 2
Properties of the film	Glass transition temperature Tg (DSC)	°C	ca. 6
	Mechanical strength*		
	Tensile strength	psi	ca. 600
		N/mm²	ca. 4
	Elongation at break	%	ca. 200
	Appearance		slight yellow, transparent
	Surface		tack-free

* The above values should not be taken as specification

Application

Fields of application

Styrofan 1186 is used mainly for modifying concrete mixtures. The most notable applications are concrete for bridge deck and parking garage overlays. The addition of Styrofan 1186 to conventional unmodified concrete mixtures reduces the amount of water required for the placement of the mix. The lower water typically results in a cured concrete with higher compressive strength. The polymer forms an elastic membrane throughout the matrix of the cured concrete, reducing the formation of voids and hairline cracks therein. Moreover, the resulting concrete mixture shows improved resistance to the penetration of oil, salts and aids in the adhesion of the new concrete to old. Flexural strength and abrasion resistance are also increased.

Styrofan 1186 has been pre-qualified by the FHWA under FHWA RD-78-35

Safety

General

The usual safety precautions when handling chemicals must be observed. These include the measures described in Federal, State and Local health and safety regulations, thorough ventilation of the workplace, good skin care and wearing of protective goggles.

Safety Data Sheet

All safety information is provided in the Safety Data Sheet for Styrofan 1186.

January 2020 rev7 page 1 of 2

FIGURE A.8: Polymer latex admixture data sheet

TABLE A.1: #67 coarse aggregate properties

Property	Sample 1	Sample 2	Sample 3	Average
Bulk specific gravity (bulk SG)	2.57	2.57	2.49	2.54
Bulk specific gravity (saturated surface dry)	2.61	2.62	2.56	2.60
Apparent specific gravity (apparent SG)	2.67	2.69	2.69	2.68
Absorption (%)	1.49	1.63	2.95	2.02

TABLE A.2: Fine aggregate properties

Property	Sample 1	Sample 2	Sample 3	Average
Bulk specific gravity (bulk SG)	2.58	2.54	2.58	2.56
Bulk specific gravity (saturated surface dry)	2.61	2.59	2.61	2.60
Apparent specific gravity (apparent SG)	2.66	2.67	2.68	2.67
Absorption (%)	1.26	1.91	1.52	1.56

APPENDIX B: BRIDGE DECK MOCKUP SCHEMATIC

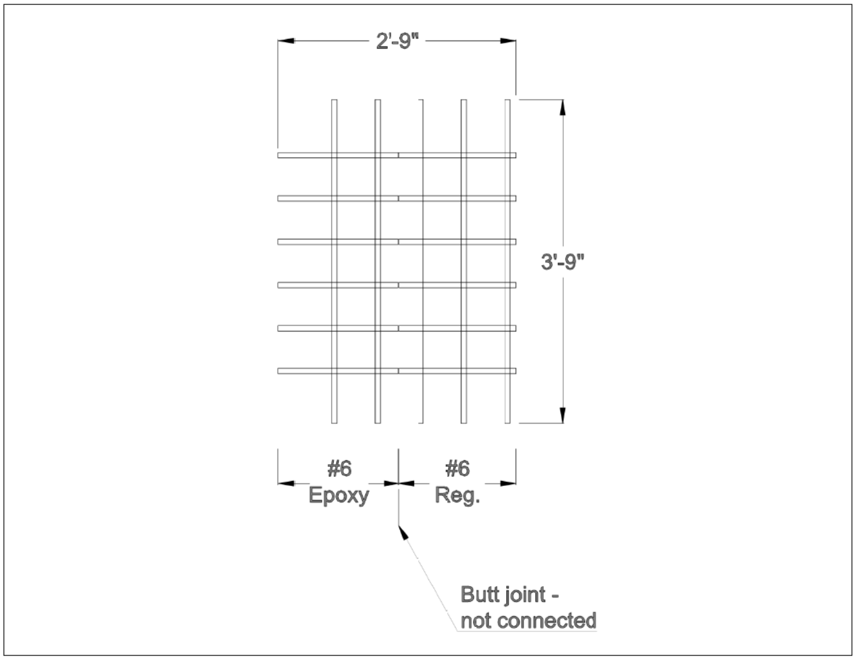

FIGURE B.1: Mockup reinforcement

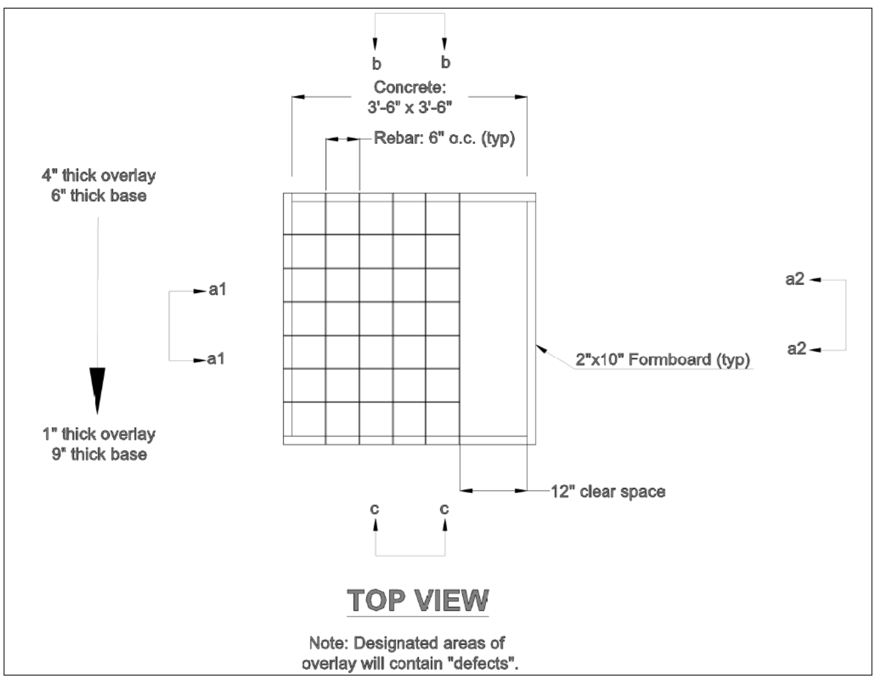

FIGURE B.2: Mockup top view

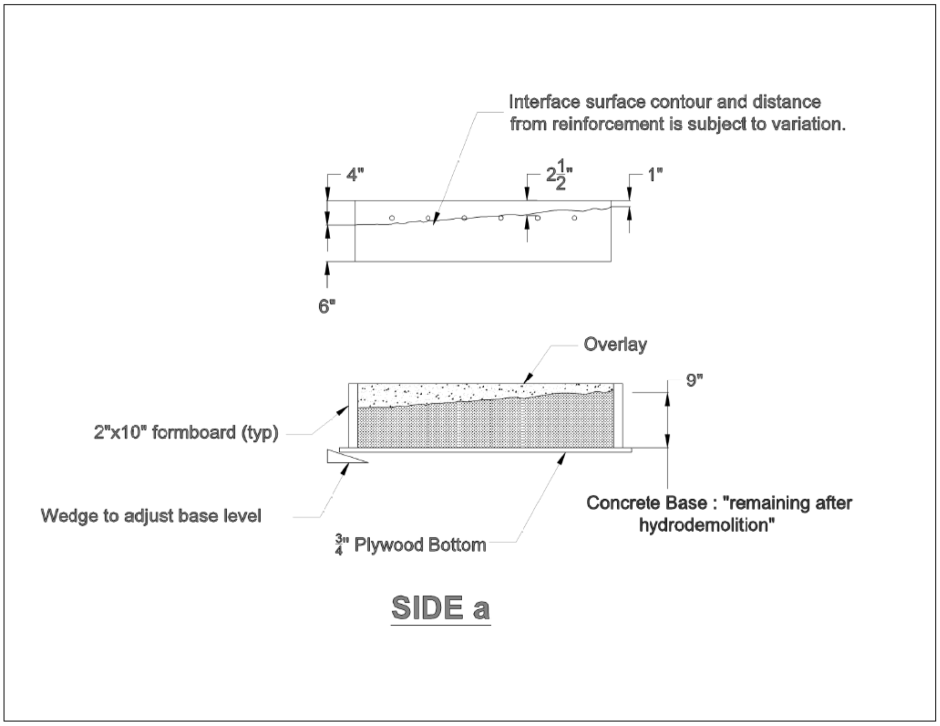

FIGURE B.3: Mockup side a

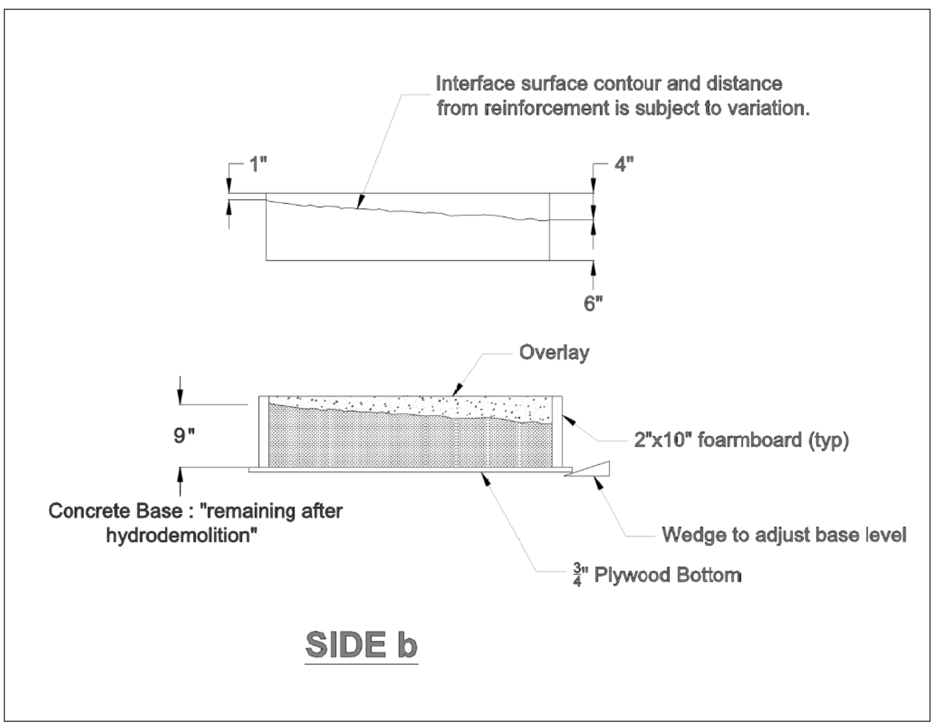

FIGURE B.4: Mockup side b

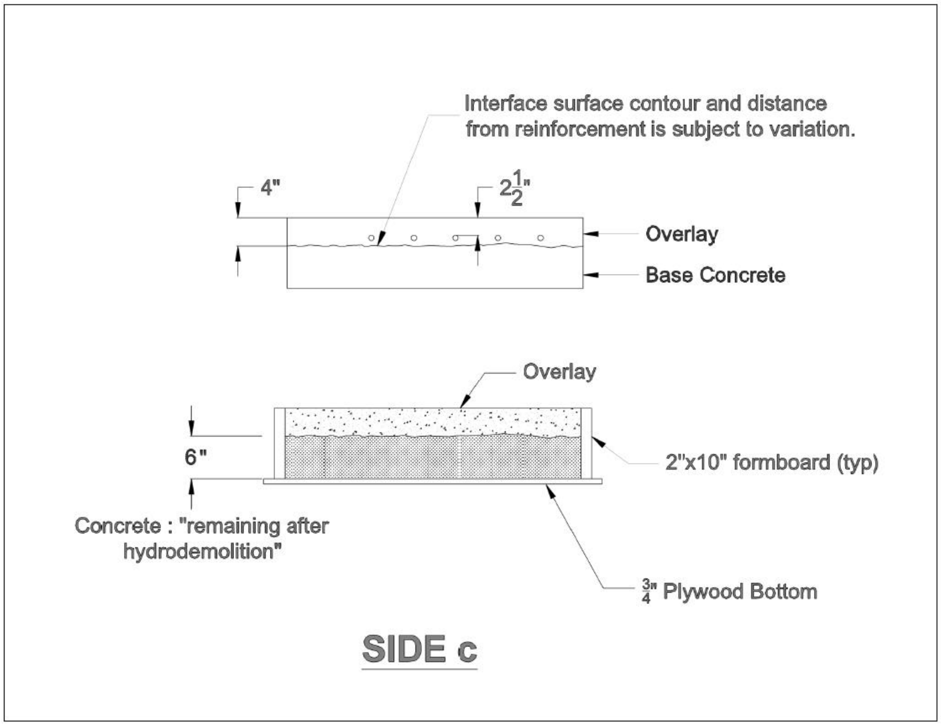

FIGURE B.5: Mockup side c

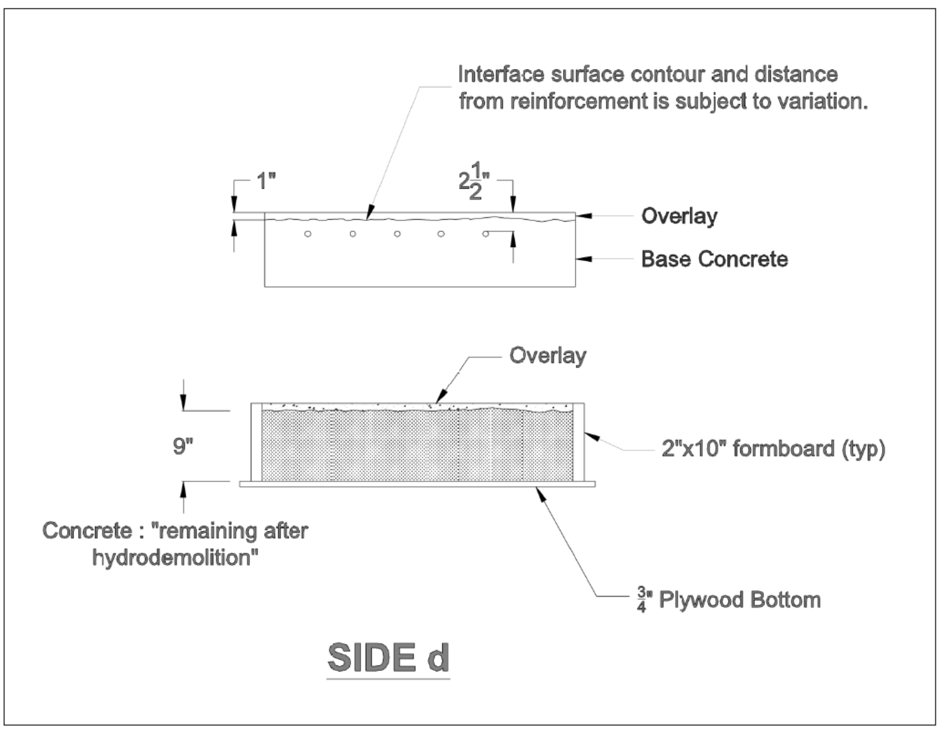

FIGURE B.6: Mockup side d

APPENDIX C: PRELIMINARY ANALYSIS RESULTS

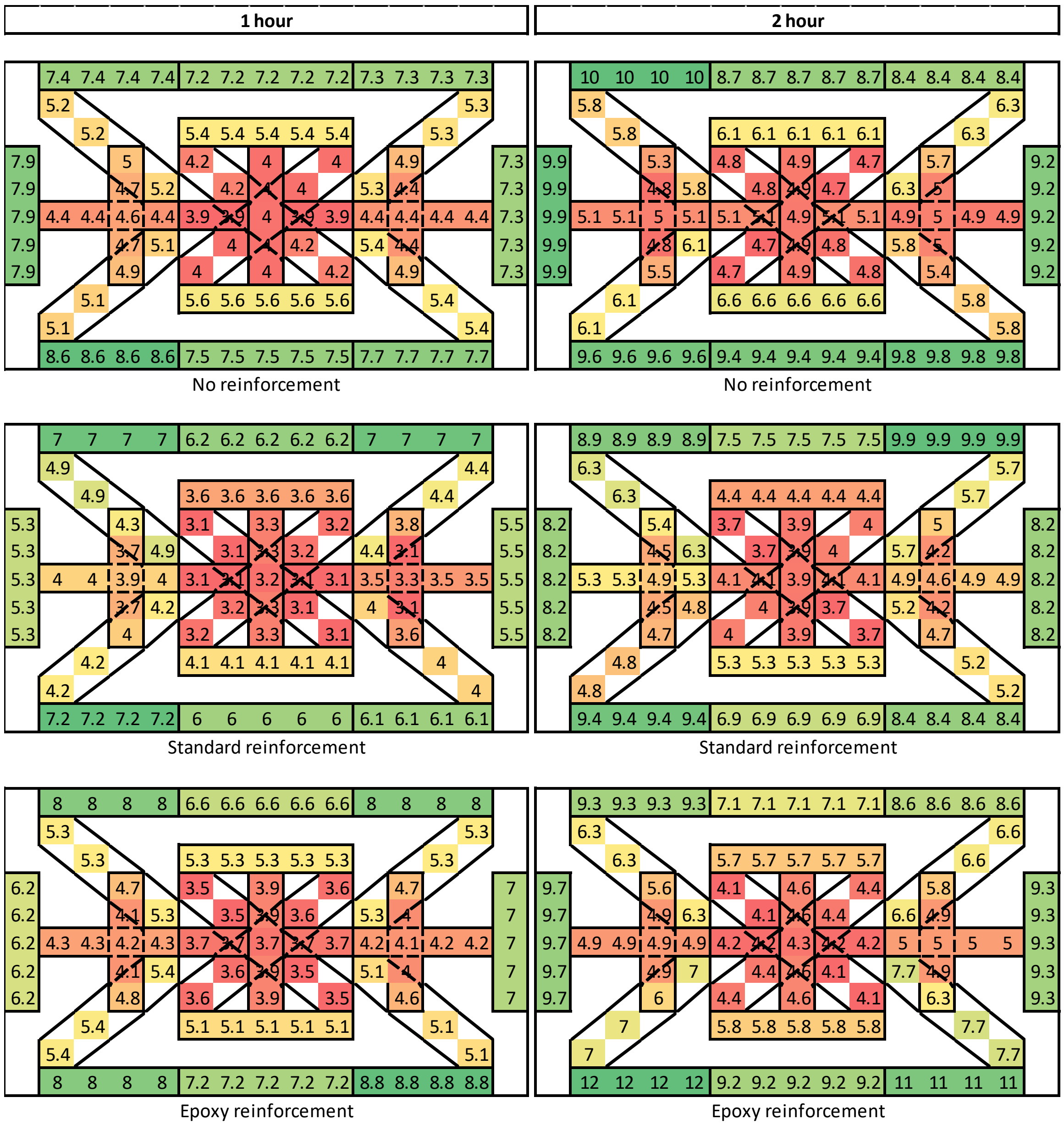

FIGURE C.1: 1 and 2 hour VHES miniature slab data

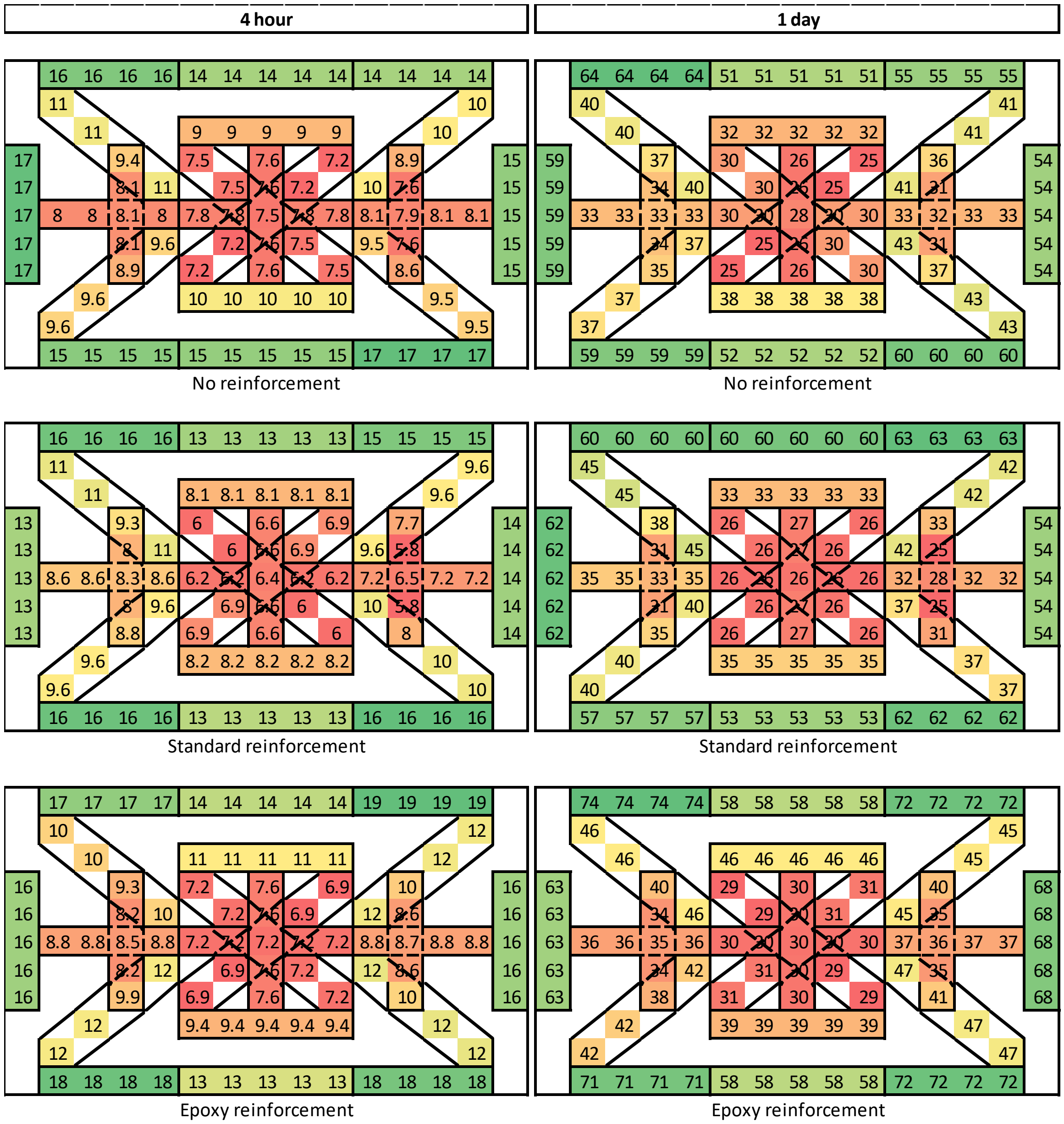

FIGURE C.2: 4 hour and 1 day VHES miniature slab data

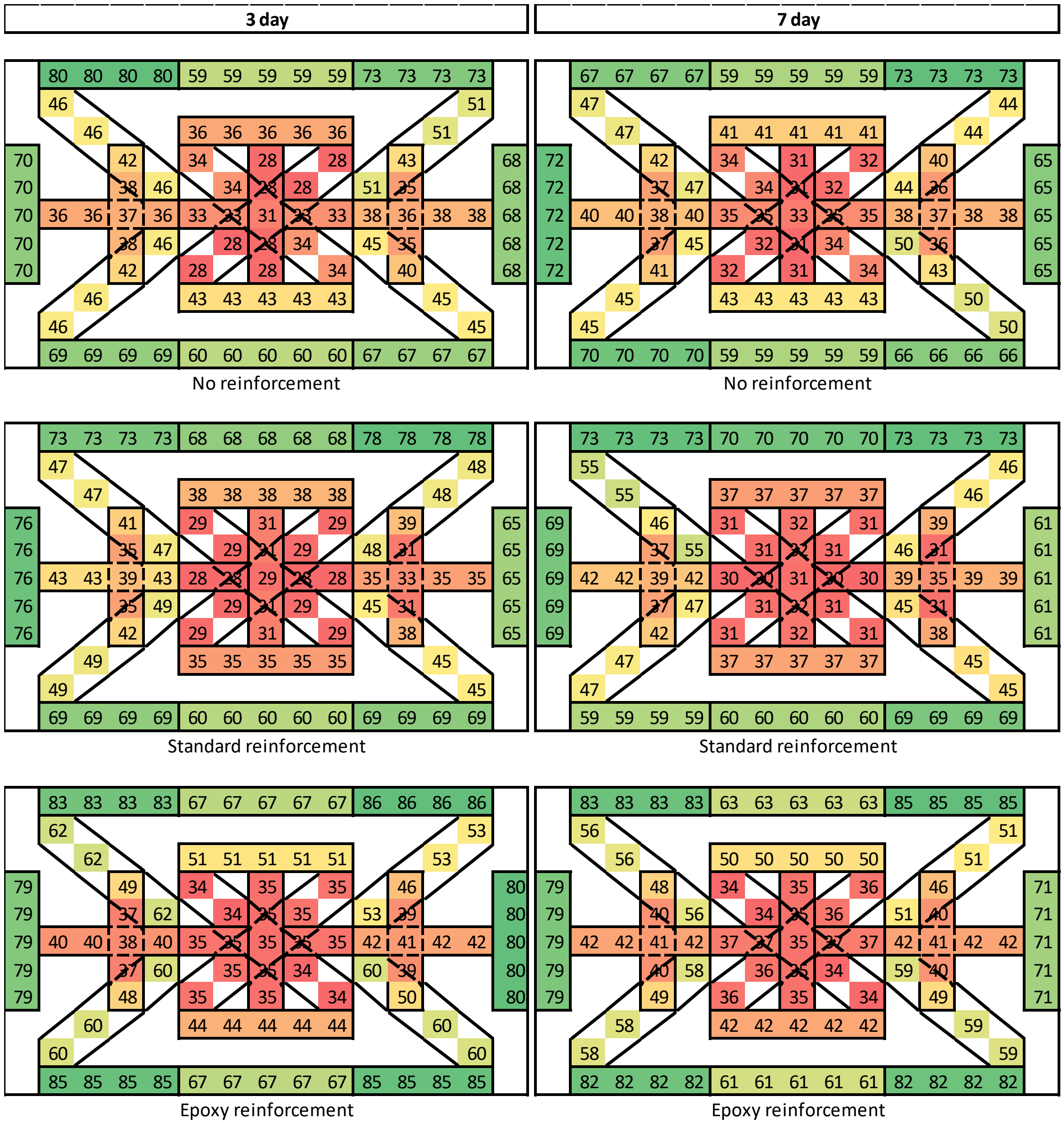

FIGURE C.3: 3 and 7 day VHES miniature slab data

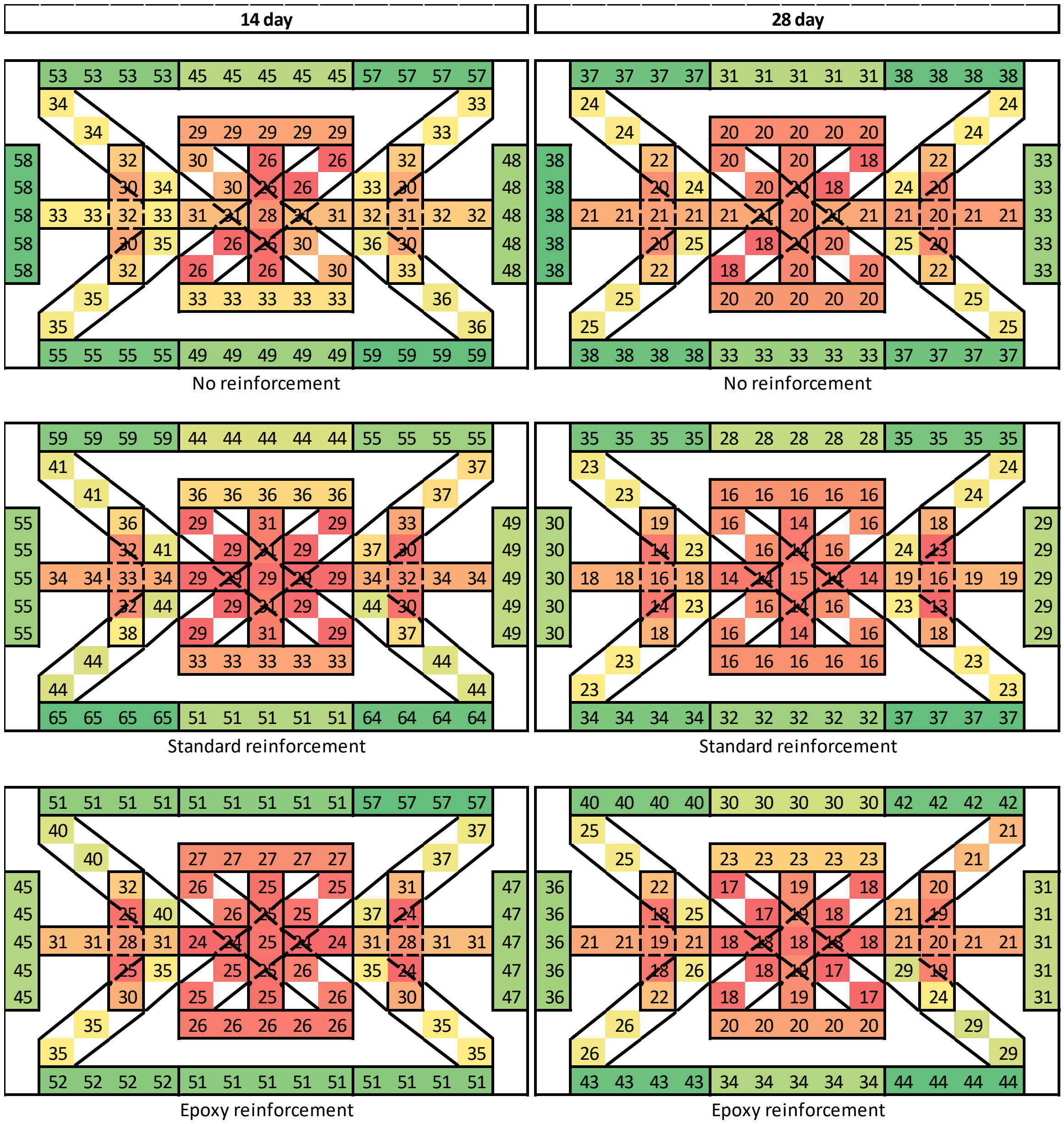

FIGURE C.4: 14 and 28 day VHES miniature slab data

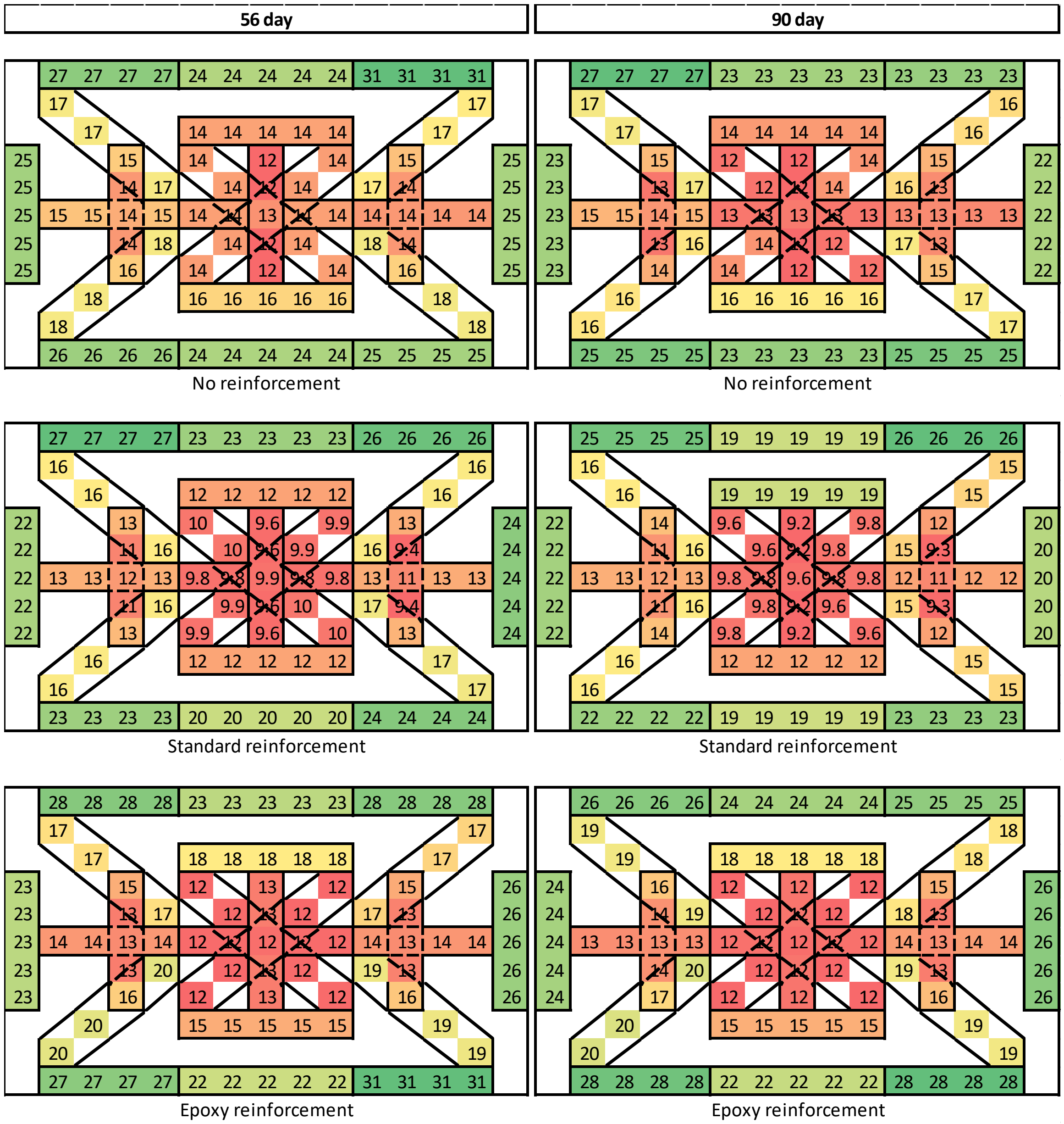

FIGURE C.5: 56 and 90 day VHES miniature slab data

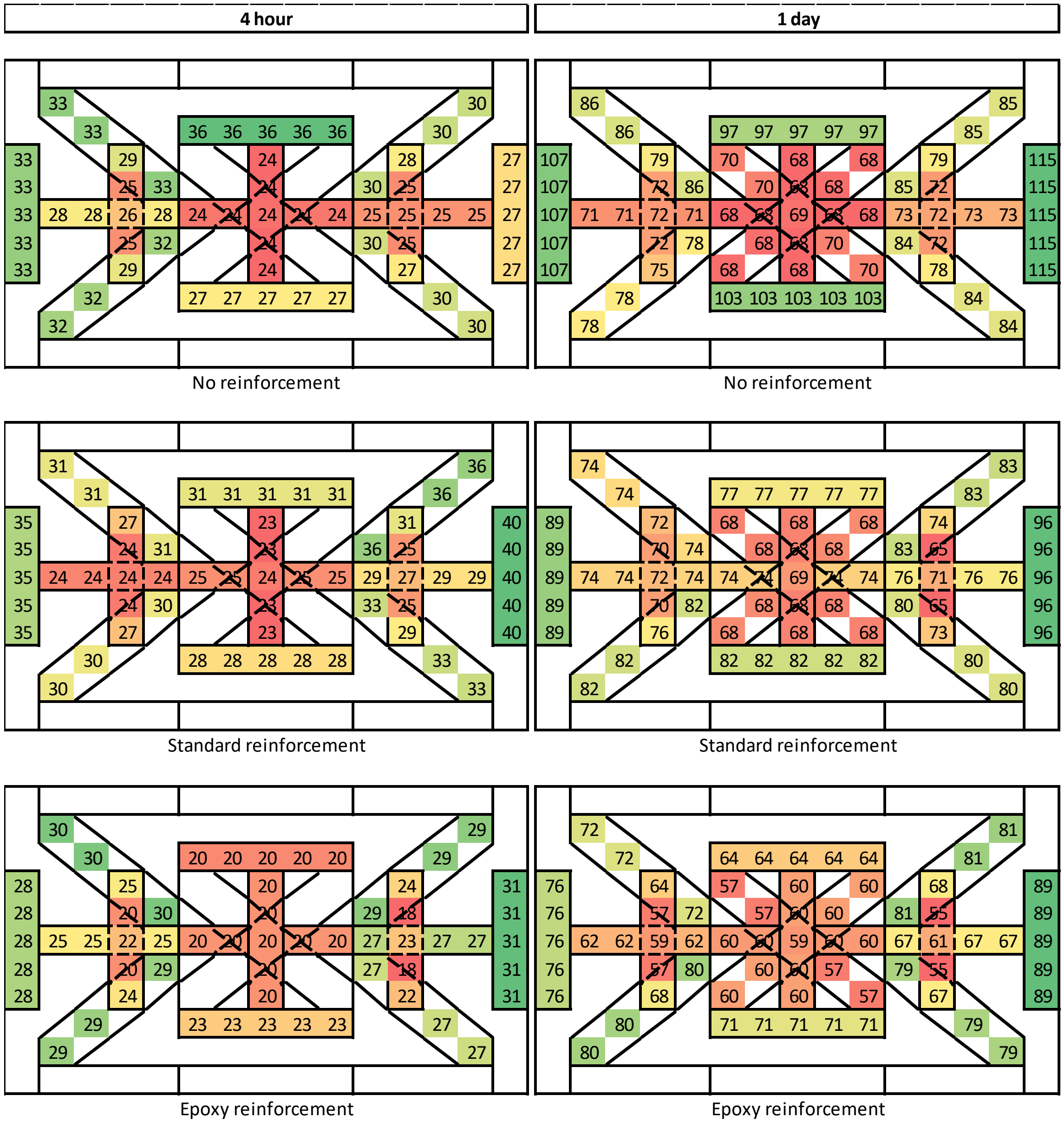

FIGURE C.6: 4 hour and 1 day VHES-LMC miniature slab data

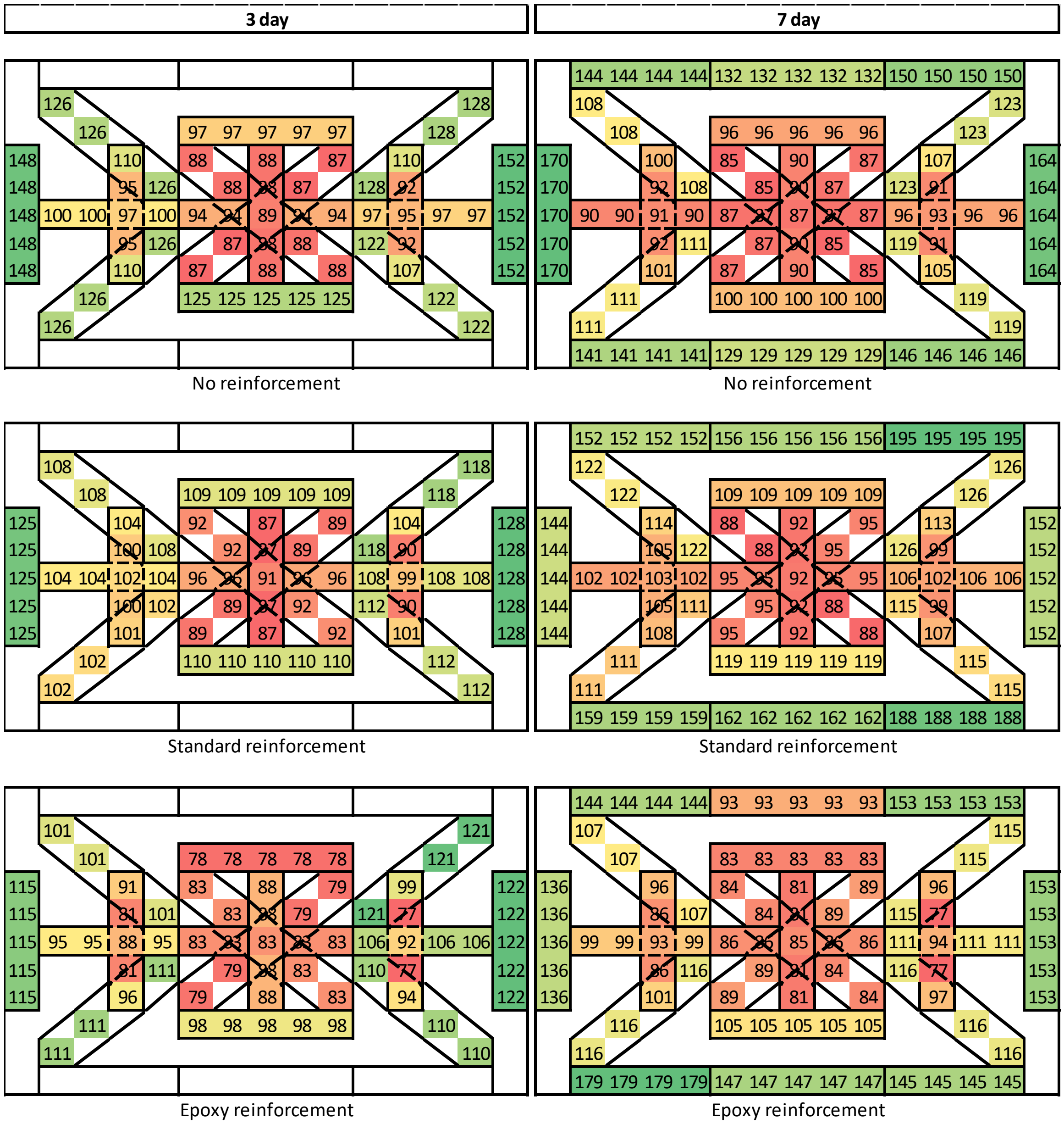

FIGURE C.7: 3 and 7 day VHES-LMC miniature slab data

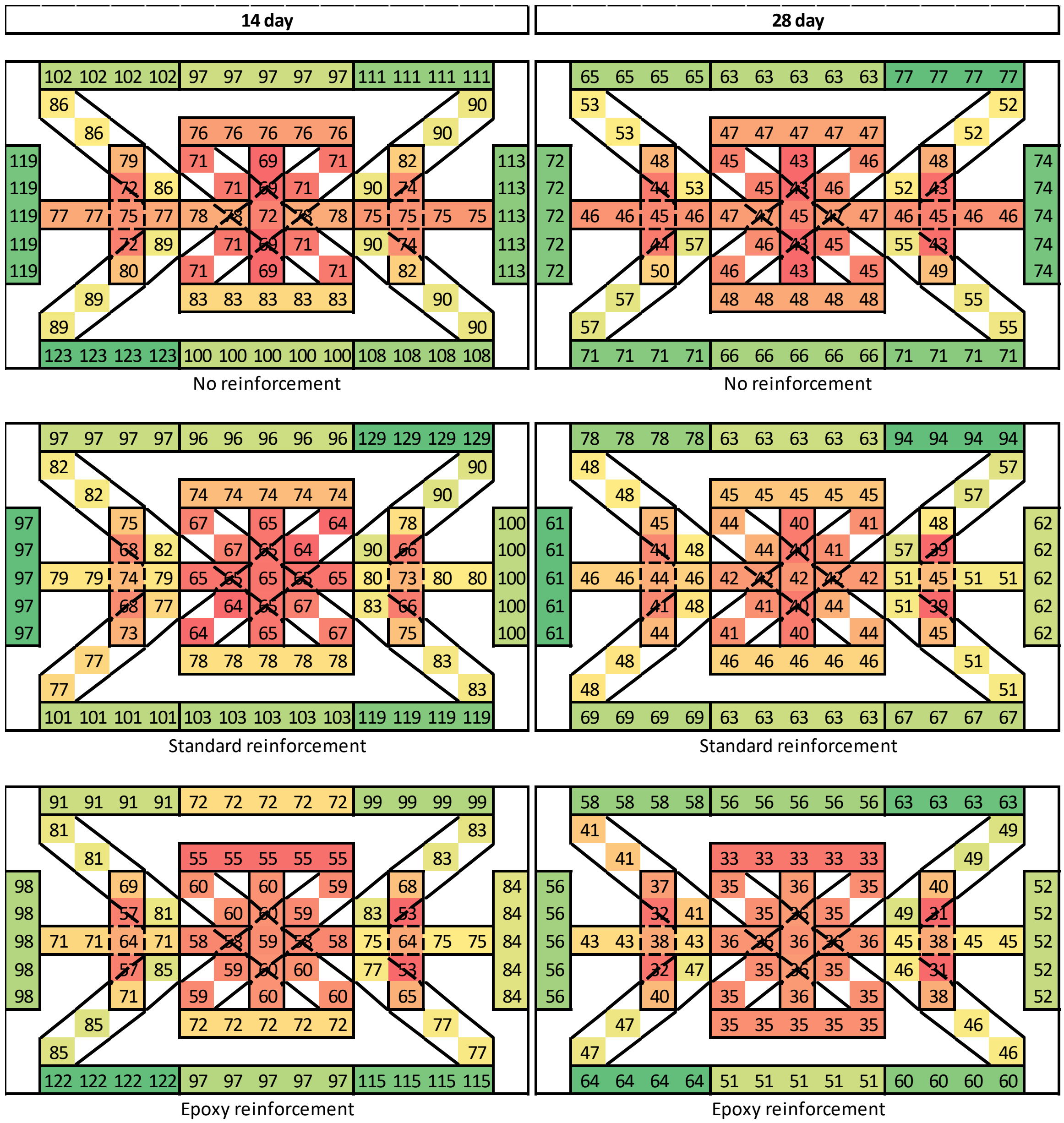

FIGURE C.8: 14 and 28 day VHES-LMC miniature slab data

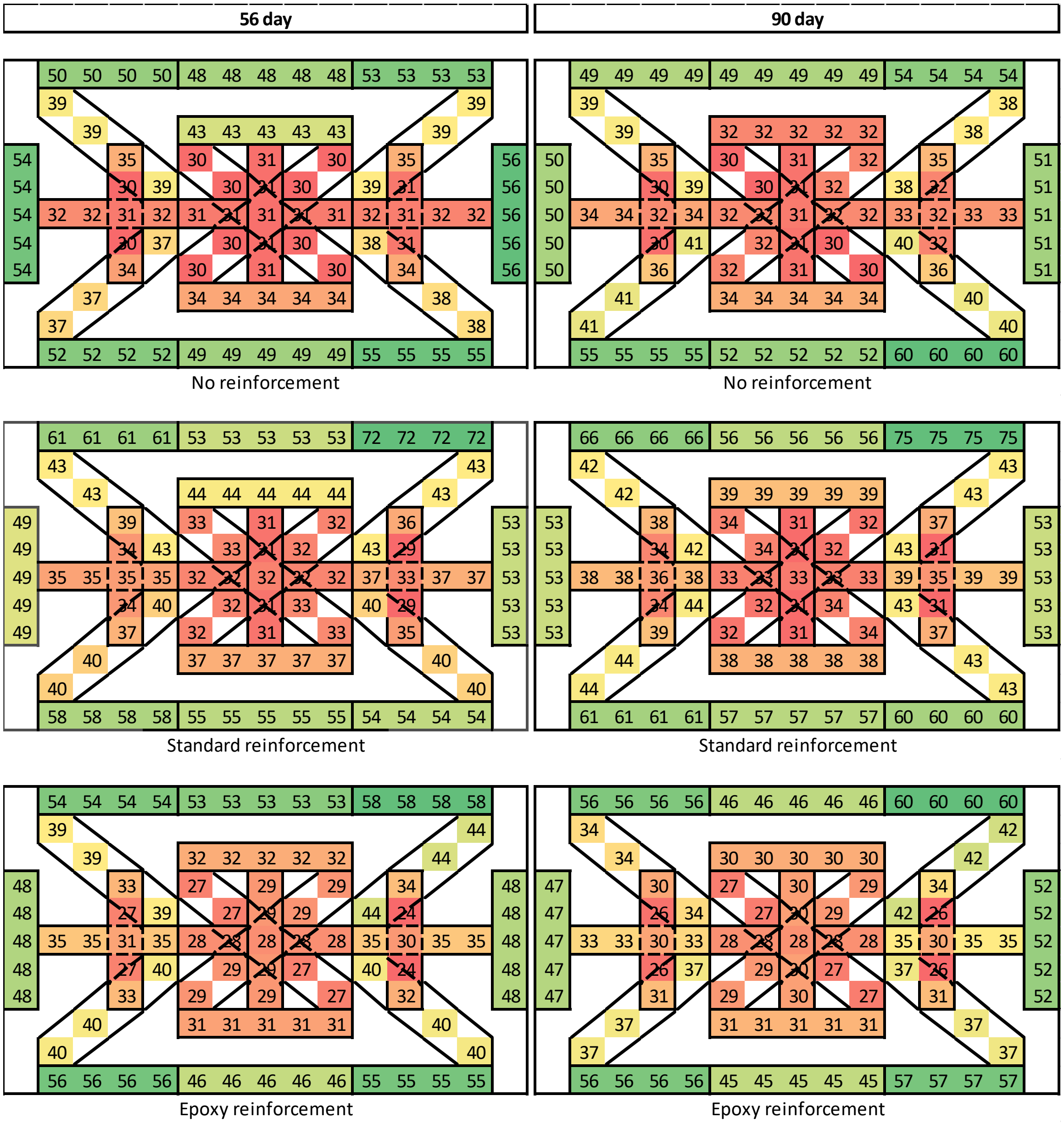

FIGURE C.9: 56 and 90 day VHES-LMC miniature slab data

APPENDIX D: SUPPLEMTAL INFORMATION FOR CHAPTER 4

Diagonal														Row Average	
	Rebar										No Rebar			All points	No vert. rebar
	1	2	3	4	5	6	7	8	9	10	11	12	13		
1	1.5	1.4	1.5	1.6	1.4	1.5	1.5	1.3	1.3	1.7	1.4	1.4	1.5	1.46	1.44
2	1.5	1.4	1.4	1.4	1.3	1.3	1.2	1.2	1.2	1.5	1.5	1.2	1.3	1.34	1.33
3	1.3	1.4	1.3	1.3	1.3	1.3	1.4	1.2	1.3	1.5	1.4	1.3	1.4	1.34	1.34
4	1.7	1.5	1.3	1.4	1.4	1.5	1.5	1.2	1.3	1.4	1.4	1.5	1.6	1.44	1.46
5	1.5	1.6	1.6	1.6	1.3	1.4	1.3	1.2	1.5	1.3	1.4	1.4	1.4	1.42	1.43
6	1.6	1.4	1.5	1.4	1.3	1.3	1.3	1.4	1.4	1.4	1.2	1.3	1.6	1.39	1.40
7	1.3	1.4	1.5	1.4	1.4	1.4	1.4	1.4	1.2	1.3	1.3	1.3	1.4	1.36	1.35
8	1.4	1.5	1.5	1.8	1.3	1.4	1.5	1.5	1.4	1.4	1.4	1.4	1.4	1.45	1.41
9	1.5	1.4	1.5	1.3	1.3	1.1	1.5	1.2	1.2	1.3	1.5	1.5	1.6	1.38	1.45
10	1.5	1.4	1.5	1.5	1.5	1.5	1.5	1.4	1.4	1.2	1.3	1.3	1.4	1.42	1.43
11	1.5	1.4	1.3	1.4	1.4	1.3	1.5	1.4	1.3	1.3	1.3	1.3	1.4	1.37	1.38
12	1.6	1.4	1.4	1.7	1.3	1.3	1.4	1.5	1.3	1.2	1.4	1.3	1.3	1.39	1.38
13	1.5	1.5	1.5	1.6	1.6	1.6	1.7	1.6	1.5	1.5	1.6	1.3	1.6	1.55	1.54
														1.408	1.409

Average														Row Average	
	Rebar										No Rebar			All points	No vert. rebar
	1	2	3	4	5	6	7	8	9	10	11	12	13		
1	1.5	1.3	1.5	1.6	1.4	1.5	1.4	1.3	1.5	1.6	1.5	1.4	1.5	1.46	1.46
2	1.5	1.5	1.4	1.3	1.3	1.2	1.3	1.3	1.3	1.5	1.5	1.3	1.3	1.37	1.36
3	1.4	1.4	1.2	1.3	1.3	1.4	1.4	1.3	1.3	1.5	1.4	1.3	1.5	1.36	1.35
4	1.7	1.5	1.3	1.3	1.4	1.5	1.4	1.3	1.3	1.5	1.5	1.4	1.5	1.43	1.44
5	1.6	1.5	1.5	1.6	1.3	1.3	1.3	1.3	1.4	1.3	1.4	1.4	1.4	1.41	1.41
6	1.6	1.5	1.5	1.4	1.3	1.3	1.3	1.3	1.3	1.2	1.2	1.3	1.6	1.37	1.38
7	1.4	1.3	1.5	1.5	1.4	1.4	1.4	1.3	1.3	1.3	1.3	1.3	1.5	1.37	1.38
8	1.4	1.5	1.5	1.5	1.3	1.3	1.4	1.4	1.4	1.4	1.4	1.4	1.4	1.41	1.40
9	1.5	1.4	1.4	1.3	1.4	1.3	1.3	1.4	1.2	1.3	1.4	1.4	1.5	1.36	1.39
10	1.6	1.4	1.4	1.5	1.5	1.5	1.4	1.4	1.3	1.3	1.3	1.4	1.5	1.42	1.43
11	1.5	1.4	1.3	1.3	1.4	1.4	1.4	1.3	1.3	1.3	1.3	1.4	1.4	1.37	1.38
12	1.6	1.4	1.4	1.6	1.3	1.4	1.5	1.5	1.3	1.3	1.4	1.4	1.4	1.41	1.41
13	1.6	1.5	1.6	1.6	1.6	1.5	1.5	1.5	1.5	1.4	1.5	1.3	1.5	1.52	1.52
														1.406	1.409

Horizontal														Row Average	
	Rebar										No Rebar			All points	No vert. rebar
	1	2	3	4	5	6	7	8	9	10	11	12	13		
1	1.5	1.2	1.5	1.6	1.4	1.4	1.2	1.3	1.6	1.6	1.5	1.6	1.5	1.45	1.48
2	1.5	1.7	1.5	1.2	1.1	1.2	1.3	1.3	1.3	1.5	1.5	1.3	1.3	1.36	1.35
3	1.2	1.4	1.2	1.2	1.2	1.4	1.3	1.3	1.3	1.5	1.4	1.3	1.5	1.32	1.30
4	1.7	1.4	1.3	1.2	1.3	1.5	1.4	1.3	1.3	1.5	1.5	1.5	1.5	1.42	1.44
5	1.6	1.6	1.5	1.5	1.3	1.3	1.3	1.2	1.4	1.2	1.4	1.5	1.6	1.42	1.45
6	1.7	1.6	1.5	1.4	1.2	1.2	1.3	1.2	1.2	1.2	1.3	1.2	1.5	1.35	1.36
7	1.6	1.4	1.4	1.5	1.4	1.3	1.3	1.3	1.3	1.4	1.2	1.2	1.5	1.37	1.36
8	1.5	1.6	1.5	1.4	1.2	1.3	1.3	1.4	1.4	1.3	1.4	1.5	1.5	1.41	1.41
9	1.4	1.3	1.3	1.3	1.2	1.4	1.2	1.4	1.2	1.2	1.3	1.4	1.5	1.32	1.31
10	1.7	1.4	1.5	1.4	1.6	1.5	1.4	1.4	1.5	1.3	1.4	1.6	1.6	1.48	1.54
11	1.5	1.5	1.3	1.3	1.5	1.3	1.3	1.2	1.3	1.4	1.4	1.4	1.5	1.38	1.40
12	1.6	1.5	1.5	1.6	1.3	1.4	1.6	1.6	1.3	1.3	1.4	1.4	1.6	1.47	1.46
13	1.5	1.4	1.6	1.4	1.4	1.3	1.4	1.5	1.4	1.3	1.5	1.2	1.4	1.41	1.43
														1.396	1.407

Standard Deviation													
	Rebar										No Rebar		
	1	2	3	4	5	6	7	8	9	10	11	12	13
1	0.1	0.1	0.1	0.1	0.1	0.1	0.2	0.1	0.2	0.1	0.1	0.2	0.1
2	0	0.2	0.1	0.1	0.2	0.1	0.2	0.1	0.1	0.1	0	0.1	0
3	0.2	0	0.1	0.1	0.2	0.1	0.2	0.1	0.1	0.1	0.1	0	0.1
4	0	0.1	0.1	0.1	0.1	0	0.1	0.1	0.1	0.2	0.1	0.2	0.1
5	0.1	0.2	0.1	0.1	0.1	0.1	0.1	0.2	0.1	0.1	0	0.1	0.2
6	0.2	0.1	0.1	0.1	0.1	0.2	0	0.1	0.1	0.2	0.1	0.1	0.2
7	0.2	0.1	0.1	0.1	0.1	0.1	0.1	0.1	0.1	0.1	0.1	0.1	0.1
8	0.1	0.2	0.1	0.2	0.1	0.1	0.1	0.1	0	0.1	0	0.1	0.1
9	0.1	0.1	0.1	0.1	0.2	0.2	0.2	0.2	0.1	0.1	0.1	0.1	0.1
10	0.1	0.1	0.2	0.1	0.1	0.1	0.1	0.1	0.2	0.1	0.1	0.2	0.1
11	0.1	0.1	0.1	0.1	0.1	0.2	0.1	0.1	0	0.1	0.1	0.1	0.1
12	0.1	0.1	0.1	0.2	0.1	0.1	0.1	0.2	0.1	0.1	0.1	0.1	0.2
13	0.1	0.2	0.1	0.2	0.3	0.2	0.2	0.1	0.1	0.1	0.1	0.2	0.1

Vertical														Row Average	
	Rebar										No Rebar			All points	No vert. rebar
	1	2	3	4	5	6	7	8	9	10	11	12	13		
1	1.6	1.4	1.4	1.5	1.3	1.5	1.6	1.4	1.5	1.6	1.6	1.3	1.4	1.47	1.46
2	1.5	1.5	1.4	1.4	1.4	1.2	1.5	1.4	1.4	1.4	1.5	1.3	1.3	1.40	1.41
3	1.6	1.4	1.2	1.4	1.5	1.5	1.6	1.3	1.4	1.6	1.3	1.3	1.5	1.43	1.43
4	1.7	1.5	1.4	1.4	1.4	1.5	1.3	1.4	1.4	1.7	1.5	1.2	1.4	1.45	1.41
5	1.6	1.3	1.5	1.7	1.2	1.3	1.2	1.5	1.4	1.4	1.4	1.3	1.3	1.39	1.36
6	1.4	1.4	1.4	1.5	1.4	1.5	1.3	1.4	1.3	1.1	1.2	1.3	1.8	1.38	1.39
7	1.4	1.2	1.5	1.5	1.3	1.5	1.5	1.3	1.3	1.2	1.4	1.3	1.6	1.38	1.41
8	1.4	1.3	1.4	1.4	1.3	1.3	1.5	1.4	1.4	1.4	1.4	1.4	1.3	1.38	1.39
9	1.5	1.5	1.4	1.2	1.6	1.3	1.3	1.5	1.3	1.4	1.4	1.3	1.5	1.40	1.41
10	1.5	1.5	1.2	1.5	1.4	1.4	1.4	1.3	1.1	1.3	1.3	1.3	1.5	1.36	1.34
11	1.4	1.4	1.4	1.2	1.4	1.6	1.4	1.4	1.3	1.2	1.3	1.4	1.4	1.37	1.38
12	1.5	1.4	1.4	1.4	1.4	1.4	1.4	1.3	1.2	1.3	1.5	1.4	1.3	1.38	1.39
13	1.7	1.7	1.6	1.7	1.9	1.6	1.4	1.5	1.6	1.5	1.4	1.5	1.6	1.59	1.59
														1.414	1.413

FIGURE D.1: 1 day CC control mockup SR heatmaps

Diagonal														Row Average	
	Rebar										No Rebar			All points	No vert. rebar
	1	2	3	4	5	6	7	8	9	10	11	12	13		
1	2.3	2.2	2.3	2.2	2.4	2.3	2.2	2.1	2.1	2.5	2.1	2.1	2.4	2.25	2.24
2	2.4	2.2	2.1	2	2	1.9	2.1	2	2.1	2.2	2.3	1.9	2	2.09	2.11
3	2.2	2.1	2.2	2.2	2.1	2	2	2	2.3	2.3	2.1	2	2.3	2.14	2.15
4	2.5	2.2	2.3	2.1	2.2	2.3	2	2.3	2.1	2.1	2	2.1	2.1	2.18	2.16
5	2.3	2.4	2.2	2.3	2.1	2.1	2	2.3	1.9	2	1.9	2.1	2	2.12	2.06
6	2.5	2.2	2.2	2	2	2.1	2.3	2.2	2.2	1.9	1.9	2.3	2.2	2.15	2.20
7	2.5	2.2	2.1	2.1	2.1	2.2	2	1.9	2.1	2	1.9	2	2.1	2.09	2.10
8	2.2	2	2.1	2.6	1.8	2.2	2.1	2.4	2.4	2	1.9	2.1	2.1	2.15	2.09
9	2	2.3	2.3	2.1	2	2	2	2.5	2.1	1.9	1.9	2.1	2.2	2.11	2.08
10	2.3	2.1	1.9	2	2.2	2.6	2.2	2.1	2.2	1.8	1.9	2.2	2.2	2.13	2.14
11	2.1	2.1	2.1	2	2	1.9	2	1.9	2.1	1.8	2.1	2.2	2.3	2.05	2.11
12	2.2	2.2	2	2	2.3	1.9	2.4	2.3	1.8	1.9	2	1.9	2.1	2.08	2.09
13	2.3	2.6	2.3	2.4	2.3	2.6	2.4	2.4	2.3	2.3	2	2	3	2.38	2.33
														2.147	2.142

Average														Row Average	
	Rebar										No Rebar			All points	No vert. rebar
	1	2	3	4	5	6	7	8	9	10	11	12	13		
1	2.3	2.1	2.3	2.3	2.1	2.3	2.2	2.1	2.1	2.4	2.1	2	2.3	2.20	2.18
2	2.3	2.2	2	2.1	1.9	1.9	2.1	2.1	2.1	2.2	2.1	1.9	2.1	2.08	2.08
3	2.2	2	2.1	2.4	2	1.9	1.9	2.1	2.1	2.2	2	2	2.3	2.10	2.08
4	2.3	2.2	2.2	2.1	2	2.1	2	2.3	2.1	2.1	2	2	2.2	2.12	2.11
5	2.4	2.3	2.2	2.2	2	2.1	2	2.2	2.1	2	1.9	2	2.1	2.11	2.09
6	2.4	2.3	2.2	2.1	1.9	2	2.1	2.1	2	1.8	1.8	2.1	2.3	2.08	2.09
7	2.4	2.1	2.1	2.2	2.1	2.1	2.1	2	2	1.9	1.8	2	2.2	2.06	2.08
8	2.3	2.1	2.1	2.4	1.8	1.9	2.1	2.3	2.2	2	2	2.1	2.3	2.12	2.10
9	2	2.1	2	2	2	2	1.9	2.4	2	2	1.9	2	2.4	2.05	2.03
10	2.3	2.1	2	2	2.2	2.2	2	2.1	2.1	1.9	2	2.2	2.3	2.11	2.15
11	2.2	2.1	2	2.1	2.2	1.9	1.8	1.8	2	2	2	2.1	2.3	2.03	2.06
12	2.2	2.2	2	2	2.2	2	2.3	2.1	1.8	1.9	2	2	2.2	2.06	2.07
13	2.2	2.4	2.3	2.2	2.1	2.2	2.1	2.3	2.2	2.1	1.9	1.8	2.5	2.18	2.14
														2.101	2.096

Horizontal														Row Average	
	Rebar										No Rebar			All points	No vert. rebar
	1	2	3	4	5	6	7	8	9	10	11	12	13		
1	2.3	2	2.2	2.3	2	2.1	1.8	2	2.1	2.3	2	2	2.2	2.10	2.08
2	2.3	2.2	2	2	1.9	1.9	2	2	2.1	2.1	2.2	1.9	2.2	2.06	2.08
3	2.1	1.8	2	2.1	2	2	1.9	2.1	2	2.1	2.1	1.9	2.3	2.03	2.04
4	2.2	2.1	2.1	2	2	2.1	2.1	2.4	2	2	2	2.1	2.2	2.10	2.09
5	2.7	2.1	2.2	2.2	2	2	2.2	2.3	2.1	2	2	2	2.1	2.15	2.16
6	2.5	2.5	2.2	2	1.7	1.8	2	2	1.9	1.8	1.8	2	2.2	2.03	2.04
7	2.4	2	2.1	2.1	2.1	2	2	2	1.9	2	1.8	1.9	2.3	2.05	2.06
8	2.4	2.2	2.1	2.2	1.7	1.8	2	2.2	2.1	2	2.1	2	2.4	2.09	2.10
9	2	1.9	1.9	2	1.9	2.1	1.9	2.4	2.1	2.1	1.8	1.9	2.5	2.04	2.00
10	2.3	2.1	2	1.9	2.1	2.1	1.9	2.1	2.1	1.9	2.1	2.3	2.4	2.10	2.15
11	2.3	2.1	1.9	2.1	2.3	1.9	1.7	1.8	1.9	2.1	1.9	2	2.4	2.03	2.05
12	2.2	2.1	1.8	1.8	2.1	2.1	2.1	2.1	1.8	1.9	2	2	2.2	2.02	2.03
13	2.1	2.5	2.3	2.2	2.1	2	1.9	2.2	2.2	2	1.9	1.8	2.2	2.11	2.06
														2.069	2.071

Standard Deviation													
	Rebar										No Rebar		
	1	2	3	4	5	6	7	8	9	10	11	12	13
1	0.1	0.1	0.1	0.1	0.2	0.2	0.4	0.1	0.1	0.1	0.1	0.1	0.1
2	0.1	0.1	0.1	0.1	0.1	0	0.1	0.1	0	0.1	0.2	0.1	0.1
3	0.1	0.2	0.1	0.4	0.1	0.1	0.1	0.1	0.2	0.1	0.1	0.1	0
4	0.2	0.1	0.1	0.1	0.2	0.2	0.1	0.1	0.1	0.1	0	0.1	0.1
5	0.3	0.2	0.1	0.1	0.2	0.1	0.2	0.2	0.2	0	0.1	0.1	0.1
6	0.2	0.2	0	0.1	0.2	0.2	0.2	0.1	0.2	0.1	0.1	0.2	0.2
7	0.2	0.1	0	0.1	0.1	0.1	0.1	0.1	0.1	0.1	0.1	0.1	0.1
8	0.1	0.1	0.1	0.2	0.1	0.2	0.1	0.1	0.2	0.1	0.1	0.1	0.2
9	0	0.2	0.3	0.1	0.1	0.1	0.1	0.1	0.1	0.1	0.1	0.1	0.2
10	0	0	0.1	0.1	0.1	0.3	0.2	0	0.1	0.1	0.1	0.1	0.1
11	0.1	0	0.1	0.1	0.2	0.1	0.2	0.1	0.1	0.2	0.1	0.1	0.1
12	0.1	0.1	0.2	0.2	0.1	0.1	0.2	0.2	0.1	0.1	0.1	0.1	0.2
13	0.1	0.2	0.1	0.2	0.2	0.4	0.3	0.1	0.1	0.2	0.1	0.2	0.5

Vertical														Row Average	
	Rebar										No Rebar			All points	No vert. rebar
	1	2	3	4	5	6	7	8	9	10	11	12	13		
1	2.4	2.2	2.3	2.4	2	2.4	2.5	2.1	2.2	2.3	2.2	2	2.2	2.25	2.23
2	2.3	2.1	1.9	2.2	1.9	1.9	2.2	2.2	2.1	2.2	1.9	2	2.1	2.08	2.05
3	2.3	2.2	2	2.9	2	1.8	1.9	2.1	2.1	2.3	1.9	2	2.3	2.14	2.06
4	2.2	2.2	2.3	2.1	1.8	2	2	2.2	2.2	2.1	2	1.9	2.2	2.09	2.08
5	2.1	2.3	2.3	2.1	1.8	2.1	1.9	2	2.3	2	1.9	1.9	2.2	2.07	2.05
6	2.1	2.3	2.2	2.2	2	2.1	1.9	2.1	2	1.7	1.7	1.9	2.5	2.05	2.04
7	2.2	2.1	2.1	2.3	2	2	2.2	2	2	1.8	1.8	2	2.2	2.05	2.06
8	2.3	2.1	2.2	2.4	1.8	1.8	2.1	2.3	2.1	2.1	2	2.1	2.4	2.13	2.13
9	2	2	1.8	1.9	2	1.9	1.8	2.3	1.9	2	2	1.9	2.6	2.01	2.00
10	2.3	2.1	2	2	2.2	2	2	2.1	2.1	2	2.1	2.2	2.3	2.11	2.15
11	2.1	2.1	1.9	2.2	2.3	2	1.8	1.8	1.9	2	1.9	2	2.2	2.02	2.01
12	2.1	2.3	2.2	2.2	2.1	2.1	2.3	2	1.7	1.8	1.9	2	2.4	2.08	2.09
13	2.1	2.2	2.4	2	2	1.9	1.9	2.2	2.1	2.1	1.9	1.7	2.2	2.05	2.04
														2.087	2.075

FIGURE D.2: 3 day CC control mockup SR heatmaps

Diagonal														Row Average	
	Rebar										No Rebar			All points	No vert. rebar
	1	2	3	4	5	6	7	8	9	10	11	12	13		
1	3.6	3	3	3.6	3.5	3.5	3.7	3.6	3.6	3.6	3.6	3.2	3.7	3.48	3.49
2	3.1	3.1	3.6	3	3.1	3.3	3.5	3.7	4.1	3.2	3.2	3.3	3.7	3.38	3.45
3	3.1	3.1	3.5	3.1	2.9	3.1	2.8	3.3	3.6	3.2	3.2	3.3	4	3.25	3.30
4	3.4	3.3	3.4	3.2	3	3.1	3.3	3.4	3.5	3.6	3.3	3.1	3.3	3.30	3.29
5	3.4	3.2	3.6	3.8	2.9	3.1	3.3	3.3	3.4	3.8	3	3.1	3.4	3.33	3.26
6	3	3.2	3.4	3.3	3.6	3.5	3.4	2.9	3.4	2.9	3.2	3.3	3.7	3.29	3.38
7	3.3	3.4	3.1	3.6	3.3	3.3	3.1	2.7	3.3	3	3	3.2	3.9	3.25	3.28
8	3.4	3.1	3.4	3.6	3.3	3.4	3.1	3.3	3.6	3.3	3.1	3	3.6	3.33	3.31
9	3.3	3.1	3.2	2.9	3.4	3.7	3.7	3.9	3.1	3.4	3.2	2.9	3.7	3.35	3.31
10	3.1	3.1	3.2	2.9	3.4	2.9	3.6	3.4	3.3	3.4	3	3.3	3.4	3.23	3.29
11	3.2	3.4	3.4	2.7	3.1	3.1	3.3	3.7	3	3.5	3.2	3.3	3.3	3.25	3.23
12	3.3	3.6	3.2	3.2	3.3	3	3.7	3.7	3.1	3.2	3.5	3.1	3.4	3.33	3.33
13	3.6	3.7	3.6	3.2	3.5	3.4	3.7	3.9	3.4	3.5	3.1	3.3	3.6	3.50	3.48
														3.327	3.337

Average														Row Average	
	Rebar										No Rebar			All points	No vert. rebar
	1	2	3	4	5	6	7	8	9	10	11	12	13		
1	3.5	3.3	3.3	3.7	3.5	3.6	3.4	3.3	3.7	3.6	3.5	3.2	3.8	3.49	3.49
2	3.3	3.3	3.5	3.2	3.1	3.3	3.5	3.4	3.7	3.4	3.3	3.1	3.7	3.37	3.40
3	3.3	3.2	3.2	3.3	3.2	3	3.3	3.5	3.6	3.3	3.2	3.1	3.8	3.31	3.35
4	3.4	3.3	3.3	3.3	3	3.1	3.4	3.5	3.3	3.6	3.3	3.4	3.5	3.33	3.32
5	3.6	3.4	3.7	3.8	3	3.3	3.2	3.4	3.3	3.5	3.1	3.2	3.5	3.38	3.31
6	3.4	3.4	3.3	3.4	3.2	3.4	3.3	3	3.4	3	3	3.2	3.7	3.27	3.31
7	3.3	3.3	3.3	3.5	3.3	3.4	3.3	3	3.3	3.3	3	3.4	3.9	3.33	3.35
8	3.4	3.2	3.3	3.5	3.2	3.2	3.3	3.5	3.5	3.5	3.2	3.3	3.6	3.36	3.35
9	3.4	3.1	3.1	3	3.2	3.4	3.5	3.7	3.3	3.4	3.1	3	3.8	3.32	3.30
10	3.2	3.2	3.2	3	3.3	3.2	3.4	3.4	3.5	3.2	3.2	3.4	3.8	3.31	3.38
11	3.3	3.2	3.3	3.1	3.2	3.4	3.3	3.4	3.4	3.3	3.1	3.3	3.6	3.31	3.33
12	3.4	3.6	3.3	3.1	3.3	3.3	3.4	3.4	3.1	3.3	3.5	3.2	3.5	3.33	3.32
13	3.9	3.7	3.6	3.6	3.3	3.4	3.5	3.8	3.5	3.5	3.3	3.3	3.4	3.52	3.47
														3.356	3.360

Horizontal														Row Average	
	Rebar										No Rebar			All points	No vert. rebar
	1	2	3	4	5	6	7	8	9	10	11	12	13		
1	3.3	3.3	3.5	3.7	3.3	3.3	2.9	3.1	3.5	3.6	3.4	3.2	3.7	3.37	3.35
2	3.2	3.3	3.3	3.5	3.1	3.2	3.3	3	3.5	3.3	3.5	3	3.7	3.30	3.33
3	3.4	3.1	3.4	3.6	3.1	2.9	3.4	3.6	3.4	3.3	3.3	2.9	3.7	3.32	3.33
4	3.6	3.2	3	3.2	3	3.2	3.3	3.6	3.3	3.3	3.3	3.6	3.6	3.32	3.34
5	4	3.5	3.8	3.7	3.2	3.3	3.4	3.6	3.3	3.3	3	3.1	3.7	3.45	3.44
6	3.7	3.6	3.3	3.2	2.8	3	3.4	2.8	3.3	3.1	3	2.9	3.6	3.21	3.25
7	3.3	3.1	3.4	3.1	3.3	3.6	3	3.1	3.2	3.1	2.9	3.3	3.7	3.24	3.26
8	3.4	3.3	3.3	3.7	3.1	3.1	3.4	3.9	3.7	3.6	3.3	3.5	3.7	3.46	3.43
9	3.7	3.2	2.9	3.2	3	3.3	3.5	3.6	3.4	3.3	2.9	2.9	4	3.30	3.29
10	3.5	3.3	3.3	2.9	3.3	3.3	3.1	3.6	3.8	3.3	3.5	3.6	4.2	3.44	3.54
11	3.5	3.4	3.4	3.6	3.4	3.5	3.1	3.3	3.7	3.4	3.1	3.4	3.6	3.42	3.40
12	3.4	3.6	3.1	2.9	3.4	3.5	3.4	3.3	3	3.3	3.4	3.2	3.6	3.32	3.31
13	4	3.4	3.6	3.4	3.3	3.4	3	3.7	3.5	3.3	3.1	2.9	3.3	3.38	3.34
														3.347	3.353

Standard Deviation													
	Rebar										No Rebar		
	1	2	3	4	5	6	7	8	9	10	11	12	13
1	0.2	0.3	0.3	0.1	0.2	0.4	0.4	0.3	0.3	0	0.1	0	0.2
2	0.2	0.2	0.2	0.3	0.1	0.1	0.3	0.4	0.3	0.2	0.2	0.2	0.1
3	0.2	0.1	0.4	0.3	0.3	0.1	0.5	0.2	0.2	0.1	0.1	0.2	0.2
4	0.3	0.2	0.3	0.1	0.1	0.1	0.2	0.1	0.2	0.3	0	0.3	0.2
5	0.3	0.2	0.1	0.1	0.2	0.2	0.3	0.2	0.2	0.3	0.2	0.1	0.2
6	0.4	0.2	0.1	0.2	0.4	0.3	0.2	0.3	0.1	0.1	0.2	0.2	0.1
7	0	0.2	0.2	0.3	0	0.2	0.5	0.3	0.1	0.4	0.2	0.2	0.2
8	0.1	0.1	0.1	0.2	0.1	0.2	0.2	0.3	0.2	0.2	0.1	0.3	0.1
9	0.2	0.1	0.2	0.2	0.2	0.3	0.2	0.2	0.2	0.1	0.2	0.1	0.2
10	0.2	0.1	0.1	0.2	0.2	0.3	0.3	0.2	0.3	0.2	0.3	0.2	0.4
11	0.2	0.3	0.1	0.5	0.2	0.3	0.3	0.3	0.4	0.3	0.1	0.1	0.3
12	0.1	0.1	0.2	0.2	0.1	0.3	0.3	0.3	0.1	0.1	0.1	0.1	0.1
13	0.3	0.4	0.1	0.5	0.2	0	0.4	0.1	0.2	0.2	0.3	0.4	0.2

Vertical														Row Average	
	Rebar										No Rebar			All points	No vert. rebar
	1	2	3	4	5	6	7	8	9	10	11	12	13		
1	3.6	3.5	3.4	3.7	3.6	4	3.6	3.3	4	3.6	3.5	3.2	4.1	3.62	3.63
2	3.5	3.5	3.5	3.2	3	3.4	3.8	3.5	3.6	3.6	3.2	3.1	3.8	3.44	3.44
3	3.4	3.3	2.8	3.1	3.5	3	3.7	3.5	3.7	3.4	3.2	3.2	3.8	3.35	3.41
4	3.1	3.5	3.5	3.4	2.9	3	3.7	3.4	3.2	3.9	3.3	3.4	3.6	3.38	3.34
5	3.4	3.6	3.7	3.9	2.9	3.5	2.9	3.4	3.1	3.3	3.3	3.3	3.3	3.35	3.24
6	3.6	3.3	3.3	3.6	3.1	3.6	3.1	3.4	3.4	2.9	2.8	3.3	3.8	3.32	3.30
7	3.3	3.5	3.3	3.7	3.3	3.3	3.9	3.3	3.4	3.7	3.2	3.6	4	3.50	3.50
8	3.3	3.1	3.2	3.3	3.3	3.2	3.4	3.3	3.3	3.6	3.1	3.3	3.5	3.30	3.30
9	3.3	3.1	3.1	3	3.3	3.2	3.3	3.7	3.5	3.5	3.2	3.1	3.7	3.31	3.31
10	3.1	3.2	3.1	3.2	3.1	3.4	3.4	3.3	3.5	3	3.1	3.3	3.8	3.27	3.30
11	3.3	2.9	3.2	2.9	3.1	3.6	3.6	3.1	3.6	2.9	3.1	3.3	3.8	3.26	3.38
12	3.4	3.5	3.5	3.2	3.2	3.5	3.1	3.1	3.2	3.4	3.5	3.3	3.4	3.33	3.33
13	4.1	4.1	3.5	4.1	3.1	3.4	3.7	3.8	3.7	3.7	3.6	3.7	3.4	3.68	3.60
														3.394	3.389

FIGURE D.3: 7 day CC control mockup SR heatmaps

Diagonal														Row Average	
	Rebar										No Rebar			All points	No vert. rebar
	1	2	3	4	5	6	7	8	9	10	11	12	13		
1	6.2	5.1	5.5	5.7	5.3	5.4	6.1	5.5	6.1	6.3	5.2	5.6	6.2	5.71	5.78
2	5.4	5	5.5	5.2	5.3	5.4	5.2	5	5.2	5.8	5.8	5	5.6	5.34	5.38
3	5.4	4.8	5	5.1	4.9	5.2	5.9	5.5	6.9	6.3	5.9	5.3	5.8	5.54	5.64
4	5.9	5.6	4.7	5.1	4.9	5.8	5.7	6.1	5.6	5.4	5.1	5	5.6	5.42	5.31
5	5.1	5.9	5.6	5.7	4.6	5	5	6	5.5	5.3	4.6	5	5.7	5.31	5.14
6	6.6	5.1	5.5	4.7	4.6	5.4	5.4	4.9	5.3	5	4.8	4.9	7	5.32	5.51
7	6	5	4.9	5.6	5.3	5.5	5.1	4.9	5.5	5.1	5	4.9	6.9	5.36	5.45
8	5.4	4.9	5.6	6.2	4.5	5.2	5.4	5.7	5.4	5.5	5.4	5.3	5.6	5.39	5.33
9	5.1	5.3	4.4	5.2	5.7	5.2	5.5	6.2	5.5	5.5	4.9	5.3	6.5	5.41	5.37
10	5.2	5.3	5	5.4	5.5	6.2	5.6	5.4	5.8	5.1	5.1	5.3	5.7	5.43	5.40
11	5.3	5	5.1	4.8	5	5	5	5.4	6.5	5.5	4.8	5	5.8	5.25	5.31
12	5	5.2	4.7	5	5.1	5.1	6.1	6	5.1	5.1	5.5	5	5.5	5.26	5.25
13	6	5.7	5.9	5.6	5.9	6.1	7.2	6.1	5.7	5.7	5.7	5.1	6.8	5.96	6.04
														5.439	5.453

Average														Row Average	
	Rebar										No Rebar			All points	No vert. rebar
	1	2	3	4	5	6	7	8	9	10	11	12	13		
1	6	5.4	5.6	5.8	5.7	5.9	6.1	5.5	6.2	6.2	5.6	5.9	6.4	5.87	5.93
2	5.5	5.1	5.2	5.3	5.1	5.3	5.2	5.2	5.7	5.8	5.7	5.2	5.9	5.40	5.43
3	5.3	4.8	5	5.1	5.1	5.1	5.4	5.6	6.2	6.1	5.7	5.2	6	5.43	5.48
4	5.6	5.4	4.9	5.1	5	5.5	5.6	5.9	5.6	5.6	5.1	5.1	6.1	5.42	5.37
5	5.6	5.6	5.7	5.2	4.9	5	5.1	6	5.6	5.4	4.9	5.1	6.4	5.42	5.40
6	6	5.2	5.5	4.9	4.5	5	5.4	5.1	5.2	5.4	5	4.9	6.7	5.31	5.41
7	5.7	5	5.2	5.4	5.3	5.5	4.9	5.1	5.2	5.4	5	5.1	6.6	5.34	5.38
8	5.6	5.3	5.6	5.8	4.6	4.9	5.4	5.8	5.6	5.6	5.5	5.6	6.1	5.49	5.50
9	5.3	5.2	4.8	5	5.6	5.3	5.3	5.9	5.6	5.3	4.8	5.2	6.4	5.37	5.38
10	5.5	5.2	5.1	4.9	5.4	5.6	5.4	5.5	5.7	5.1	5.3	5.4	6.3	5.42	5.52
11	5.5	5	5.3	4.8	5.4	5.3	4.8	5	6	5.3	4.9	5.1	5.9	5.26	5.36
12	5.3	5.2	4.7	4.9	5.2	5.1	5.7	5.3	4.9	5	5.3	4.9	5.6	5.17	5.21
13	6.1	5.9	6	5.8	6	5.8	6.4	5.9	6	6	5.7	5.4	6.7	5.97	6.03
														5.453	5.492

Horizontal														Row Average	
	Rebar										No Rebar			All points	No vert. rebar
	1	2	3	4	5	6	7	8	9	10	11	12	13		
1	5.5	5.2	5.5	5.4	5.4	5.5	5	5.2	5.9	5.9	5.3	5.8	6.7	5.56	5.64
2	5.5	5.2	5.3	5.7	5	5.3	5	5.3	5.8	5.6	5.9	5.4	6.5	5.50	5.55
3	5.1	4.6	5.1	5	5.1	5.2	4.9	5.6	6.1	6	5.8	5.2	6.3	5.38	5.45
4	5.6	5	4.9	4.8	4.9	5.6	5.7	6.4	5.3	5.3	4.9	5.4	6.6	5.42	5.41
5	5.8	5.5	5.7	5	5	4.7	5	6	5.5	5.4	5	5.2	6.6	5.42	5.48
6	6	5.2	5.5	5	4.5	4.9	5.5	5.3	5.4	5.6	5.2	4.9	6.3	5.33	5.41
7	5.7	5	5.3	5.2	5.3	5.3	4.7	5.3	5	5.4	5.1	5.3	6.6	5.32	5.38
8	5.7	5.5	5.6	5.6	4.6	4.5	5.6	6.2	5.9	5.7	5.5	5.9	6.5	5.60	5.66
9	5.5	5	4.9	4.8	5.2	5.6	5.2	6	5.8	5.4	4.6	5.1	6.9	5.38	5.40
10	5.6	5.4	5.2	4.4	5.2	5.4	5	5.8	6.1	5.4	5.7	5.8	7.3	5.56	5.74
11	5.3	5.3	5.6	4.8	5.6	5.2	4.2	4.6	5.7	5.6	5	5	6.2	5.24	5.33
12	5.6	5.3	4.9	4.5	4.8	5.2	5.5	5.1	4.7	4.8	4.7	4.9	6	5.08	5.14
13	6	5.7	6.1	5.3	5.5	5.6	5.2	5.5	5.7	5.3	5.2	5.3	6.2	5.58	5.65
														5.414	5.479

Standard Deviation													
	Rebar										No Rebar		
	1	2	3	4	5	6	7	8	9	10	11	12	13
1	0.4	0.4	0.2	0.5	0.6	0.8	1.1	0.4	0.3	0.3	0.6	0.3	0.3
2	0.1	0.1	0.3	0.3	0.2	0.1	0.2	0.2	0.4	0.2	0.3	0.2	0.5
3	0.2	0.3	0.1	0.2	0.3	0.2	0.5	0.1	0.7	0.2	0.3	0.2	0.3
4	0.3	0.3	0.3	0.4	0.2	0.4	0.2	0.6	0.4	0.5	0.2	0.3	0.5
5	0.4	0.2	0.1	0.4	0.2	0.3	0.2	0.1	0.1	0.1	0.2	0.1	0.6
6	0.6	0.2	0	0.2	0.1	0.3	0.1	0.2	0.2	0.4	0.2	0	0.4
7	0.3	0.1	0.3	0.2	0	0.3	0.2	0.2	0.3	0.3	0.1	0.2	0.3
8	0.2	0.3	0.1	0.3	0.2	0.4	0.3	0.4	0.3	0.1	0.1	0.3	0.5
9	0.2	0.2	0.4	0.2	0.3	0.3	0.2	0.4	0.2	0.2	0.2	0.1	0.5
10	0.3	0.2	0.1	0.5	0.2	0.5	0.4	0.3	0.5	0.4	0.4	0.3	0.9
11	0.3	0.3	0.3	0	0.3	0.4	0.6	0.4	0.4	0.4	0.1	0.1	0.3
12	0.3	0.1	0.2	0.3	0.4	0.1	0.3	0.6	0.2	0.2	0.5	0.1	0.3
13	0.2	0.3	0.1	0.6	0.6	0.3	1	0.4	0.5	0.8	0.5	0.4	0.4

Vertical														Row Average	
	Rebar										No Rebar			All points	No vert. rebar
	1	2	3	4	5	6	7	8	9	10	11	12	13		
1	6.2	5.8	5.9	6.4	6.3	6.9	7.2	5.9	6.5	6.5	6.2	6.2	6.4	6.34	6.36
2	5.5	5.2	4.9	5.1	5.1	5.3	5.3	5.2	6	6	5.4	5.2	5.6	5.37	5.38
3	5.4	5.1	4.9	5.3	5.4	4.8	5.3	5.7	5.5	6.1	5.3	5	6	5.37	5.35
4	5.3	5.5	5.2	5.5	5.2	5.1	5.4	5.2	6	6.2	5.2	4.8	6	5.43	5.39
5	5.9	5.5	5.7	5	5	5.3	5.4	6.1	5.7	5.5	5	5.2	6.8	5.55	5.59
6	5.4	5.4	5.5	5.1	4.5	4.8	5.3	5.2	5	5.7	5.1	4.9	6.7	5.28	5.30
7	5.5	4.9	5.4	5.3	5.3	5.8	4.8	5.2	5.2	5.7	5	5	6.4	5.35	5.33
8	5.7	5.4	5.7	5.6	4.8	5.1	5.1	5.5	5.4	5.7	5.5	5.7	6.1	5.48	5.50
9	5.3	5.3	5.1	4.9	5.8	5.1	5.3	5.5	5.4	5.1	5	5.2	5.9	5.30	5.38
10	5.8	5	5	5	5.6	5.3	5.7	5.2	5.2	4.7	5	5.2	5.8	5.27	5.41
11	5.9	4.8	5.2	4.8	5.5	5.7	5.3	4.9	5.9	4.9	4.9	5.2	5.7	5.28	5.45
12	5.4	5.2	4.5	5.1	5.6	5.1	5.5	4.9	5	5.1	5.7	4.9	5.4	5.18	5.25
13	6.3	6.3	6	6.4	6.7	5.7	6.7	6.2	6.6	6.9	6.2	5.8	7	6.37	6.41
														5.505	5.545

FIGURE D.4: 14 day CC control mockup SR heatmaps

Diagonal	Rebar										No Rebar			Row Average	
	1	2	3	4	5	6	7	8	9	10	11	12	13	All points	No vert. rebar
1	10	8	8.3	9.5	9	9.7	9.4	9.4	9.6	9.2	9.7	8.4	10	9.29	9.37
2	8.3	8	7.6	8.3	7.9	7.3	8.5	8.7	9.3	9.5	8.4	8.2	8.9	8.38	8.39
3	7.9	7.5	8.5	7.7	7.5	7.3	6.5	8.5	8.6	8.5	7.6	8.9	8.8	7.99	8.04
4	9.4	8	8.2	8.1	7.7	7.9	7.5	7.8	8.3	8.4	8.3	7.8	8.1	8.12	8.16
5	8.6	7.4	7.7	8.2	7.2	7.7	7.4	8.2	8.4	8.2	7.5	8.2	8.6	7.95	7.95
6	8.1	8	7.8	7.5	7.8	8	8.3	7.4	7.5	6.8	7.3	7.2	9.5	7.78	7.94
7	8.8	7.8	7.8	7.3	7.8	7.8	8.4	7.1	7.4	7.9	7.7	8	10	8.00	8.26
8	8.9	8.1	7.5	8.1	8	8.3	8.6	8.8	7.6	8	8.3	7.8	9.1	8.24	8.23
9	8.2	7.9	7.9	7.4	9.8	7.5	8.7	9.1	8.8	8.7	7.7	8.4	10	8.48	8.70
10	8.1	7.6	8.5	7.4	7.9	7.7	7.7	8	9.2	7.8	8	9.2	8.6	8.13	8.40
11	8.5	8.4	7.8	7.6	7	7.2	9.2	10	7.4	8.3	7.1	8.1	9.4	8.16	8.06
12	8.1	8.5	8.9	7.9	8.6	7	9	8.4	7.8	7.3	7.3	7	8.3	8.01	8.13
13	9.5	8.4	8	8.3	9.9	10	8.6	10	9.1	9.4	8.4	8.6	9.6	9.08	8.96
														8.276	8.353

Average	Rebar										No Rebar			Row Average	
	1	2	3	4	5	6	7	8	9	10	11	12	13	All points	No vert. rebar
1	10	8.8	8.5	9.5	8.8	9.4	8.7	8.7	9.1	8.8	8.6	8.3	9.6	8.99	8.96
2	8.5	7.9	7.4	8.3	7.5	7.5	8.2	8.2	8.7	8.9	8.1	7.9	9	8.17	8.18
3	8.4	7.5	7.7	7.5	8.1	7.4	7.5	8.2	8.4	8.4	8.1	7.9	9.3	8.04	8.20
4	8.7	8	7.9	7.7	7.4	7.8	7.8	8	8.2	8.7	8.1	8.1	8.9	8.10	8.13
5	8.5	8	8.1	8.5	7.3	7.9	7.3	8.4	7.8	8.1	7.4	7.7	9	7.99	7.89
6	8.4	8.1	8.2	7.6	7.8	7.7	7.9	7.5	7.4	7.1	7.3	7.1	9.5	7.82	7.94
7	8.6	7.3	7.6	7.6	8	7.8	7.9	7.3	7.7	8.1	7.5	8.1	9.7	7.95	8.15
8	8.7	7.7	8	8.1	7.5	8	8.6	8.7	8	8.3	8	8	8.7	8.18	8.20
9	8.1	7.8	7.6	7.2	9.2	8	8.1	8.7	8.5	8	7.4	8	9.6	8.16	8.31
10	8.6	7.8	7.5	7.7	8	7.7	7.4	7.6	8.4	7.7	7.8	8.5	9.1	7.98	8.17
11	8.5	7.8	7.3	7.2	7.3	7.6	8.6	8.6	7.9	7.8	7.4	7.7	9	7.90	7.97
12	8.6	8.4	7.7	7.5	7.7	7.5	8.3	8.4	7.8	7.6	7.5	7.4	8.8	7.93	7.97
13	9.7	9	8.4	9.1	8.8	8.8	8.5	9.6	9.2	9.4	8.8	8.7	9.6	9.05	8.97
														8.175	8.233

Horizontal	Rebar										No Rebar			Row Average	
	1	2	3	4	5	6	7	8	9	10	11	12	13	All points	No vert. rebar
1	9.7	8.5	7.8	9	8.2	7.9	7.4	8	9.1	8.8	7.8	7.9	9.7	8.45	8.45
2	8.7	8	7.3	7.9	7.3	7.3	7.4	7.6	8	8.5	8.2	7.4	9.7	7.95	8.00
3	8.3	7.8	7.9	7.3	8.2	7.6	7.4	8.1	8.1	7.8	8.7	7.2	9.6	8.00	8.18
4	9.1	7.8	7.2	7.1	7.5	8.1	7.6	8.8	7.8	7.9	7.8	7.8	10	8.06	8.14
5	8.9	7.9	8.6	7.9	7.6	7.6	7.1	8.8	7.4	7.5	7.4	7.5	9.8	8.00	8.04
6	9.7	8.4	8.4	7.5	7	7.1	7.8	7	6.4	7.8	7.5	6.8	8.9	7.72	7.81
7	9.4	7.4	7	7.3	8.3	8.1	7.4	7.5	8.2	8.4	7.4	7.9	10	8.02	8.20
8	8.7	8.1	8.6	8.3	7	7.3	8.4	9.4	8.2	8.4	8.5	8	8.8	8.28	8.28
9	8.1	7.5	7.4	7.1	7.9	8.6	8.5	8.4	8.3	7.6	7	7.7	9.9	8.00	8.10
10	8.8	7.6	7.1	7.8	8.7	8.2	6.5	6.9	8.3	8.3	7.4	8	9.6	7.94	8.05
11	9.4	7.7	7.4	6.8	7.2	7.7	8.9	8.3	7.4	7.4	7.6	7.4	8.7	7.84	8.00
12	9.3	8.3	7.4	7.1	6.8	7.6	8.4	9.3	7.9	7.4	7.4	7.4	9.1	7.95	7.96
13	9.8	8.4	8.5	9	8	8	7.4	8.7	8.8	8.6	8	8.1	8.8	8.47	8.43
														8.052	8.125

Standard Deviation	Rebar										No Rebar		
	1	2	3	4	5	6	7	8	9	10	11	12	13
1	0.3	0.9	0.8	0.5	0.5	1.4	1.2	0.7	0.5	0.5	1	0.4	0.7
2	0.2	0.2	0.2	0.4	0.3	0.3	0.7	0.6	0.7	0.6	0.3	0.5	0.6
3	0.6	0.4	0.9	0.2	0.6	0.2	1.1	0.3	0.3	0.5	0.6	0.9	0.5
4	1	0.2	0.6	0.6	0.4	0.3	0.4	0.7	0.4	1	0.3	0.5	1.2
5	0.4	0.6	0.5	0.7	0.3	0.5	0.2	0.4	0.6	0.5	0.1	0.4	0.7
6	1.1	0.3	0.3	0.2	0.8	0.6	0.4	0.6	1	0.6	0.3	0.2	0.6
7	0.9	0.6	0.6	0.5	0.3	0.3	0.5	0.2	0.4	0.3	0.2	0.3	0.7
8	0.2	0.8	0.6	0.2	0.5	0.6	0.3	0.8	0.3	0.2	0.6	0.2	0.5
9	0.1	0.2	0.3	0.2	1.1	0.6	0.9	0.4	0.3	0.6	0.4	0.4	0.8
10	0.5	0.3	0.8	0.2	0.7	0.4	0.8	0.6	0.7	0.7	0.3	0.6	0.5
11	0.9	0.5	0.6	0.4	0.4	0.3	0.8	1.4	0.9	0.5	0.3	0.4	0.4
12	0.6	0.1	1	0.4	0.9	0.4	0.8	1	0.2	0.4	0.3	0.4	0.4
13	0.2	1	0.4	0.9	1	1	1.1	0.8	0.5	0.8	1.1	0.7	0.8

Vertical	Rebar										No Rebar			Row Average	
	1	2	3	4	5	6	7	8	9	10	11	12	13	All points	No vert. rebar
1	10	9.8	9.4	10	9.2	11	9.4	8.8	8.7	8.3	8.2	8.6	8.9	9.24	9.08
2	8.6	7.7	7.2	8.7	7.4	7.8	8.8	8.3	8.8	8.6	7.8	8.2	8.5	8.18	8.16
3	9	7.1	6.8	7.5	8.7	7.2	8.6	7.9	8.6	8.8	8.1	7.7	9.6	8.12	8.39
4	7.5	8.2	8.3	8	6.9	7.5	8.3	7.5	8.6	9.8	8.2	8.6	8.2	8.13	8.08
5	8.1	8.6	8	9.3	7.1	8.5	7.3	8.1	7.5	8.5	7.4	7.4	8.7	8.04	7.69
6	7.5	7.9	8.4	7.9	8.5	8.1	7.5	8.2	8.4	6.8	7	7.2	10	7.95	8.06
7	7.7	6.7	8.1	8.2	7.9	7.6	8	7.4	7.6	7.9	7.3	8.5	8.9	7.83	8.00
8	8.6	6.8	7.9	8	7.6	8.4	8.9	7.9	8.1	8.4	7.3	8.1	8.2	8.02	8.09
9	8	7.9	7.5	7.2	9.9	7.9	7	8.6	8.3	7.6	7.5	8	8.7	8.01	8.12
10	9	8.1	7	7.8	7.4	7.3	8.1	7.8	7.8	6.9	7.9	8.2	9.1	7.88	8.06
11	7.6	7.4	6.7	7.2	7.8	7.8	7.7	7.4	8.9	7.6	7.5	7.7	8.9	7.71	7.85
12	8.3	8.5	6.9	7.6	7.6	7.8	7.5	7.4	7.6	8.1	7.9	7.8	8.9	7.84	7.81
13	9.7	10	8.7	10	8.5	8.5	9.6	9.9	9.8	10	10	9.4	10	9.60	9.51
														8.196	8.223

FIGURE D.5: 28 day CC control mockup SR heatmaps

Diagonal														Row Average	
	Rebar										No Rebar			All points	No vert. rebar
	1	2	3	4	5	6	7	8	9	10	11	12	13		
1	18	18	16	17	16	17	18	16	17	20	15	17	19	16.98	16.69
2	17	14	14	15	13	15	14	14	18	16	17	14	16	15.12	15.34
3	15	14	14	15	14	13	15	15	17	16	15	15	16	14.87	15.01
4	16	15	14	15	14	15	14	15	15	15	14	15	17	14.82	14.79
5	16	16	15	14	13	14	13	14	14	14	13	15	15	14.14	14.15
6	18	16	15	14	15	14	14	14	15	15	14	14	18	15.05	15.31
7	17	14	14	15	14	14	13	14	14	15	14	15	18	14.52	14.71
8	15	14	14	14	14	14	13	13	15	14	13	14	15	13.94	14.16
9	18	16	14	14	14	15	13	16	15	16	15	14	16	15.01	14.85
10	15	16	14	14	16	15	14	16	15	14	13	13	16	14.52	14.39
11	15	13	13	13	13	14	14	14	16	14	13	13	15	13.88	14.21
12	18	14	15	15	15	14	14	15	14	14	15	13	15	14.54	14.70
13	19	17	15	16	16	18	16	18	18	16	17	16	18	16.91	16.79
														14.946	15.008

Average														Row Average	
	Rebar										No Rebar			All points	No vert. rebar
	1	2	3	4	5	6	7	8	9	10	11	12	13		
1	17	17	17	17	15	17	18	16	17	18	15	17	19	16.93	16.93
2	16	13	14	15	13	14	14	14	15	15	14	15	16	14.55	14.69
3	15	14	14	14	13	14	14	14	15	16	14	14	16	14.38	14.36
4	15	14	13	14	13	14	14	14	14	14	13	14	17	14.12	14.08
5	15	15	14	14	13	13	13	15	13	13	13	14	15	13.76	13.70
6	17	14	14	13	13	13	14	14	14	13	13	14	17	14.04	14.43
7	15	14	14	14	13	13	13	13	13	14	13	14	16	13.72	13.79
8	15	14	14	14	13	13	13	13	14	14	13	13	14	13.65	13.71
9	16	14	13	13	14	14	13	15	14	14	13	13	15	13.95	13.90
10	15	14	12	13	15	14	13	14	14	13	13	14	16	13.75	13.89
11	14	13	13	13	13	13	13	13	15	14	12	13	14	13.22	13.38
12	16	14	13	14	14	13	14	15	14	13	13	13	14	13.85	13.94
13	17	16	15	15	14	16	15	17	16	15	16	16	17	15.76	15.70
														14.283	14.347

Horizontal														Row Average	
	Rebar										No Rebar			All points	No vert. rebar
	1	2	3	4	5	6	7	8	9	10	11	12	13		
1	16	16	17	15	14	16	17	16	17	17	15	16	19	16.18	16.44
2	16	14	15	15	13	14	14	14	15	15	15	16	17	14.69	14.95
3	14	14	13	14	14	14	13	15	14	15	15	13	16	14.08	14.05
4	16	14	13	13	12	15	14	15	13	13	14	14	18	14.04	14.18
5	15	15	14	14	12	12	13	17	15	13	12	14	17	13.97	13.96
6	18	14	14	12	12	13	14	13	13	13	13	14	16	13.81	14.29
7	14	13	13	13	13	12	12	12	15	15	13	14	17	13.49	13.73
8	16	15	14	14	13	13	12	13	14	14	13	13	15	13.68	13.71
9	15	13	14	14	15	14	13	16	14	14	13	13	14	13.92	13.76
10	17	14	12	12	13	14	14	14	12	13	13	15	17	13.88	14.21
11	14	13	14	14	14	13	12	12	14	14	12	14	14	13.42	13.48
12	16	14	14	14	13	13	14	16	14	12	10	12	15	13.61	13.59
13	17	15	15	15	14	14	13	15	15	14	15	13	16	14.58	14.65
														14.105	14.230

Standard Deviation													
	Rebar										No Rebar		
	1	2	3	4	5	6	7	8	9	10	11	12	13
1	1.2	0.7	1	2.5	0.8	0.8	2.2	0.6	0.4	1.8	1.2	0.6	0.7
2	0.8	0.9	1.3	0.1	0.4	1.1	0.9	0.2	2.8	0.7	3	1.4	0.8
3	0.7	0.7	0.4	0.9	1.1	0.9	1.1	0.9	1.6	0.6	1	1	0.2
4	1.5	0.6	0.8	0.8	0.7	1.4	0.2	0.2	1.1	1	1.1	0.9	1.9
5	1.1	1.3	1.2	0.3	0.4	0.8	0.3	1.9	1.8	0.5	0.7	0.8	1.2
6	1.4	1.3	0.9	0.9	1.3	1.4	0.7	0.6	1.1	1.8	1.1	0.7	0.9
7	1.8	0.3	0.7	0.7	0.7	1.1	1.1	0.8	2.2	1.1	1.3	0.4	3
8	0.8	0.4	0.6	0.4	0.5	0.4	0.7	0.3	1.1	0.5	0.4	0.8	1.1
9	2.2	1.7	0.7	1.7	0.7	1.5	0.3	1.2	1.4	1.5	1.2	0.7	1.3
10	1.8	1	1	1.1	1.4	1.3	0.7	1.4	1.3	1.2	0.9	1.2	1.6
11	1.2	0.3	1	0.7	1.5	1.7	1.5	0.7	1.7	0.8	0.7	0.3	1.2
12	1.3	0.4	2	0.8	1	0.6	0.9	1.4	0.6	1.3	2.4	0.6	0.6
13	1.1	1.3	0.1	0.7	1.3	2	1.7	1.7	1.6	1.1	1	2.7	0.8

Vertical														Row Average	
	Rebar										No Rebar			All points	No vert. rebar
	1	2	3	4	5	6	7	8	9	10	11	12	13		
1	18	17	18	20	15	17	21	17	18	17	17	17	18	17.61	17.68
2	17	12	13	15	13	13	15	14	12	15	11	14	15	13.84	13.79
3	15	15	14	13	12	15	14	13	14	17	13	14	16	14.20	14.01
4	13	15	13	14	13	13	14	14	14	14	12	13	15	13.52	13.26
5	14	13	13	13	13	13	14	14	11	13	12	13	15	13.17	13.00
6	15	13	13	13	13	12	13	14	13	12	12	13	18	13.25	13.70
7	13	13	14	14	13	14	14	13	11	13	11	14	12	13.15	12.94
8	15	14	13	14	13	13	13	13	13	13	13	13	13	13.32	13.25
9	14	14	13	11	14	12	12	14	12	13	12	13	14	12.92	13.08
10	13	14	12	12	15	12	13	13	14	12	12	13	14	12.86	13.08
11	13	13	12	12	11	11	13	13	13	13	12	13	13	12.37	12.46
12	15	14	11	13	13	13	13	13	15	13	14	13	14	13.39	13.53
13	17	16	15	15	13	16	15	18	16	15	15	18	17	15.78	15.68
														13.798	13.803

FIGURE D.6: 56 day CC control mockup SR heatmaps

Diagonal	Rebar										No Rebar			Row Average	
	1	2	3	4	5	6	7	8	9	10	11	12	13	All points	No vert. rebar
1	29	26	28	27	25	28	31	26	25	27	24	24	25	26.46	26.23
2	25	21	22	22	19	24	22	21	25	23	25	20	25	22.42	22.75
3	23	19	18	21	20	20	24	30	23	23	22	22	24	22.21	22.08
4	22	22	19	21	21	23	19	19	20	21	21	24	24	21.11	21.16
5	26	22	20	22	20	19	20	21	21	22	22	21	23	21.56	21.71
6	24	23	24	19	19	22	20	22	22	22	22	22	22	21.75	21.90
7	25	20	20	21	20	22	22	20	22	20	21	23	22	21.37	21.88
8	24	20	21	24	21	22	21	21	24	22	21	22	23	22.03	22.13
9	24	22	19	21	21	18	19	24	20	20	22	24	22	21.20	21.39
10	23	20	21	23	23	25	22	20	22	20	19	25	24	22.03	22.39
11	24	19	19	19	21	21	20	19	22	22	20	20	23	20.58	20.94
12	24	22	19	19	21	20	21	20	22	20	24	21	25	21.25	21.98
13	27	24	23	24	23	22	22	28	27	24	27	22	27	24.49	24.53
														22.189	22.388

Average	Rebar										No Rebar			Row Average	
	1	2	3	4	5	6	7	8	9	10	11	12	13	All points	No vert. rebar
1	25	23	24	25	23	26	27	24	24	25	22	23	25	24.26	24.06
2	22	20	21	21	18	21	21	20	22	21	21	19	25	20.95	21.12
3	21	19	19	20	20	19	20	23	21	22	21	20	24	20.64	20.63
4	19	20	19	20	19	21	20	20	20	20	20	21	24	20.23	20.26
5	23	21	20	22	19	19	20	22	23	21	20	20	23	21.08	21.10
6	23	21	22	18	18	20	21	20	20	19	19	21	23	20.27	20.74
7	22	21	20	20	20	21	21	19	19	20	20	21	22	20.42	20.62
8	23	20	19	21	20	20	20	21	21	20	20	20	22	20.51	20.60
9	21	20	19	20	22	18	18	21	19	20	20	21	21	19.96	20.15
10	22	20	19	21	22	22	20	20	21	19	19	23	22	20.71	20.89
11	22	20	18	18	20	21	19	18	20	20	19	19	21	19.56	19.78
12	23	21	19	18	20	20	20	21	20	19	20	20	22	20.16	20.49
13	25	23	22	23	22	22	21	25	24	23	24	23	26	23.33	23.37
														20.930	21.061

Horizontal	Rebar										No Rebar			Row Average	
	1	2	3	4	5	6	7	8	9	10	11	12	13	All points	No vert. rebar
1	22	22	23	24	20	24	23	23	25	24	22	22	28	23.05	22.96
2	22	22	22	22	18	20	20	18	22	22	19	19	26	20.85	20.93
3	20	22	21	20	20	19	18	20	19	22	20	19	25	20.30	20.24
4	20	20	18	19	19	22	21	22	20	19	19	20	27	20.41	20.37
5	24	21	21	22	19	19	22	25	22	21	20	21	25	21.58	21.64
6	24	20	21	17	16	18	21	17	18	18	20	21	25	19.59	20.60
7	22	23	19	18	20	21	20	19	19	21	19	18	22	20.12	20.01
8	22	20	19	20	19	19	20	23	20	20	19	20	22	20.19	20.15
9	19	19	18	21	19	18	18	21	21	20	18	21	21	19.52	19.20
10	23	21	18	19	22	21	19	22	20	20	19	22	21	20.61	20.48
11	23	20	18	17	22	23	17	17	19	21	18	20	20	19.59	19.63
12	24	22	20	17	21	21	22	26	21	18	16	19	21	20.58	20.55
13	25	22	22	24	23	23	20	23	22	23	22	21	23	22.56	22.31
														20.689	20.697

Standard Deviation	Rebar										No Rebar		
	1	2	3	4	5	6	7	8	9	10	11	12	13
1	3.4	2.4	3.4	1.3	2.7	2.2	4.5	1.9	1.3	2.5	1.1	1	2.6
2	2.5	2.3	1.6	0.7	0.5	2.5	0.9	1.6	2.9	1.9	3.4	0.7	1.2
3	1.7	2.4	1.7	0.9	1	1.1	2.9	5.6	2.5	0.8	1.5	2.2	0.6
4	2.5	1	0.3	1.1	2.2	2.7	0.8	1.7	0.4	1	0.9	2.3	2.6
5	3.4	1	0.6	0.9	1.4	0.7	1	2.5	2.1	0.8	2.3	1.2	1.5
6	2.8	1.6	2.3	1.1	1.7	1.8	0.2	2.7	2.1	2.4	2.2	0.8	1.5
7	3.2	1.7	0.6	1.4	0.4	1	0.9	0.6	2.1	0.9	0.9	2.3	0.6
8	0.9	0.5	1.8	2.7	1.2	2.3	0.8	1.6	3	1.5	1.3	1.7	0.9
9	2.3	1.6	0.9	2.2	2.6	0.6	0.6	2.3	1.4	1.4	2.4	2.3	1.1
10	2.1	1.1	1.2	2.2	1.6	2.6	1.4	2.1	1.4	1.6	0.8	1.8	1.9
11	2	0.3	0.7	1	2	2.3	1.4	1.1	1.7	1.9	1.4	1	1.3
12	2.5	1.8	0.9	1.4	1.4	1	2.2	4	1.9	1.2	4	0.8	2.2
13	2.4	1	0.9	1.3	1.5	1.3	0.8	2.5	2.5	0.6	2.3	2.2	2.1

Vertical	Rebar										No Rebar			Row Average	
eadin	1	2	3	4	5	6	7	8	9	10	11	12	13	All points	No vert. rebar
1	24	21	21	25	23	26	27	23	22	23	21	23	23	23.26	22.99
2	20	18	19	20	18	19	21	21	19	19	18	19	24	19.56	19.69
3	20	17	18	20	19	17	20	20	20	22	19	18	24	19.43	19.56
4	17	20	19	20	16	18	20	19	20	19	20	20	22	19.18	19.25
5	19	20	20	21	17	20	20	20	25	21	18	19	22	20.11	19.95
6	19	21	20	18	20	19	21	20	19	17	17	20	22	19.45	19.72
7	19	19	19	20	21	20	21	19	18	19	20	21	21	19.76	19.97
8	23	20	18	19	19	18	19	20	19	19	19	19	21	19.32	19.53
9	21	19	19	17	25	17	18	19	18	18	20	19	20	19.17	19.88
10	20	19	18	20	20	20	20	18	20	17	18	21	21	19.49	19.81
11	20	19	17	18	18	18	20	18	18	18	18	18	21	18.52	18.77
12	20	19	19	17	19	19	17	18	18	19	18	20	21	18.66	18.94
13	23	23	22	22	20	20	20	24	25	23	23	25	27	22.95	23.26
														19.912	20.099

FIGURE D.7: 90 day CC control mockup SR heatmaps

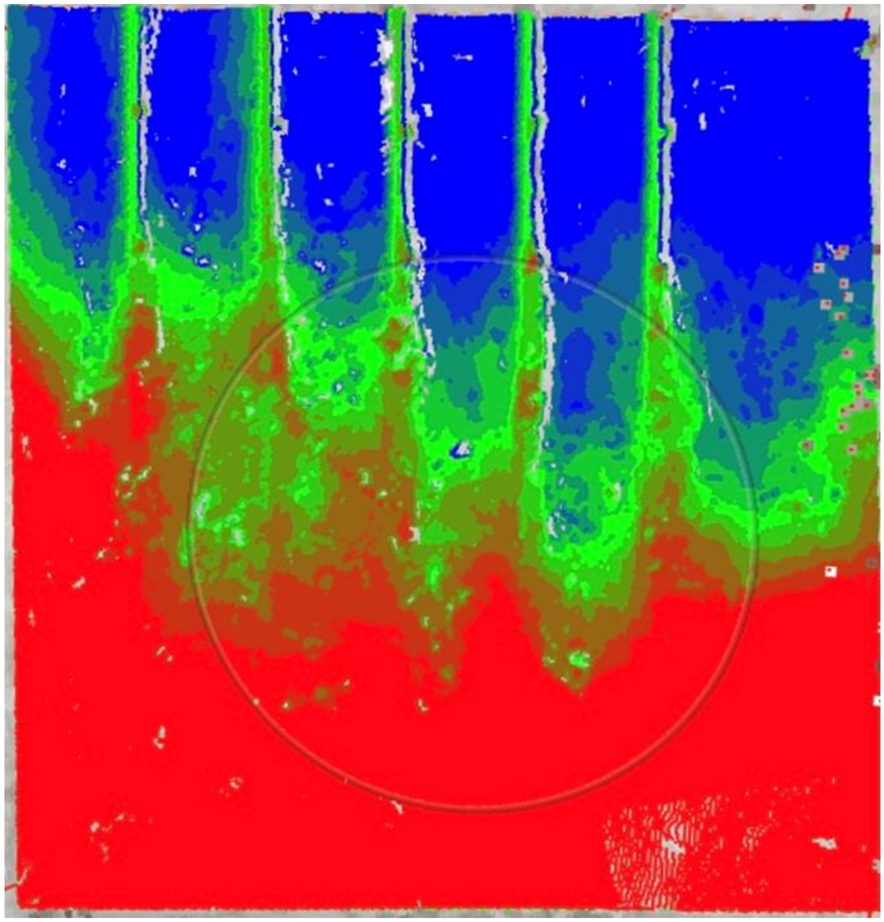

FIGURE D.8: LMC 3D surface scan

Diagonal	Rebar										No Rebar			Row Average		
	1	2	3	4	5	6	7	8	9	10	11	12	13	All Points	No vert bar	No vert bar/void
1	2.3	2.2	2.3	2.2	2.2	1.8	2.2	2	2	2.1	2	2	2.2	2.115	2.150	2.143
2	2.3	2.1	2	2	2	1.9	2	1.9	1.9	2	2	1.9	2.4	2.031	2.063	2.063
3	2.5	2.2	2.1	2	2	1.9	1.9	1.8	2.1	1.9	2	2	2.2	2.046	2.100	2.100
4	2.3	2.2	2.1	2	2.1	2	2	1.9	2	2	2	2.1	2.2	2.069	2.100	2.100
5	2.1	2	1.9	2.1	2	2	2	2	1.9	1.9	2	2.1	2.1	2.008	2.013	2.014
6	2.3	2	1.9	1.8	1.8	2	2	2	2.2	1.9	1.9	2.1	2.4	2.023	2.075	2.071
7	2.2	2.1	2.1	2	2	2	1.9	2	2	2	2	2	2.4	2.054	2.075	2.100
8	2.2	2	2.1	2	1.9	1.8	1.8	1.9	2	1.9	1.9	1.9	2.4	1.985	2.025	2.025
9	2.2	2	2	1.7	2	1.9	1.8	1.8	1.8	1.9	1.9	2	2.2	1.938	1.988	1.988
10	2.4	2	1.9	1.8	2	1.9	2.1	1.8	1.9	1.9	2	2	2.1	1.985	2.050	2.050
11	2.2	2.2	2	1.9	1.9	1.9	2	1.9	1.8	1.9	2	2	2.2	1.992	2.013	2.013
12	2.4	2	1.9	2.1	2	1.9	2	2	1.9	2	2	2.2	2.6	2.077	2.125	2.125
13	2.6	2.4	2.3	2.5	2.3	2.1	2.5	2	2	2.2	2.2	2.4	3.1	2.354	2.425	2.414
														2.052	2.092	2.093

Average	Rebar										No Rebar			Row Average		
	1	2	3	4	5	6	7	8	9	10	11	12	13	All Points	No vert bar	No vert bar/void
1	2.3	2.2	2.3	2.2	2.1	1.9	2.2	2.1	2.1	2	2.1	2.1	2.3	2.151	2.196	2.200
2	2.4	2.1	2.1	2.2	2.1	2	2	1.9	2	2	2	2.1	2.4	2.095	2.125	2.125
3	2.4	2.3	2.2	2.1	2	2	1.9	1.9	2	2	2	2.1	2.2	2.085	2.113	2.113
4	2.4	2.2	2	2	2.1	2	2	2	2.1	2.1	2.1	2.1	2.2	2.090	2.117	2.117
5	2.3	2.1	2	2.1	2	2	2	2	2	2	2.1	2.2	2.3	2.079	2.113	2.124
6	2.4	2.1	2	1.9	1.9	2	2	2	2	2	2	2.1	2.4	2.051	2.079	2.076
7	2.3	2.1	2	2	2	2	2	2	1.9	2	2.1	2.1	2.4	2.067	2.096	2.117
8	2.3	2.1	2.1	2	1.9	1.9	1.9	2	2	1.9	2	2	2.3	2.026	2.067	2.067
9	2.4	2.1	2	1.8	2	2	1.8	1.9	1.9	1.9	2	2.1	2.2	2.010	2.038	2.038
10	2.5	2.1	2	1.8	1.8	1.9	2	1.8	1.9	2	2	2	2.2	1.995	2.033	2.033
11	2.4	2.2	2	1.9	1.9	1.9	2	1.9	1.9	2	2.1	2.1	2.3	2.051	2.100	2.100
12	2.4	2.2	2.1	2.1	2	1.9	2.2	2	1.9	2.1	2.1	2.2	2.5	2.141	2.192	2.192
13	2.9	2.6	2.6	2.5	2.3	2.3	2.6	2.1	2.1	2.3	2.4	2.5	2.9	2.467	2.533	2.529
														2.101	2.138	2.141

Horizontal	Rebar										No Rebar			Row Average		
	1	2	3	4	5	6	7	8	9	10	11	12	13	All Points	No vert bar	No vert bar/void
1	2.3	2.1	2.4	2.2	2	2.1	1.9	2.1	2	2.1	2.2	2.2	2.4	2.154	2.175	2.214
2	2.5	2.2	2.2	2.5	2.2	2.1	2	1.9	2	2.1	2	2	2.4	2.162	2.163	2.163
3	2.4	2.4	2.4	2.2	2.1	2.1	2	1.8	1.9	1.9	1.9	2	2.2	2.100	2.113	2.113
4	2.5	2.1	2	2	2	2	2	2	2	2.1	2.1	2.1	2.1	2.077	2.100	2.100
5	2.6	2.1	2.1	2.2	2	2	2	2	2	2	2.1	2.2	2.4	2.131	2.175	2.200
6	2.5	2.1	2	1.9	1.7	2	2	2	1.9	1.9	2	2.1	2.4	2.038	2.075	2.071
7	2.4	2.2	2	2	1.9	2.1	2	2	1.9	2	2.1	2.2	2.4	2.092	2.113	2.133
8	2.5	2.1	2.1	2	1.9	2	2	2	1.8	1.7	1.9	2	2.3	2.023	2.063	2.063
9	2.7	2.1	2	1.9	2	2.2	1.9	2	1.8	1.9	2	2	2.2	2.054	2.075	2.075
10	2.5	2.2	2	1.8	1.7	1.9	2.1	1.9	1.8	2.1	2	2	2.4	2.031	2.063	2.063
11	2.7	2.2	2	2	2	1.8	1.9	2	2	2.1	2.2	2.2	2.5	2.123	2.188	2.188
12	2.5	2.2	2.1	2.1	2.2	1.9	2.4	2.2	1.9	2.1	2.2	2.3	2.4	2.192	2.250	2.250
13	3	2.7	2.5	2.5	2.3	2.2	2.5	2.2	2.1	2.2	2.3	2.4	2.7	2.431	2.475	2.471
														2.124	2.156	2.162

Standard Deviation	Rebar										No Rebar		
	1	2	3	4	5	6	7	8	9	10	11	12	13
1	0	0.1	0.1	0	0.1	0.2	0.3	0.1	0.1	0.1	0.1	0.1	0.1
2	0.1	0.1	0.1	0.3	0.1	0.1	0.1	0.1	0.1	0.1	0.1	0.2	0.1
3	0.1	0.1	0.2	0.1	0.1	0.1	0.1	0.1	0.1	0.2	0.2	0.1	0.1
4	0.1	0.1	0.1	0	0.1	0	0	0.1	0.1	0.1	0.1	0.1	0.1
5	0.3	0.1	0.1	0.1	0.1	0.1	0	0	0.1	0.1	0.1	0.1	0.2
6	0.1	0.1	0.1	0.2	0.2	0.1	0.1	0	0.2	0.1	0.1	0	0
7	0.1	0.1	0.1	0	0.1	0.1	0.1	0	0.1	0.1	0.1	0.1	0.1
8	0.2	0.1	0.1	0.1	0	0.1	0.1	0.1	0.2	0.2	0.1	0.2	0.1
9	0.3	0.1	0	0.1	0.1	0.2	0.1	0.1	0.1	0.1	0.1	0.1	0.1
10	0.1	0.1	0.1	0	0.2	0.1	0.1	0.1	0.1	0.1	0	0.1	0.2
11	0.3	0	0.1	0.2	0.1	0.1	0.1	0.1	0.1	0.1	0.1	0.1	0.2
12	0.1	0.2	0.2	0	0.2	0.1	0.2	0.2	0.1	0.1	0.1	0.1	0.1
13	0.2	0.2	0.3	0.1	0.1	0.3	0.1	0.1	0.2	0.2	0.2	0.2	0.2

Vertical	Rebar										No Rebar			Row Average		
	1	2	3	4	5	6	7	8	9	10	11	12	13	All Points	No vert bar	No vert bar/void
1	2.3	2.3	2.3	2.2	2.2	1.8	2.4	2.1	2.2	1.9	2.1	2.2	2.4	2.185	2.263	2.243
2	2.3	2	2.1	2	2	2	2.1	2	2	2	2.1	2.3	2.3	2.092	2.150	2.150
3	2.3	2.2	2	2	2	2	1.9	2	2.1	2.2	2.2	2.2	2.3	2.108	2.125	2.125
4	2.3	2.2	2	2	2.2	2	2	2.1	2.2	2.1	2.1	2.2	2.2	2.123	2.150	2.150
5	2.3	2.1	2.1	2.1	2.1	1.9	2	2	2	2	2.1	2.2	2.4	2.100	2.150	2.157
6	2.3	2.2	2	2.1	2.1	2.1	1.9	2	1.9	2.1	2	2.1	2.4	2.092	2.088	2.086
7	2.4	2.1	1.9	2	2	1.9	2	2	1.9	1.9	2.1	2.2	2.3	2.054	2.100	2.117
8	2.2	2.2	2.2	1.9	1.9	1.9	1.9	2	2.1	2	2.1	2.2	2.3	2.069	2.113	2.113
9	2.4	2.2	2	1.9	1.9	2	1.8	2	2	2	2	2.2	2.1	2.038	2.050	2.050
10	2.5	2.2	2	1.8	1.7	2	1.9	1.8	1.9	1.9	2	1.9	2	1.969	1.988	1.988
11	2.4	2.2	2.1	1.7	1.9	2	2	1.9	1.9	1.9	2.2	2.2	2.1	2.038	2.100	2.100
12	2.4	2.3	2.2	2.1	1.9	2	2.2	1.9	2	2.1	2.2	2.2	2.5	2.154	2.200	2.200
13	3	2.7	2.9	2.4	2.4	2.6	2.7	2.2	2.3	2.5	2.6	2.7	3	2.615	2.700	2.700
														2.126	2.167	2.167

FIGURE D.9: 1 day LMC overlay mockup SR heatmaps

Diagonal														Row Average		
	Rebar										No Rebar			All Points	No vert bar	No vert bar/void
	1	2	3	4	5	6	7	8	9	10	11	12	13			
1	4.8	4.8	4.7	4.8	4.5	3.8	4.8	4.3	4.3	4	4.1	4.4	4.6	4.454	4.525	4.486
2	4.9	4.4	4.5	4	4.2	4	4	3.9	4	4.2	4	4.2	4.7	4.231	4.313	4.313
3	5	4.4	4.4	4.4	4.1	3.9	3.9	3.6	4.3	4	4.1	4.2	4.9	4.246	4.363	4.363
4	4.7	4.5	4.2	4.1	4.1	4.1	4.1	4.1	3.9	4.1	4.1	4.7	4.3	4.231	4.263	4.263
5	4.4	4.2	4	4.1	4	4	4.2	4.1	4	3.8	3.9	4.1	4.6	4.108	4.150	4.171
6	4.7	4.4	4.2	3.9	3.9	4.2	3.9	3.8	3.7	3.8	3.9	4.2	4.9	4.115	4.175	4.171
7	4.5	4.4	4.3	3.8	3.9	3.9	3.9	4.1	3.9	3.8	4	4	5.1	4.123	4.200	4.283
8	4.5	4.5	4.1	4.2	4.3	3.9	3.9	3.6	3.7	3.7	3.8	3.9	4.5	4.046	4.088	4.088
9	5.1	4.3	4.1	4	3.9	3.9	3.8	4.1	3.5	3.9	3.9	4	4	4.038	4.038	4.038
10	4.9	4.1	4	3.9	3.9	3.9	4.1	3.7	3.6	3.9	4.1	4.1	4.4	4.046	4.138	4.138
11	5	4.4	4.1	4	3.7	3.9	3.9	3.7	3.8	3.9	4.2	4.5	4.7	4.138	4.238	4.238
12	4.9	4.3	4.3	4.3	4.2	4.1	4.2	4.1	3.9	4.3	4.3	4.4	5	4.331	4.400	4.400
13	5.7	4.9	4.6	4.5	4.4	4.3	4.9	4.3	4.5	4.5	4.6	5	5.8	4.769	4.938	4.943
														4.221	4.294	4.299

Average														Row Average		
	Rebar										No Rebar			All Points	No vert bar	No vert bar/void
	1	2	3	4	5	6	7	8	9	10	11	12	13			
1	4.8	4.6	4.8	4.7	4.4	3.8	4.4	4.2	4.2	4	4.1	4.3	4.8	4.385	4.463	4.467
2	4.8	4.5	4.4	4.2	4.3	4.1	4	4	4.1	4.2	4.1	4.4	4.7	4.295	4.354	4.354
3	4.8	4.4	4.3	4.2	4.1	4	4.1	4	4.1	4.1	4.1	4.3	4.9	4.267	4.338	4.338
4	4.8	4.5	4.2	4.2	4.2	4.1	4.1	4	4	4.2	4.2	4.4	4.6	4.267	4.313	4.313
5	4.6	4.3	4.2	4.3	4	4	4.1	4.1	3.9	3.9	4	4.3	4.9	4.210	4.258	4.290
6	4.8	4.4	4.3	4.1	4.1	4	4	4	3.8	3.8	4	4.2	5	4.193	4.267	4.281
7	4.6	4.3	4.2	4	4.1	4	4	4	3.9	3.9	4	4.2	5.3	4.190	4.283	4.361
8	4.7	4.4	4.2	4.2	4.2	3.8	4.2	3.9	3.9	3.8	3.8	3.9	4.6	4.115	4.167	4.167
9	5.1	4.4	4.2	4.1	4.1	4	3.8	4	3.7	3.9	3.9	4.1	4.3	4.121	4.150	4.150
10	5.1	4.2	4.1	3.9	3.8	4	4.1	3.8	3.7	3.9	4.1	4.1	4.3	4.072	4.150	4.150
11	5.1	4.4	4.1	4	3.8	3.9	4	3.9	3.8	4	4.2	4.5	4.6	4.164	4.246	4.246
12	5	4.5	4.3	4.2	4.2	4.2	4.7	4.4	4.1	4.3	4.4	4.5	5	4.441	4.513	4.513
13	5.5	4.9	4.7	4.6	4.4	4.4	4.9	4.4	4.4	4.5	4.6	4.9	5.4	4.736	4.846	4.843
														4.266	4.334	4.344

Horizontal														Row Average		
											No Rebar			All Points	No vert bar	No vert bar/void
	1	2	3	4	5	6	7	8	9	10	11	12	13			
1	4.6	4.4	4.9	4.5	4.1	3.8	4.1	4.1	4	4.1	4	4.3	4.9	4.292	4.363	4.400
2	5	4.5	4.5	4.3	4.3	4.2	4	4	4.3	4.4	4.1	4.5	4.7	4.369	4.425	4.425
3	4.9	4.4	4.3	4.2	4.3	4.2	4.2	4.1	3.9	4	4.2	4.3	5	4.308	4.388	4.388
4	5	4.6	4.1	4.2	4.1	4.1	4	3.9	3.9	4.1	4.2	4.4	4.8	4.262	4.313	4.313
5	4.8	4.4	4.3	4.4	4	4.1	4.1	4.1	3.8	3.9	4	4.5	5.3	4.285	4.350	4.400
6	4.9	4.3	4.3	4.5	4.3	4	4.1	4.1	3.7	3.9	4	4.2	5.3	4.279	4.350	4.371
7	4.9	4.3	4	3.8	4	4	4	4	3.8	4	4.2	4.4	6	4.262	4.413	4.517
8	4.7	4.3	4.1	3.9	4	3.7	3.8	4.1	4.1	3.9	3.8	3.8	5	4.092	4.163	4.163
9	5.1	4.3	4.1	4.2	4.2	4.2	3.8	3.9	3.6	3.8	3.9	4.1	4.5	4.131	4.163	4.163
10	5.2	4.1	4	3.9	3.7	4	4	4	3.7	3.9	4	4.1	4	4.046	4.088	4.088
11	5.3	4.4	4	4.1	4	3.9	3.9	3.9	3.8	4.1	4.2	4.5	4.6	4.208	4.288	4.288
12	5.3	4.6	4.1	4.3	4.3	4.4	5.3	5.1	4.2	4.3	4.6	4.4	5	4.608	4.650	4.650
13	5.5	4.7	4.9	4.6	4.4	4.2	4.7	4.4	4.2	4.5	4.7	4.6	5	4.646	4.750	4.757
														4.291	4.362	4.378

Standard Deviation													
	Rebar										No Rebar		
	1	2	3	4	5	6	7	8	9	10	11	12	13
1	0.2	0.2	0.1	0.2	0.2	0.1	0.4	0.1	0.2	0.1	0.1	0.1	0.2
2	0.3	0.1	0.1	0.2	0.1	0.1	0.1	0.2	0.2	0.2	0.1	0.2	0.1
3	0.2	0.1	0.1	0.2	0.2	0.2	0.2	0.4	0.2	0.1	0.1	0.1	0.1
4	0.2	0.1	0.1	0.1	0.1	0	0.1	0.1	0.2	0.1	0.1	0.3	0.3
5	0.2	0.1	0.2	0.2	0.1	0.1	0.1	0	0.1	0.1	0.2	0.2	0.4
6	0.1	0	0.2	0.3	0.2	0.2	0.1	0.2	0.1	0.1	0.1	0.1	0.2
7	0.2	0.1	0.2	0.3	0.2	0.1	0.1	0.1	0.1	0.1	0.3	0.2	0.6
8	0.2	0.1	0.1	0.3	0.2	0.1	0.6	0.3	0.2	0.1	0.1	0.1	0.4
9	0	0.1	0.2	0.1	0.2	0.2	0.1	0.1	0.2	0.1	0.1	0.1	0.3
10	0.2	0.2	0.1	0	0.1	0.1	0.1	0.2	0.2	0.1	0.1	0	0.3
11	0.2	0.1	0.1	0.1	0.2	0.1	0.1	0.2	0	0.1	0.1	0	0.1
12	0.2	0.2	0.2	0.1	0.2	0.2	0.6	0.6	0.2	0	0.2	0.2	0.1
13	0.2	0.3	0.2	0.1	0.1	0.2	0.2	0.1	0.2	0.1	0.2	0.2	0.4

Vertical														Row Average		
	Rebar										No Rebar			All Points	No vert bar	No vert bar/void
	1	2	3	4	5	6	7	8	9	10	11	12	13			
1	4.9	4.5	4.7	4.8	4.5	3.9	4.4	4.1	4.3	4	4.1	4.3	4.8	4.408	4.500	4.514
2	4.5	4.5	4.3	4.3	4.4	4	4.1	4.2	4.1	4.1	4.2	4.4	4.6	4.285	4.325	4.325
3	4.6	4.5	4.3	4.1	3.9	3.9	4.1	4.4	4	4.2	4.1	4.3	4.8	4.246	4.263	4.263
4	4.8	4.4	4.2	4.2	4.3	4.1	4.2	4.1	4.3	4.3	4.2	4.2	4.7	4.308	4.363	4.363
5	4.6	4.4	4.2	4.5	4.1	4	4	4.1	3.9	3.9	4.2	4.3	4.9	4.238	4.275	4.300
6	4.7	4.4	4.5	4	4.1	3.9	4	4.1	3.9	3.8	4	4.1	4.9	4.185	4.275	4.300
7	4.5	4.3	4.4	4.4	4.3	4	4	3.9	4	3.9	3.7	4.2	4.8	4.185	4.238	4.283
8	4.8	4.5	4.3	4.4	4.2	3.9	4.8	4	3.9	3.9	3.7	4	4.3	4.208	4.250	4.250
9	5.1	4.5	4.4	4.1	4.1	4	3.9	3.9	3.9	4	4	4.2	4.4	4.192	4.250	4.250
10	5.1	4.4	4.2	3.9	3.8	4	4.1	3.7	3.9	3.8	4.1	4.1	4.5	4.123	4.225	4.225
11	4.9	4.5	4.1	4	3.7	3.8	4.1	4	3.8	3.9	4.1	4.5	4.5	4.146	4.213	4.213
12	4.9	4.7	4.4	4.1	4	4.1	4.5	3.9	4.1	4.3	4.4	4.7	4.9	4.385	4.488	4.488
13	5.3	5.2	4.7	4.6	4.3	4.6	5	4.5	4.6	4.6	4.4	5	5.5	4.792	4.850	4.829
														4.285	4.347	4.354

FIGURE D.10: 3 day LMC overlay mockup SR heatmaps

Diagonal														Row Average		
	Rebar										No Rebar			All Points	No vert bar	No vert bar/void
	1	2	3	4	5	6	7	8	9	10	11	12	13			
1	6.5	6.6	6.7	6.6	6.3	6.1	6.4	5.7	6.2	5.6	5.8	6.2	6.3	6.231	6.300	6.286
2	6.7	5.9	5.9	5.8	5.8	5.4	5.7	6.6	5.6	5.8	5.6	5.7	5.3	5.831	5.788	5.788
3	6.6	6.5	5.6	5.9	5.6	5.5	5.3	5	5.8	5.7	5.8	5.6	6.4	5.792	5.838	5.838
4	5.6	5.4	5.5	5.7	6.3	5.7	5.7	5.7	5.3	5.9	5.7	5.9	6	5.723	5.750	5.750
5	6.2	6.1	5.9	5.7	5.5	5.9	5.7	5.4	5.2	5.3	5.7	5.7	6	5.715	5.738	5.771
6	6.3	5.7	5.6	5.3	4.8	5.8	5.5	5.5	5.4	5.3	5.1	6.1	6.6	5.615	5.675	5.614
7	6.4	5.7	6	5.1	5.2	5.3	5.3	5.5	5.2	5.4	5.5	5.8	6.5	5.608	5.738	5.817
8	6.7	6	5.9	5.4	5.3	5.2	5.5	5.3	5	5.3	5	5.5	5.9	5.538	5.600	5.600
9	6.8	5.9	5.7	5.4	5.2	5.2	5.3	5.3	5.1	5.3	5.3	5.7	5.9	5.548	5.625	5.625
10	6.9	5.9	5.5	5.3	5.2	5.7	5.6	5.1	4.8	5	5.3	5.5	5.6	5.492	5.550	5.550
11	6.7	6.1	5.3	5.4	5	5.2	5.3	4.9	5.2	5.3	5.7	5.9	6.1	5.548	5.650	5.650
12	6.7	5.9	5.7	5.7	5.7	5.7	6	5.4	5.3	5.7	5.7	5.7	6.6	5.831	5.925	5.925
13	7.1	6.4	6	6.5	5.9	5.8	6.5	5.5	5.9	5.9	6	6.7	7.4	6.277	6.438	6.429
														5.750	5.816	5.819

Average														Row Average		
	Rebar										No Rebar			All Points	No vert bar	No vert bar/void
	1	2	3	4	5	6	7	8	9	10	11	12	13			
1	6.7	6.4	6.7	6.4	6.1	5.4	5.8	5.9	6	5.7	5.5	6.1	6.3	6.060	6.139	6.181
2	6.9	6.3	6	6	5.9	5.5	5.7	5.8	5.6	5.7	5.7	5.9	6.1	5.928	5.967	5.967
3	6.6	6.4	5.9	5.8	5.6	5.5	5.5	5.1	5.6	5.7	5.8	5.8	6.7	5.851	5.942	5.942
4	6	6.1	5.7	5.6	5.9	5.6	5.6	5.7	5.5	5.9	5.9	5.9	6.3	5.838	5.875	5.875
5	6.5	6.1	6	5.7	5.6	5.8	5.7	5.7	5.5	5.5	5.8	6	6.3	5.862	5.925	5.976
6	6	5.7	5.8	5.6	5.5	5.7	5.6	5.6	5.4	5.4	5.4	6.1	6.9	5.741	5.825	5.790
7	6.1	5.9	5.9	5.6	5.4	5.4	5.4	5.5	5.3	5.4	5.6	5.7	6.4	5.667	5.725	5.794
8	6.6	5.9	5.9	5.6	5.4	5.3	5.4	5.4	5.1	5.3	5.2	5.6	6	5.579	5.642	5.642
9	6.8	6	5.6	5.5	5.4	5.4	5.3	5.4	5.2	5.3	5.4	5.7	6	5.614	5.679	5.679
10	6.8	6	5.6	5.4	5.1	5.5	5.6	5.2	4.9	5.1	5.4	5.7	5.5	5.529	5.583	5.583
11	6.8	6.1	5.5	5.3	5.2	5.3	5.4	5	5.2	5.4	5.8	5.6	6	5.580	5.675	5.675
12	6.8	6	5.7	5.7	5.6	5.7	6	5.7	5.3	5.7	5.9	5.8	6.5	5.862	5.942	5.942
13	7.2	6.3	6.3	6.2	6	5.9	6.5	5.9	5.9	6.1	5.9	6.5	7.4	6.323	6.471	6.462
														5.803	5.876	5.885

Horizontal														Row Average		
	Rebar										No Rebar			All Points	No vert bar	No vert bar/void
	1	2	3	4	5	6	7	8	9	10	11	12	13			
1	6.5	6	6.5	6.1	5.7	4.9	5.8	5.9	5.8	5.6	5.3	6	6.1	5.862	5.963	5.986
2	7.3	6.6	6	6.2	6.1	5.6	5.7	5.5	5.4	5.8	5.8	5.9	6.5	6.031	6.088	6.088
3	7	6.4	6.2	5.9	5.7	5.6	6	5	5.3	5.9	5.7	6.1	6.7	5.962	6.088	6.088
4	5.9	6.3	5.9	5.4	5.5	5.8	5.5	5.6	5.5	5.9	5.8	6.1	6.6	5.831	5.850	5.850
5	6.4	6.1	6.1	5.8	5.3	5.9	5.9	6	5.6	5.6	5.8	6	6.5	5.923	5.950	6.043
6	6.3	5.8	5.9	5.5	5.8	5.6	5.7	5.8	5.5	5.6	5.5	6	7.6	5.892	6.038	6.043
7	6.5	6	5.8	5.5	5.3	5.4	5.4	5.5	5.3	5.4	5.8	5.7	6.3	5.685	5.763	5.850
8	6.3	5.8	5.9	5.5	5.4	5.3	5.4	5.4	4.9	5.3	5.3	5.5	6.2	5.554	5.613	5.613
9	7.2	6.1	5.5	5.6	5.6	5.7	5.3	5.4	5	5.3	5.4	5.5	6.3	5.685	5.725	5.725
10	6.9	6	5.7	5.6	5	5.4	5.7	5.4	4.8	5.2	5.5	5.7	5.3	5.554	5.575	5.575
11	7	6	5.6	5.3	5.5	5.4	5.3	5	5.1	5.6	6.1	5.9	6.1	5.685	5.825	5.825
12	7.2	6	5.6	5.8	5.7	5.7	5.9	6.1	5.3	5.5	5.9	6	6.4	5.931	6.000	6.000
13	7.1	6.2	6.5	6.1	5.8	5.7	6.3	5.9	5.4	5.7	5.2	6.2	7.3	6.108	6.225	6.214
														5.823	5.900	5.915

Standard Deviation													
	Rebar										No Rebar		
	1	2	3	4	5	6	7	8	9	10	11	12	13
1	0.3	0.3	0.2	0.3	0.4	0.6	0.5	0.2	0.2	0.1	0.3	0.1	0.2
2	0.4	0.4	0.1	0.2	0.2	0.1	0	0.7	0.2	0.2	0.1	0.2	0.7
3	0.4	0.1	0.3	0.2	0.1	0.2	0.4	0.2	0.3	0.2	0.2	0.3	0.3
4	0.5	0.6	0.2	0.2	0.4	0.2	0.1	0.1	0.2	0.1	0.3	0.2	0.3
5	0.4	0.1	0.1	0.1	0.3	0.1	0.2	0.3	0.2	0.2	0.2	0.3	0.3
6	0.5	0.1	0.2	0.3	0.6	0.1	0.1	0.2	0.2	0.2	0.2	0.1	0.6
7	0.6	0.2	0.1	0.6	0.3	0.2	0.1	0.1	0.1	0.1	0.2	0.1	0.1
8	0.3	0.1	0	0.2	0.1	0.1	0.1	0.1	0.2	0	0.2	0.1	0.2
9	0.4	0.1	0.1	0.1	0.2	0.3	0	0	0.2	0.1	0.2	0.2	0.2
10	0.2	0.1	0.1	0.2	0.1	0.2	0.1	0.2	0.2	0.1	0.1	0.2	0.2
11	0.2	0.1	0.2	0.1	0.3	0.1	0.1	0.2	0.1	0.2	0.3	0.5	0.2
12	0.4	0.1	0.2	0.1	0.2	0.1	0.2	0.4	0	0.2	0.2	0.2	0.1
13	0.2	0.1	0.3	0.2	0.2	0.3	0.3	0.4	0.5	0.5	0.7	0.3	0.1

Vertical														Row Average		
	Rebar										No Rebar			All Points	No vert bar	No vert bar/void
	1	2	3	4	5	6	7	8	9	10	11	12	13			
1	7	6.5	6.8	6.5	6.4	5.1	5.3	6	5.9	5.8	5.4	6	6.4	6.087	6.154	6.271
2	6.6	6.3	6.1	6.1	5.9	5.5	5.7	5.4	5.7	5.5	5.7	6	6.5	5.923	6.025	6.025
3	6.2	6.3	5.9	5.6	5.5	5.3	5.2	5.4	5.7	5.6	6	5.8	6.9	5.800	5.900	5.900
4	6.6	6.6	5.8	5.7	6	5.4	5.6	5.8	5.7	5.8	6.3	5.8	6.4	5.962	6.025	6.025
5	6.9	6	5.9	5.7	5.9	5.7	5.6	5.6	5.6	5.6	6	6.3	6.5	5.946	6.088	6.114
6	5.4	5.7	6	5.9	5.8	5.7	5.5	5.6	5.2	5.3	5.5	6.1	6.6	5.715	5.763	5.714
7	5.5	6.1	5.9	6.2	5.7	5.6	5.5	5.4	5.4	5.5	5.4	5.7	6.3	5.708	5.675	5.717
8	6.8	5.9	5.9	5.8	5.5	5.3	5.3	5.4	5.3	5.3	5.4	5.7	5.8	5.646	5.713	5.713
9	6.5	6	5.7	5.4	5.3	5.2	5.3	5.4	5.4	5.4	5.6	5.8	5.9	5.608	5.688	5.688
10	6.6	6	5.6	5.4	5	5.3	5.6	5.1	5.2	5.2	5.5	5.8	5.7	5.541	5.625	5.625
11	6.7	6.1	5.5	5.3	5	5.3	5.5	5.2	5.2	5.3	5.6	5.1	5.8	5.508	5.550	5.550
12	6.5	6	5.9	5.6	5.3	5.6	6.2	5.5	5.3	5.8	6	5.6	6.4	5.823	5.900	5.900
13	7.4	6.4	6.5	6.1	6.2	6.3	6.8	6.2	6.4	6.6	6.6	6.6	7.5	6.585	6.750	6.743
														5.835	5.912	5.922

FIGURE D.11: 7 day LMC overlay mockup SR heatmaps

Diagonal														Row Average		
	Rebar										No Rebar			All	No vert	No vert
	1	2	3	4	5	6	7	8	9	10	11	12	13	Points	bar	bar/void
1	9.5	9.3	9	9.1	8.6	6.9	9	7.9	8.1	8.1	9.1	8.4	8.7	8.592	8.800	8.771
2	9.2	8.9	8.8	8.7	8.5	7.5	7.4	7.6	7.8	8.1	7.8	8	9.2	8.269	8.338	8.338
3	9.1	8.4	8.8	8.2	7.7	7.5	7.9	7.6	7.8	7.9	8.1	7.7	9	8.131	8.263	8.263
4	9.3	9.1	8.2	7.5	8.5	8.1	8	8	7.9	8.4	8.3	7.4	8.3	8.231	8.238	8.238
5	8.1	8.2	7.7	8.2	8.3	8.5	8.4	7.6	7.8	7.4	7.8	8.8	8.5	8.100	8.175	8.157
6	8.8	8.2	7.8	7.3	8.1	7.9	8	7.9	7.9	8.4	7.5	8.3	9.9	8.154	8.288	8.286
7	8.8	8.2	8.6	7	7.1	8.1	7.6	7.9	7.7	7.9	8.6	8.2	9.3	8.077	8.238	8.333
8	8.7	8.5	8.6	7.5	7.8	7.2	7.9	7.7	7.8	7.7	7.5	8.2	8.8	7.992	8.163	8.163
9	9.6	8.2	7.9	7.3	7.7	8	7.3	8.5	7.3	7.3	7.8	8.1	7.9	7.918	7.954	7.954
10	9.8	8.3	7.8	7.6	7.5	7.9	7.1	7.5	7.1	7.1	7.7	8.1	7.5	7.769	7.825	7.825
11	9.1	8	7.7	7.6	7.6	7.6	7.5	7.5	7.7	7.8	7.8	8.5	8.8	7.938	8.088	8.088
12	9.8	8.5	7.8	8.1	8	7.9	8.1	7.8	7.4	8.2	7.9	8.4	9.5	8.262	8.363	8.363
13	9.9	8.4	9.2	9.3	9.1	8.3	9.6	8.6	8	8.4	8.4	9.6	10	8.992	9.238	9.186
														8.187	8.305	8.305

Average														Row Average		
	Rebar										No Rebar			All	No vert	No vert
	1	2	3	4	5	6	7	8	9	10	11	12	13	Points	bar	bar/void
1	9.7	9.2	9.1	9	8.5	6.5	9	8.4	8.3	8.2	8.4	8.7	9.3	8.649	8.883	8.862
2	9.4	8.7	8.6	8.5	8.1	7.6	7.8	7.5	7.6	7.8	7.9	8.2	9.3	8.237	8.368	8.368
3	9.1	8.9	8.6	8.3	7.9	7.6	7.6	7.1	7.7	8	8.3	8.1	9.1	8.174	8.296	8.296
4	9.4	8.9	8.2	7.6	8.5	8.1	8.1	7.9	7.8	8.1	8.1	8.1	8.9	8.269	8.371	8.371
5	8.7	8.5	8.1	8.1	7.7	8	8.1	7.9	7.8	7.8	8	8.5	8.7	8.154	8.208	8.281
6	9	8.7	7.9	7.7	8.1	7.9	7.9	7.8	7.8	8	7.7	8.3	10	8.223	8.350	8.357
7	9.1	8.2	8.2	7.5	7.5	7.9	7.6	7.9	7.7	7.7	8.3	8.2	9.5	8.095	8.258	8.367
8	8.8	8.3	8.1	7.4	7.6	7.2	7.7	7.8	7.6	7.4	7.8	8.1	8.8	7.893	8.064	8.064
9	9.7	8.5	7.7	7.5	7.6	7.6	7.5	8	7.2	7.6	7.9	8	8.4	7.934	7.997	7.997
10	9.6	8.4	7.7	7.3	7.4	7.6	7.5	7.5	7.2	7.1	7.8	8	8	7.782	7.896	7.896
11	9.4	7.9	7.7	7.8	7.8	7.7	7.4	7.5	7.7	7.9	8	8.3	9	8.013	8.163	8.163
12	9.6	8.5	7.8	8	8.1	7.9	8.7	8.1	7.6	7.9	8.3	8.1	9.4	8.321	8.467	8.467
13	10	8.8	9.2	9.6	9.1	9	9.7	8.7	8.2	8.5	8.9	9.3	10	9.223	9.400	9.352
														8.228	8.363	8.372

Horizontal														Row Average		
	Rebar										No Rebar			All	No vert	No vert
	1	2	3	4	5	6	7	8	9	10	11	12	13	Points	bar	bar/void
1	9.6	8.8	8.8	8.7	8.2	6.2	8.4	8.3	7.7	8.3	7.8	8.7	9.7	8.400	8.613	8.643
2	10	9.2	8.8	8.4	8	8.1	8.2	7.6	7.3	7.9	7.6	8.1	9.4	8.354	8.425	8.425
3	9.6	9	9.1	8.6	8.1	8.1	7.6	6.3	7.3	7.9	8.1	8.5	9.3	8.269	8.450	8.450
4	9.7	8.7	8.1	7.7	8.3	8.1	8.1	8.1	7.4	7.5	7.2	8.9	9.8	8.277	8.438	8.438
5	9.4	8.8	8.2	8.2	7.1	7.7	8	8.3	7.9	7.7	8	8.5	9.1	8.223	8.275	8.443
6	9	9	8	7.8	8.2	7.6	7.8	8.3	7.6	7.8	7.7	8.1	11	8.308	8.438	8.486
7	9.4	8	8.4	7.4	7.4	7.9	7.8	8.1	7.5	7.6	8.1	8	9.6	8.092	8.275	8.450
8	9.2	8.1	7.9	7.2	7.2	7.5	7.5	7.9	7.1	7.4	7.8	7.8	9.3	7.841	7.979	7.979
9	9.9	8.6	7.5	7.6	7.3	7.9	7.7	7.6	7	7.6	8.1	7.8	9.1	7.977	8.050	8.050
10	9.9	8.5	7.5	6.9	7	7.5	8	8.1	6.8	6.9	7.9	7.9	8.2	7.777	7.900	7.900
11	10	7.9	7.9	7.8	8.1	7.9	7.2	7.5	7.7	8.2	7.9	8.3	9.2	8.131	8.300	8.300
12	10	8.6	7.9	7.6	8.3	8	8.9	9.2	7.6	7.4	8.7	8.1	9	8.408	8.563	8.563
13	11	9	8.9	9	8.8	9	9	8.8	7.9	8.2	8.6	8.5	9.8	8.938	9.025	9.029
														8.230	8.364	8.396

Standard Deviation													
	Rebar										No Rebar		
	1	2	3	4	5	6	7	8	9	10	11	12	13
1	0.2	0.3	0.4	0.3	0.3	0.4	0.7	0.6	0.7	0.1	0.7	0.3	0.6
2	0.6	0.6	0.3	0.2	0.4	0.5	0.4	0.2	0.3	0.4	0.4	0.3	0.1
3	0.5	0.5	0.6	0.3	0.2	0.4	0.4	0.7	0.4	0.2	0.3	0.4	0.2
4	0.3	0.2	0.1	0.1	0.2	0.1	0.1	0.3	0.3	0.5	0.8	0.8	0.8
5	0.7	0.3	0.4	0.1	0.6	0.4	0.3	0.4	0.1	0.4	0.3	0.3	0.3
6	0.2	0.4	0.1	0.4	0.2	0.3	0.1	0.6	0.2	0.3	0.2	0.2	0.9
7	0.3	0.3	0.5	0.5	0.5	0.2	0.2	0.3	0.2	0.2	0.3	0.2	0.2
8	0.3	0.2	0.4	0.2	0.3	0.3	0.2	0.1	0.4	0.3	0.3	0.3	0.5
9	0.2	0.2	0.2	0.2	0.3	0.6	0.2	0.5	0.2	0.3	0.2	0.2	0.6
10	0.4	0.1	0.2	0.4	0.3	0.3	0.5	0.6	0.4	0.3	0.1	0.1	0.4
11	0.6	0.1	0.2	0.2	0.3	0.2	0.2	0	0	0.2	0.2	0.3	0.2
12	0.5	0.2	0.1	0.3	0.2	0.1	0.5	0.9	0.3	0.5	0.4	0.3	0.4
13	0.4	0.4	0.4	0.9	0.4	0.8	0.8	0.1	0.4	0.3	0.7	0.7	0.7

Vertical														Row Average		
	Rebar										No Rebar			All	No vert	No vert
	1	2	3	4	5	6	7	8	9	10	11	12	13	Points	bar	bar/void
1	9.9	9.4	9.6	9.3	8.7	6.5	9.7	9.1	9	8.2	8.4	9	9.6	8.954	9.238	9.171
2	8.9	8.1	8.3	8.5	7.7	7.1	7.9	7.3	7.6	7.4	8.3	8.6	9.4	8.087	8.341	8.341
3	8.7	9.3	7.9	8.1	7.8	7.3	7.2	7.3	8	8.2	8.7	8	9.1	8.123	8.175	8.175
4	9.1	8.9	8.2	7.6	8.7	8	8.1	7.5	8	8.4	8.7	8.1	8.6	8.300	8.438	8.438
5	8.6	8.4	8.4	8	7.7	7.9	7.9	7.9	7.8	8.2	8.3	8.2	8.5	8.138	8.175	8.243
6	9.2	8.9	7.8	8	7.9	8.2	8	7.2	8	7.8	7.9	8.5	9.3	8.208	8.325	8.300
7	9	8.5	7.6	8	8.1	7.7	7.4	7.6	7.9	7.6	8.2	8.3	9.6	8.115	8.263	8.317
8	8.6	8.2	7.9	7.6	7.7	6.9	7.7	7.8	7.8	7.1	8.1	8.3	8.3	7.846	8.050	8.050
9	9.6	8.6	7.8	7.5	7.8	7	7.4	8	7.4	7.8	7.8	8	8.1	7.908	7.988	7.988
10	9.2	8.5	7.9	7.4	7.6	7.4	7.5	7	7.6	7.4	7.8	7.9	8.2	7.800	7.963	7.963
11	9	7.9	7.6	7.9	7.8	7.7	7.5	7.5	7.7	7.8	8.2	8	9	7.969	8.100	8.100
12	9	8.3	7.7	8.2	8.1	7.9	9	7.4	7.9	8.2	8.4	7.9	9.8	8.292	8.475	8.475
13	11	9.1	9.6	11	9.5	9.8	11	8.8	8.6	8.8	9.7	9.8	11	9.738	9.938	9.843
														8.268	8.420	8.416

FIGURE D.12: 14 day LMC overlay mockup SR heatmaps

	Diagonal													Row Average		
	Rebar										No Rebar			All Points	No vert bar	No vert bar/void
	1	2	3	4	5	6	7	8	9	10	11	12	13			
1	12	11	12	12	12	8.3	11	10	11	11	11	11	12	11.185	11.613	11.757
2	12	12	12	11	10	10	9.5	9.9	10	10	10	11	12	10.692	10.750	10.750
3	12	11	11	11	9.9	10	9.5	8.7	10	9.8	11	10	12	10.469	10.700	10.700
4	13	12	10	9.9	11	11	10	9.8	10	11	11	11	12	10.815	10.975	10.975
5	12	11	11	11	11	10	10	9.6	10	9.6	9.8	11	12	10.562	10.763	10.786
6	12	11	10	10	9.9	10	9.9	9.7	10	9.5	10	11	13	10.431	10.663	10.600
7	11	11	11	9.3	9.5	10	9.6	10	9.6	9.9	11	11	12	10.323	10.488	10.633
8	12	10	10	9.7	9.4	8.9	9.9	9.8	9.4	9.8	9.4	11	11	10.031	10.225	10.225
9	12	11	9.8	9.6	8.9	9.8	9.5	11	9.9	9.9	10	11	10	10.192	10.163	10.163
10	13	11	9.6	9.6	9	11	9.9	9.4	9.4	8.6	9.9	10	9.7	9.915	10.025	10.025
11	13	11	9.9	10	9.5	11	9.7	9.4	10	9.8	9.8	10	11	10.415	10.500	10.500
12	13	11	10	10	11	10	11	10	9.4	10	9.8	10	12	10.685	10.838	10.838
13	14	12	11	12	11	11	12	11	11	10	11	11	14	11.623	11.863	11.800
														10.564	10.736	10.750

	Average													Row Average		
	Rebar										No Rebar			All Points	No vert bar	No vert bar/void
	1	2	3	4	5	6	7	8	9	10	11	12	13			
1	12	12	12	12	11	8.8	11	10	11	11	11	11	13	11.185	11.467	11.543
2	12	12	11	11	10	9.7	10	9.7	9.6	10	10	11	12	10.692	10.854	10.854
3	12	12	11	11	10	9.8	9.2	8.5	9.9	10	11	11	13	10.508	10.733	10.733
4	13	11	10	9.6	11	9.8	10	9.8	9.8	11	11	11	12	10.682	10.938	10.938
5	12	11	11	10	10	9.7	10	10	10	9.7	10	11	12	10.556	10.846	10.938
6	12	11	10	10	10	10	10	9.7	9.9	9.9	10	11	13	10.560	10.847	10.859
7	12	11	10	9.3	9.7	10	9.8	9.9	9.8	10	11	11	13	10.421	10.688	10.783
8	12	10	10	9.3	9.3	9.2	9.5	9.8	9.4	9.6	9.7	10	12	9.964	10.183	10.183
9	12	11	9.7	9.5	9.3	9.8	9.5	10	9.5	9.8	10	11	11	10.179	10.288	10.288
10	13	11	9.8	9.2	8.9	10	10	9.7	9.5	8.9	9.7	9.9	10	9.969	10.142	10.142
11	13	11	9.9	9.5	9.5	10	9.6	9.4	9.9	9.9	10	11	11	10.231	10.408	10.408
12	13	11	10	10	11	10	11	10	9.5	9.9	10	10	12	10.659	10.908	10.908
13	14	12	12	12	12	11	12	11	11	11	11	11	13	11.815	12.108	12.100
														10.571	10.801	10.821

	Horizontal													Row Average		
	Rebar										No Rebar			All Points	No vert bar	No vert bar/void
	1	2	3	4	5	6	7	8	9	10	11	12	13			
1	13	12	11	12	10	8.8	10	11	11	11	11	11	13	10.992	11.188	11.357
2	13	12	11	12	10	10	10	9.7	9.1	10	11	10	13	10.885	10.988	10.988
3	13	13	12	11	10	10	9.2	7.5	9.2	9.9	10	11	13	10.592	10.825	10.825
4	13	11	10	9.5	9.9	9.4	9.7	9.7	9.2	11	11	12	13	10.631	10.925	10.925
5	12	11	11	11	10	9.3	10	11	9.7	9.8	11	11	13	10.646	10.938	11.071
6	13	11	11	9.8	10	9.9	10	10	10	10	10	11	15	10.800	11.150	11.214
7	12	11	10	9.1	9.6	11	10	9.7	10	10	11	12	14	10.685	10.988	11.033
8	12	9.7	10	9	9	9.5	9.2	9.7	9.3	9.1	9.9	9.8	12	9.877	10.175	10.175
9	13	10	9.3	9.9	9.6	10	9.6	9.7	9	9.5	11	11	12	10.208	10.400	10.400
10	14	11	9.8	8.9	8.6	9.6	10	10	9.4	8.7	9.3	9.6	10	9.931	10.125	10.125
11	13	10	10	9.5	9.6	10	9	9.5	9.7	10	11	11	11	10.292	10.488	10.488
12	14	11	10	11	11	9.7	11	11	9.4	9.2	11	11	11	10.715	10.963	10.963
13	15	11	12	12	13	11	11	11	10	10	11	11	14	11.638	12.113	12.214
														10.607	10.866	10.906

	Standard Deviation												
	Rebar										No Rebar		
	1	2	3	4	5	6	7	8	9	10	11	12	13
1	0.1	0.4	0.6	0.2	1.2	0.5	1.1	0.2	0.1	0.4	0.3	0.6	0.5
2	0.9	0.3	0.8	0.7	0.2	0.8	0.5	0.3	0.7	0.3	0.3	0.8	0.7
3	0.6	0.7	1.1	0.5	0.4	0.5	0.3	0.9	0.6	0.3	0.7	0.5	0.2
4	0.1	0.3	0.1	0.3	0.5	0.7	0.3	0.1	0.6	0.2	0.1	0.7	0.7
5	0.3	0.5	0.2	0.5	0.3	0.4	0.1	0.5	0.3	0.1	0.5	0.2	0.6
6	0.8	0.3	0.4	0.3	0.2	0.3	0.3	0.6	0.4	0.3	0.4	0.3	1.2
7	0.5	0.6	0.7	0.2	0.2	0.5	0.3	0.3	0.3	0.4	0.2	0.5	1.1
8	0.4	0.4	0.2	0.4	0.3	0.3	0.4	0.1	0.1	0.4	0.3	0.4	0.6
9	0.3	0.5	0.3	0.5	0.4	0.4	0.2	0.5	0.5	0.3	0.2	0.2	0.7
10	0.5	0.1	0.3	0.4	0.3	0.5	0.3	0.5	0.2	0.4	0.4	0.3	0.4
11	0.9	0.6	0.2	0.6	0.2	0.6	0.5	0.1	0.3	0.4	0.5	0.1	0.1
12	0.4	0.3	0.1	0.6	0.7	0.3	0.1	0.6	0.2	0.6	0.5	0.2	0.2
13	0.7	0.9	0.8	0.5	0.8	0.6	0.7	0.3	0.5	0.4	0.6	0.4	0.5

	Vertical													Row Average		
	Rebar										No Rebar			All Points	No vert bar	No vert bar/void
	1	2	3	4	5	6	7	8	9	10	11	12	13			
1	13	12	11	12	12	9.2	12	10	11	11	11	10	13	11.377	11.600	11.514
2	12	11	10	11	10	8.8	11	9.4	9.4	9.9	11	12	12	10.500	10.825	10.825
3	12	12	9.5	10	9.7	9.3	8.9	9.3	10	10	11	11	13	10.464	10.675	10.675
4	13	11	10	9.4	11	9.4	10	9.9	10	11	11	11	12	10.600	10.913	10.913
5	12	10	11	9.8	10	9.6	10	9.8	10	9.7	11	11	12	10.462	10.838	10.957
6	11	11	10	10	10	9.9	11	9.1	9.4	10	11	11	13	10.448	10.729	10.761
7	12	10	9.5	9.5	9.9	9.6	9.8	9.8	9.7	9.6	10	11	12	10.254	10.588	10.683
8	11	10	10	9.2	9.6	9.2	9.4	9.9	9.4	9.9	9.8	10	11	9.985	10.150	10.150
9	12	11	9.9	9	9.5	9.4	9.3	9.9	9.6	10	11	11	11	10.138	10.300	10.300
10	13	11	10	9	9.2	10	10	9.4	9.7	9.4	10	10	10	10.062	10.275	10.275
11	12	10	9.7	9	9.3	9.6	10	9.4	9.7	9.6	10	11	11	9.985	10.238	10.238
12	13	11	10	9.5	9.9	10	11	9.8	9.8	10	11	11	12	10.577	10.925	10.925
13	14	12	13	13	12	12	13	11	11	11	12	12	13	12.185	12.350	12.286
														10.541	10.800	10.808

FIGURE D.13: 28 day LMC overlay mockup SR heatmaps

	Diagonal													Row Average		
	Rebar										No Rebar			All	No vert	No vert
	1	2	3	4	5	6	7	8	9	10	11	12	13	Points	bar	bar/void
1	17	14	14	14	15	10	14	13	15	14	15	15	16	14.295	15.075	15.229
2	16	14	14	14	13	13	12	13	13	12	13	13	15	13.400	13.575	13.575
3	16	15	13	13	13	12	12	9.4	13	12	13	13	14	12.900	13.300	13.300
4	14	15	13	12	13	12	13	12	12	13	13	13	14	12.954	13.000	13.000
5	15	15	12	13	12	13	14	13	12	12	13	14	14	13.115	13.225	13.357
6	14	13	13	13	13	13	13	12	13	12	12	13	15	12.848	13.204	13.190
7	15	14	13	12	12	12	13	12	12	13	13	13	15	12.892	13.163	13.500
8	14	13	12	12	12	11	12	12	12	12	12	13	15	12.162	12.488	12.488
9	15	13	12	11	11	11	11	13	11	12	13	13	14	12.387	12.579	12.579
10	16	13	12	12	12	12	12	11	11	9.8	12	13	13	12.233	12.679	12.679
11	15	14	12	12	13	13	12	11	12	12	12	14	15	12.754	13.075	13.075
12	16	14	12	13	14	12	13	12	12	13	13	15	18	13.741	14.279	14.279
13	18	14	14	14	15	13	15	13	13	14	15	17	21	15.031	16.000	16.100
														13.132	13.511	13.565

	Average													Row Average		
	Rebar										No Rebar			All	No vert	No vert
	1	2	3	4	5	6	7	8	9	10	11	12	13	Points	bar	bar/void
1	17	15	14	15	14	9.8	14	15	14	14	15	15	16	14.504	15.042	15.181
2	16	14	14	13	12	12	12	12	12	12	13	13	16	13.238	13.517	13.517
3	15	14	13	13	13	12	12	9.9	12	12	13	13	15	12.842	13.242	13.242
4	15	14	13	12	13	12	12	12	12	13	13	14	15	13.029	13.292	13.292
5	15	14	13	13	13	12	13	12	12	12	13	14	15	13.043	13.343	13.438
6	14	13	13	13	13	12	12	12	12	12	13	13	16	12.903	13.230	13.297
7	15	13	13	12	12	12	12	12	12	13	13	14	16	13.023	13.492	13.600
8	15	13	12	12	12	11	12	12	12	12	12	13	14	12.362	12.704	12.704
9	15	13	12	11	12	11	11	13	11	12	13	13	14	12.432	12.689	12.689
10	16	13	12	11	11	12	13	12	12	11	12	13	13	12.373	12.693	12.693
11	15	13	12	12	12	12	12	12	12	12	12	14	15	12.683	13.093	13.093
12	16	14	12	13	13	12	13	13	12	13	14	15	18	13.689	14.143	14.143
13	19	14	14	15	15	14	15	14	13	14	15	16	20	15.197	15.942	16.033
														13.178	13.571	13.609

	Horizontal													Row Average		
	Rebar										No Rebar			All	No vert	No vert
	1	2	3	4	5	6	7	8	9	10	11	12	13	Points	bar	bar/void
1	17	15	15	14	13	9.1	12	14	13	13	14	14	16	13.787	14.313	14.614
2	16	15	14	14	12	12	13	12	12	12	13	13	17	13.385	13.650	13.650
3	16	14	13	13	13	12	12	10	11	12	13	13	16	12.923	13.388	13.388
4	16	14	12	12	12	12	12	12	11	13	14	14	16	13.046	13.325	13.325
5	15	13	13	13	12	11	12	12	12	13	13	14	15	12.943	13.354	13.500
6	15	14	14	13	12	12	13	12	12	12	13	12	18	13.154	13.500	13.657
7	15	14	13	12	12	12	12	12	13	13	13	15	18	13.354	13.838	13.833
8	15	13	12	11	11	11	12	12	12	12	12	12	15	12.292	12.675	12.675
9	16	13	12	12	12	12	12	12	10	10	12	13	15	12.392	12.825	12.825
10	17	14	13	11	11	13	13	13	12	11	12	12	13	12.500	12.738	12.738
11	17	13	12	12	12	12	11	12	12	12	13	14	15	12.795	13.279	13.279
12	17	14	13	13	13	12	12	15	12	12	14	15	17	13.731	14.138	14.138
13	20	15	14	15	15	13	14	14	13	14	16	16	20	15.208	15.913	16.143
														13.193	13.610	13.674

	Standard Deviation												
	Rebar										No Rebar		
	1	2	3	4	5	6	7	8	9	10	11	12	13
1	0.2	0.7	0.4	1.1	1.4	0.6	1.9	2.3	1.1	1.5	0.5	1	0.7
2	0.8	0.4	0.5	1	0.4	0.7	0.3	0.5	0.3	0.2	0.3	0.5	1
3	1	0.5	0.7	0.4	0.3	0.5	0.4	0.5	0.8	0.8	0.3	0.3	1.2
4	0.8	0.7	0.3	0.5	0.6	0.2	0.4	0.2	0.8	0.1	0.6	0.3	0.8
5	0.4	1	0.6	0.3	0.6	0.7	0.7	0.6	0.2	0.4	0.5	0.8	1
6	0.5	0.6	1	0.4	0.4	0.6	0.4	0.3	0.4	0.2	0.4	0.5	1.3
7	0.1	1.1	0.7	0.5	0.6	0.4	0.3	0.3	0.7	0.5	0.5	1.1	1.6
8	0.9	0.1	0.3	0.5	0.4	0.3	0.2	0.5	0.1	0.5	0.7	0.7	1.1
9	1	0.6	0.4	0.7	0.5	0.3	0.4	0.7	1	1.1	0.2	0.1	0.9
10	0.7	0.5	0.4	0.7	0.4	0.5	0.5	0.8	0.7	0.9	0.2	0.7	0.5
11	1.2	0.6	0.2	0.7	0.3	0.5	0.8	0.3	0.3	0.2	0.6	0.2	0.7
12	0.6	0.6	0.3	0.3	1	0.3	0.5	1.4	0.8	0.8	0.7	0.4	0.5
13	0.9	0.3	0.3	1	0.2	0.5	1	1.1	0.1	0.3	0.5	0.6	0.8

	Vertical													Row Average		
	Rebar										No Rebar			All	No vert	No vert
	1	2	3	4	5	6	7	8	9	10	11	12	13	Points	bar	bar/void
1	17	16	15	16	16	10	16	17	15	16	15	16	17	15.431	15.738	15.700
2	15	14	13	12	12	11	12	12	12	12	13	14	15	12.931	13.325	13.325
3	14	14	12	12	13	11	12	10	13	13	13	13	15	12.702	13.038	13.038
4	15	14	12	12	13	12	13	12	13	13	14	14	15	13.087	13.550	13.550
5	14	14	13	12	13	12	12	11	12	13	14	13	16	13.072	13.450	13.457
6	14	13	12	13	13	12	12	12	12	12	13	13	16	12.708	12.988	13.043
7	15	12	12	11	13	12	13	12	13	12	14	14	15	12.823	13.475	13.467
8	16	13	13	12	12	11	12	13	12	12	13	14	13	12.631	12.950	12.950
9	14	14	12	12	12	11	11	13	12	12	13	14	13	12.515	12.663	12.663
10	16	13	13	12	12	12	12	12	12	12	12	12	13	12.385	12.663	12.663
11	14	13	12	11	12	12	13	12	12	12	12	14	14	12.500	12.925	12.925
12	16	13	12	13	12	13	12	12	13	13	15	15	18	13.597	14.013	14.013
13	19	14	14	16	15	14	16	15	13	13	15	17	19	15.354	15.913	15.857
														13.210	13.591	13.588

FIGURE D.14: 56 day LMC overlay mockup SR heatmaps

Diagonal														Row Average		
	Rebar										No Rebar			All	No vert	No vert
	1	2	3	4	5	6	7	8	9	10	11	12	13	Points	bar	bar/void
1	19	16	16	17	15	12	14	15	15	15	17	17	19	15.895	16.450	16.771
2	18	16	15	15	13	13	13	14	13	14	14	15	17	14.600	14.875	14.875
3	16	16	15	14	14	13	13	11	14	14	14	14	17	14.300	14.738	14.738
4	16	15	14	13	14	13	14	14	13	15	16	14	16	14.231	14.425	14.425
5	16	14	13	13	13	14	14	14	14	14	14	16	16	14.100	14.363	14.586
6	14	14	13	12	13	14	13	12	14	12	14	14	17	13.615	13.988	13.929
7	17	14	14	12	13	13	12	13	13	14	15	14	18	13.908	14.450	14.717
8	14	14	13	12	12	11	14	13	13	14	14	14	17	13.385	13.675	13.675
9	15	14	13	12	11	13	13	12	12	12	13	15	14	12.977	13.150	13.150
10	17	14	13	12	13	13	12	12	12	12	13	15	15	13.154	13.538	13.538
11	17	15	13	13	12	13	14	13	13	13	14	15	19	13.954	14.400	14.400
12	19	13	14	14	15	13	13	13	13	14	15	17	21	14.800	15.700	15.700
13	21	17	17	17	16	16	16	15	15	18	19	20	28	17.992	18.938	19.343
														14.378	14.822	14.911

Average														Row Average		
	Rebar										No Rebar			All	No vert	No vert
	1	2	3	4	5	6	7	8	9	10	11	12	13	Points	bar	bar/void
1	20	16	16	16	15	12	14	15	15	16	16	17	19	15.891	16.488	16.819
2	18	16	15	15	14	13	13	13	13	14	14	15	18	14.619	14.926	14.926
3	16	16	14	14	13	13	13	11	14	14	14	15	18	14.091	14.535	14.535
4	16	15	14	13	14	13	13	13	13	15	15	15	16	14.279	14.604	14.604
5	16	14	14	13	13	13	13	13	13	14	14	15	17	14.051	14.463	14.695
6	15	14	13	12	14	13	13	12	13	13	14	14	17	13.679	14.146	14.124
7	16	14	13	12	13	13	13	13	13	13	14	15	18	13.838	14.392	14.461
8	16	14	13	12	12	12	13	13	13	13	13	14	17	13.362	13.800	13.800
9	16	14	13	12	12	13	13	13	12	13	13	15	15	13.339	13.685	13.685
10	18	14	13	12	12	13	13	12	12	12	13	14	15	13.292	13.650	13.650
11	18	14	13	12	13	13	13	12	13	13	14	15	18	13.849	14.463	14.463
12	18	15	14	13	15	14	13	14	13	14	15	17	20	14.892	15.642	15.642
13	21	18	17	18	16	16	16	15	15	17	19	21	26	17.908	18.704	19.095
														14.392	14.884	14.961

Horizontal														Row Average		
	Rebar										No Rebar			All	No vert	No vert
	1	2	3	4	5	6	7	8	9	10	11	12	13	Points	bar	bar/void
1	19	16	16	14	13	12	12	15	14	15	16	16	19	15.169	15.700	16.186
2	18	16	15	16	14	14	13	13	12	14	14	15	20	14.869	15.100	15.100
3	16	16	14	14	13	13	12	9.9	13	13	14	15	19	14.077	14.613	14.613
4	17	15	14	13	12	14	13	13	12	15	15	16	18	14.431	14.638	14.638
5	17	14	14	14	12	14	13	14	14	14	15	15	18	14.408	14.775	15.114
6	16	14	13	12	13	13	13	13	13	13	14	15	20	14.008	14.638	14.586
7	15	15	14	12	12	14	12	13	14	14	15	16	21	14.269	14.813	14.883
8	17	13	13	12	11	12	12	13	12	13	13	14	18	13.246	13.725	13.725
9	18	13	12	13	13	13	13	13	11	13	14	14	17	13.533	13.966	13.966
10	20	15	14	11	11	13	14	13	12	11	13	13	15	13.462	13.988	13.988
11	18	14	14	13	14	12	12	12	12	14	15	15	17	13.969	14.613	14.613
12	19	15	14	13	15	14	13	14	13	13	14	17	20	14.862	15.475	15.475
13	21	18	15	17	17	15	14	15	13	17	19	20	25	17.269	17.888	18.400
														14.429	14.918	15.022

Standard Deviation													
	Rebar										No Rebar		
	1	2	3	4	5	6	7	8	9	10	11	12	13
1	0.6	0.6	0.8	1.5	1.4	0.4	1.9	0.2	0.8	0.9	0.6	0.3	0.8
2	0.7	0.2	0.3	0.8	0.3	0.3	0.3	0.8	0.6	0.3	0.4	0.3	1.6
3	0.4	0.3	1.2	0.6	0.2	0.3	0.2	0.8	0.6	0.6	0.4	0.4	1.2
4	1	0.3	0.3	0.5	1.6	0.6	0.5	0.6	1.4	0.6	0.2	0.9	1.8
5	0.8	0.4	0.7	0.5	0.5	0.9	0.4	1.4	0.7	0.1	0.5	0.7	1
6	1.4	0.6	0.2	0.1	1	0.8	0.3	0.4	0.2	0.9	0.2	0.8	2
7	0.9	1	0.9	0.3	0.8	0.4	0.4	0.3	0.3	1	0.6	0.8	3.1
8	1.3	0.4	0.3	0.3	0.6	0.2	1.2	0	0.4	0.6	0.4	1.1	1
9	1.5	0.5	0.9	0.5	0.9	0.6	0.2	0.6	1.2	0.3	0.6	0.3	1.3
10	1.8	0.6	0.3	0.6	0.7	0.2	1	0.8	0.6	0.8	0.2	1.1	0.8
11	0.9	0.5	0.5	1.1	0.7	0.2	1.2	0.5	0.3	0.8	0.6	0.4	0.9
12	0.5	1	0.3	0.6	0.1	0.7	0.5	0.5	0.5	0.6	0.6	0.2	0.6
13	0.3	0.6	1.2	1.3	0.6	0.8	1.6	0.7	1.3	0.7	0.3	0.7	2

Vertical														Row Average		
	Rebar										No Rebar			All	No vert	No vert
	1	2	3	4	5	6	7	8	9	10	11	12	13	Points	bar	bar/void
1	20	17	17	17	16	12	16	15	16	17	16	17	20	16.608	17.313	17.500
2	17	15	15	15	14	13	13	12	13	13	14	15	17	14.387	14.804	14.804
3	16	15	13	13	13	13	13	11	14	15	14	15	17	13.895	14.254	14.254
4	16	15	13	12	15	13	14	13	15	14	16	15	15	14.177	14.750	14.750
5	16	14	15	13	13	12	13	12	13	13	14	14	16	13.646	14.250	14.386
6	14	13	13	12	15	13	13	12	13	14	14	14	16	13.415	13.813	13.857
7	15	13	12	12	14	13	13	12	13	12	14	15	15	13.338	13.913	13.783
8	16	14	13	12	13	12	12	13	13	13	13	16	16	13.454	14.000	14.000
9	16	14	14	12	13	12	13	13	14	13	13	15	15	13.508	13.938	13.938
10	17	15	13	12	11	13	13	13	13	13	13	13	14	13.262	13.425	13.425
11	18	14	13	11	13	13	13	12	13	13	14	15	17	13.623	14.375	14.375
12	18	15	14	12	15	14	14	13	14	15	15	17	21	15.015	15.750	15.750
13	21	18	18	19	17	16	18	16	16	17	19	21	25	18.462	19.288	19.543
														14.368	14.913	14.951

FIGURE D.15: 90 day LMC overlay mockup SR heatmaps

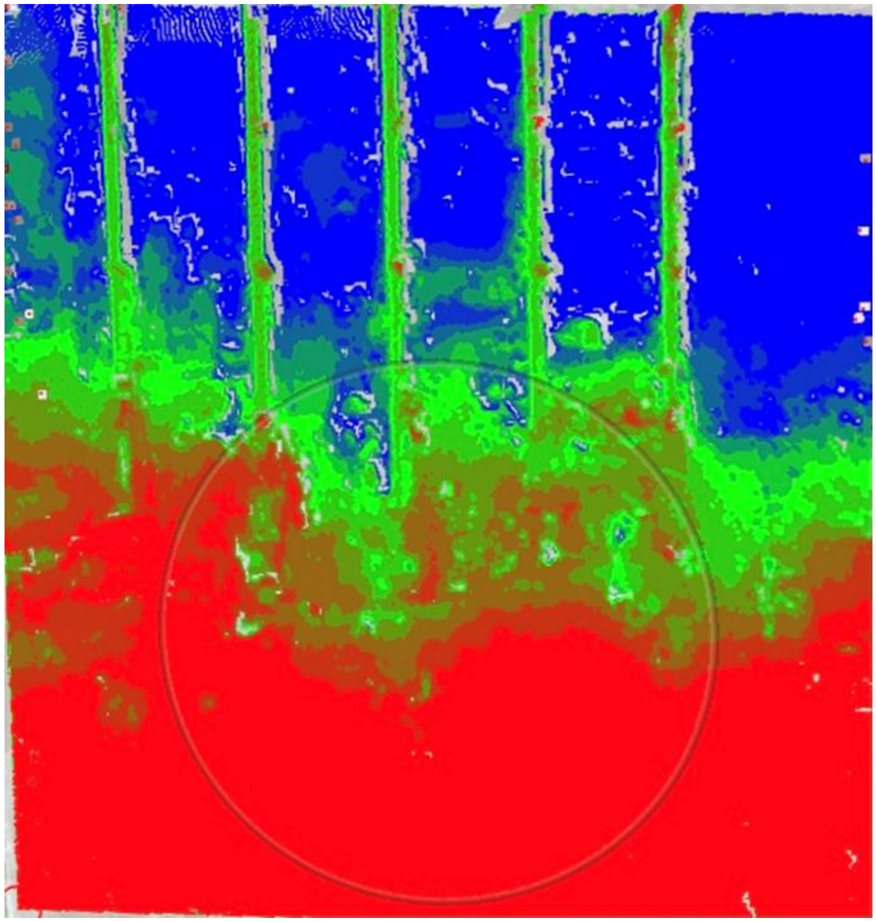

FIGURE D.16: VHES 3D surface scan

	Diagonal													Row Average		
	Rebar										No Rebar			All	No vert	No vert
	1	2	3	4	5	6	7	8	9	10	11	12	13	Points	bar	bar/void
1	1.4	1.2	1.5	1.3	1.2	1.1	1.2	1.2	1	1.3	1.3	1.2	1.2	1.24	1.25	1.22
2	1.3	1.2	1.4	1.2	1.2	1.1	1.1	1.1	1.1	1.2	1.2	1.2	1.3	1.20	1.23	1.23
3	1.1	1.2	1.2	1.2	1.2	1.1	1.1	1	1.1	1.2	1.3	1.1	1.4	1.17	1.19	1.20
4	1.4	1.3	1.3	1.2	1.2	1.2	1.1	1.2	1.1	1.2	1.2	1.3	1.4	1.24	1.25	1.25
5	1.4	1.2	1.1	1.3	1.4	1.1	1.2	1.2	1.1	1.2	1.3	1.2	1.3	1.23	1.25	1.23
6	1.4	1.2	1.2	1.2	1.3	1.4	1.2	1.3	1.3	1.2	1.4	1.4	1.4	1.30	1.33	1.31
7	1.4	1.3	1.3	1.2	1.2	1.3	1.2	1.3	1.4	1.3	1.3	1.3	1.4	1.30	1.31	1.28
8	1.4	1.3	1.2	1.2	1.2	1.2	1.2	1.2	1.3	1.3	1.2	1.4	1.5	1.28	1.30	1.30
9	1.4	1.4	1.3	1.3	1.2	1.2	1.3	1.4	1.2	1.3	1.3	1.4	1.4	1.32	1.31	1.31
10	1.4	1.4	1.4	1.3	1.3	1.3	1.3	1.3	1.4	1.4	1.5	1.6	1.6	1.40	1.44	1.44
11	1.5	1.4	1.3	1.4	1.4	1.4	1.4	1.3	1.3	1.4	1.5	1.4	1.6	1.41	1.43	1.43
12	1.6	1.5	1.4	1.4	1.6	1.4	1.5	1.6	1.4	1.4	1.5	1.6	1.7	1.51	1.54	1.54
13	2.2	1.7	1.8	1.7	1.7	1.7	2	1.7	1.6	1.5	1.6	1.7	2.1	1.77	1.84	1.75
														1.335	1.358	1.345

	Average													Row Average		
	Rebar										No Rebar			All	No vert	No vert
	1	2	3	4	5	6	7	8	9	10	11	12	13	Points	bar	bar/void
1	1.4	1.4	1.5	1.3	1.3	1.1	1.3	1.3	1.1	1.3	1.3	1.3	1.3	1.31	1.33	1.29
2	1.3	1.3	1.3	1.3	1.2	1.1	1.2	1.2	1.2	1.2	1.2	1.3	1.5	1.25	1.27	1.27
3	1.2	1.2	1.2	1.2	1.2	1.2	1.1	1.1	1.1	1.2	1.3	1.2	1.4	1.20	1.22	1.22
4	1.4	1.3	1.3	1.3	1.3	1.1	1.2	1.2	1.1	1.2	1.3	1.3	1.4	1.27	1.29	1.29
5	1.4	1.3	1.2	1.3	1.5	1.2	1.2	1.2	1.1	1.2	1.3	1.4	1.4	1.29	1.32	1.30
6	1.4	1.2	1.2	1.3	1.2	1.4	1.3	1.3	1.3	1.3	1.4	1.4	1.4	1.31	1.33	1.31
7	1.5	1.3	1.3	1.2	1.2	1.3	1.3	1.3	1.4	1.3	1.3	1.4	1.4	1.33	1.36	1.33
8	1.4	1.3	1.3	1.3	1.2	1.3	1.3	1.3	1.4	1.3	1.3	1.4	1.5	1.34	1.36	1.36
9	1.4	1.4	1.3	1.4	1.3	1.3	1.3	1.3	1.3	1.3	1.4	1.4	1.5	1.36	1.36	1.36
10	1.4	1.4	1.4	1.3	1.3	1.4	1.4	1.4	1.4	1.4	1.4	1.5	1.6	1.42	1.43	1.43
11	1.6	1.5	1.4	1.4	1.4	1.4	1.4	1.3	1.4	1.4	1.5	1.5	1.6	1.44	1.46	1.46
12	1.7	1.6	1.5	1.5	1.6	1.6	1.5	1.6	1.4	1.4	1.5	1.6	1.9	1.56	1.58	1.58
13	2.2	1.8	1.8	1.7	1.7	1.7	1.9	1.8	1.6	1.5	1.7	1.8	2.1	1.79	1.84	1.77
														1.375	1.394	1.382

	Horizontal													Row Average		
	Rebar										No Rebar			All	No vert	No vert
	1	2	3	4	5	6	7	8	9	10	11	12	13	Points	bar	bar/void
1	1.3	1.4	1.5	1.3	1.3	1.2	1.3	1.3	1.1	1.3	1.2	1.2	1.3	1.28	1.28	1.24
2	1.3	1.3	1.3	1.3	1.2	1.2	1.2	1.2	1.2	1.3	1.2	1.3	1.5	1.27	1.28	1.28
3	1.2	1.2	1.2	1.2	1.2	1.2	1.1	1.1	1.1	1.3	1.2	1.2	1.4	1.20	1.20	1.20
4	1.4	1.3	1.3	1.3	1.2	1.1	1.3	1.2	1.1	1.2	1.2	1.3	1.4	1.25	1.28	1.28
5	1.4	1.4	1.3	1.3	1.5	1.2	1.2	1.1	1.1	1.3	1.3	1.4	1.6	1.32	1.35	1.33
6	1.4	1.2	1.2	1.3	1.2	1.4	1.2	1.2	1.2	1.3	1.3	1.4	1.4	1.28	1.29	1.27
7	1.6	1.3	1.2	1.2	1.2	1.3	1.4	1.3	1.4	1.3	1.4	1.4	1.4	1.34	1.38	1.36
8	1.5	1.3	1.3	1.3	1.2	1.3	1.3	1.3	1.3	1.4	1.4	1.3	1.6	1.35	1.36	1.36
9	1.4	1.3	1.3	1.4	1.3	1.4	1.3	1.2	1.4	1.4	1.4	1.5	1.6	1.38	1.40	1.40
10	1.5	1.4	1.4	1.3	1.3	1.4	1.5	1.5	1.4	1.4	1.4	1.4	1.6	1.42	1.44	1.44
11	1.6	1.4	1.3	1.4	1.4	1.4	1.4	1.4	1.4	1.4	1.4	1.5	1.6	1.43	1.45	1.45
12	1.7	1.5	1.6	1.5	1.5	1.7	1.5	1.6	1.3	1.4	1.5	1.6	2	1.57	1.59	1.59
13	2.2	1.7	1.7	1.7	1.7	1.7	1.7	1.8	1.6	1.6	1.7	1.8	2	1.76	1.80	1.75
														1.374	1.390	1.380

	Standard Deviation												
	Rebar										No Rebar		
	1	2	3	4	5	6	7	8	9	10	11	12	13
1	0.1	0.2	0.1	0	0.2	0.1	0.2	0.1	0.2	0.1	0.2	0.1	0.1
2	0	0.1	0.1	0.1	0	0.1	0.1	0.1	0.1	0.1	0.1	0.1	0.2
3	0.2	0.1	0.1	0	0	0.1	0.1	0.1	0	0.1	0.1	0.1	0.1
4	0.1	0.1	0	0.1	0.1	0.1	0.1	0	0.1	0	0.1	0	0
5	0.1	0.1	0.1	0.1	0.1	0.1	0.1	0.1	0.1	0.1	0.1	0.2	0.2
6	0	0.1	0.1	0.1	0.1	0	0.1	0.1	0.1	0.1	0.1	0	0.1
7	0.1	0	0.1	0.1	0.1	0.1	0.1	0	0.1	0	0.1	0.1	0.1
8	0.1	0.1	0.1	0.2	0.1	0.1	0.1	0.2	0.1	0.1	0.1	0.1	0.1
9	0	0.1	0.1	0.1	0.1	0.1	0	0.1	0.1	0.1	0.1	0.1	0.1
10	0.1	0.1	0.1	0.1	0.1	0.1	0.1	0.1	0.1	0	0.1	0.1	0
11	0.1	0.1	0.1	0.1	0.1	0.1	0	0.1	0.1	0	0.1	0.1	0
12	0.1	0.2	0.1	0.1	0.1	0.2	0	0	0.1	0.1	0.1	0	0.2
13	0.1	0.1	0.1	0.1	0	0.1	0.2	0.2	0.1	0.1	0.1	0.1	0.1

	Vertical													Row Average		
	Rebar										No Rebar			All	No vert	No vert
	1	2	3	4	5	6	7	8	9	10	11	12	13	Points	bar	bar/void
1	1.4	1.5	1.6	1.3	1.5	1.1	1.5	1.4	1.3	1.4	1.5	1.4	1.4	1.41	1.45	1.42
2	1.3	1.3	1.3	1.4	1.2	1.1	1.2	1.2	1.2	1.2	1.3	1.3	1.6	1.28	1.30	1.30
3	1.4	1.3	1.1	1.2	1.2	1.2	1.2	1.2	1.1	1.1	1.3	1.3	1.5	1.24	1.26	1.26
4	1.5	1.4	1.3	1.3	1.4	1.1	1.3	1.2	1.2	1.2	1.4	1.3	1.4	1.31	1.35	1.35
5	1.3	1.4	1.2	1.4	1.5	1.2	1.3	1.2	1.2	1.2	1.4	1.5	1.4	1.32	1.35	1.33
6	1.4	1.3	1.3	1.3	1.2	1.4	1.4	1.3	1.3	1.3	1.4	1.4	1.5	1.35	1.36	1.36
7	1.4	1.3	1.4	1.3	1.3	1.4	1.3	1.3	1.5	1.3	1.3	1.4	1.5	1.36	1.39	1.34
8	1.3	1.4	1.4	1.5	1.3	1.3	1.4	1.5	1.5	1.3	1.4	1.5	1.5	1.41	1.41	1.41
9	1.4	1.5	1.4	1.4	1.3	1.4	1.3	1.4	1.3	1.3	1.4	1.4	1.4	1.38	1.36	1.36
10	1.4	1.5	1.5	1.4	1.4	1.4	1.3	1.5	1.3	1.4	1.3	1.6	1.6	1.43	1.43	1.43
11	1.6	1.6	1.5	1.5	1.5	1.5	1.4	1.3	1.4	1.4	1.5	1.5	1.6	1.48	1.50	1.50
12	1.7	1.8	1.5	1.5	1.6	1.6	1.5	1.6	1.5	1.5	1.6	1.6	1.9	1.61	1.61	1.61
13	2.1	1.9	1.8	1.8	1.7	1.8	2	2	1.7	1.5	1.7	1.8	2.2	1.85	1.88	1.82
														1.417	1.435	1.422

FIGURE D.17: 1 hour VHES overlay mockup SR heatmaps

Diagonal														Row Average		
Rebar										No Rebar				All	No vert	No vert
	1	2	3	4	5	6	7	8	9	10	11	12	13	Points	bar	bar/void
1	2	2	2	1.8	1.7	1.6	1.8	1.6	1.9	1.8	1.9	1.8	1.8	1.82	1.86	1.86
2	1.8	1.8	1.7	1.8	1.9	1.6	1.5	1.6	1.5	1.8	1.6	1.8	1.9	1.72	1.71	1.71
3	1.7	1.7	1.5	1.6	1.6	1.6	1.6	1.4	1.6	1.5	1.8	1.8	2.1	1.65	1.71	1.70
4	1.8	1.9	1.8	1.7	1.7	1.4	1.6	1.5	1.6	1.6	1.8	1.9	2.1	1.72	1.79	1.79
5	1.9	1.7	1.7	1.8	1.9	1.5	1.6	1.6	1.5	1.7	1.7	1.9	2	1.73	1.78	1.76
6	1.8	1.7	1.7	1.7	1.6	1.8	1.7	1.6	1.6	1.6	1.8	2	2	1.74	1.78	1.74
7	1.8	1.9	1.8	1.6	1.7	1.9	1.7	1.9	2	1.8	1.6	1.8	2	1.81	1.80	1.72
8	1.8	1.8	1.7	1.6	1.6	1.7	1.6	1.9	1.7	1.8	1.6	1.8	2.2	1.75	1.75	1.75
9	1.8	1.9	1.6	1.8	1.8	1.7	1.6	1.8	1.7	1.7	1.7	2	2	1.78	1.78	1.78
10	1.8	1.9	1.9	1.7	1.7	1.6	1.7	1.8	1.8	1.7	2	1.8	2.2	1.82	1.86	1.86
11	1.9	1.9	1.7	1.7	1.9	1.7	1.8	1.6	1.6	2	2	1.8	2	1.82	1.84	1.84
12	2	1.9	1.8	2	2	1.8	1.8	1.9	1.7	1.8	1.9	2	2.3	1.92	1.94	1.94
13	2.7	2.1	2.2	2	2.1	2.1	2.4	2.1	2	1.8	2.2	2.2	2.7	2.20	2.31	2.23
														1.805	1.838	1.821

Average														Row Average		
	Rebar										No Rebar			All	No vert	No vert
	1	2	3	4	5	6	7	8	9	10	11	12	13	Points	bar	bar/void
1	1.8	2	2	1.8	1.7	1.6	1.9	1.7	1.7	1.8	1.8	1.8	1.8	1.80	1.82	1.78
2	1.8	1.8	1.7	1.7	1.7	1.6	1.6	1.6	1.5	1.7	1.6	1.7	2	1.70	1.71	1.71
3	1.8	1.8	1.7	1.7	1.6	1.5	1.5	1.5	1.6	1.6	1.7	1.8	2.1	1.67	1.70	1.70
4	1.8	1.8	1.7	1.7	1.7	1.5	1.6	1.6	1.5	1.5	1.8	1.8	2.1	1.70	1.75	1.75
5	1.9	1.8	1.6	1.8	1.9	1.5	1.6	1.6	1.5	1.7	1.8	1.9	2.1	1.74	1.78	1.77
6	1.8	1.7	1.7	1.7	1.6	1.8	1.7	1.6	1.6	1.6	1.7	2	2	1.73	1.75	1.72
7	1.9	1.7	1.8	1.7	1.6	1.8	1.8	1.9	1.9	1.8	1.7	1.8	2.1	1.81	1.82	1.74
8	1.9	1.8	1.7	1.7	1.7	1.7	1.7	1.9	1.7	1.8	1.7	1.8	2.1	1.78	1.79	1.79
9	1.8	1.8	1.7	1.8	1.8	1.7	1.6	1.8	1.7	1.7	1.7	1.9	1.9	1.77	1.77	1.77
10	1.9	1.9	1.8	1.7	1.7	1.7	1.7	1.8	1.8	1.8	1.8	1.9	2.1	1.82	1.84	1.84
11	2	1.9	1.7	1.8	1.8	1.8	1.8	1.7	1.7	2	1.9	1.9	2	1.84	1.85	1.85
12	2	2	1.9	1.8	1.9	1.8	1.9	1.9	1.7	1.8	1.9	2.1	2.3	1.93	1.96	1.96
13	2.7	2.3	2.2	2	2.1	2.1	2.3	2.1	1.9	1.9	2.2	2.2	2.6	2.20	2.26	2.18
														1.806	1.832	1.813

Horizontal														Row Average		
	Rebar										No Rebar			All	No vert	No vert
	1	2	3	4	5	6	7	8	9	10	11	12	13	Points	bar	bar/void
1	1.6	2	2	1.7	1.7	1.6	1.8	1.7	1.5	1.8	1.7	1.6	1.8	1.73	1.71	1.66
2	1.8	1.8	1.8	1.6	1.7	1.6	1.6	1.6	1.5	1.7	1.7	1.7	2.2	1.72	1.75	1.75
3	1.7	1.7	1.8	1.8	1.6	1.6	1.5	1.5	1.6	1.8	1.7	1.8	2.1	1.71	1.73	1.71
4	2	1.8	1.7	1.7	1.6	1.6	1.6	1.6	1.3	1.6	1.7	1.7	2.1	1.69	1.71	1.71
5	1.9	1.9	1.7	1.8	2	1.6	1.5	1.6	1.5	1.7	1.8	1.8	2.1	1.76	1.79	1.76
6	1.8	1.7	1.7	1.7	1.6	1.8	1.7	1.6	1.6	1.6	1.7	2	1.9	1.72	1.75	1.71
7	2	1.7	1.7	1.9	1.6	1.8	1.8	2.1	1.9	2	1.8	1.9	2.2	1.88	1.86	1.78
8	2	1.8	1.8	1.7	1.7	1.7	1.8	1.9	1.6	1.9	1.7	1.8	2.2	1.82	1.83	1.83
9	1.8	1.8	1.7	1.8	1.8	1.8	1.7	1.8	1.7	1.9	1.8	2	2	1.82	1.81	1.81
10	2	1.9	1.8	1.8	1.7	1.7	1.9	1.9	1.8	1.9	1.8	1.9	2.2	1.87	1.89	1.89
11	2.1	1.8	1.7	1.9	1.8	1.8	1.8	1.9	1.8	1.9	1.9	2	2	1.88	1.89	1.89
12	2.2	2	2	1.8	2	2	2	2	1.7	1.8	1.9	2.2	2.5	2.01	2.06	2.06
13	2.8	2.2	2.1	2	2.1	2.1	2.2	2.1	1.8	2	2.1	2.1	2.4	2.15	2.20	2.10
														1.827	1.844	1.820

Standard Deviation													
	Rebar										No Rebar		
	1	2	3	4	5	6	7	8	9	10	11	12	13
1	0.2	0	0	0.1	0.1	0.1	0.1	0.1	0.2	0	0.1	0.2	0
2	0	0	0.1	0.1	0.2	0.1	0.1	0.1	0	0.1	0.1	0.1	0.2
3	0.1	0.1	0.2	0.1	0	0.1	0.1	0.1	0.1	0.2	0.2	0.1	0.1
4	0.2	0.1	0.1	0	0.1	0.1	0	0.1	0.2	0.1	0.1	0.1	0.1
5	0	0.1	0.1	0	0.2	0.1	0.1	0	0.1	0.1	0.1	0.1	0.1
6	0	0	0	0	0	0.1	0.1	0	0	0.1	0.1	0.1	0.1
7	0.1	0.2	0.1	0.2	0.1	0.1	0.1	0.2	0.1	0.2	0.1	0.1	0.1
8	0.1	0.1	0.1	0.1	0.1	0.1	0.1	0.1	0.1	0.1	0.1	0.1	0.1
9	0	0.1	0.1	0.1	0.1	0.1	0.1	0.1	0.1	0.2	0.1	0.1	0.1
10	0.1	0.1	0.1	0.1	0	0.1	0.2	0.1	0.1	0.1	0.2	0.1	0.2
11	0.1	0.1	0.1	0.1	0.1	0.1	0	0.2	0.1	0.1	0.1	0.1	0
12	0.2	0.1	0.1	0.2	0.1	0.2	0.1	0.1	0.1	0.1	0.1	0.1	0.2
13	0.2	0.2	0.1	0.1	0	0.1	0.1	0.1	0.1	0.1	0.1	0.1	0.2

Vertical														Row Average		
	Rebar										No Rebar			All	No vert	No vert
	1	2	3	4	5	6	7	8	9	10	11	12	13	Points	bar	bar/void
1	1.9	2	2	1.8	1.8	1.5	2	1.8	1.7	1.8	1.9	2	1.8	1.85	1.89	1.82
2	1.8	1.8	1.7	1.8	1.5	1.5	1.6	1.5	1.5	1.6	1.6	1.7	2	1.66	1.68	1.68
3	1.9	1.9	1.7	1.7	1.6	1.4	1.5	1.6	1.5	1.5	1.5	1.7	2	1.65	1.68	1.67
4	1.7	1.8	1.6	1.7	1.8	1.5	1.6	1.6	1.5	1.4	1.9	1.8	2	1.68	1.74	1.74
5	1.9	1.7	1.5	1.8	1.7	1.4	1.7	1.6	1.6	1.6	1.8	1.9	2.1	1.72	1.78	1.79
6	1.8	1.7	1.7	1.7	1.6	1.7	1.6	1.6	1.6	1.7	1.6	1.9	2.1	1.72	1.74	1.71
7	1.8	1.6	1.8	1.5	1.6	1.7	1.8	1.8	1.8	1.7	1.6	1.8	2.1	1.74	1.79	1.72
8	1.8	1.7	1.7	1.7	1.7	1.6	1.8	1.8	1.8	1.7	1.7	1.9	2	1.76	1.80	1.80
9	1.8	1.8	1.8	1.7	1.7	1.6	1.6	1.7	1.6	1.6	1.7	1.8	1.8	1.71	1.73	1.73
10	1.9	1.8	1.7	1.7	1.7	1.7	1.6	1.8	1.7	1.9	1.7	1.9	1.9	1.77	1.76	1.76
11	1.9	1.9	1.8	1.8	1.8	1.8	1.8	1.6	1.6	2	1.9	1.9	2	1.83	1.84	1.84
12	1.9	2	1.8	1.7	1.8	1.7	1.8	1.9	1.8	1.9	1.8	2	2.2	1.87	1.89	1.89
13	2.5	2.5	2.2	2.1	2.1	2.2	2.4	2.2	2	2	2.2	2.2	2.6	2.25	2.28	2.22
														1.785	1.813	1.796

FIGURE D.18: 4 hour VHES overlay mockup SR heatmaps

Diagonal														Row Average		
	Rebar										No Rebar			All	No vert	No vert
	1	2	3	4	5	6	7	8	9	10	11	12	13	Points	bar	bar/void
1	7.9	7.6	8.3	7.4	7	7.7	7.4	6.3	6.3	6.8	6.6	7	7.1	7.18	7.20	6.98
2	7.1	7.4	7.9	8	8	6.6	6.3	5.8	5.9	6.5	6.5	6.5	7.8	6.95	7.00	7.00
3	7.2	7.4	6.5	7.1	6.8	6.8	6.4	6.1	6.2	6.4	6.7	6.3	8.7	6.82	6.85	6.93
4	7	7.7	7.2	6.9	6.5	4.6	6.5	6.3	6.8	7.2	7.5	7.5	8.3	6.92	7.16	7.16
5	7.3	7.5	6.9	7.5	7.1	5.7	6.3	6.4	6.4	7.5	7.4	7.9	8.3	7.09	7.20	7.21
6	7.8	7.5	7	7.1	6.6	7	7	7.2	6.8	7.4	7.8	8.3	8.8	7.41	7.51	7.40
7	8.3	7.9	8	6.4	7.1	7.1	7	7.3	7	7.3	7.4	8.7	9.1	7.58	7.83	7.56
8	8.3	7.9	8	8.2	8.2	7.3	6.9	7.7	7	7.8	8.3	8.5	9.3	7.95	8.06	8.06
9	8.7	8.5	8	8.2	8.7	8.1	8.4	8.5	7.7	8.2	8.6	8.8	9.4	8.45	8.54	8.54
10	9.4	9.3	8.4	9	8.5	8.2	8.6	8.4	8.2	9.2	9.4	9.4	11	8.96	9.05	9.05
11	9.8	8.9	8.8	9.4	9.4	9.4	9.1	8.8	7.8	9.2	9.6	9.6	10	9.23	9.29	9.29
12	11	9.6	9.5	8.6	9.1	8.8	9.1	9.5	8.9	9.1	9.6	9.9	9.9	9.40	9.58	9.58
13	12	10	10	9.9	10	9.3	11	9.2	9.3	9.7	9.8	10	11	10.18	10.50	10.21
														8.010	8.135	8.074

Average														Row Average		
	Rebar										No Rebar			All	No vert	No vert
	1	2	3	4	5	6	7	8	9	10	11	12	13	Points	bar	bar/void
1	7.5	7.3	7.7	7	6.5	6.8	7	6	6	6.7	6.1	6.3	7.2	6.78	6.79	6.67
2	7	6.9	7	7	7.1	6.3	6.1	5.8	5.9	6.3	6.1	6.4	7.6	6.57	6.64	6.64
3	6.7	7	6.8	6.7	6.6	6.3	6.1	6	6	6.2	6.4	6.5	8.1	6.56	6.64	6.66
4	6.9	7.3	6.8	6.4	6.3	5	6.2	6.1	6.3	6.8	7.1	7.1	8.9	6.71	6.95	6.95
5	7.1	7.1	6.5	7	7	5.8	6.3	6.3	6.5	7.2	7.3	7.5	8.3	6.92	7.07	7.08
6	7.4	7.1	7.1	6.9	6.6	7.1	6.8	6.7	6.5	7.1	7.4	7.9	8.6	7.18	7.30	7.21
7	8	7.4	7.5	6.7	7.1	6.8	6.8	7	6.9	7.1	7.3	8.3	8.7	7.37	7.58	7.35
8	8.2	7.3	7.5	7.8	7.5	7.5	7.1	7.8	7.2	7.7	8	8.2	9.3	7.77	7.87	7.87
9	8.3	8.1	7.9	7.9	8.2	7.9	7.9	8	7.6	8.2	8.1	8.5	9	8.14	8.20	8.20
10	9.3	8.6	8.3	8.4	8.1	8.3	8.5	8.4	7.8	8.6	8.8	9	10	8.65	8.74	8.74
11	10	8.9	8.6	8.8	8.9	8.8	8.8	8.4	8	8.9	9.2	9.2	9.5	8.92	9.01	9.01
12	10	9.2	8.9	8.8	9.2	8.8	8.9	9.1	8.5	8.9	9.2	9.5	10	9.19	9.34	9.34
13	12	10	9.7	9.6	9.9	9.1	10	9.6	8.6	9.5	9.6	10	11	9.93	10.15	9.83
														7.744	7.868	7.811

Horizontal														Row Average		
	Rebar										No Rebar			All	No vert	No vert
	1	2	3	4	5	6	7	8	9	10	11	12	13	Points	bar	bar/void
1	7.3	7	7.3	6.2	6.2	6.2	6.3	5.9	5.6	6.4	5.7	5.7	7.2	6.38	6.41	6.40
2	7.2	6.8	7	6.3	6.6	6.1	5.9	6	6	6.5	6.1	6.4	7.6	6.50	6.60	6.60
3	6.6	6.5	6.8	6.4	6.4	6.4	6	5.9	6	6.1	6.5	6.3	7.7	6.43	6.54	6.57
4	7.7	6.8	6.6	6.2	6	5.3	5.8	6.1	5.9	6.5	6.6	6.8	11	6.68	7.00	7.00
5	7.2	6.9	6.1	6.6	7.1	5.7	6.2	6.1	6.4	7.1	7.2	7.3	8.8	6.82	7.04	7.03
6	7.3	6.8	7.2	7	6.5	7	6.6	6.4	6.2	7.2	7.3	7.9	8.7	7.09	7.22	7.12
7	8.5	7.3	7.4	7	6.9	6.4	6.6	6.8	6.7	7.2	7.4	8.1	8.7	7.31	7.54	7.36
8	8.3	7.1	6.8	8	7	7.6	7.5	7.9	7.5	7.8	7.8	8.1	9.7	7.78	7.84	7.84
9	8.4	7.9	7.9	8	8.2	8.2	8	8.1	7.8	8.7	7.9	8.3	9.4	8.22	8.24	8.24
10	9.8	8.2	7.9	8.1	8	8.6	8.6	8.4	8	8.2	8.5	9.3	10	8.59	8.77	8.77
11	11	8.8	8.5	8.6	8.6	8.7	8.8	8.6	8.4	8.8	9.1	8.9	9.4	8.91	9.04	9.04
12	11	9.5	9.1	9.3	9.6	9.4	9	8.9	8.5	9	8.7	9.7	11	9.38	9.48	9.48
13	12	9.7	9.4	9.1	9.5	8.8	9.8	9.7	7.9	9.1	9.1	9.9	11	9.62	9.84	9.42
														7.670	7.810	7.758

Standard Deviation													
	Rebar										No Rebar		
	1	2	3	4	5	6	7	8	9	10	11	12	13
1	0.3	0.3	0.6	0.7	0.4	0.8	0.6	0.2	0.4	0.3	0.5	0.7	0.1
2	0.3	0.4	0.9	0.9	0.8	0.3	0.2	0.3	0.2	0.3	0.4	0.1	0.3
3	0.5	0.5	0.3	0.4	0.2	0.6	0.3	0.1	0.2	0.2	0.3	0.3	0.5
4	0.8	0.5	0.4	0.4	0.3	0.4	0.4	0.2	0.5	0.4	0.5	0.4	1.5
5	0.3	0.4	0.4	0.5	0.1	0.2	0.1	0.2	0.2	0.2	0.1	0.3	0.5
6	0.3	0.4	0.1	0.3	0.2	0.2	0.2	0.4	0.3	0.4	0.4	0.4	0.2
7	0.8	0.4	0.4	0.3	0.2	0.4	0.2	0.3	0.2	0.3	0.1	0.3	0.4
8	0.2	0.5	0.6	0.5	0.6	0.2	0.3	0.1	0.3	0.2	0.3	0.2	0.4
9	0.4	0.3	0.1	0.3	0.5	0.4	0.6	0.5	0.2	0.5	0.4	0.3	0.6
10	0.5	0.6	0.4	0.5	0.3	0.2	0.1	0.1	0.5	0.5	0.5	0.6	0.6
11	0.5	0.1	0.2	0.5	0.5	0.6	0.3	0.5	0.4	0.2	0.4	0.4	0.7
12	0.3	0.6	0.7	0.4	0.3	0.6	0.3	0.4	0.4	0.3	0.5	0.6	0.5
13	0.4	0.3	0.6	0.4	0.4	0.3	0.6	0.3	0.7	0.4	0.4	0.3	0.4

Vertical														Row Average		
	Rebar										No Rebar			All	No vert	No vert
	1	2	3	4	5	6	7	8	9	10	11	12	13	Points	bar	bar/void
1	7.3	7.3	7.4	7.4	6.4	6.5	7.2	5.9	6.2	7	5.9	6.3	7.3	6.78	6.75	6.62
2	6.7	6.6	6.1	6.8	6.6	6.1	6.1	5.5	5.7	5.9	5.8	6.3	7.3	6.27	6.33	6.33
3	6.2	7	7	6.6	6.5	5.7	5.8	6	5.9	6	6.1	6.8	7.9	6.42	6.53	6.49
4	6.1	7.4	6.5	6.1	6.3	5.2	6.2	6	6.3	6.6	7.2	7	7.9	6.52	6.69	6.69
5	6.8	6.8	6.4	6.8	6.9	6	6.4	6.5	6.7	7.1	7.3	7.4	7.9	6.85	6.98	6.99
6	7.2	7	7	6.5	6.8	7.4	6.7	6.5	6.5	6.7	7.1	7.6	8.4	7.03	7.16	7.10
7	7.1	7.1	7.2	6.7	7.3	7	6.8	7	7	6.8	7.2	8.1	8.4	7.21	7.39	7.12
8	7.9	7	7.8	7.3	7.3	7.5	6.9	7.7	7	7.4	7.8	8.1	8.9	7.58	7.71	7.71
9	7.9	8	7.8	7.6	7.7	7.4	7.3	7.5	7.3	7.8	7.8	8.4	8.3	7.76	7.82	7.82
10	8.8	8.3	8.6	8.2	7.9	8.2	8.4	8.5	7.2	8.5	8.6	8.4	9.4	8.39	8.41	8.41
11	9.6	9	8.6	8.4	8.6	8.2	8.5	7.9	7.7	8.8	8.9	9	8.8	8.62	8.71	8.71
12	10	8.5	8.2	8.5	9	8.2	8.5	8.8	8.1	8.6	9.2	8.8	9.9	8.80	8.98	8.98
13	12	10	9.4	9.7	10	9.1	10	9.8	8.6	9.8	9.8	9.8	11	9.97	10.13	9.85
														7.553	7.660	7.600

FIGURE D.19: 1 day VHES overlay mockup SR heatmaps

Diagonal														Row Average		
	Rebar										No Rebar			All Points	No vert bar	No vert bar/void
	1	2	3	4	5	6	7	8	9	10	11	12	13			
1	8.2	8.1	8.3	8.2	8	7.3	7.6	6.8	6.6	7.2	6.3	7.2	7.4	7.48	7.45	7.30
2	7.9	7.7	7.6	8.2	8.6	7.3	6.5	6.3	6.4	6.8	7	6.9	7.9	7.32	7.35	7.35
3	7.3	7.5	7.2	7.1	7.3	7.6	6.8	6.5	6.7	6.6	7.3	6.7	9.1	7.21	7.30	7.39
4	7.4	8.4	7.5	7	7	5.4	6.9	6.7	7.4	7.1	7.8	7.8	8.7	7.32	7.56	7.56
5	7.5	7.7	6.9	7.7	7.9	6.4	7.2	7.6	7.1	8.3	8.2	8.4	9.6	7.73	7.85	7.84
6	8.3	7.8	7.5	7.7	7.6	7.8	7.7	7.6	7.6	7.9	8.8	9.1	9.5	8.07	8.27	8.15
7	9.4	8.9	8.6	6.9	7.6	7.9	7.8	7.7	7.9	8	7.3	8.5	9.7	8.17	8.35	8.14
8	9.5	8.9	8.3	8.2	8.2	7.8	7.8	8	7.7	8.8	7.8	9.2	10	8.50	8.60	8.60
9	9.4	9.1	8.6	8.6	8.8	8.6	7.6	8.9	8.1	8.5	9.4	9.7	10	8.89	8.99	8.99
10	9.6	9.5	9.8	9.9	9.4	8.5	9.4	9.3	9	9.4	10	10	12	9.69	9.93	9.93
11	11	9.6	9.5	9.7	9.7	8.3	10	9.7	8.7	10	11	11	12	9.99	10.32	10.32
12	11	9.8	9.9	9.6	10	9.1	9.2	11	9.6	9.9	11	11	11	10.18	10.41	10.41
13	15	11	11	10	10	9.7	11	11	11	11	12	12	13	11.31	11.68	11.30
														8.605	8.773	8.713

Average														Row Average		
	Rebar										No Rebar			All Points	No vert bar	No vert bar/void
	1	2	3	4	5	6	7	8	9	10	11	12	13			
1	8.1	8.1	8.1	7.4	7.4	7.1	7.5	6.5	6.5	7.1	6.4	6.8	7.3	7.25	7.26	7.15
2	7.8	7.4	7.5	7.7	7.7	6.9	6.6	6.2	6.4	6.8	6.6	6.9	8.1	7.12	7.20	7.20
3	7.2	7.5	7.2	7.1	7.2	7.2	6.6	6.4	6.5	6.5	6.9	7	8.8	7.10	7.18	7.21
4	7.7	7.8	7.2	6.9	7.1	5.5	6.7	6.6	7	6.9	7.6	7.6	8.5	7.16	7.42	7.42
5	7.6	7.5	6.8	7.5	7.4	6.3	6.9	7.2	7.1	8	8	8.4	9.5	7.56	7.72	7.77
6	8.2	7.5	7.3	7.4	7.3	7.5	7.3	7.1	7.4	7.6	8.2	8.7	9.8	7.80	8.03	7.93
7	8.9	8.5	7.8	6.8	7.4	7.4	7.2	7	7.1	7.1	7.7	8.4	9.5	7.76	8.00	7.81
8	9.1	8.6	8.2	8.2	7.9	7.9	7.5	8	7.9	8.6	8	9.1	10	8.38	8.46	8.46
9	9.2	8.9	8.4	8.6	8.6	8.4	8.1	8.6	8.1	8.3	9.1	9.3	10	8.75	8.86	8.86
10	9.4	9	9.3	9.3	9	8.6	9.1	9.1	8.5	9.2	9.8	10	11	9.33	9.50	9.50
11	10	9.8	9.3	9.4	9.7	8.6	9.7	9.2	8.7	9.7	10	10	11	9.72	9.96	9.96
12	11	9.9	9.6	9.5	10	9.2	9.3	10	9.2	9.7	10	11	11	9.99	10.17	10.17
13	13	11	10	9.9	10	9.9	11	10	9.6	11	11	11	12	10.68	10.93	10.56
														8.353	8.515	8.462

Horizontal														Row Average		
											No Rebar			All Points	No vert bar	No vert bar/void
	1	2	3	4	5	6	7	8	9	10	11	12	13			
1	8.1	8	7.8	6.8	7.2	6.9	7.1	6.3	6.3	7	6.6	6.5	7.4	7.08	7.13	7.12
2	8	7.2	7.4	7.6	7.3	7.1	6.5	6.1	6.7	7.4	6.7	7	8.8	7.22	7.30	7.30
3	7.2	7.3	7.3	7.3	7.2	7.3	6.7	6.5	6.3	6.5	6.7	7	9.3	7.13	7.22	7.25
4	8.5	7.3	7.2	7	7.6	5.5	6.4	6.7	6.8	7	7.5	8	8.7	7.25	7.59	7.59
5	7.8	7.5	6.6	7.4	7.5	6.1	6.6	6.8	7	8.2	8	8.8	10	7.57	7.80	7.84
6	8.1	7.2	7.2	7.4	6.7	7.8	6.9	7	7	8	8.2	8.6	11	7.75	7.91	7.81
7	9.2	8.7	7.3	6.9	6.5	6.8	6.9	6.9	7	7.3	8.2	8.1	9.3	7.62	7.81	7.62
8	9.4	8.4	8	8.3	7.8	8	7.4	7.5	8	8.5	8.1	9.3	10	8.38	8.54	8.54
9	9.4	8.8	8.1	8.6	8.6	8.6	8.8	9.1	8.6	8.9	8.8	9.1	10	8.90	8.96	8.96
10	9.5	9	9.2	9.5	8.7	8.8	8.9	9.1	9	9.4	9.6	10	11	9.38	9.53	9.53
11	11	10	9.1	9.1	9.5	8.8	9.4	9.5	8.8	8.9	9.8	11	11	9.61	9.83	9.83
12	11	9.8	9.7	9.6	10	11	9.8	11	9.6	9.8	9.8	11	12	10.26	10.39	10.39
13	12	10	9.6	9.5	9.9	9.5	9.7	9.3	8.9	9.9	11	9.4	11	10.00	10.20	9.95
														8.319	8.477	8.440

Standard Deviation													
	Rebar										No Rebar		
	1	2	3	4	5	6	7	8	9	10	11	12	13
1	0.1	0.1	0.3	0.7	0.5	0.2	0.3	0.3	0.2	0.1	0.2	0.4	0.2
2	0.2	0.3	0.1	0.5	0.8	0.5	0.2	0.1	0.3	0.6	0.4	0.2	0.7
3	0.1	0.3	0.1	0.2	0.1	0.5	0.3	0.1	0.2	0.1	0.4	0.3	0.6
4	0.7	0.6	0.3	0.2	0.5	0.1	0.3	0.2	0.4	0.2	0.2	0.5	0.3
5	0.2	0.2	0.2	0.2	0.6	0.2	0.3	0.4	0.1	0.4	0.2	0.4	0.6
6	0.1	0.3	0.2	0.4	0.6	0.5	0.4	0.4	0.3	0.6	0.6	0.3	0.7
7	0.6	0.6	0.7	0.1	0.8	0.6	0.5	0.7	0.7	1	0.5	0.3	0.2
8	0.7	0.3	0.2	0.1	0.2	0.1	0.3	0.5	0.2	0.2	0.2	0.2	0.5
9	0.4	0.2	0.3	0.1	0.2	0.4	0.6	0.6	0.5	0.7	0.3	0.4	0.3
10	0.2	0.5	0.5	0.8	0.4	0.2	0.3	0.2	0.8	0.3	0.5	0.2	1
11	0.8	0.2	0.2	0.3	0.3	0.3	0.4	0.6	0.1	0.7	0.9	0.2	0.6
12	0.1	0.1	0.4	0.2	0.1	1.3	0.4	0.8	0.7	0.2	0.5	0.9	0.6
13	1.4	0.5	0.8	0.5	0.2	0.5	1.2	0.9	0.9	0.8	0.6	1.1	0.7

Vertical														Row Average		
											No Rebar			All Points	No vert bar	No vert bar/void
	1	2	3	4	5	6	7	8	9	10	11	12	13			
1	8.1	8.1	8.1	7.3	7.1	7	7.7	6.5	6.6	7	6.3	6.6	7.1	7.19	7.20	7.04
2	7.6	7.3	7.4	7.2	7.1	6.4	6.9	6.1	6.1	6.2	6.2	6.7	7.5	6.82	6.94	6.94
3	7.2	7.8	7.2	7	7.1	6.6	6.3	6.3	6.5	6.5	6.6	7.2	8.1	6.95	7.03	7.00
4	7.2	7.8	7	6.6	6.7	5.5	6.7	6.4	6.7	6.7	7.4	7	8.2	6.92	7.11	7.11
5	7.5	7.4	7	7.5	6.8	6.4	7	7.2	7.1	7.5	7.8	8	8.9	7.39	7.51	7.61
6	8.2	7.4	7.1	7	7.7	7	7.4	6.8	7.5	6.9	7.7	8.5	9.3	7.58	7.93	7.84
7	8.2	7.8	7.6	6.7	8	7.5	7	6.4	6.5	6	7.5	8.6	9.4	7.48	7.85	7.66
8	8.3	8.6	8.2	8.2	7.8	7.8	7.2	8.4	8.1	8.5	8.1	8.9	9.4	8.27	8.25	8.25
9	8.7	8.8	8.5	8.5	8.4	7.9	8	7.9	7.7	7.6	9.1	9	9.7	8.45	8.64	8.64
10	9.2	8.6	8.8	8.4	8.9	8.6	8.9	9	7.6	8.9	9.4	9.8	9.7	8.91	9.04	9.04
11	9.6	9.8	9.3	9.4	10	8.8	9.5	8.5	8.6	10	9.9	10	11	9.57	9.74	9.74
12	11	10	9.1	9.3	10	8	9	9.3	8.4	9.5	9.8	9.5	11	9.52	9.70	9.70
13	13	11	10	9.8	10	10	12	10	9.4	11	10	11	12	10.73	10.91	10.43
														8.136	8.295	8.231

FIGURE D.20: 3 day VHES overlay mockup SR heatmaps

Diagonal	Rebar										No Rebar			Row Average		
	1	2	3	4	5	6	7	8	9	10	11	12	13	All Points	No vert bar	No vert bar/void
1	11	8.8	9	7.9	8.3	7.9	8.7	7.8	7.5	8	7.9	7.8	8	8.34	8.50	8.50
2	9	8.7	8.1	7.8	9.1	7.9	7.1	7.2	6.9	7.7	7.7	7.6	8.6	7.95	8.01	8.01
3	8.4	8.1	7.5	7.8	7.6	7.6	7.8	7.4	7.7	7.2	8.2	7.6	9.8	7.90	8.08	8.14
4	8.5	8.5	8.3	8.2	7.6	6.6	7.5	7.9	7.9	7.6	8.2	8.2	8.7	7.98	8.11	8.11
5	8.5	8.7	7.6	8.4	8.5	6.5	7.7	8.2	7.9	8.9	8.5	9	9.4	8.29	8.39	8.37
6	9.2	8.3	8.6	8.2	8.2	8.7	8.3	8	7.5	8	9	9.3	9.5	8.52	8.70	8.61
7	9.7	9.6	9.1	8	8.5	8.3	8.6	9.6	9	8.9	8.6	9.1	10	9.03	9.13	8.90
8	8.9	9	8.8	8.8	8.5	8.8	8.8	8.5	9.5	8.7	9	10	10	9.05	9.23	9.23
9	9.3	9.2	8.7	9.3	9.2	9.2	8.8	8.7	8.7	9	10	10	11	9.37	9.55	9.55
10	9.8	9.9	9.3	9.9	9.7	9.2	9.8	9.7	9.4	9.4	11	11	12	9.95	10.15	10.15
11	11	10	9.7	10	10	9.7	10	10	9.1	9.9	11	11	12	10.18	10.33	10.33
12	12	10	9.5	9.8	11	10	9.3	10	9.5	10	11	11	12	10.37	10.54	10.54
13	13	11	11	11	10	9.5	12	11	10	11	11	11	12	10.96	11.27	10.94
														9.068	9.228	9.183

Average	Rebar										No Rebar			Row Average		
	1	2	3	4	5	6	7	8	9	10	11	12	13	All Points	No vert bar	No vert bar/void
1	9.6	8.5	8.3	7.4	7.8	7.7	8.4	7.6	7.2	7.6	7.2	7.4	8.5	7.95	8.06	8.07
2	8.3	7.9	7.5	6.9	7.7	7.3	7	6.9	6.8	7.1	7.1	7.3	8.5	7.41	7.52	7.52
3	8.2	7.6	7	7	7.1	7.1	7.2	7.1	7.1	7.2	7.5	7.5	9.1	7.46	7.61	7.62
4	8.1	7.9	7.7	7.5	7.3	6.4	7.2	7.4	7.4	7.4	7.6	8	8.9	7.60	7.78	7.78
5	8.1	8.2	7.1	8.1	8.1	6.5	7.4	7.6	7.4	7.8	8.1	8.8	9.4	7.89	8.05	8.04
6	8.7	8	7.9	7.7	7.7	8.1	7.4	7.7	7.2	7.9	8.4	9	9.5	8.09	8.23	8.11
7	9	8.5	8.2	7.2	7.7	8	7.7	8.3	8	7.4	8.3	9.1	9.8	8.25	8.47	8.17
8	8.7	8.3	8.3	8.5	8.2	8.3	8.3	8.4	8.4	8.5	8.6	9.3	9.8	8.59	8.72	8.72
9	8.9	8.8	8.4	8.8	8.8	8.8	8.5	8.4	8.4	8.6	9.5	9.7	10	8.92	9.07	9.07
10	9.8	9.2	8.8	9	9.1	8.9	9	9.1	8.9	9.2	9.9	10	11	9.40	9.60	9.60
11	10	9.6	9.2	9.2	9.6	9.1	9.4	9.3	8.8	9.7	10	10	11	9.66	9.83	9.83
12	11	9.7	9	9.3	9.8	9.4	9.2	9.6	9.2	9.7	10	11	11	9.83	10.02	10.02
13	12	10	9.8	9.9	9.6	9.3	10	9.9	9.3	10	11	11	12	10.28	10.52	10.27
														8.564	8.728	8.679

Horizontal	Rebar										No Rebar			Row Average		
	1	2	3	4	5	6	7	8	9	10	11	12	13	All Points	No vert bar	No vert bar/void
1	9	8.3	8	7.1	7.3	7.6	7.7	7.8	6.8	6.9	6.3	6.6	9.2	7.58	7.61	7.72
2	8.5	7.4	7	6.5	7.3	7.2	7	6.9	7	7.2	7	7.5	8.9	7.34	7.53	7.53
3	8.7	7.2	7	6.6	7.1	7	7.1	7	6.8	7.5	7.4	7.6	9.2	7.40	7.61	7.61
4	8.6	7.7	7.5	7	7	6.7	7	7.3	7.4	7.6	7.7	7.9	9.6	7.62	7.84	7.84
5	8.2	7.9	6.9	8.1	8.1	7.3	7.3	7.5	7.3	7.8	8.2	8.9	10	7.97	8.13	8.13
6	8.6	7.6	7.3	7	7.1	8.1	7.6	7.3	7.2	7.7	8.4	8.7	9.8	7.88	8.09	8.00
7	9.4	8.2	7.4	6.5	7	8.2	7	8.2	8	7.3	8	8.8	9.6	7.97	8.15	7.76
8	9	7.8	8.3	8.4	7.9	8	8.2	8.9	7.9	8.3	8.4	9.2	10	8.49	8.62	8.62
9	9	8.6	8.2	8.5	8.5	9	8.8	8.8	8.4	9.1	8.9	9.4	10	8.88	8.93	8.93
10	10	9	8.9	8.8	8.8	8.9	8.6	9.2	9.3	9.3	9.8	11	11	9.41	9.64	9.64
11	11	9.4	9	8.9	9.4	9.2	9	9.1	9.2	9.7	10	10	11	9.58	9.78	9.78
12	11	9.5	9.1	9.3	9.7	9.5	9.2	9.5	9.1	9.4	9.5	10	11	9.68	9.84	9.84
13	12	9.7	9.5	9.5	9.1	8.9	9.3	9.4	8.7	9.9	10	10	11	9.82	10.03	9.78
														8.431	8.597	8.551

Standard Deviation	Rebar										No Rebar		
	1	2	3	4	5	6	7	8	9	10	11	12	13
1	1	0.3	0.6	0.4	0.5	0.2	0.6	0.3	0.4	0.6	0.8	0.7	0.6
2	0.8	0.7	0.6	0.8	1.2	0.6	0.2	0.3	0.3	0.6	0.5	0.5	0.5
3	0.6	0.5	0.6	0.7	0.5	0.5	0.5	0.2	0.5	0.3	0.6	0.1	0.7
4	0.8	0.5	0.6	0.6	0.3	0.5	0.3	0.4	0.5	0.4	0.6	0.2	0.7
5	0.5	0.4	0.4	0.4	0.4	0.9	0.3	0.6	0.5	1.1	0.4	0.3	0.7
6	0.4	0.4	0.7	0.6	0.6	0.7	1	0.4	0.3	0.2	0.6	0.3	0.4
7	1	0.9	0.9	0.8	0.8	0.4	0.8	1.2	1	1.5	0.3	0.3	0.5
8	0.4	0.6	0.5	0.3	0.3	0.5	0.4	0.6	0.9	0.2	0.3	0.7	0.6
9	0.4	0.3	0.3	0.5	0.4	0.5	0.5	0.6	0.4	0.7	0.8	0.3	1
10	0.4	0.6	0.6	0.8	0.6	0.4	0.7	0.6	0.7	0.3	0.6	0.5	1
11	0.9	0.3	0.4	0.7	0.4	0.7	0.6	0.7	0.6	0.2	0.3	0.4	0.7
12	1.1	0.5	0.6	0.6	0.7	0.8	0.1	0.5	0.2	0.4	0.7	0.4	0.2
13	0.7	0.5	0.6	0.6	0.6	0.3	1.3	0.9	0.9	0.4	0.5	0.6	0.5

Vertical	Rebar										No Rebar			Row Average		
	1	2	3	4	5	6	7	8	9	10	11	12	13	All Points	No vert bar	No vert bar/void
1	9.1	8.3	8	7.3	7.8	7.5	8.9	7.3	7.4	8	7.4	7.7	8.2	7.92	8.06	7.98
2	7.5	7.7	7.4	6.5	6.8	6.7	6.8	6.6	6.4	6.5	6.7	6.7	7.9	6.94	7.03	7.03
3	7.6	7.6	6.4	6.5	6.7	6.7	6.8	7	6.8	7	7	7.4	8.4	7.07	7.14	7.10
4	7.2	7.6	7.2	7.3	7.3	5.8	7.1	7.1	7	6.9	7	7.9	8.3	7.21	7.38	7.38
5	7.6	8.1	6.9	7.7	7.8	5.6	7.1	7	6.9	6.7	7.7	8.4	8.7	7.40	7.64	7.61
6	8.4	8.1	7.7	7.8	7.8	7.4	6.4	7.7	6.9	8.1	7.8	9	9.1	7.86	7.89	7.73
7	7.9	7.8	8.1	7.1	7.6	7.6	7.5	7.2	7	6	8.2	9.3	9.4	7.75	8.13	7.86
8	8.2	8	7.9	8.2	8.2	8	8	7.8	7.9	8.6	8.4	8.7	9.2	8.24	8.31	8.31
9	8.5	8.6	8.4	8.5	8.8	8.3	8	7.7	8	7.8	9.1	9.7	9.4	8.53	8.74	8.74
10	9.4	8.7	8.1	8.3	8.7	8.5	8.6	8.5	8.1	8.9	9.4	9.8	10	8.85	9.03	9.03
11	9	9.4	8.9	8.7	9.3	8.4	9.1	8.7	8.2	9.5	9.9	9.8	11	9.22	9.39	9.39
12	9.7	9.3	8.4	8.7	9.2	8.5	9.1	9.2	9.1	9.5	9.8	11	11	9.44	9.69	9.69
13	11	10	9.3	9.5	9.5	9.5	10	9.4	8.9	10	11	11	12	10.06	10.26	10.08
														8.191	8.360	8.302

FIGURE D.21: 7 day VHES overlay mockup SR heatmaps

Diagonal														Row Average		
	Rebar										No Rebar			All	No vert	No vert
	1	2	3	4	5	6	7	8	9	10	11	12	13	Points	bar	bar/void
1	9.2	9.2	9	8	8.2	8.6	9	8.5	8.2	8.7	8.6	9	9.4	8.74	8.83	8.72
2	9.1	8	8.1	8.1	8.9	7.9	7.7	7.6	7.2	7.6	7.4	8.6	10	8.18	8.39	8.39
3	8.4	8.1	7.4	7.5	7.8	8.2	8.2	7.4	7.5	8	8.8	8.4	10	8.16	8.36	8.36
4	8.8	9.1	7.9	8.2	7.9	8.3	7.9	8	8	7.6	9	9.2	10	8.49	8.64	8.64
5	9	8.3	7.6	8.5	9.3	7.5	8.4	8.6	8.3	9.1	9.1	9.9	12	8.86	9.15	9.13
6	9.1	8.6	8.6	8.2	8.9	8.3	7.7	9.4	8.7	8.4	9.8	11	11	9.02	9.29	9.10
7	10	9.4	8.6	7.6	8.2	7.8	8.4	9	8.7	8.9	8.5	9.1	11	8.88	9.09	8.76
8	9.8	9	8.4	8.9	8.9	8.7	9.2	9.4	9.3	8.8	8.8	10	11	9.22	9.39	9.39
9	9.2	9.4	8.7	9.3	9.2	8.7	8.3	9.3	9	9.1	10	10	10	9.30	9.39	9.39
10	10	9.5	9.2	9.4	9.2	9.2	9.1	9.5	9.8	9.5	11	11	11	9.78	10.01	10.01
11	9.7	9.4	9.1	9.5	9.4	8.2	9.6	9.4	9.4	9.4	11	11	12	9.75	10.11	10.11
12	11	9.5	9	9.2	9.7	9	9.7	9.8	9.2	9.6	10	12	13	10.03	10.41	10.41
13	14	11	10	10	10	9.8	12	10	10	11	11	12	13	10.99	11.41	11.00
														9.185	9.420	9.339

Average														Row Average		
	Rebar										No Rebar			All	No vert	No vert
	1	2	3	4	5	6	7	8	9	10	11	12	13	Points	bar	bar/void
1	9.1	8.9	8.7	7.7	7.9	8.3	9	8.3	8	8.3	8	8.4	9.5	8.46	8.57	8.49
2	9	8.1	7.8	7.6	8.3	7.7	7.7	7.4	7.2	7.6	7.5	8.5	9.8	8.02	8.22	8.22
3	8.3	8	7.4	7.3	7.7	7.7	7.6	7.4	7.4	7.8	8.3	8.4	10	7.98	8.18	8.15
4	8.6	8.6	7.8	7.8	8.3	7.5	7.6	7.7	7.8	7.5	8.4	8.9	9.8	8.18	8.39	8.39
5	9	8.3	7.6	8.5	9.2	7.8	8	8	8	8.8	9	9.6	11	8.68	8.92	8.88
6	9.7	8.7	8.4	8.4	8.8	8.5	7.9	8.3	8.1	8.1	9.2	9.9	11	8.79	9.05	8.93
7	9.5	8.7	8.4	8	8.2	7.9	7.8	8.9	8.8	8.7	8.5	9.1	10	8.69	8.84	8.50
8	9.2	8.6	8.3	8.8	8.9	8.3	8.6	9	8.6	8.9	8.9	10	10	8.95	9.10	9.10
9	9.2	9.2	8.7	8.9	8.9	8.5	8.6	9	8.5	9	9.4	9.9	11	9.11	9.22	9.22
10	9.9	9	9	9	8.9	8.8	9	9.2	9.2	9.5	10	10	11	9.46	9.69	9.69
11	9.8	9.5	8.7	9.1	9.1	8.4	9.3	9	9.3	9.6	10	11	11	9.55	9.83	9.83
12	11	9.6	9	9	9.5	9	9.5	9.6	8.9	9.6	10	11	12	9.80	10.08	10.08
13	13	10	9.8	9.9	9.9	9.7	11	10	9.3	10	11	11	12	10.60	10.95	10.53
														8.944	9.157	9.078

Horizontal														Row Average		
	Rebar										No Rebar			All	No vert	No vert
	1	2	3	4	5	6	7	8	9	10	11	12	13	Points	bar	bar/void
1	9.2	8.7	8.7	7.6	7.7	8.3	9	8.2	7.5	7.9	7.5	7.7	9.5	8.27	8.35	8.28
2	9.2	8.1	7.7	7.4	8.1	7.9	7.3	7.4	7.5	8.1	7.9	8.4	10	8.08	8.26	8.26
3	8.4	7.7	7.3	7.3	7.4	7.6	7.6	7.7	7.6	7.8	8.4	8.6	11	8.01	8.25	8.20
4	9	8.2	7.7	7.7	8.1	7.3	7.4	7.8	7.7	7.7	8.4	8.8	9.9	8.13	8.38	8.38
5	9	8	7.3	8.5	9.3	7.9	7.8	7.6	8	8.9	8.9	9.9	11	8.64	8.93	8.87
6	9.8	8.8	8.5	8.5	8.5	8.1	8	7.7	7.3	8.2	9.2	9.8	11	8.69	8.96	8.84
7	9.7	8.6	8.5	8.3	7.9	7.9	7.5	9.5	9.8	9.4	8.9	9.2	10	8.87	8.95	8.50
8	9.5	8.3	8	9.2	8.8	7.8	8.2	9	8.1	9.2	9	11	11	8.94	9.09	9.09
9	9.4	9.1	8.6	9	8.8	8.7	8.8	9.2	8.6	9.2	9	10	11	9.20	9.30	9.30
10	10	9	9	9	8.8	8.8	8.7	9	9.1	9.5	9.9	11	11	9.44	9.68	9.68
11	10	9.6	8.7	9.1	8.7	8.8	9.2	9	9.4	9.9	10	11	11	9.60	9.80	9.80
12	11	9.3	9.4	9.2	9.4	9.3	9.4	9.7	8.8	9.9	9.9	11	12	9.89	10.14	10.14
13	13	10	9.7	9.1	9.8	9.4	10	10	8.8	10	10	11	12	10.32	10.66	10.28
														8.929	9.134	9.047

Standard Deviation													
	Rebar										No Rebar		
	1	2	3	4	5	6	7	8	9	10	11	12	13
1	0.2	0.3	0.3	0.3	0.3	0.4	0	0.2	0.4	0.4	0.6	0.7	0.1
2	0.3	0.1	0.3	0.4	0.6	0.3	0.4	0.2	0.3	0.6	0.3	0.1	0.4
3	0.1	0.3	0.2	0.2	0.2	0.5	0.6	0.3	0.2	0.3	0.6	0.2	0.5
4	0.5	0.5	0.1	0.4	0.5	0.7	0.3	0.3	0.2	0.2	0.6	0.3	0.6
5	0.1	0.4	0.3	0.1	0.2	0.3	0.4	0.5	0.3	0.4	0.1	0.5	0.7
6	0.5	0.1	0.3	0.2	0.2	0.5	0.2	1	0.7	0.4	0.7	0.7	0.4
7	0.8	0.7	0.2	0.4	0.4	0.2	0.5	0.7	1	0.8	0.4	0.1	0.6
8	0.7	0.4	0.2	0.4	0.1	0.5	0.5	0.4	0.6	0.3	0.1	0.7	0.5
9	0.2	0.2	0.2	0.5	0.3	0.3	0.3	0.4	0.6	0.3	0.5	0.4	0.6
10	0.5	0.5	0.3	0.4	0.2	0.4	0.2	0.3	0.5	0.1	0.4	0.4	0.4
11	0.3	0.1	0.4	0.5	0.4	0.3	0.3	0.5	0.2	0.3	0.3	0.4	0.5
12	0.6	0.4	0.5	0.3	0.2	0.4	0.2	0.3	0.2	0.3	0.3	0.9	0.6
13	0.5	0.4	0.2	0.7	0.1	0.2	0.8	0.2	0.7	0.3	0.3	0.9	0.3

Vertical														Row Average		
	Rebar										No Rebar			All	No vert	No vert
	1	2	3	4	5	6	7	8	9	10	11	12	13	Points	bar	bar/void
1	8.8	8.9	8.4	7.4	7.9	7.9	9	8.1	8.2	8.3	8	8.5	9.5	8.38	8.54	8.48
2	8.6	8.2	7.6	7.4	7.8	7.4	8	7.2	7	7	7.3	8.4	9.4	7.79	8.01	8.01
3	8.2	8.3	7.6	7.1	7.8	7.3	7	7.1	7.2	7.5	7.7	8.3	9.7	7.75	7.94	7.89
4	8	8.5	7.7	7.5	8.8	7	7.6	7.4	7.6	7.3	7.8	8.6	9.2	7.92	8.16	8.16
5	8.9	8.7	7.8	8.4	9	8.1	7.7	7.9	7.7	8.4	9	9	10	8.53	8.68	8.63
6	10	8.7	8.1	8.4	8.9	9	7.9	7.8	8.2	7.7	8.5	9.2	10	8.67	8.89	8.84
7	8.6	8	8.2	8.2	8.6	8.1	7.6	8.2	7.8	7.9	8.2	9	9.9	8.33	8.49	8.24
8	8.4	8.5	8.4	8.4	9	8.3	8.4	8.7	8.5	8.6	8.9	9.3	9.7	8.70	8.83	8.83
9	9	9	8.9	8.4	8.7	8.2	8.6	8.5	7.9	8.7	9.2	9.5	10	8.82	8.98	8.98
10	9.3	8.5	8.7	8.7	8.8	8.5	9.1	9	8.8	9.4	9.8	10	11	9.17	9.39	9.39
11	9.5	9.6	8.4	8.6	9.2	8.3	9	8.5	9	9.4	10	10	11	9.30	9.56	9.56
12	10	10	8.5	8.7	9.3	8.6	9.3	9.2	8.8	9.4	10	10	11	9.49	9.69	9.69
13	13	10	9.7	10	9.8	9.8	12	9.9	9.1	10	11	11	12	10.49	10.79	10.32
														8.719	8.917	8.847

FIGURE D.22: 14 day VHES overlay mockup SR heatmaps

Diagonal														Row Average		
	Rebar										No Rebar			All	No vert	No vert
	1	2	3	4	5	6	7	8	9	10	11	12	13	Points	bar	bar/void
1	11	9.2	9	7.7	7.8	8.4	8.9	8.7	7.8	8.5	8.8	9.3	10	8.83	9.03	9.00
2	8.6	7.9	7.6	7.4	7.2	7.6	7.2	7.5	6.7	7.6	7.9	8.5	10	7.84	7.99	7.99
3	8.2	7.6	7.4	6.8	7.6	8.1	7.9	6.9	7.2	7.1	7.9	8.2	10	7.79	8.10	8.09
4	8.1	8.7	8.3	7.6	8.8	7.9	7.7	7.4	7.5	7.6	8.1	8.2	9.4	8.10	8.26	8.26
5	8.6	8	7.4	8.4	9.2	7.5	7.7	8	7.4	8.5	8.7	8.9	9.8	8.32	8.46	8.36
6	9.2	7.9	8.2	8.1	8.5	8.4	7.8	7.9	7.9	7.7	9.1	9.3	9.5	8.42	8.69	8.60
7	9.2	8.4	7.8	7.1	8.1	8.7	7.2	9.3	8	8.3	8.7	8.8	11	8.48	8.55	8.20
8	8.7	8.1	7.6	8.6	8.3	8.1	8	8.8	8.4	8	8	9	10	8.43	8.50	8.50
9	9.1	8.3	7.7	8	8.2	7.6	7.8	8.6	8.3	8.4	9.1	9.1	9.8	8.46	8.64	8.64
10	9.1	8.6	8.9	8.2	8	7.9	8.3	8.7	9.1	8.7	9.4	10	10	8.89	9.18	9.18
11	9.6	8.6	8.2	8.5	8.6	7.8	9.1	8.5	8.3	8.7	9.7	9.6	11	8.92	9.24	9.24
12	10	8.6	8.5	8.6	9.6	9.1	9	9	8.2	8.6	10	10	12	9.35	9.70	9.70
13	13	9.6	9.3	10	9.8	9.6	12	9.7	9	10	10	12	14	10.54	10.99	10.59
														8.643	8.871	8.795

Average														Row Average		
	Rebar										No Rebar			All	No vert	No vert
	1	2	3	4	5	6	7	8	9	10	11	12	13	Points	bar	bar/void
1	9.4	8.9	8.7	7.3	7.5	8	8.9	8	7.7	8.1	8.1	8.7	10	8.41	8.63	8.53
2	8.3	7.7	7.4	7	7.4	7.4	7.2	7.2	6.8	7.2	7.5	8.6	9.8	7.68	7.90	7.90
3	8.1	7.5	7.2	6.6	7.6	7.6	7.5	6.9	7.1	7.1	7.6	8.3	10	7.64	7.95	7.90
4	8.2	8.3	7.7	7.5	8.5	7.7	7.3	7.2	7.3	7.4	8.1	8.4	9.1	7.91	8.08	8.08
5	8.6	8.1	7.4	8.2	9.1	7.8	7.4	7.7	7.4	8.2	8.4	8.8	9.7	8.21	8.34	8.24
6	8.8	7.9	7.9	8	8.2	8.3	7.5	7.6	7.6	7.6	8.3	8.8	9.3	8.13	8.30	8.23
7	8.9	8.1	7.7	7.6	8	7.7	7.1	8.5	8.5	7.9	8.1	8.6	9.6	8.19	8.33	7.98
8	8.5	7.8	7.6	8.1	7.9	7.6	7.7	8.1	8	7.8	7.9	8.5	9.4	8.07	8.18	8.18
9	8.4	8.2	7.6	7.8	8.1	7.5	7.9	8.1	8	8.1	8.6	8.7	9.3	8.17	8.33	8.33
10	8.7	8.2	8.3	8	8	7.9	8.1	8.5	8.7	8.6	8.9	9.6	9.9	8.57	8.78	8.78
11	8.9	8.4	7.9	8.2	8.2	7.7	8.8	8.2	8.3	8.5	9.2	9.7	10	8.64	8.93	8.93
12	10	8.6	8.2	8.4	9.2	9.3	8.8	9	8.2	8.4	9.4	9.9	12	9.16	9.42	9.42
13	12	9.4	8.7	9.5	9.7	9.4	11	9.5	8.9	9.6	9.9	10	13	10.02	10.37	10.00
														8.370	8.580	8.499

Horizontal														Row Average		
	Rebar										No Rebar			All	No vert	No vert
	1	2	3	4	5	6	7	8	9	10	11	12	13	Points	bar	bar/void
1	8.8	9	8.8	7.1	7.2	8.1	8.6	7.8	7.1	7.6	7.9	8	10	8.15	8.30	8.20
2	8	7.6	7.3	6.8	7.6	7.6	7.1	7.2	7.2	7.4	7.7	8.9	9.8	7.71	7.95	7.95
3	8.2	7.2	6.9	6.5	7.5	7.5	7.7	7.1	7.4	7.2	7.8	8.5	10	7.68	8.04	7.97
4	9.1	7.9	7.5	7.7	8.2	7.6	7.1	7.3	7	7.5	8.3	8.5	9.3	7.93	8.13	8.13
5	8.7	8.1	7.5	8.3	8.9	7.8	7.4	7.4	7.4	8.2	8.5	9.1	10	8.25	8.44	8.37
6	8.7	7.8	7.9	7.9	8.1	8.1	7.4	7.3	7.2	7.8	8.3	8.8	9.1	8.03	8.19	8.10
7	9.6	7.8	7.8	8.1	7.9	7.1	7.3	9.1	9	9	8.3	8.8	9.2	8.39	8.49	8.19
8	8.9	7.7	7.3	8.1	7.5	7.3	7.7	7.9	8	8	8.2	8.5	9.2	8.03	8.17	8.17
9	8.2	8.1	7.5	8.1	7.8	7.4	8.5	7.9	8.6	8.2	8.6	8.9	9.9	8.28	8.50	8.50
10	8.8	8	8.2	8.3	7.9	7.9	7.9	8.8	8.9	8.8	8.8	9.4	10	8.62	8.78	8.78
11	8.6	8.2	7.8	8.4	7.9	7.4	8.5	8.5	8.3	8.4	9.1	10	10	8.56	8.80	8.80
12	9.9	8.1	8.2	8.4	9.1	9.3	8.7	9.1	8.2	8.6	9.1	10	12	9.18	9.49	9.49
13	13	9.1	8.1	9	9.5	9.8	9.9	9.8	9	9.2	10	9.6	12	9.85	10.15	9.80
														8.359	8.570	8.495

Standard Deviation													
	Rebar										No Rebar		
	1	2	3	4	5	6	7	8	9	10	11	12	13
1	1	0.3	0.3	0.4	0.3	0.5	0.4	0.6	0.5	0.5	0.7	0.7	0.1
2	0.3	0.2	0.2	0.3	0.2	0.3	0.2	0.3	0.3	0.5	0.5	0.2	0.4
3	0.2	0.3	0.3	0.2	0.1	0.4	0.5	0.2	0.4	0.1	0.5	0.2	0.2
4	0.9	0.4	0.5	0.3	0.3	0.2	0.4	0.3	0.3	0.2	0.2	0.2	0.4
5	0.1	0.1	0.1	0.2	0.2	0.3	0.4	0.3	0.1	0.3	0.3	0.4	0.4
6	0.3	0.1	0.3	0.1	0.3	0.2	0.3	0.3	0.4	0.3	0.9	0.5	0.2
7	0.8	0.3	0.2	0.5	0.1	0.9	0.2	1.2	0.5	1.3	0.7	0.3	0.8
8	0.6	0.3	0.2	0.5	0.4	0.4	0.3	0.6	0.4	0.3	0.4	0.6	0.5
9	0.6	0.1	0.1	0.5	0.2	0.1	0.6	0.4	0.9	0.4	0.5	0.5	0.9
10	0.5	0.3	0.5	0.4	0.1	0.1	0.2	0.4	0.6	0.3	0.5	0.7	0.6
11	0.6	0.2	0.3	0.5	0.4	0.2	0.3	0.5	0.1	0.2	0.5	0.4	0.4
12	0.2	0.5	0.4	0.1	0.3	0.2	0.2	0.1	0.1	0.3	0.6	0.6	0.9
13	0.7	0.3	0.6	0.5	0.2	0.5	1	0.4	0.2	0.6	0.4	1.2	1.1

Vertical														Row Average		
	Rebar										No Rebar			All	No vert	No vert
	1	2	3	4	5	6	7	8	9	10	11	12	13	Points	bar	bar/void
1	8.8	8.6	8.4	7	7.5	7.4	9.3	7.5	8.1	8.1	7.5	8.9	10	8.25	8.58	8.40
2	8.3	7.7	7.3	6.9	7.5	7.1	7.4	6.9	6.6	6.7	7	8.5	9.4	7.49	7.75	7.75
3	7.8	7.7	7.4	6.5	7.6	7.3	7	6.7	6.7	7	7	8.1	10	7.45	7.71	7.66
4	7.4	8.2	7.4	7.2	8.6	7.6	7	6.9	7.4	7.2	8	8.4	8.7	7.69	7.86	7.86
5	8.5	8.2	7.3	8	9.1	8.1	7	7.6	7.5	8	8.1	8.3	9.2	8.07	8.13	7.99
6	8.6	7.9	7.6	7.9	8	8.3	7.3	7.7	7.7	7.2	7.4	8.3	9.3	7.94	8.03	7.99
7	8	8.1	7.4	7.5	8	7.2	6.9	7.2	8.5	6.5	7.4	8.3	9.1	7.70	7.95	7.54
8	7.8	7.5	7.8	7.7	7.9	7.5	7.3	7.7	7.7	7.4	7.5	7.9	9	7.75	7.87	7.87
9	7.9	8.2	7.7	7.2	8.2	7.4	7.4	7.8	7	7.7	8.1	8.2	8.3	7.78	7.85	7.85
10	8.2	8	7.9	7.6	8.1	7.8	8.1	8.1	8	8.3	8.4	9.1	9.2	8.22	8.38	8.38
11	8.6	8.5	7.6	7.6	8.2	7.8	8.8	7.6	8.4	8.4	8.7	9.3	10	8.45	8.74	8.74
12	10	9	7.8	8.3	9	9.5	8.7	8.9	8.1	8.1	9	9.2	11	8.95	9.06	9.06
13	11	9.5	8.7	9.4	9.7	8.8	11	9	8.6	9.3	9.5	9.6	12	9.68	9.98	9.62
														8.108	8.298	8.207

FIGURE D.23: 28 day VHES overlay mockup SR heatmaps

Diagonal

	Rebar										No Rebar			Row Average		
	1	2	3	4	5	6	7	8	9	10	11	12	13	All Points	No vert bar	No vert bar/void
1	16	13	13	12	12	12	13	13	11	13	13	14	15	12.98	13.29	13.28
2	12	11	11	10	12	12	11	11	9.9	10	11	12	15	11.41	11.71	11.71
3	12	10	9.3	9.1	11	12	12	10	9.8	8.9	11	12	16	10.93	11.45	11.45
4	11	12	9.9	10	10	11	11	11	11	9.7	11	11	14	10.89	11.08	11.08
5	12	11	9	11	12	9.5	11	11	10	12	11	12	14	11.08	11.33	11.27
6	12	11	10	10	10	10	9.5	11	10	10	13	12	14	11.03	11.45	11.32
7	13	11	10	8.9	9.3	9.7	9.5	11	9.9	11	10	11	14	10.59	10.84	10.45
8	11	11	9.7	11	11	10	9.4	10	12	11	11	12	13	10.76	10.95	10.95
9	12	11	9.7	10	11	11	10	11	11	11	12	12	13	11.15	11.33	11.33
10	12	11	12	11	11	11	11	11	12	12	12	13	14	11.62	11.96	11.96
11	13	12	11	11	12	11	12	12	11	12	13	13	15	11.93	12.35	12.35
12	15	12	11	12	13	12	12	12	11	12	14	16	17	12.93	13.63	13.63
13	18	14	14	15	14	14	16	14	13	14	14	16	19	14.77	15.26	14.83
														11.698	12.048	11.969

Average

	Rebar										No Rebar			Row Average		
	1	2	3	4	5	6	7	8	9	10	11	12	13	All Points	No vert bar	No vert bar/void
1	14	12	12	10	11	11	12	11	10	12	12	12	14	11.87	12.22	12.30
2	12	10	9.8	9.4	11	11	10	9.9	9.5	9.7	10	11	14	10.61	10.97	10.97
3	11	9.9	9	8.7	10	11	10	9.6	9.3	8.7	10	11	14	10.21	10.63	10.59
4	11	11	9.4	9.5	10	10	10	9.8	9.7	9	10	11	13	10.23	10.50	10.50
5	11	10	8.7	10	11	9.8	10	9.8	9.5	11	11	11	13	10.42	10.62	10.59
6	12	10	9.5	9.7	10	9.7	9.2	10	9.3	9.7	11	12	13	10.30	10.61	10.47
7	12	9.7	9.8	8.6	9.4	9.1	8.7	10	9.7	10	10	11	13	10.03	10.33	9.94
8	11	9.8	9	10	10	9.4	9.3	10	10	9.9	10	11	12	10.13	10.30	10.30
9	11	10	9.6	9.8	10	9.9	9.5	10	10	11	11	11	12	10.37	10.50	10.50
10	11	10	11	10	10	10	10	11	10	11	11	12	13	10.87	11.12	11.12
11	12	11	10	11	11	10	11	11	10	11	12	12	14	11.23	11.59	11.59
12	13	12	11	12	12	12	12	12	12	11	13	14	16	12.44	12.92	12.92
13	17	13	13	13	13	13	14	14	12	13	14	15	18	13.95	14.33	13.95
														10.974	11.280	11.211

Horizontal

	Rebar										No Rebar			Row Average		
	1	2	3	4	5	6	7	8	9	10	11	12	13	All Points	No vert bar	No vert bar/void
1	14	11	12	9.8	10	11	12	11	9.9	10	11	11	15	11.23	11.65	11.78
2	12	10	9.3	9.4	11	11	10	9.7	9.7	10	10	12	14	10.56	10.91	10.91
3	11	9.3	8.5	8.8	10	11	11	9.6	9	9	9.8	11	14	10.07	10.44	10.36
4	11	9.8	9.3	9.8	10	9.8	9.6	9.8	9.1	9.7	10	11	14	10.27	10.58	10.58
5	11	10	8.7	10	11	9.8	9.3	9.2	9.5	10	11	12	13	10.38	10.69	10.62
6	11	9.8	9.5	9.8	10	9.7	9.2	9.2	9	10	11	12	12	10.20	10.50	10.34
7	12	9.5	9.7	9.4	9.3	9.1	8.5	10	11	11	10	11	13	10.25	10.49	9.92
8	12	9.3	9.1	9.9	9.6	9.2	9.2	10	9.2	10	11	11	12	10.13	10.34	10.34
9	10	9.8	9.5	9.8	9.3	9.6	9.6	10	9.8	11	11	11	13	10.27	10.39	10.39
10	11	10	11	10	10	11	9.9	11	11	11	12	12	14	10.96	11.16	11.16
11	12	11	10	11	11	10	11	11	11	11	12	13	14	11.25	11.65	11.65
12	13	11	11	11	12	12	11	12	11	11	12	14	16	12.05	12.54	12.54
13	17	13	12	13	13	13	13	14	11	13	13	14	17	13.48	13.73	13.35
														10.855	11.158	11.072

Standard Deviation

	Rebar										No Rebar		
	1	2	3	4	5	6	7	8	9	10	11	12	13
1	1.4	0.7	0.9	0.9	0.9	1.3	0.7	1	0.7	1.5	1	1.7	0.7
2	0.3	1	0.8	0.7	0.8	1.1	0.7	1.1	0.6	0.7	1.2	0.7	1
3	0.6	0.6	0.4	0.4	0.6	1.1	1.4	0.6	0.4	0.4	0.9	0.6	1.4
4	0.9	0.9	0.5	0.6	0.2	1.1	0.5	0.8	0.7	1.2	0.7	0.5	1.7
5	1.1	0.6	0.3	0.5	1.1	0.3	0.7	0.8	0.5	1.2	0.8	1	1.1
6	0.9	0.5	0.6	0.6	0.2	0.4	0.3	0.9	1	0.7	1.8	0.9	1.1
7	1.3	0.9	0.3	1	0.2	0.6	0.7	0.7	1.5	1.4	0.4	0.3	1.1
8	0.8	0.8	0.7	0.8	0.6	0.5	0.1	0.2	1.4	0.9	0.6	1	1
9	1	0.8	0.1	0.5	1.1	0.9	0.7	0.9	0.9	0.7	1	0.7	1.1
10	0.7	0.7	1	1.2	0.6	0.7	0.6	0.5	1.3	0.6	0.6	1.3	1.2
11	1.2	0.5	0.6	0.5	0.6	0.5	0.7	1	0.7	0.6	1	0.6	1.3
12	1.3	0.7	0.3	0.4	0.4	0.6	0.8	0.3	1.4	0.3	1.1	1.1	1
13	0.6	0.5	0.9	1.1	0.2	0.5	1.4	0.2	1	0.7	0.4	1.1	1.3

Vertical

	Rebar										No Rebar			Row Average		
	1	2	3	4	5	6	7	8	9	10	11	12	13	All Points	No vert bar	No vert bar/void
1	13	12	11	10	10	9.8	11	11	10	12	12	12	14	11.40	11.73	11.83
2	12	9.4	9.4	8.7	10	9.9	9.9	9	8.8	8.9	8.8	11	13	9.86	10.28	10.28
3	11	9.9	9.2	8.3	9.8	9.7	9	9	9.2	8.3	9.2	10	13	9.64	10.01	9.96
4	9.6	11	8.9	8.8	10	9	9.9	9.1	9.4	7.6	9.7	10	11	9.54	9.85	9.85
5	10	9.6	8.3	9.6	9.6	10	10	9.4	9.1	9.8	9.9	10	12	9.79	9.84	9.88
6	11	9.6	8.9	9	10	9.3	9	9.9	8.5	8.9	9.1	11	12	9.67	9.88	9.76
7	10	9	9.5	7.5	9.7	8.5	8.2	9.3	8.1	8.8	9.6	10	11	9.26	9.65	9.46
8	10	9.4	8.3	9.3	9.7	9	9.3	9.9	9.1	8.9	9.5	9.8	11	9.49	9.62	9.62
9	10	9.8	9.6	9.4	9.5	9.3	8.8	9.3	9.2	9.8	10	11	11	9.69	9.80	9.80
10	10	9.8	9.9	8.9	9.7	9.4	9.9	10	9	10	11	11	12	10.03	10.24	10.24
11	11	11	9.8	10	11	9.8	11	9.6	9.4	10	11	12	13	10.49	10.76	10.76
12	12	12	12	12	12	13	11	12	13	11	12	13	16	12.34	12.59	12.59
13	17	13	12	13	13	13	13	14	12	13	13	15	17	13.61	13.99	13.67
														10.370	10.633	10.591

FIGURE D.24: 56 day VHES overlay mockup SR heatmaps

90 day

Wednesday October 21st

Diagonal	Rebar										No Rebar			Row Average		
	1	2	3	4	5	6	7	8	9	10	11	12	13	All Points	No vert bar	No vert bar/void
1	16	14	14	12	12	13	12	12	11	13	13	14	14	13.03	13.28	13.26
2	13	12	11	11	14	13	11	11	10	11	12	13	16	12.15	12.48	12.48
3	12	11	11	11	12	12	12	11	11	9.9	11	12	15	11.45	11.90	11.95
4	12	12	11	11	11	11	11	11	12	12	12	12	15	11.69	11.93	11.93
5	12	11	10	11	12	10	11	10	11	13	13	13	14	11.69	12.02	12.00
6	13	11	11	11	11	11	11	12	11	11	13	13	14	11.61	11.99	11.83
7	13	11	11	10	10	10	10	12	11	12	12	12	15	11.52	11.86	11.40
8	13	12	12	11	11	10	10	10	11	12	12	13	14	11.64	11.91	11.91
9	14	13	12	12	12	11	10	13	12	12	12	13	13	12.20	12.25	12.25
10	13	14	14	14	13	12	11	12	12	12	14	14	16	13.08	13.15	13.15
11	15	14	13	14	14	13	14	14	12	13	14	14	14	13.65	13.78	13.78
12	16	16	14	15	15	15	13	14	13	13	15	16	16	14.58	14.74	14.74
13	19	17	18	18	17	16	17	14	14	15	16	18	19	16.61	17.10	16.78
														12.683	12.952	12.881

Average	Rebar										No Rebar			Row Average		
	1	2	3	4	5	6	7	8	9	10	11	12	13	All Points	No vert bar	No vert bar/void
1	15	13	13	11	11	12	12	12	11	13	13	13	14	12.56	12.84	12.83
2	13	11	11	11	13	12	11	11	11	11	11	12	15	11.78	12.08	12.08
3	12	11	10	11	11	11	11	11	11	9.7	11	11	14	11.10	11.47	11.49
4	12	12	11	11	11	10	11	11	11	11	12	12	14	11.40	11.67	11.67
5	12	11	9.6	11	11	9.6	11	10	11	12	13	12	14	11.35	11.65	11.71
6	12	11	11	11	10	11	11	11	10	11	13	12	14	11.29	11.58	11.48
7	13	11	11	9.9	11	9.9	9.7	11	11	11	12	12	14	11.19	11.58	11.19
8	13	12	11	11	11	9.9	10	10	11	12	12	13	14	11.55	11.83	11.83
9	13	13	12	12	11	11	11	12	12	12	12	12	13	11.96	12.01	12.01
10	14	14	14	13	12	12	12	12	11	13	13	14	15	13.01	13.18	13.18
11	15	14	13	14	13	12	14	13	12	13	13	14	14	13.36	13.49	13.49
12	16	15	14	15	15	14	14	14	13	13	14	16	16	14.57	14.77	14.77
13	18	17	17	17	17	15	16	15	14	15	16	17	18	16.23	16.58	16.39
														12.412	12.670	12.624

Horizontal	Rebar										No Rebar			Row Average		
	1	2	3	4	5	6	7	8	9	10	11	12	13	All Points	No vert bar	No vert bar/void
1	15	13	13	11	11	11	12	11	11	12	12	12	14	12.13	12.38	12.46
2	13	10	11	12	12	12	11	11	11	11	11	13	15	11.80	12.15	12.15
3	12	11	10	10	12	11	11	11	12	9.9	11	12	15	11.22	11.68	11.69
4	13	11	10	11	10	9.9	11	11	11	12	12	13	14	11.40	11.69	11.69
5	12	12	9.7	11	12	9.9	11	11	11	12	13	12	15	11.64	11.90	11.96
6	12	11	11	11	10	11	11	11	10	11	13	12	13	11.35	11.58	11.51
7	13	12	11	11	11	9.9	9.7	11	11	12	12	12	14	11.39	11.70	11.20
8	14	12	11	12	11	9.6	10	11	11	13	11	13	14	11.78	11.99	11.99
9	13	12	12	12	11	11	11	12	12	13	12	13	14	12.09	12.13	12.13
10	14	14	14	12	12	13	13	12	11	13	13	14	16	13.22	13.46	13.46
11	14	14	13	14	13	11	14	13	12	13	13	15	15	13.36	13.50	13.50
12	16	14	15	15	15	15	14	15	13	13	14	16	17	14.72	14.98	14.98
13	19	17	17	16	16	15	16	16	14	15	17	18	18	16.45	16.83	16.65
														12.504	12.764	12.720

Standard Deviation	Rebar										No Rebar		
	1	2	3	4	5	6	7	8	9	10	11	12	13
1	1.2	0.5	0.5	0.7	0.8	0.9	0.6	0.4	0.1	0.3	0.7	0.9	0.1
2	0.6	1	0.6	0.3	1.1	0.5	0.4	0.6	0.6	0.2	0.9	0.6	0.6
3	0.3	0.2	0.8	0.3	0.3	0.7	0.7	0.4	0.5	0.3	0.8	0.5	0.9
4	1	0.5	0.6	0.2	0.4	0.6	0.2	0.5	0.4	0.6	0.2	0.3	1.3
5	0.8	0.2	0.5	0.6	1	0.7	0.3	0.6	0.2	1	0.4	0.9	0.9
6	0.4	0.3	0.6	0.4	0.3	0.8	0.4	0.4	0.6	0.1	0.3	0.7	0.4
7	0.6	0.7	0.3	0.9	0.3	0.3	0.6	1	1.1	0.8	0.2	0.3	0.6
8	0.7	0.6	0.2	0.4	0.4	0.4	0.1	0.7	0.5	0.6	0.3	0.4	0.4
9	0.4	0.3	0.1	0.3	0.3	0.2	0.3	0.7	1	0.9	0.2	0.8	0.8
10	0.7	0.2	0.5	1	0.2	0.4	0.8	0.3	0.5	0.4	0.4	0.6	1
11	0.3	0.5	0.2	0.5	0.9	0.6	0.4	0.7	0.3	0.4	0.5	0.6	0.7
12	1	1	0.8	0.3	0.2	0.6	0.4	0.6	0.6	0.3	0.6	0.9	1.3
13	1.2	0.6	0.5	0.7	0.3	0.3	1	0.8	0.2	0.5	1	1.6	0.6

Vertical	Rebar										No Rebar			Row Average		
	1	2	3	4	5	6	7	8	9	10	11	12	13	All Points	No vert bar	No vert bar/
1	14	13	13	11	12	11	13	12	11	13	13	14	14	12.52	12.88	12.78
2	12	11	10	12	13	12	11	10	10	11	9.8	12	15	11.38	11.61	11.61
3	11	11	9.1	11	11	10	11	10	11	9.3	9.8	11	14	10.63	10.83	10.84
4	11	12	10	11	11	9.5	11	10	12	11	12	12	13	11.11	11.40	11.40
5	11	11	9.1	10	10	8.8	10	10	11	11	12	12	13	10.74	11.04	11.16
6	12	11	10	10	10	9.7	10	11	9.6	11	12	12	14	10.93	11.19	11.10
7	12	10	11	8.9	11	9.7	9.2	9.8	9.4	10	12	12	14	10.65	11.19	10.98
8	13	11	11	11	11	9.8	9.9	9.9	11	12	12	12	13	11.22	11.58	11.58
9	13	13	12	11	12	11	11	11	10	12	12	11	12	11.59	11.65	11.65
10	13	13	13	12	12	12	12	12	11	13	14	13	15	12.72	12.91	12.91
11	15	15	13	13	13	12	13	12	11	12	13	13	13	13.08	13.19	13.19
12	18	16	13	15	15	14	14	14	14	13	14	15	15	14.42	14.59	14.59
13	17	16	17	17	16	15	15	15	14	14	15	15	18	15.65	15.80	15.73
														12.049	12.295	12.271

FIGURE D.25: 90 day VHES overlay mockup SR heatmaps

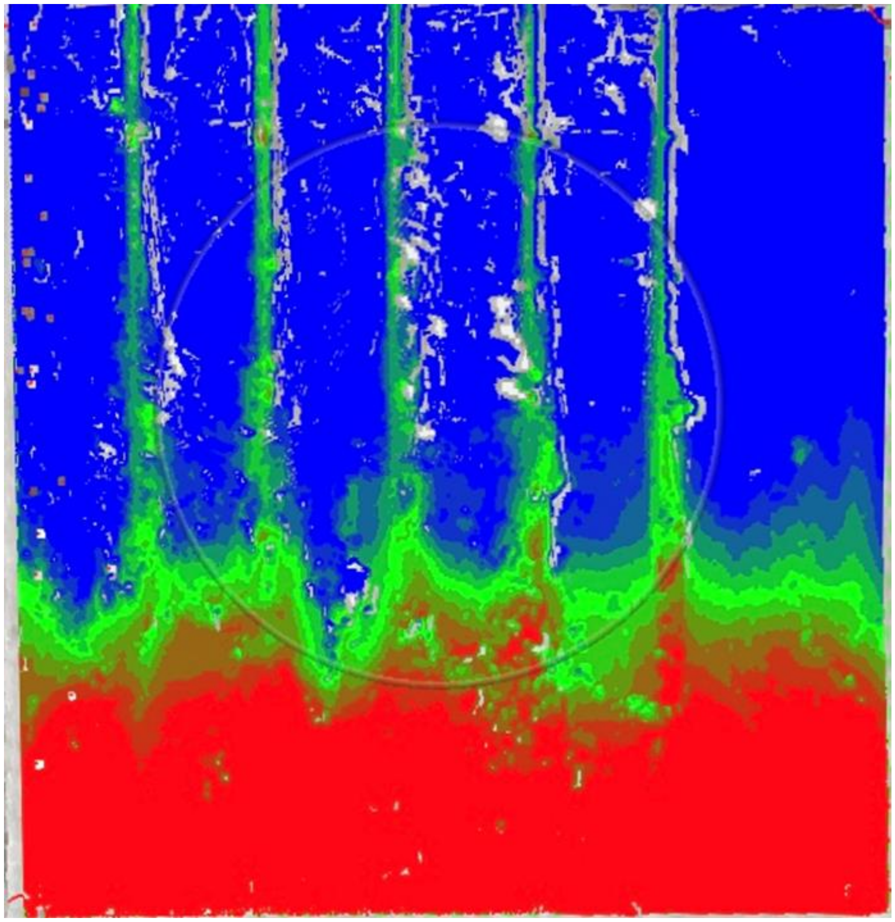

FIGURE D.26: VHES-LMC 3D surface scan

Diagonal	Rebar										No Rebar			Row Average		
	1	2	3	4	5	6	7	8	9	10	11	12	13	All Points	No vert bar	No vert bar/void
1	3	2.5	2.2	2.4	2.4	2.6	2.4	2.3	2.3	2.2	2.4	2.8	2.6	2.469	2.513	2.583
2	2.4	2.4	2.2	2.1	2.1	2.1	2.1	2.1	2.3	2.3	2.3	2.2	2.6	2.246	2.275	2.275
3	2.4	2.5	2.3	2	2.1	1.9	2.2	2	2.1	2.1	2.3	2.2	2.4	2.192	2.250	2.271
4	2.6	2.9	2.9	2.1	2.5	2.2	2.1	2.1	2.5	2.2	2.3	2.3	2.5	2.400	2.463	2.463
5	2.3	2.4	2.3	2.3	2.4	2.3	2.3	2.4	2.3	2.3	2.3	2.4	2.6	2.354	2.363	2.320
6	2.5	2.4	2.5	2.5	2.5	2.5	2.4	2.3	2.4	2.2	2.3	2.2	2.4	2.392	2.400	2.433
7	2.6	2.6	2.5	2.5	2.4	2.3	2.1	2.4	2.5	2.4	2.5	2.4	2.7	2.456	2.463	2.457
8	2.7	2.6	2.6	2.6	2.3	2.5	2.5	2.6	2.6	2.8	2.4	2.5	2.6	2.562	2.525	2.525
9	2.9	2.5	2.5	2.5	2.5	2.5	2.5	2.4	2.3	2.4	2.5	2.9	2.9	2.562	2.625	2.625
10	3.2	2.5	2.5	2.6	2.4	2.4	2.5	2.5	2.5	2.6	2.5	2.6	2.9	2.592	2.638	2.638
11	2.7	2.6	2.6	2.8	2.4	2.5	2.6	2.6	2.7	2.5	2.7	2.6	3	2.638	2.663	2.663
12	2.9	2.6	2.9	2.8	2.7	2.6	3	2.8	2.6	2.7	2.7	2.9	3.3	2.808	2.875	2.875
13	3.5	3.2	3	3	2.9	2.9	3.4	3.4	2.9	2.8	3.1	3.2	3.5	3.138	3.188	3.100
														2.524	2.557	2.556

Average	Rebar										No Rebar			Row Average		
	1	2	3	4	5	6	7	8	9	10	11	12	13	All Points	No vert bar	No vert bar/void
1	3.0	2.7	2.5	2.5	2.5	2.5	2.5	2.3	2.4	2.2	2.5	2.9	2.9	2.582	2.667	2.717
2	2.6	2.5	2.4	2.1	2.1	2.2	2.2	2.2	2.4	2.3	2.4	2.4	2.9	2.368	2.418	2.418
3	2.7	2.6	2.5	2.3	2.2	2.2	2.2	2.2	2.2	2.2	2.4	2.4	2.6	2.367	2.408	2.438
4	2.8	2.8	2.6	2.5	2.5	2.4	2.3	2.3	2.5	2.4	2.3	2.4	2.7	2.500	2.513	2.513
5	2.6	2.6	2.4	2.4	2.6	2.5	2.5	2.4	2.5	2.5	2.3	2.5	2.7	2.500	2.517	2.480
6	2.7	2.7	2.5	2.6	2.6	2.6	2.6	2.4	2.5	2.4	2.4	2.5	2.6	2.538	2.546	2.544
7	2.7	2.7	2.6	2.7	2.4	2.5	2.4	2.5	2.7	2.7	2.5	2.6	2.8	2.598	2.583	2.567
8	2.8	2.6	2.6	2.6	2.4	2.7	2.6	2.7	2.6	2.8	2.5	2.6	2.8	2.628	2.596	2.596
9	3.0	2.7	2.6	2.6	2.6	2.6	2.6	2.6	2.4	2.6	2.6	2.9	3.0	2.664	2.700	2.700
10	3.2	2.7	2.7	2.7	2.6	2.5	2.6	2.7	2.6	2.7	2.6	2.7	3.0	2.721	2.758	2.758
11	2.8	2.7	2.8	2.9	2.6	2.6	2.6	2.7	2.8	2.6	2.8	2.8	3.1	2.754	2.779	2.779
12	3.1	2.9	2.9	3.0	3.0	3.0	3.1	3.1	2.7	2.8	2.8	3.0	3.4	2.995	3.004	3.004
13	3.6	3.3	3.1	3.1	3.1	3.1	3.4	3.6	3.0	2.9	3.2	3.2	3.5	3.238	3.254	3.172
														2.650	2.673	2.668

Horizontal	Rebar										No Rebar			Row Average		
	1	2	3	4	5	6	7	8	9	10	11	12	13	All Points	No vert bar	No vert bar/void
1	3	2.7	2.5	2.4	2.4	2.4	2.5	2.4	2.2	2.1	2.3	2.6	2.7	2.477	2.525	2.533
2	2.7	2.7	2.5	2.1	2	2.3	2	2.1	2.3	2.3	2.2	2.4	3.1	2.366	2.404	2.404
3	2.8	2.6	2.6	2.4	2.3	2.3	2.1	2.2	2.3	2.2	2.4	2.4	2.6	2.400	2.438	2.457
4	2.9	2.7	2.6	2.6	2.6	2.4	2.2	2.4	2.4	2.4	2.3	2.4	2.5	2.492	2.488	2.488
5	2.8	2.7	2.4	2.4	2.7	2.6	2.4	2.4	2.5	2.5	2.3	2.5	2.8	2.538	2.550	2.520
6	3.1	2.9	2.2	2.4	2.5	2.5	2.7	2.4	2.4	2.4	2.5	2.6	2.6	2.554	2.575	2.567
7	2.7	2.6	2.6	2.6	2.4	2.4	2.5	2.4	2.7	2.6	2.4	2.5	2.9	2.562	2.588	2.571
8	2.7	2.6	2.4	2.5	2.5	2.6	2.3	2.5	2.5	2.6	2.5	2.6	2.9	2.554	2.550	2.550
9	2.9	3	2.6	2.5	2.6	2.6	2.3	2.5	2.4	2.7	2.6	2.8	3	2.654	2.650	2.650
10	2.9	2.8	2.8	2.9	2.7	2.5	2.5	2.6	2.6	2.8	2.7	2.7	3.2	2.746	2.763	2.763
11	2.7	2.8	2.8	2.8	2.5	2.6	2.5	2.7	2.8	2.5	2.6	2.9	3.3	2.731	2.763	2.763
12	3.3	3	3	3	3.2	3.2	3.1	3.2	2.6	2.7	2.9	3	3.3	3.038	3.050	3.050
13	3.5	3.5	3	3.1	3.1	3.2	3.6	3.6	3	2.7	3	3	3.4	3.208	3.200	3.083
														2.640	2.657	2.646

Standard Deviation	Rebar										No Rebar		
	1	2	3	4	5	6	7	8	9	10	11	12	13
1	0.1	0.3	0.4	0.1	0.2	0.1	0.1	0.1	0.3	0.1	0.3	0.3	0.5
2	0.2	0.2	0.2	0.1	0.1	0.1	0.2	0.2	0.1	0.1	0.2	0.2	0.3
3	0.3	0.2	0.2	0.2	0.1	0.2	0.1	0.2	0.1	0.2	0.1	0.2	0.3
4	0.2	0.1	0.4	0.4	0.1	0.2	0.2	0.2	0.1	0.2	0	0.2	0.3
5	0.3	0.2	0.1	0.2	0.2	0.2	0.3	0.1	0.2	0.2	0	0.2	0.1
6	0.3	0.3	0.3	0.2	0.1	0.1	0.2	0.2	0.2	0.2	0.1	0.3	0.2
7	0.1	0.2	0.1	0.3	0.1	0.2	0.3	0.2	0.2	0.4	0.1	0.2	0.1
8	0.1	0.1	0.2	0.1	0.1	0.2	0.3	0.2	0.1	0.3	0.1	0.1	0.2
9	0.1	0.3	0.2	0.1	0.2	0.1	0.3	0.3	0.1	0.2	0.1	0.1	0.1
10	0.3	0.2	0.2	0.2	0.2	0.1	0.2	0.2	0.1	0.1	0.1	0.2	0.2
11	0.1	0.1	0.2	0.1	0.2	0.1	0.2	0.2	0.1	0.2	0.2	0.2	0.2
12	0.2	0.3	0.1	0.3	0.3	0.3	0.1	0.3	0.2	0.2	0.1	0.1	0.1
13	0.1	0.2	0.1	0.2	0.3	0.2	0.2	0.3	0.1	0.3	0.2	0.2	0.1

Vertical	Rebar										No Rebar			Row Average		
	1	2	3	4	5	6	7	8	9	10	11	12	13	All Points	No vert bar	No vert bar/void
1	3.1	3	2.9	2.6	2.7	2.5	2.6	2.3	2.8	2.3	2.9	3.2	3.5	2.800	2.963	3.033
2	2.8	2.5	2.6	2.2	2.1	2.2	2.4	2.5	2.5	2.4	2.6	2.6	3	2.492	2.575	2.575
3	3	2.8	2.6	2.4	2.2	2.3	2.3	2.4	2.2	2.4	2.5	2.6	2.9	2.508	2.538	2.586
4	3	2.8	2.2	2.9	2.5	2.6	2.5	2.3	2.5	2.6	2.3	2.6	3.1	2.608	2.588	2.588
5	2.6	2.6	2.5	2.6	2.7	2.5	2.9	2.5	2.7	2.6	2.3	2.7	2.7	2.608	2.638	2.600
6	2.6	2.8	2.7	2.8	2.7	2.7	2.6	2.6	2.8	2.5	2.4	2.7	2.8	2.669	2.663	2.633
7	2.7	2.9	2.6	3	2.5	2.7	2.6	2.8	2.9	3.1	2.6	2.8	2.9	2.777	2.700	2.671
8	2.9	2.7	2.7	2.7	2.5	2.9	2.9	2.9	2.6	3.1	2.5	2.7	2.9	2.769	2.713	2.713
9	3.1	2.6	2.8	2.7	2.8	2.7	2.9	2.9	2.4	2.6	2.7	2.9	3	2.777	2.825	2.825
10	3.4	2.9	2.9	2.6	2.7	2.6	2.9	2.9	2.7	2.7	2.6	2.9	2.9	2.823	2.875	2.875
11	2.9	2.8	2.9	3	2.8	2.7	2.8	2.9	2.9	2.9	3	2.9	3.1	2.892	2.913	2.913
12	3.2	3.2	2.9	3.3	3	3.2	3.1	3.4	3	3	2.9	3.1	3.5	3.138	3.088	3.088
13	3.7	3.1	3.2	3.3	3.4	3.2	3.3	3.9	3.1	3.3	3.4	3.3	3.6	3.369	3.375	3.333
														2.787	2.804	2.802

FIGURE D.27: 1 hour VHES-LMC overlay mockup SR heatmaps

Diagonal

	Rebar										No Rebar			Row Average		
	1	2	3	4	5	6	7	8	9	10	11	12	13	All Points	No vert bar	No vert bar/void
1	4.7	4	3.7	3.6	3.7	3.3	3.6	3.8	3.7	3.1	3.9	4.1	4.1	3.792	3.938	4.033
2	4.1	3.3	3.4	2.9	3.2	2.9	2.9	3.1	3.7	3.5	3.4	3.6	4.2	3.402	3.563	3.563
3	3.8	4.3	3.7	3.4	3.3	3.2	3.1	3.1	3.3	3.3	3.5	3.6	3.7	3.485	3.500	3.529
4	4.5	4.5	3.8	3.8	3.9	3.5	3.4	3.4	3.8	3.6	3.6	3.8	4.4	3.846	3.900	3.900
5	3.9	3.9	4	4	4.1	3.6	3.9	3.6	3.7	3.9	3.8	3.9	4.2	3.885	3.938	3.940
6	4	4.4	3.9	4.2	3.9	4.2	3.8	3.8	3.7	3.9	3.4	3.7	3.7	3.892	3.763	3.783
7	4.5	4.8	4.3	4.6	4.5	4.4	4.1	4.5	4.2	3.7	4.1	4.1	4.4	4.323	4.275	4.286
8	4.6	4.3	4.5	4.3	4.5	3.9	4	4.2	4	4.3	4	4.1	4.3	4.231	4.250	4.250
9	4.5	4.2	4.3	4.2	3.9	3.9	4	4	3.7	4.2	3.9	4.8	4.3	4.146	4.175	4.175
10	4.9	4.4	4.2	4	3.9	3.7	3.8	4.1	3.9	3.9	3.7	4.1	4.2	4.062	4.088	4.088
11	4.4	3.7	4.3	4.4	3.9	3.8	4	4.1	3.7	4.2	4.1	4.1	4.6	4.100	4.138	4.138
12	4.2	4.2	4.1	3.8	3.9	4	4.1	4.1	3.5	3.7	3.8	4	4.7	4.008	4.038	4.038
13	4.4	4.4	4	4.2	4	4	4.5	4.8	4.2	3.9	4.2	4.2	4.4	4.246	4.238	4.167
														3.955	3.985	3.991

Average

	Rebar										No Rebar			Row Average		
	1	2	3	4	5	6	7	8	9	10	11	12	13	All Points	No vert bar	No vert bar/void
1	4.5	4.0	3.7	3.9	3.6	3.6	3.5	3.7	3.6	3.3	3.7	4.0	3.9	3.774	3.817	3.883
2	4.0	3.5	3.3	3.0	3.0	3.0	3.0	3.1	3.4	3.7	3.6	3.6	4.2	3.403	3.500	3.500
3	4.0	4.2	3.5	3.4	3.2	3.2	3.0	3.1	3.2	3.3	3.4	3.5	3.8	3.444	3.450	3.490
4	4.3	4.0	3.7	3.6	3.6	3.6	3.2	3.2	3.6	3.5	3.4	3.7	4.2	3.656	3.708	3.708
5	3.8	3.9	3.8	3.7	3.8	3.7	3.6	3.4	3.5	3.6	3.6	3.8	4.2	3.738	3.775	3.733
6	4.0	4.1	3.5	3.9	3.9	4.1	3.6	3.7	3.7	3.7	3.4	3.8	3.8	3.787	3.713	3.689
7	4.0	4.1	3.8	4.1	3.7	4.1	3.8	4.0	3.9	3.9	3.7	3.9	4.1	3.936	3.867	3.857
8	4.2	4.0	4.1	3.8	3.9	3.9	3.6	3.8	3.6	4.1	3.8	3.8	4.0	3.887	3.871	3.871
9	4.3	4.0	3.9	3.8	3.8	3.7	3.5	3.9	3.5	3.8	3.6	4.2	4.3	3.864	3.883	3.883
10	4.6	4.2	4.0	3.8	3.8	3.6	3.6	4.1	3.7	3.9	3.7	4.0	4.2	3.923	3.933	3.933
11	4.2	3.8	4.0	4.2	3.8	3.8	3.7	3.9	3.7	3.9	3.9	4.2	4.4	3.972	3.992	3.992
12	4.2	4.1	4.1	4.1	4.1	4.2	4.0	4.1	3.6	3.8	3.8	4.1	4.6	4.059	4.063	4.063
13	4.6	4.7	4.3	4.3	4.2	4.2	4.5	4.8	4.0	4.0	4.0	4.2	4.3	4.318	4.267	4.167
														3.828	3.834	3.828

Horizontal

	Rebar										No Rebar			Row Average		
	1	2	3	4	5	6	7	8	9	10	11	12	13	All Points	No vert bar	No vert bar/void
1	4.4	3.9	3.6	3.7	3.5	3.7	3.3	3.6	3.3	3.2	3.3	4	3.7	3.631	3.638	3.700
2	4	3.8	3.3	3	2.8	3	2.9	3.1	3.2	4.1	3.5	3.5	4.3	3.423	3.438	3.438
3	3.7	4.2	3.5	3.3	3	3.3	2.8	2.9	3.2	3.4	3.4	3.5	3.7	3.377	3.350	3.400
4	4	3.8	3.6	3.4	3.7	3.5	3	3.2	3.5	3.5	3.4	3.8	3.9	3.562	3.613	3.613
5	3.7	3.9	3.8	3.5	3.9	3.9	3.4	3.3	3.3	3.6	3.4	3.7	4.3	3.669	3.688	3.640
6	4.1	4	3.3	3.5	4.3	4	3.4	3.5	3.4	3.7	3.5	3.7	4.1	3.731	3.725	3.667
7	3.7	3.7	3.7	3.6	3.3	3.5	3.7	3.8	3.7	3.6	3.5	3.6	3.9	3.638	3.638	3.629
8	4	4	3.9	3.4	3.6	3.9	3.3	3.4	3.5	3.6	3.7	3.5	3.7	3.654	3.650	3.650
9	4.1	3.9	3.6	3.7	3.7	3.4	3	3.6	3.5	3.6	3.3	3.8	4.3	3.654	3.663	3.663
10	4.4	4	3.8	3.7	3.8	3.5	3.4	3.9	3.6	3.9	3.7	3.9	4.2	3.831	3.850	3.850
11	4	3.9	3.8	4.1	3.7	4	3.3	3.7	3.8	3.6	3.6	4.2	4.7	3.877	3.888	3.888
12	4.4	3.9	4.2	4.1	4.3	4.2	4.1	4.1	3.7	3.6	3.5	3.9	4.4	4.031	4.063	4.063
13	4.6	4.7	4.2	4.2	4.2	4.1	4.5	4.9	4	4.2	3.7	4	4.1	4.262	4.163	4.033
														3.718	3.720	3.710

Standard Deviation

	Rebar										No Rebar		
	1	2	3	4	5	6	7	8	9	10	11	12	13
1	0.2	0.1	0.2	0.4	0.1	0.3	0.2	0.1	0.3	0.3	0.3	0.1	0.2
2	0.2	0.3	0.1	0.1	0.2	0.1	0.2	0.1	0.3	0.4	0.2	0.1	0.2
3	0.4	0.2	0.2	0.1	0.2	0.2	0.2	0.3	0.2	0.1	0.1	0.1	0.1
4	0.3	0.5	0.1	0.2	0.3	0.1	0.2	0.2	0.2	0.2	0.2	0.2	0.3
5	0.1	0.1	0.2	0.3	0.3	0.2	0.3	0.2	0.2	0.3	0.2	0.1	0.2
6	0.1	0.2	0.3	0.4	0.4	0.1	0.2	0.2	0.3	0.2	0.1	0.1	0.3
7	0.4	0.6	0.4	0.5	0.7	0.5	0.2	0.4	0.3	0.4	0.3	0.3	0.3
8	0.3	0.3	0.3	0.5	0.6	0.1	0.4	0.4	0.3	0.4	0.2	0.3	0.3
9	0.2	0.2	0.4	0.3	0.1	0.3	0.5	0.3	0.2	0.3	0.3	0.5	0.1
10	0.3	0.2	0.2	0.2	0.2	0.1	0.2	0.2	0.2	0	0	0.1	0.1
11	0.2	0.1	0.3	0.2	0.1	0.2	0.4	0.2	0.1	0.3	0.3	0.1	0.4
12	0.2	0.2	0.2	0.4	0.2	0.2	0.2	0	0.1	0.3	0.3	0.2	0.2
13	0.3	0.4	0.3	0.1	0.3	0.2	0	0.1	0.2	0.2	0.3	0.3	0.2

Vertical

	Rebar										No Rebar			Row Average		
	1	2	3	4	5	6	7	8	9	10	11	12	13	All Points	No vert bar	No vert bar/void
1	4.4	4.1	3.9	4.3	3.6	3.9	3.6	3.7	3.9	3.7	3.8	3.9	3.9	3.900	3.875	3.917
2	3.8	3.4	3.2	3	3	3	3.2	3.2	3.3	3.4	3.8	3.7	4	3.385	3.500	3.500
3	4.5	4	3.4	3.4	3.2	3	3.1	3.4	3	3.3	3.4	3.5	3.9	3.469	3.500	3.543
4	4.3	3.6	3.7	3.7	3.3	3.7	3.3	3.1	3.5	3.3	3.2	3.4	4.2	3.562	3.613	3.613
5	3.8	3.8	3.7	3.7	3.5	3.7	3.6	3.4	3.6	3.4	3.5	3.9	4	3.662	3.700	3.620
6	3.9	4	3.4	3.9	3.6	4.2	3.5	3.8	4	3.5	3.3	3.9	3.6	3.738	3.650	3.617
7	3.8	3.9	3.5	4	3.3	4.4	3.7	3.8	3.9	4.4	3.5	3.9	3.9	3.846	3.688	3.657
8	4	3.7	4	3.7	3.5	3.8	3.6	3.9	3.4	4.3	3.6	3.7	3.9	3.777	3.713	3.713
9	4.2	3.8	3.9	3.6	3.9	3.7	3.5	4.1	3.3	3.6	3.5	4	4.2	3.792	3.813	3.813
10	4.4	4.2	4	3.6	3.6	3.6	3.6	4.2	3.6	3.9	3.7	3.9	4.1	3.877	3.863	3.863
11	4.1	3.9	4	4.1	3.9	3.7	3.7	4	3.7	3.9	4	4.2	4	3.938	3.950	3.950
12	4.1	4.1	3.9	4.5	4.1	4.3	3.8	4.1	3.7	4.1	4	4.3	4.8	4.138	4.088	4.088
13	4.9	5.1	4.6	4.4	4.5	4.4	4.5	4.8	3.8	3.9	4	4.5	4.4	4.446	4.400	4.300
														3.810	3.796	3.784

FIGURE D.28: 4 hour VHES-LMC overlay mockup SR heatmaps

Diagonal

	Rebar										No Rebar			Row Average: All Points	No vert bar	No vert bar/void
	1	2	3	4	5	6	7	8	9	10	11	12	13			
1	12	9.9	9	8.8	9.4	9	10	11	9.1	7.6	7.6	8.8	8.9	9.300	9.388	9.300
2	9.8	8.6	8.5	8.1	7.8	7.8	7.4	6.9	7.9	7.4	7.6	7.3	8.7	7.985	8.125	8.125
3	11	10	6.5	8.8	8.7	8.5	7.4	7.6	7	7.7	7.8	7.8	8.2	8.215	8.013	7.914
4	11	11	9.7	8.6	8.3	8.3	8.5	7.8	8.2	8.3	7.7	8.3	9.6	8.800	8.850	8.850
5	9.8	10	9.1	9.5	8.8	8.7	8.9	7.8	9.5	8.9	8.1	8.6	9.1	9.008	8.988	8.940
6	10	11	9.8	9.8	9.1	9.7	9	11	8.6	8.8	8.6	8.8	9	9.477	9.125	9.200
7	10	9.9	9.8	10	8.6	9.4	8.5	9.5	10	9.7	9.6	9.4	9.4	9.562	9.475	9.371
8	11	9.4	9.9	10	9.4	10	9.4	9.5	9.7	10	9.1	10	11	9.900	9.963	9.963
9	11	10	11	9.8	10	9.4	9.2	9.6	10	10	10	11	11	10.192	10.400	10.400
10	13	12	10	9.3	10	9.1	9.8	10	10	11	11	12	12	10.723	10.975	10.975
11	12	12	12	12	10	10	10	11	11	12	12	12	13	11.462	11.550	11.550
12	13	13	12	12	12	12	12	12	12	12	13	13	14	12.477	12.688	12.688
13	14	13	13	14	12	13	14	15	13	13	13	13	14	13.362	13.225	12.883
														10.036	10.059	10.012

Average

	Rebar										No Rebar			Row Average: All Points	No vert bar	No vert bar/void
	1	2	3	4	5	6	7	8	9	10	11	12	13			
1	11	9	8.2	8.2	8.1	8	8.3	8.7	7.7	7.3	7.6	8.2	8.6	8.369	8.450	8.517
2	9.4	8	7.8	6.8	6.9	7	6.7	6.7	7.1	7	6.9	6.8	8	7.321	7.458	7.458
3	9.6	9.1	7.1	7.5	7.1	7.5	6.7	7.1	6.6	7	7.1	7.2	8	7.510	7.417	7.457
4	9.7	9.1	8.5	8.1	7.6	7.5	7.4	7.1	7.4	7.5	6.9	7.4	8.7	7.909	7.951	7.951
5	9.2	9.3	8.3	8.6	8.1	8.3	7.9	7.6	8.3	8.2	7.5	7.8	8.3	8.256	8.171	8.207
6	9.5	9.4	8.9	8.7	8.6	8.5	8.1	9.4	8.1	8.3	8.1	8.2	8.6	8.644	8.500	8.544
7	9.4	9.3	9.1	9.3	8.2	8.7	8.2	8.8	9.3	9.4	8.6	8.7	9.3	8.937	8.839	8.778
8	10	9.2	9.2	9.4	9.2	9.3	8.6	8.8	8.8	9.5	8.8	9	10	9.259	9.279	9.279
9	10	9.2	9.4	9.3	9.4	8.7	8.2	9.3	8.9	9.5	9.2	10	11	9.413	9.542	9.542
10	12	11	9.8	9.2	9.4	9.1	9	9.7	9.4	10	10	11	12	10.044	10.238	10.238
11	12	11	11	11	9.9	10	9.9	10	11	11	11	12	12	10.844	11.004	11.004
12	13	12	11	12	12	12	11	12	11	11	11	12	14	11.807	11.875	11.875
13	14	13	13	12	12	12	13	15	12	12	12	12	13	12.805	12.704	12.444
														9.317	9.341	9.330

Horizontal

	Rebar										No Rebar			Row Average: All Points	No vert bar	No vert bar/void
	1	2	3	4	5	6	7	8	9	10	11	12	13			
1	11	8.8	7.4	7.4	7	7.3	7.4	7.7	6.5	6.8	6.8	7.3	7.8	7.646	7.675	7.767
2	9.5	8.3	7.6	6.1	6.2	6.8	6.1	6.4	6.5	7	6.3	6.4	7.5	6.977	7.013	7.013
3	9.2	8.6	7.5	7	6.2	7.2	6.5	6.8	6.6	6.7	6.7	7	7.9	7.223	7.200	7.343
4	9.2	8.5	8.3	7.7	7.5	6.8	6.8	6.9	7	7.5	6.7	7.1	8.1	7.546	7.588	7.588
5	9.1	9.1	7.9	8.2	8.3	8	7.5	7.5	7.3	7.7	7.1	7.5	7.7	7.915	7.800	7.980
6	10	9.2	8.5	7.9	8.5	7.8	7.8	8.7	7.4	8	8.2	8	8.8	8.400	8.450	8.467
7	8.6	9.3	8.9	8.5	7.9	8.4	8	8.6	8.6	9	7.9	8.3	9.3	8.564	8.441	8.419
8	9.7	9.3	9.7	9.5	9.3	8.7	8.2	8.3	8.7	9.3	8.9	8.7	10	9.108	9.163	9.163
9	10	8.9	9.1	9	9.1	8.2	7.2	8.8	8.6	9.2	8.4	9.6	11	8.992	9.100	9.100
10	12	10	9.7	9.5	9	9.3	8.8	9.7	9.2	9.4	10	10	12	9.900	10.100	10.100
11	12	11	10	11	10	10	9.7	10	11	9.8	10	12	13	10.746	10.988	10.988
12	14	11	11	11	11	12	11	11	11	10	9.8	11	14	11.435	11.575	11.575
13	14	13	13	12	12	12	13	15	13	12	12	12	12	12.585	12.588	12.267
														9.003	9.052	9.059

Standard Deviation

	Rebar										No Rebar		
	1	2	3	4	5	6	7	8	9	10	11	12	13
1	1.2	0.8	0.8	0.7	1.2	0.9	1.7	1.6	1.3	0.4	0.8	0.8	0.7
2	0.5	0.9	0.7	1.1	0.8	0.7	0.7	0.3	0.7	0.4	0.7	0.5	0.6
3	1	0.8	0.5	1.1	1.4	0.9	0.6	0.4	0.5	0.6	0.6	0.6	0.2
4	0.7	1.3	1.1	0.5	0.7	0.8	1	0.6	0.7	0.9	0.7	0.8	0.8
5	0.6	1	0.7	0.8	0.8	0.4	0.9	0.2	1.1	0.6	0.5	0.7	0.7
6	1.3	1.1	0.8	1	0.5	1	0.8	1.7	0.6	0.4	0.6	0.6	0.6
7	0.9	0.6	0.6	0.8	0.4	0.6	0.3	0.7	0.8	0.4	0.9	0.6	0.1
8	0.7	0.3	1	0.7	0.3	0.7	0.7	0.6	0.9	0.6	0.4	0.9	0.6
9	0.5	1	1	0.4	0.6	0.6	1	0.4	1	0.6	1.1	0.6	0.4
10	0.9	0.9	0.5	0.4	0.5	0.2	0.7	0.6	0.9	1.1	0.7	0.8	0.7
11	1	0.9	1.1	0.9	0.3	0.4	0.4	0.5	0.3	1	0.7	0.5	1
12	0.4	0.8	0.8	0.4	0.9	0.2	1	0.6	0.7	0.7	1.4	1.2	0.8
13	0.6	0.3	0.1	1.1	0.3	0.4	1.1	0.3	1	0.8	0.7	0.6	1

Vertical

	Rebar										No Rebar			Row Average: All Points	No vert bar	No vert bar/void
	1	2	3	4	5	6	7	8	9	10	11	12	13			
1	9.7	8.3	8.2	8.5	7.8	7.7	7.2	7.8	7.5	7.5	8.4	8.4	9.1	8.162	8.288	8.483
2	8.9	7	7.2	6.3	6.7	6.5	6.6	6.7	6.9	6.6	6.9	6.8	7.9	7.000	7.238	7.238
3	8.9	8.7	7.3	6.8	6.5	6.8	6.2	7	6.1	6.6	6.8	6.7	7.8	7.092	7.038	7.114
4	9.5	8.2	7.5	7.9	7	7.3	6.8	6.6	7.1	6.6	6.3	6.7	8.4	7.379	7.417	7.417
5	8.7	8.4	7.9	8	7.3	8.2	7.3	7.5	8	8.1	7.3	7.3	8	7.846	7.725	7.700
6	8.1	8.5	8.3	8.5	8.2	8.1	7.5	8.1	8.2	8.1	7.5	7.7	7.9	8.054	7.925	7.967
7	9.4	8.8	8.7	9.4	8	8.2	8	8.2	9	9.5	8.2	8.3	9.2	8.685	8.600	8.543
8	10	8.9	8	8.6	8.8	9.3	8.1	8.5	8	9	8.4	8.3	9.9	8.769	8.713	8.713
9	10	8.4	8.6	9.2	9	8.6	8.2	9.5	8.1	9	8.8	9.9	10	9.054	9.125	9.125
10	11	10	9.4	8.8	9.2	8.9	8.5	9.2	8.7	9.4	9.4	10	11	9.508	9.638	9.638
11	11	10	10	10	9.5	9.7	9.6	9.8	10	11	11	11	11	10.323	10.475	10.475
12	13	12	11	12	11	12	10	12	10	11	11	12	13	11.508	11.363	11.363
13	13	13	13	12	12	12	12	14	11	12	13	11	14	12.469	12.300	12.183
														8.911	8.911	8.920

FIGURE D.29: 1 day VHES-LMC overlay mockup SR heatmaps

Diagonal														Row Average		
	Rebar										No Rebar			All	No vert	No vert
	1	2	3	4	5	6	7	8	9	10	11	12	13	Points	bar	bar/void
1	14	11	11	11	11	11	12	12	9.9	9.4	9.4	11	11	10.985	11.025	10.917
2	12	11	9.3	9.2	9.4	9.8	9.9	8.9	9.1	9.5	9.6	9.3	10	9.815	9.888	9.888
3	12	12	8	10	12	11	9.7	9.3	9.8	8.9	9.3	9.4	11	10.233	10.100	9.886
4	13	11	12	11	10	9.5	11	9.6	9.9	9.6	10	9.8	12	10.635	10.920	10.920
5	12	12	12	12	10	10	11	11	11	11	10	11	12	11.046	11.063	10.940
6	13	13	13	13	12	12	12	14	11	11	11	11	11	12.069	11.725	11.983
7	12	13	12	11	12	12	10	12	12	12	12	12	12	11.785	11.750	11.686
8	14	12	13	13	11	12	12	12	12	13	11	12	13	12.154	12.163	12.163
9	15	13	13	13	13	12	12	13	12	13	13	13	14	12.877	12.975	12.975
10	16	14	14	11	13	12	12	13	13	14	14	14	17	13.492	13.838	13.838
11	15	14	15	14	13	14	13	13	14	14	15	16	17	14.300	14.588	14.588
12	16	16	15	17	16	16	16	16	14	15	14	16	17	15.569	15.400	15.400
13	18	16	16	16	15	16	17	18	16	16	16	17	18	16.277	16.388	16.167
														12.403	12.448	12.411

Average														Row Average		
	Rebar										No Rebar			All Points	No vert	No vert
	1	2	3	4	5	6	7	8	9	10	11	12	13		bar	bar/void
1	13	11	10	9.7	10	9.8	10	10	9.3	9	9.1	9.7	11	10.115	10.250	10.244
2	11	10	9.3	8.5	8.5	8.5	8.6	8.4	8.6	8.6	9.1	9.1	10	9.164	9.346	9.346
3	12	11	8.6	9.3	10	9.5	8.4	8.4	8.4	8.2	8.8	8.9	10	9.358	9.397	9.273
4	12	11	10	10	9.6	9	9	8.8	9.2	9	9.3	9.1	11	9.851	10.000	10.000
5	11	12	11	11	9.7	10	9.9	9.7	10	9.9	9.4	9.5	11	10.275	10.251	10.287
6	12	12	12	11	10	11	11	11	10	10	9.8	10	10	10.821	10.650	10.806
7	12	12	12	11	12	11	10	11	11	12	11	11	12	11.296	11.264	11.240
8	13	11	12	11	11	11	11	11	11	12	11	11	13	11.515	11.588	11.588
9	14	13	12	13	12	12	11	12	12	12	12	13	14	12.454	12.488	12.488
10	15	14	13	12	12	12	12	12	13	14	13	14	16	13.113	13.354	13.354
11	14	14	14	14	13	13	12	13	13	14	14	15	16	13.715	13.958	13.958
12	16	16	15	15	15	15	15	15	14	14	13	15	17	14.856	14.838	14.838
13	17	16	15	15	15	15	16	18	15	16	16	16	16	15.764	15.704	15.361
														11.715	11.776	11.752

Horizontal														Row Average		
	Rebar										No Rebar			All	No vert	No vert
	1	2	3	4	5	6	7	8	9	10	11	12	13	Points	bar	bar/void
1	12	11	10	9.1	9.4	9.2	10	10	9	9.4	9.3	9.1	11	9.869	9.925	9.867
2	11	10	9.4	8.1	7.8	8.1	8	7.9	8	8.5	8.6	9.4	10	8.862	9.063	9.063
3	12	10	8.8	9.5	9.8	9.1	7.3	7	7.6	7.9	8.7	8.8	10	8.964	9.079	8.976
4	12	11	10	11	9.1	8.6	7.9	8.4	8.6	9	8.9	8.8	11	9.587	9.616	9.616
5	11	12	11	10	9.2	9.9	9.9	9.5	9.7	9.5	8.9	8.3	12	10.025	9.979	10.060
6	12	12	11	9.9	9.4	10	10	11	9.6	10	9.9	10	10	10.377	10.338	10.383
7	11	12	12	11	11	11	11	11	11	12	11	10	11	11.156	10.979	10.976
8	14	11	11	11	11	11	11	11	11	11	11	11	13	11.446	11.700	11.700
9	13	13	12	13	12	11	10	12	11	12	11	13	14	12.108	12.013	12.013
10	15	13	12	12	13	11	11	12	12	13	13	13	15	12.677	12.900	12.900
11	14	14	14	14	13	13	12	13	14	13	13	15	16	13.723	13.988	13.988
12	17	16	15	14	15	14	15	14	14	13	12	13	17	14.492	14.650	14.650
13	18	16	14	15	15	15	16	19	15	15	16	15	15	15.462	15.250	14.767
														11.442	11.498	11.458

Standard Deviation													
	Rebar										No Rebar		
	1	2	3	4	5	6	7	8	9	10	11	12	13
1	1.1	0.5	0.3	0.9	0.6	0.9	1.8	2.3	0.6	0.7	0.4	0.7	0.7
2	0.8	0.7	0.1	0.6	0.8	1.2	1.1	0.5	0.6	0.8	0.5	0.4	0.2
3	0.6	1.2	0.5	1	1.2	1.7	1.2	1.2	1.2	0.6	0.5	0.5	0.4
4	0.5	0.5	1.2	0.7	0.6	0.5	1.4	0.7	0.7	0.6	0.9	0.6	1
5	0.5	0.6	0.6	0.9	0.6	0.2	0.7	0.8	1	0.8	0.8	1.1	1.3
6	1.2	1.1	1.3	1.5	1.4	1.4	1.3	2	0.7	0.8	1	0.4	1.2
7	0.8	0.6	0.1	0.2	0.4	1.6	0.6	0.5	0.7	0.3	1	0.8	0.6
8	1.4	0.6	0.9	1.1	0.5	0.3	1	0.7	0.7	1	0.8	0.7	0.3
9	0.7	0.4	0.7	0.9	0.6	0.5	0.7	0.5	0.5	0.2	1	0.4	0.6
10	0.9	0.7	0.8	1.6	0.5	0.5	0.5	0.6	0.7	0.4	0.6	0.5	0.8
11	1	0.6	0.9	0.6	0.5	0.9	0.9	0.4	0.5	0.3	1.1	0.8	0.5
12	0.8	0.4	0.9	1.2	1.2	0.9	0.8	0.7	0.1	1.1	1	1.4	0.2
13	0.3	0.3	1	0.5	0.2	0.5	0.4	1.1	0.9	0.8	0.4	1.1	1.4

Vertical														Row Average		
	Rebar										No Rebar			All	No vert	No vert
	1	2	3	4	5	6	7	8	9	10	11	12	13	Points	bar	bar/void
1	13	10	10	9.2	10	9.4	8.7	7.8	8.9	8.2	8.7	9.5	9.8	9.492	9.800	9.950
2	11	9.8	9.3	8.2	8.4	7.6	8	8.4	8.7	7.9	9	8.7	10	8.815	9.088	9.088
3	11	10	8.9	8.3	9.4	8	8.1	8.9	7.7	7.8	8.4	8.5	9.9	8.877	9.013	8.957
4	12	10	9.2	9.4	9.4	8.9	8.6	8.5	9.1	8.4	8.8	8.8	10	9.331	9.463	9.463
5	11	11	10	10	9.6	9.8	9.2	9	9.3	9.3	9	9.5	9.6	9.754	9.713	9.860
6	11	11	11	11	9.8	9.9	9.4	9.7	11	9.8	8.7	9.9	8.9	10.015	9.888	10.050
7	12	12	11	11	12	8.8	9.8	11	11	12	10	11	11	10.946	11.063	11.057
8	12	11	11	11	11	11	10	12	11	11	9.8	10	13	10.946	10.900	10.900
9	14	13	12	12	12	12	11	12	12	13	13	13	15	12.377	12.475	12.475
10	14	13	13	14	12	12	12	12	13	13	13	14	15	13.169	13.325	13.325
11	13	13	13	13	12	12	12	13	13	14	14	14	16	13.123	13.300	13.300
12	16	15	14	15	13	14	14	14	14	14	13	15	17	14.508	14.463	14.463
13	17	16	15	16	14	15	16	16	14	16	16	15	16	15.554	15.475	15.150
														11.301	11.382	11.387

FIGURE D.30: 3 day VHES-LMC overlay mockup SR heatmaps

Diagonal

	Rebar 1	2	3	4	5	6	7	8	9	10	No Rebar 11	12	13	Row Average: All Points	No vert bar	No vert bar/void
1	16	12	12	13	11	12	12	9.6	11	12	11	11	12	11.877	11.963	11.950
2	13	11	12	10	9.4	10	9.3	9.6	9.8	11	11	11	12	10.762	10.988	10.988
3	13	12	9.6	11	12	12	11	10	10	11	11	11	13	11.223	11.213	11.100
4	13	13	13	12	11	11	11	9.4	11	10	11	12	12	11.469	11.688	11.688
5	13	14	13	12	11	11	11	12	11	11	12	11	13	11.933	11.925	11.920
6	13	14	13	13	12	12	13	12	12	12	12	12	11	12.446	12.363	12.533
7	13	13	14	12	12	12	12	13	13	13	13	13	13	12.823	12.800	12.829
8	15	13	14	13	12	14	13	14	14	14	13	14	14	13.731	13.800	13.800
9	16	14	14	14	14	14	13	14	15	14	14	16	16	14.300	14.575	14.575
10	17	15	15	13	14	13	13	15	15	16	15	15	18	14.885	15.125	15.125
11	16	15	16	16	15	15	14	15	15	16	16	17	19	15.823	16.163	16.163
12	16	17	16	18	17	17	18	17	16	17	17	18	20	17.231	17.250	17.250
13	18	17	16	18	17	17	19	19	18	18	18	18	17	17.708	17.650	17.300
														13.555	13.654	13.632

Average

	Rebar 1	2	3	4	5	6	7	8	9	10	No Rebar 11	12	13	Row Average: All Points	No vert bar	No vert bar/void
1	14	12	12	12	11	11	11	9.6	11	11	10	11	12	11.262	11.454	11.500
2	13	11	11	9.6	9.3	9.8	9.3	9.4	9.7	9.8	11	10	12	10.346	10.638	10.638
3	13	12	9.8	9.9	11	11	9.8	9.7	9.3	10	10	11	12	10.542	10.618	10.620
4	13	12	12	12	10	10	10	9.6	11	10	11	11	12	11.029	11.171	11.171
5	12	13	12	12	11	11	11	11	11	11	11	11	13	11.614	11.533	11.553
6	14	13	13	12	12	12	12	12	12	12	11	12	11	12.049	11.979	12.178
7	13	13	13	12	12	12	12	13	12	13	12	12	13	12.497	12.346	12.395
8	15	13	13	13	12	13	12	13	13	14	13	13	14	13.249	13.242	13.242
9	15	14	14	13	13	13	12	14	14	14	13	14	15	13.708	13.804	13.804
10	16	15	14	14	13	13	13	15	14	15	14	15	17	14.541	14.671	14.671
11	16	15	15	15	15	15	14	15	15	15	15	17	19	15.567	15.854	15.854
12	17	16	16	17	17	17	17	16	16	16	16	17	19	16.644	16.779	16.779
13	18	18	16	17	16	17	18	19	17	17	17	18	17	17.236	17.108	16.894
														13.099	13.169	13.177

Horizontal

	1	2	3	4	5	6	7	8	9	10	No Rebar 11	12	13	Row Average: All Points	No vert bar	No vert bar/void
1	13	13	12	11	11	9.6	10	9.6	10	10	9.6	10	12	10.838	11.013	11.050
2	12	11	11	9.2	9	9.4	8.9	8.7	9.8	9.7	9.5	10	13	10.115	10.413	10.413
3	13	12	10	9.8	10	11	9.1	8.6	9	9.7	10	11	12	10.269	10.413	10.471
4	14	13	12	12	10	9.1	8.9	9.5	10	10	11	11	13	10.933	11.125	11.125
5	12	13	13	12	11	11	11	11	11	12	11	10	13	11.631	11.588	11.660
6	14	14	12	12	12	11	11	12	11	12	12	11	12	11.962	11.925	12.050
7	13	13	13	12	13	12	12	13	12	14	12	12	13	12.477	12.400	12.443
8	15	14	13	13	12	13	12	13	13	14	13	13	14	13.169	13.163	13.163
9	15	15	14	12	13	13	11	14	14	14	13	14	15	13.700	13.700	13.700
10	16	15	14	14	13	13	13	15	14	15	14	15	17	14.469	14.550	14.550
11	17	16	15	15	15	15	14	15	15	16	15	18	20	15.738	16.000	16.000
12	18	16	16	16	17	17	17	16	16	16	15	17	18	16.377	16.688	16.688
13	19	18	16	16	16	16	18	20	17	16	16	18	17	17.200	17.113	16.733
														12.991	13.084	13.080

Standard Deviation

	Rebar 1	2	3	4	5	6	7	8	9	10	No Rebar 11	12	13
1	1.3	0.5	0.2	1.4	0.2	1.2	1.1	0.1	0.6	0.9	0.6	0.6	0.2
2	0.5	0.6	0.4	0.6	0.2	0.4	0.4	0.6	0.2	0.8	1	0.5	0.9
3	0.2	0.9	0.3	0.7	1.2	1.2	0.8	1	0.6	0.7	0.3	1	0.7
4	0.4	0.8	0.8	0.1	0.7	1	1.2	0.2	0.4	0.1	0.6	0.8	0.6
5	0.3	0.4	0.6	0.3	0.4	0.3	0.4	0.6	0.3	0.3	0.7	0.6	0.9
6	0.4	0.7	0.5	0.6	0.2	0.6	1.1	0.4	0.6	0.2	0.8	0.6	0.8
7	0.3	0.2	0.8	0.8	0.8	0.3	0.1	0.2	0.7	0.1	0.7	0.6	0.8
8	0.9	0.7	0.9	0.1	0.3	0.6	0.7	0.4	1	0.3	0.1	0.9	0.2
9	0.3	1.1	1	0.8	0.6	0.3	1.2	0.2	1.1	0.7	0.6	1.4	0.7
10	0.8	0.3	0.4	0.6	0.3	0.2	0.2	0.5	0.4	0.8	0.5	0.2	1
11	0.6	0.8	0.9	0.2	0.5	0.5	0.5	0.5	0.2	0.3	0.6	1	0.7
12	0.8	0.8	0.1	0.9	0.8	0.5	1.3	0.6	0.1	1.3	0.8	0.9	1.1
13	1.2	0.8	0.1	0.8	0.5	0.6	1.4	0.7	0.8	0.9	0.7	0.3	0.5

Vertical

	1	2	3	4	5	6	7	8	9	10	No Rebar 11	12	13	Row Average: All Points	No vert bar	No vert bar/void
1	13	12	11	11	11	11	11	9.5	11	10	11	11	12	11.069	11.388	11.500
2	13	10	11	9.3	9.4	9.7	9.7	9.8	9.4	9	11	10	11	10.162	10.513	10.513
3	13	11	9.8	9.3	9.8	9.8	9.6	11	9	9.6	10	9.5	11	10.133	10.229	10.290
4	13	12	11	11	9.5	10	9.8	9.8	11	10	10	10	12	10.685	10.700	10.700
5	12	13	12	12	11	12	11	11	11	11	10	11	12	11.277	11.088	11.080
6	13	13	13	12	12	12	11	12	12	11	11	11	10	11.738	11.650	11.950
7	13	13	12	13	11	12	12	12	11	13	12	11	12	12.192	11.838	11.914
8	14	12	13	13	12	13	12	13	13	14	13	13	14	12.846	12.763	12.763
9	15	13	13	12	13	13	12	15	13	13	13	13	14	13.123	13.138	13.138
10	16	15	14	13	13	13	13	15	14	15	14	15	16	14.269	14.338	14.338
11	16	15	15	15	14	14	15	14	15	15	15	16	18	15.138	15.400	15.400
12	16	16	16	17	16	16	15	17	16	15	16	18	19	16.323	16.400	16.400
13	16	17	16	17	16	16	16	18	16	17	17	17	17	16.800	16.563	16.650
														12.750	12.770	12.818

FIGURE D.31: 7 day VHES-LMC overlay mockup SR heatmaps

Diagonal														Row Average		
	Rebar										No Rebar			All	No vert	No vert
	1	2	3	4	5	6	7	8	9	10	11	12	13	Points	bar	bar/void
1	19	16	15	14	15	15	15	14	13	14	13	14	16	14.610	14.766	14.788
2	16	14	14	13	12	12	12	12	12	12	13	13	15	13.015	13.338	13.338
3	16	16	12	13	15	13	14	13	12	13	13	14	14	13.677	13.713	13.471
4	16	17	15	14	13	12	13	13	13	13	14	14	17	14.062	14.438	14.438
5	17	16	15	15	14	13	14	13	14	14	14	14	16	14.585	14.838	14.980
6	17	16	16	15	14	15	15	16	15	15	14	14	14	14.954	14.775	15.017
7	17	16	16	15	14	15	14	14	16	15	15	15	16	15.238	15.325	15.257
8	19	15	16	16	15	17	16	16	17	16	16	15	17	16.038	16.100	16.100
9	18	17	16	17	16	16	16	17	17	17	16	19	18	16.938	17.038	17.038
10	20	18	17	16	16	16	17	19	17	18	18	18	21	17.702	17.891	17.891
11	19	18	19	18	18	17	17	18	18	18	19	19	22	18.438	18.850	18.850
12	20	20	18	19	20	20	19	20	17	20	18	20	21	19.362	19.138	19.138
13	20	20	18	20	18	20	23	23	20	19	21	20	21	20.185	20.050	19.600
														16.062	16.174	16.147

Average														Row Average		
	Rebar										No Rebar			All Points	No vert	No vert
	1	2	3	4	5	6	7	8	9	10	11	12	13		bar	bar/void
1	18	16	15	14	15	15	15	15	15	14	15	15	17	15.519	15.780	15.941
2	16	14	14	12	12	13	13	12	13	13	14	14	16	13.578	14.013	14.013
3	16	16	13	13	14	13	14	13	12	13	14	14	16	14.064	14.267	14.248
4	17	16	14	14	13	12	13	13	14	13	14	14	17	14.228	14.533	14.533
5	17	17	15	15	14	14	14	14	14	15	14	14	16	14.811	14.860	15.013
6	18	15	16	15	15	15	15	16	15	15	14	15	15	15.208	15.263	15.394
7	16	16	17	16	14	15	15	15	16	16	15	15	16	15.574	15.458	15.376
8	18	16	16	16	16	17	16	17	17	17	16	16	17	16.464	16.492	16.492
9	19	18	17	17	16	16	16	18	18	17	16	18	19	17.323	17.346	17.346
10	20	18	17	16	17	16	17	19	18	18	18	18	21	17.988	18.243	18.243
11	19	19	20	20	19	18	18	19	19	19	20	21	24	19.334	19.633	19.633
12	20	20	19	20	21	21	20	21	19	20	19	21	22	20.126	19.967	19.967
13	21	21	19	20	20	21	24	24	20	21	21	21	21	20.951	20.871	20.400
														16.551	16.671	16.661

Horizontal														Row Average		
	Rebar										No Rebar			All	No vert	No vert
	1	2	3	4	5	6	7	8	9	10	11	12	13	Points	bar	bar/void
1	18	17	15	14	16	16	15	18	15	15	14	15	19	15.938	15.963	16.233
2	16	15	16	12	12	13	14	12	14	14	15	15	17	14.085	14.675	14.675
3	16	16	13	15	15	13	15	13	13	14	15	16	18	14.662	15.075	15.157
4	19	16	14	12	13	12	13	14	16	14	14	15	18	14.485	15.025	15.025
5	17	18	15	13	14	15	14	15	13	15	14	15	16	14.923	14.763	14.900
6	19	13	16	15	16	15	15	16	15	15	15	16	16	15.577	15.988	15.950
7	17	17	18	16	15	16	16	15	16	17	15	15	17	16.100	16.000	15.943
8	19	17	17	17	17	17	16	17	17	18	16	17	17	17.008	17.075	17.075
9	20	20	20	18	16	17	17	19	18	18	16	18	20	18.131	18.050	18.050
10	20	20	17	17	18	18	17	18	18	19	19	18	22	18.462	18.688	18.688
11	19	20	22	22	20	20	18	19	20	20	20	22	26	20.672	20.950	20.950
12	22	21	19	20	22	21	21	22	21	20	19	21	23	20.969	21.038	21.038
13	24	21	19	19	20	22	24	25	21	21	21	22	21	21.454	21.475	20.650
														17.113	17.289	17.256

Standard Deviation													
	Rebar										No Rebar		
	1	2	3	4	5	6	7	8	9	10	11	12	13
1	0.3	0.7	0.9	0.2	0.8	0.6	0.5	2.1	2	0.8	1.7	1.1	1.8
2	0.4	0.4	1	0.1	0.6	0.5	1.3	0.9	0.9	0.9	1	0.9	0.8
3	0.3	0.2	1	1	1.1	0.3	1.1	0.8	0.4	0.7	1.1	1.4	1.8
4	1.6	0.5	0.7	1.4	0.2	0.8	0.4	0.6	1.2	0.7	0.2	0.7	1
5	0.3	0.8	0.1	1.2	0.1	0.9	0.3	1.3	0.7	0.4	0.6	0.3	0.4
6	1.5	1.8	0.2	0.3	0.7	0.3	0.7	0.9	0.4	0.3	0.7	0.9	1.2
7	1.6	0.4	1	0.7	0.3	0.5	1	0.5	0.3	1.4	0.2	0.2	0.5
8	0.8	1.1	0.6	0.5	1.2	0.4	0.4	1.2	0.6	0.6	0.4	0.7	0.3
9	0.8	1.9	2	0.8	0.4	0.6	0.6	1.3	0.5	0.8	0.2	0.9	1.2
10	0.3	1.1	0.6	0.4	1.1	1	0.3	0.4	0.8	0.4	0.3	0.4	0.6
11	0.7	1.2	1.7	2	1.3	1.6	0.7	0.6	1.5	1	0.3	1.5	2.1
12	1.5	0.4	0.5	0.7	1.1	0.9	0.9	0.9	1.8	0.6	0.4	0.9	1.2
13	2.1	0.9	0.9	0.9	1.5	0.8	0.8	0.8	0.4	1.6	0.7	1.2	0.3

Vertical														Row Average		
											No Rebar			All	No vert	No vert
	1	2	3	4	5	6	7	8	9	10	11	12	13	Points	bar	bar/void
1	18	17	16	14	16	16	16	15	17	13	16	17	17	16.008	16.613	16.800
2	15	14	14	12	13	13	14	13	13	12	15	13	15	13.633	14.025	14.025
3	16	16	14	13	13	13	13	14	12	13	15	13	16	13.854	14.013	14.114
4	16	16	14	15	13	13	13	13	14	13	14	14	16	14.138	14.138	14.138
5	17	16	15	16	14	15	15	13	15	15	15	14	15	14.925	14.979	15.160
6	17	16	16	16	15	15	14	15	16	14	14	15	14	15.092	15.025	15.217
7	14	16	16	17	14	15	15	15	16	17	15	15	16	15.385	15.050	14.929
8	18	15	16	16	16	16	16	18	16	17	16	16	17	16.346	16.300	16.300
9	18	17	16	16	16	16	17	19	18	16	17	17	18	16.900	16.950	16.950
10	20	17	16	16	16	16	17	19	19	18	19	18	21	17.800	18.150	18.150
11	18	18	18	19	19	18	18	19	18	19	20	21	22	18.892	19.100	19.100
12	19	20	19	21	20	21	19	21	19	19	19	21	21	20.046	19.725	19.725
13	20	21	19	20	21	21	23	23	21	22	22	22	20	21.215	21.088	20.950
														16.480	16.550	16.581

FIGURE D.32: 14 day VHES-LMC overlay mockup SR heatmaps

Diagonal	Rebar										No Rebar			Row Average: All Points	Row Average: No vert bar	Row Average: No vert bar/void
	1	2	3	4	5	6	7	8	9	10	11	12	13			
1	27	27	22	21	23	25	27	27	26	22	23	24	27	24.764	24.925	25.100
2	20	22	22	19	16	24	25	17	20	19	22	21	26	20.885	21.400	21.400
3	26	24	18	18	30	29	28	20	17	22	25	24	23	23.331	23.850	23.014
4	26	28	25	20	19	21	25	22	21	19	25	21	25	22.715	23.238	23.238
5	22	24	21	20	18	17	18	19	21	21	21	20	23	20.338	20.488	20.140
6	23	26	25	20	20	22	20	20	22	20	20	18	21	21.256	21.025	21.500
7	22	24	20	18	19	19	18	19	23	22	22	20	23	20.692	20.750	20.371
8	26	20	22	21	20	23	21	22	21	23	20	22	23	21.731	21.813	21.813
9	24	24	21	23	21	23	22	25	25	23	23	27	23	23.354	23.225	23.225
10	23	21	25	19	21	22	24	24	24	25	25	21	29	23.254	23.988	23.988
11	21	22	24	25	24	24	23	24	24	24	26	25	27	24.018	24.138	24.138
12	21	26	23	26	25	22	27	25	21	25	24	25	26	24.348	24.066	24.066
13	24	24	21	24	28	28	29	28	25	20	27	24	24	24.923	25.038	24.600
														22.739	22.919	22.815

Average	Rebar										No Rebar			Row Average: All Points	Row Average: No vert bar	Row Average: No vert bar/void
	1	2	3	4	5	6	7	8	9	10	11	12	13			
1	23	22	19	18	19	21	20	19	19	17	20	20	23	20.062	20.500	20.933
2	17	18	18	16	14	17	18	15	16	16	18	18	22	17.255	17.746	17.746
3	21	19	17	16	20	20	20	17	15	18	20	19	21	18.546	18.954	18.819
4	21	21	19	17	15	15	17	17	17	17	20	18	22	18.185	18.683	18.683
5	20	20	19	17	16	15	16	16	18	18	18	17	20	17.674	17.863	17.547
6	20	21	20	18	17	18	17	18	18	17	17	17	18	18.135	17.908	18.167
7	19	20	18	18	17	17	16	17	18	18	18	17	20	17.908	17.788	17.700
8	21	17	18	18	18	19	18	19	18	19	18	18	19	18.605	18.646	18.646
9	22	20	19	20	18	19	20	22	21	20	20	22	21	20.270	20.367	20.367
10	21	19	21	18	19	19	20	21	21	21	21	20	24	20.287	20.796	20.796
11	20	20	22	22	21	21	20	21	21	21	22	22	24	21.207	21.272	21.272
12	20	22	20	23	22	20	23	23	20	21	21	22	23	21.624	21.518	21.518
13	21	21	19	21	23	24	26	26	22	21	23	22	22	22.503	22.321	21.828
														19.405	19.566	19.540

Horizontal	Rebar										No Rebar			Row Average: All Points	Row Average: No vert bar	Row Average: No vert bar/void
	1	2	3	4	5	6	7	8	9	10	11	12	13			
1	22	19	16	15	17	18	15	16	15	15	16	18	23	17.338	17.738	18.467
2	16	17	16	15	13	14	13	14	14	15	16	17	21	15.438	15.825	15.825
3	18	18	16	14	15	16	16	16	15	17	18	17	21	16.662	17.075	17.329
4	19	18	18	15	12	11	12	15	15	16	18	18	22	16.108	16.775	16.775
5	19	19	18	17	15	14	15	16	16	17	16	16	21	16.808	16.975	16.500
6	19	20	18	17	16	16	16	17	16	16	17	17	17	16.931	16.925	16.850
7	18	19	18	16	15	16	16	16	17	17	17	16	19	16.862	16.813	16.843
8	20	17	16	17	17	18	17	18	17	17	16	17	19	17.300	17.413	17.413
9	23	20	20	19	17	18	20	20	20	21	18	20	20	19.492	19.588	19.588
10	20	19	19	18	19	17	18	21	19	20	18	19	22	19.108	19.263	19.263
11	20	21	21	22	19	19	18	20	20	20	19	22	23	20.385	20.413	20.413
12	22	21	20	22	21	19	22	22	20	19	19	21	22	20.623	20.650	20.650
13	21	20	19	21	20	23	24	25	21	23	21	21	21	21.462	20.925	20.450
														18.040	18.183	18.182

Standard Deviation	Rebar										No Rebar		
	1	2	3	4	5	6	7	8	9	10	11	12	13
1	3.2	4.7	3.3	3.4	3.3	3.3	5.9	7.2	5.7	4.1	3.7	3.3	3.7
2	2.2	3.2	3.7	3	1.8	5.7	6.3	1.6	3.2	2.3	2.8	2.3	3.6
3	4.5	4.4	1.6	2	8.5	8.3	7.4	2.3	1.5	3.4	4.1	4.7	2.6
4	4.4	5.7	4.5	2.6	3.3	5	6.7	4.3	3.2	2.3	4.4	2.7	3.4
5	2.1	3.8	2.6	2.2	1.9	1.3	1.8	2.2	2.8	2.8	3.1	2.3	2.7
6	2.9	4	4.4	1.8	2.2	3.6	3	2.1	3	2.2	2.4	1.7	3.3
7	2.6	3.3	1.7	1.1	1.7	2	1.7	1.6	4.4	3.6	3.3	2.4	3.3
8	4	2.3	2.9	2.3	2.4	3.2	2.4	2.5	2.6	3.2	2.3	3.1	2.9
9	2.3	3.2	2.4	2.7	2.1	4.2	2.3	2.8	2.8	3.4	2.8	4.3	2.2
10	1.4	2.3	4.1	1.2	1.4	2.8	3.2	2.5	2.9	3.1	3.9	1.1	4.3
11	1.4	1.9	2.1	2.6	3.3	3	2.8	2.5	3	2.7	3.4	2.1	2.8
12	1.7	2.9	2.1	3.1	2.7	1.7	3.5	1.9	1.2	3.6	2.5	2.6	2.7
13	2.1	2.3	1.1	2.1	3.9	3.6	2.7	1.9	2.5	1.4	3.6	1.4	2.2

Vertical	Rebar										No Rebar			Row Average: All Points	Row Average: No vert bar	Row Average: No vert bar/void
	1	2	3	4	5	6	7	8	9	10	11	12	13			
1	21	19	17	16	18	20	18	14	17	15	20	20	20	18.085	18.838	19.233
2	16	16	16	14	14	14	15	14	15	15	18	16	19	15.441	16.013	16.013
3	18	16	15	15	15	13	15	16	14	15	18	15	18	15.646	15.938	16.114
4	18	17	16	16	14	14	14	15	15	15	17	16	19	15.731	16.038	16.038
5	19	17	16	15	15	15	14	15	16	16	16	16	17	15.877	16.125	16.000
6	18	18	17	17	16	17	14	17	17	16	15	15	14	16.218	15.775	16.150
7	17	18	17	18	16	16	15	17	15	16	15	15	17	16.169	15.800	15.886
8	18	15	17	17	16	17	17	18	16	18	16	17	17	16.785	16.713	16.713
9	20	17	17	18	17	15	18	20	20	17	19	19	19	17.964	18.288	18.288
10	20	17	18	16	19	17	18	19	20	19	19	20	21	18.500	19.138	19.138
11	18	18	20	20	18	19	18	20	18	19	20	20	22	19.218	19.266	19.266
12	18	20	19	20	21	20	21	21	19	19	19	21	21	19.900	19.838	19.838
13	19	20	19	19	22	21	26	25	21	21	20	21	20	21.123	21.000	20.433
														17.435	17.597	17.624

FIGURE D.33: 28 day VHES-LMC overlay mockup SR heatmaps

Diagonal														Row Average		
	Rebar										No Rebar			All	No vert	No vert
	1	2	3	4	5	6	7	8	9	10	11	12	13	Points	bar	bar/void
1	33	32	25	29	29	27	31	31	27	23	30	29	37	29.523	30.125	30.767
2	24	27	23	23	21	27	31	25	23	22	27	28	30	25.446	25.913	25.913
3	30	27	20	26	25	35	34	29	29	23	28	25	28	27.485	27.238	27.514
4	29	27	24	19	18	19	23	22	22	19	28	26	33	23.762	25.425	25.425
5	29	27	26	22	19	19	20	21	21	22	22	21	25	22.585	22.863	23.100
6	29	28	25	24	20	22	22	20	22	20	21	19	22	22.441	22.366	23.055
7	27	29	24	21	20	20	19	19	20	17	21	20	23	21.385	21.550	21.757
8	27	22	24	26	22	23	21	21	20	22	20	20	24	22.415	22.225	22.225
9	29	28	24	26	23	22	22	23	25	22	22	24	21	23.946	23.763	23.763
10	33	25	28	21	23	24	26	24	24	24	22	23	29	25.023	25.988	25.988
11	28	27	27	29	28	26	25	27	25	24	26	25	30	26.654	26.813	26.813
12	28	30	24	28	31	27	30	29	27	28	26	29	32	28.377	28.338	28.338
13	36	30	27	28	31	33	38	36	30	29	34	31	35	32.038	32.588	31.250
														25.468	25.784	25.839

Average														Row Average		
	Rebar										No Rebar			All Points	No vert	No vert
	1	2	3	4	5	6	7	8	9	10	11	12	13		bar	bar/void
1	33	30	26	27	28	30	30	28	26	22	28	29	35	28.500	29.217	29.778
2	25	24	22	22	21	25	25	22	22	22	25	25	31	24.036	24.600	24.600
3	28	24	20	26	27	33	33	28	24	22	27	24	28	26.392	26.179	26.100
4	29	26	24	20	18	18	20	21	22	20	27	24	30	23.108	24.379	24.379
5	29	26	26	22	19	18	19	20	21	22	21	20	26	22.177	22.575	22.800
6	29	27	25	23	20	20	20	21	21	19	20	19	22	22.006	22.030	22.429
7	28	27	24	22	20	20	20	19	19	18	19	19	25	21.574	21.808	22.148
8	29	22	24	24	22	22	21	21	20	20	20	20	23	22.136	22.429	22.429
9	30	27	24	26	23	21	21	22	24	21	21	22	22	23.474	23.529	23.529
10	29	24	25	22	23	23	25	25	24	22	22	23	27	24.169	24.696	24.696
11	26	27	26	27	26	24	24	26	24	24	26	26	31	25.928	26.138	26.138
12	29	29	24	27	28	26	29	28	27	27	24	28	31	27.528	27.550	27.550
13	34	30	27	27	30	32	36	37	29	32	32	31	33	31.613	31.713	30.600
														24.819	25.142	25.167

Horizontal														Row Average		
											No Rebar			All	No vert	No vert
	1	2	3	4	5	6	7	8	9	10	11	12	13	Points	bar	bar/void
1	35	30	27	27	29	34	31	29	24	21	26	29	37	29.077	29.625	29.833
2	25	23	23	23	21	24	23	20	21	24	22	25	34	23.585	24.100	24.100
3	28	26	19	32	29	38	36	30	22	24	26	24	31	28.054	26.950	26.600
4	31	26	25	20	17	15	18	21	22	21	25	24	30	22.692	23.863	23.863
5	30	28	27	22	20	17	18	20	20	23	21	20	27	22.431	22.763	23.060
6	32	28	26	23	20	20	18	22	19	20	18	20	25	22.392	22.438	22.350
7	30	28	25	22	20	21	20	19	20	19	19	19	30	22.392	22.850	23.314
8	32	22	23	23	23	22	19	21	20	20	21	20	25	22.169	22.700	22.700
9	33	28	25	29	23	20	20	20	23	23	20	22	24	23.869	23.713	23.713
10	26	25	25	24	24	23	24	26	23	22	22	23	28	24.300	24.388	24.388
11	25	28	27	27	27	23	22	25	26	26	25	27	35	26.369	26.688	26.688
12	34	28	23	27	24	28	30	27	27	25	22	28	33	27.400	27.750	27.750
13	36	29	28	26	29	32	35	37	28	33	33	30	35	31.531	31.650	30.433
														25.097	25.344	25.292

Standard Deviation													
	Rebar										No Rebar		
	1	2	3	4	5	6	7	8	9	10	11	12	13
1	1.7	1.7	1.7	2	1.3	3.8	2.4	3.3	1.6	1.4	1.8	0.2	2.8
2	0.5	2	0.4	1	0.2	2.2	4.7	2.5	1.2	1.5	2.7	2.7	2.4
3	2.6	2.8	0.3	6.4	2.3	6.5	3.1	2.4	4.5	1.5	0.9	1.8	2.5
4	1.4	0.7	0.7	1	1.2	2.7	2.8	0.8	0.4	1	1.9	2.1	2.8
5	1	2.4	0.9	0.2	0.9	0.9	1.3	1.6	0.6	1.2	1.1	0.4	1.2
6	2.9	1.8	1.2	0.8	0.6	0.9	1.6	0.9	1.4	1.5	1.6	0.7	2.6
7	1.7	1.3	1.1	1.1	0.6	0.9	1.4	0.5	0.8	0.9	1.4	0.4	5
8	2.3	0.7	0.8	1.7	0.6	0.6	1.1	0.4	0.7	1.3	0.6	0.8	1.6
9	2.4	2.9	0.9	3.1	0.4	0.9	1.2	1.7	0.8	2	1.2	1.1	2.4
10	3.7	2.6	2.3	1.7	1.4	0.6	0.8	1	1	1.2	0.3	0.3	2.8
11	1.7	1.9	1.3	2.1	2.3	1.5	1.5	0.8	2.1	1.8	0.9	1.1	3.4
12	3.9	1.1	1	0.4	3.2	2.5	2.2	1.6	0.8	1.9	2.2	0.7	2.8
13	2.9	1.3	0.8	1.3	1.6	1.3	1.4	0.5	0.9	2.5	2	1.7	2.7

Vertical														Row Average		
											No Rebar			All	No vert	No vert
	1	2	3	4	5	6	7	8	9	10	11	12	13	Points	bar	bar/void
1	32	29	24	25	26	27	27	24	26	21	28	29	32	26.900	27.900	28.733
2	25	23	22	21	21	24	22	21	22	21	26	23	29	23.077	23.788	23.788
3	25	21	20	19	26	26	30	25	20	21	27	22	26	23.638	24.350	24.186
4	28	25	24	21	19	20	20	20	21	20	28	22	28	22.869	23.850	23.850
5	28	24	25	22	19	19	20	18	21	20	19	20	25	21.515	22.100	22.240
6	27	24	24	23	21	20	20	21	21	17	19	19	20	21.185	21.288	21.883
7	27	26	23	23	19	20	22	18	19	17	19	19	21	20.946	21.025	21.371
8	28	21	24	23	22	21	21	21	21	19	20	21	22	21.823	22.363	22.363
9	29	23	23	23	23	21	22	23	24	19	22	22	20	22.608	23.113	23.113
10	28	21	23	22	21	23	24	25	25	21	22	23	24	23.185	23.713	23.713
11	25	24	25	25	24	24	24	27	22	23	26	27	28	24.762	24.913	24.913
12	27	29	25	27	28	23	26	29	26	27	25	28	28	26.808	26.563	26.563
13	31	32	27	28	31	31	36	37	29	33	30	33	30	31.269	30.900	30.117
														23.891	24.297	24.372

FIGURE D.34: 56 day VHES-LMC overlay mockup SR heatmaps

Diagonal														Row Average		
	Rebar										No Rebar			All	No vert	No vert
	1	2	3	4	5	6	7	8	9	10	11	12	13	Points	bar	bar/void
1	45	39	36	40	37	45	37	42	36	32	35	40	46	39.154	39.000	39.783
2	35	32	29	33	30	45	40	24	33	30	31	33	45	33.810	34.363	34.363
3	32	32	22	29	47	45	54	34	24	30	34	33	35	34.623	35.200	33.486
4	39	30	28	33	22	24	31	30	25	25	34	32	38	30.100	31.150	31.150
5	36	29	33	26	23	20	23	23	27	27	27	25	33	26.969	28.388	28.340
6	31	33	34	29	25	24	25	25	29	28	25	24	26	27.400	27.275	28.167
7	33	37	28	25	23	24	23	23	25	26	25	23	28	26.308	25.975	26.129
8	37	22	28	28	25	27	25	25	28	27	26	26	29	27.277	28.063	28.063
9	25	34	30	30	28	28	30	29	29	27	24	28	28	28.469	27.663	27.663
10	38	30	22	25	30	29	33	28	32	30	26	30	37	29.854	30.938	30.938
11	36	34	32	33	32	29	30	32	39	29	31	32	35	32.738	33.488	33.488
12	36	40	32	36	36	33	38	36	33	36	33	35	41	35.708	35.563	35.563
13	46	42	36	37	39	38	49	44	38	37	46	44	51	42.085	43.738	42.433
														31.884	32.369	32.274

Average														Row Average		
	Rebar										No Rebar			All Points	No vert bar	No vert bar/void
	1	2	3	4	5	6	7	8	9	10	11	12	13			
1	41	36	33	35	35	38	35	33	34	31	32	36	42	35.579	36.092	36.717
2	30	33	25	29	27	34	34	24	27	26	28	30	38	29.678	30.108	30.108
3	32	27	24	28	38	40	42	30	24	27	30	29	33	31.105	31.571	30.610
4	34	28	26	25	24	25	26	26	24	23	31	28	35	27.249	28.408	28.408
5	33	28	30	25	25	20	21	21	25	24	24	23	30	25.377	26.458	26.600
6	32	30	30	26	23	21	23	23	24	23	23	22	26	25.036	25.279	25.700
7	30	31	26	24	22	23	23	21	24	24	23	22	26	24.579	24.463	24.462
8	35	23	26	26	24	25	24	23	25	24	25	25	28	25.638	26.429	26.429
9	27	31	27	27	25	26	28	27	28	27	29	27	28	27.254	27.292	27.292
10	35	30	29	24	26	27	30	27	28	26	26	28	33	28.585	29.567	29.567
11	32	31	29	32	29	28	28	30	31	27	30	31	35	30.313	30.717	30.717
12	35	35	30	32	33	30	33	35	34	36	35	33	37	33.662	33.775	33.775
13	42	38	35	33	37	35	45	43	37	36	41	40	44	38.777	39.975	38.933
														29.449	30.010	29.947

Horizontal														Row Average		
											No Rebar			All	No vert	No vert
	1	2	3	4	5	6	7	8	9	10	11	12	13	Points	bar	bar/void
1	38	35	30	34	33	36	35	30	37	36	29	32	44	34.538	34.725	35.517
2	30	39	23	27	25	29	28	23	25	27	26	31	39	28.623	28.475	28.475
3	31	26	26	33	41	45	39	28	26	26	28	30	35	31.715	31.888	30.600
4	32	27	25	22	28	27	21	24	23	23	30	29	37	26.654	28.025	28.025
5	30	31	29	25	22	21	19	22	24	25	23	24	31	25.123	25.325	24.700
6	33	30	27	25	22	19	21	22	21	22	24	23	28	24.423	25.088	24.917
7	29	30	26	24	22	23	22	23	23	23	23	23	29	24.508	24.550	24.729
8	37	25	25	26	26	26	23	23	23	21	24	25	29	25.623	26.513	26.513
9	25	30	27	25	25	27	27	27	29	30	35	26	27	27.731	27.650	27.650
10	36	37	38	25	25	28	28	26	27	25	25	27	34	29.308	30.063	30.063
11	33	32	29	38	28	28	27	29	29	27	30	31	39	30.754	30.813	30.813
12	38	33	30	30	32	28	32	35	32	32	32	33	36	32.592	33.138	33.138
13	45	34	34	31	36	38	47	45	40	38	41	40	41	39.246	40.525	38.800
														29.295	29.752	29.534

Standard Deviation													
	Rebar										No Rebar		
	1	2	3	4	5	6	7	8	9	10	11	12	13
1	3.7	2.2	3.2	4.1	2.5	6.2	1.8	7.3	4.3	5.7	3	4.2	5.1
2	4.1	5.7	3.4	3.8	2.7	10	6	1	4.5	5.2	2.6	2.8	7
3	0.9	4.1	1.8	5.6	10	8.8	11	3.4	1.5	2.3	3.6	3.9	3.8
4	4.6	1.8	1.9	7	3.9	1.8	4.9	3.2	1.2	2.4	2.6	4.3	3.9
5	3	2.7	2.8	1.3	3.8	1.3	2	2.5	2.1	2.4	2.7	2.2	2.8
6	1.8	2	3.8	3.1	1.4	2.8	1.8	1.5	4	4.3	3.2	1.5	2.6
7	2.6	4.9	2.1	0.4	1.1	0.9	1.1	2.7	1	1.9	2.1	2.2	4.3
8	4.6	1.7	1.5	2	2.1	2.3	1	1.9	2.8	3.1	1.3	1.3	2.8
9	2.8	3.7	2.5	3.2	2.8	3.5	1.8	2.1	1.4	4.1	5.6	1.3	1.1
10	3.4	6.5	8.2	0.3	3.2	2.5	2.9	1	3.4	2.8	1	1.1	4
11	4.3	3.3	3	5.8	2.9	1.5	1.6	1.8	6.4	2.1	1.4	1.4	3.8
12	3.8	4.1	2.7	3.2	2.7	2.8	4.1	0.9	2.7	3.6	4.3	1.8	3.8
13	7	3.7	0.7	3.2	1.8	5.5	5.6	3.2	4.7	1.8	5.5	4.3	6.3

Vertical														Row Average		
											No Rebar			All	No vert	No vert
	1	2	3	4	5	6	7	8	9	10	11	12	13	Points	bar	bar/void
1	39	35	34	32	36	32	34	28	29	25	34	36	36	33.046	34.550	34.850
2	27	27	23	26	26	27	34	25	25	20	28	27	31	26.600	27.488	27.488
3	33	24	24	22	27	30	33	29	23	25	29	25	28	26.977	27.625	27.743
4	31	27	25	21	21	24	26	25	23	20	29	24	31	24.992	26.050	26.050
5	33	25	28	23	29	19	22	18	23	22	22	21	27	24.038	25.663	26.760
6	30	29	28	23	23	20	22	23	22	19	19	21	23	23.285	23.475	24.017
7	28	28	24	24	21	22	24	18	25	24	21	19	21	22.923	22.863	22.529
8	29	22	26	24	22	23	23	22	25	25	24	23	24	24.015	24.713	24.713
9	30	27	25	25	22	22	26	25	27	22	28	26	29	25.562	26.563	26.563
10	32	24	28	24	23	24	29	27	26	25	27	28	29	26.592	27.700	27.700
11	28	28	26	26	26	26	27	29	26	25	29	30	31	27.446	27.850	27.850
12	31	33	27	30	32	28	29	34	37	39	40	31	34	32.685	32.625	32.625
13	34	37	35	31	37	29	38	39	31	34	35	36	39	35.000	35.663	35.567
														27.166	27.910	28.035

FIGURE D.35: 90 day VHES-LMC overlay mockup SR heatmaps